Investigation into mechanisms of metastasis in breast cancer and pancreatic cancer

A thesis submitted for the degree of Ph.D. by

Gemma Moore, B.Sc. Hons

The experimental work described in this thesis was performed under the supervision of Dr. Laura Breen and Dr. Fiona O'Neill.

National Institute for Cellular Biotechnology

School of Biotechnology

Dublin City University

July 2017

I hereby certify that this material, which I now submit for assessment on the programme of study leading to the award of Ph.D. is entirely my own work, that I have exercised reasonable care to ensure that the work is original, and does not to the best of my knowledge breach any law of copyright, and has not been taken from the work of others save and to the extent that such work has been cited and acknowledged within the text of my work.

Signed: _____ ID No.: 57480571

Date:

.

This thesis is dedicated to my loving family.

My parents, Joan and Jimmy.

My sister, Deborah.

My brother, James.

Acknowledgements

Firstly, I would like to thank Dr. Laura Breen. Laura coming on board as my supervisor was the best thing that happened throughout my PhD. I am so unbelievably grateful to you. I always felt like we were a team, in it together. You always made time for me and were nothing but supportive. When things went wrong, it was usually you telling me to forget about it, go home early and start a fresh tomorrow, which was exactly what I needed to hear. I'll never be able to put into words how much easier everything was because I had you there to help me. Thank you so much, I am eternally grateful.

I would like to thank Professor Martin Clynes. If not for the opportunity you gave me I would not be where I am today. From the original just 6 weeks of Intra lab experience, to the whole Summer, to a PhD, none of this would have happened if you had not given me the opportunity, the support and guidance over the years. I am completely grateful. The NICB is a special place to train as a scientist which is down to you, the atmosphere of learning has been fostered and developed through you.

Fiona, you were such a great addition to my supervisory panel. You always had such great enthusiasm which was so refreshing especially in the final year. I appreciate all your help, advice and I appreciate that you always made time for me.

Sandra, my unofficial, surrogate supervisor. Over the last couple of years, you have given me so much of your time which I am extremely grateful for. Your advice was always helpful and you happily listened to me rant and rave.

Overall, I want to say a huge thank you to everyone in the NICB. Over the years, I have asked questions and gotten help from virtually every person in the building. The centre has such a great attitude towards collaboration and training of young scientists. I am grateful to everyone who has helped me along the way.

To everyone on the top floor over the 5 years and specifically Paul, Shane, Edel, Orla, Alan, Kevin and Laura, you guys have been the best part of the PhD process. I wouldn't want to face a PhD without all the fun and laughs we had. I love you all and will miss you so much.

To my best friend, Vanessa, I am so lucky to have you. You have listened to me rant, rave, moan and cry so patiently over the years. Your support, encouragement and enthusiasm was so important to me during the PhD. You were always so encouraging and never doubted that I would get there in the end. Our friendship is forever, we are sisters, family, and that is never ending.

Finally, to my family, this is **our** achievement, not mine. I wouldn't have been able to do any of this without you. Everyday of my life I have felt how much you love me and that you are proud of me. Your support, understanding and humour have gotten me through the tough parts. In return, I offer my unending love, support and knowledge that I am proud everyday to be a member of our little family. You are my home, my heart, my happiness.

Table of Contents

Table of Figures

Abbreviations

2D	-	2-Dimensional
3D	-	3-Dimensional
Ago-2	-	Argonaute-2
Apaf	-	Apoptotic protease activating factor
AR	-	Androgen Receptor
Bcl-2	-	B-cell Lymphoma 2
B-CLL	-	B cell chronic lymphocytic leukaemia
BL1	-	Basal-like 1
BL2	-	Basal-like 2
Bmf	-	Bcl-2 Modifying Factor
BSA	-	Bovine Serum Albumin
CAF	-	Cancer Associated Fibroblast
cDNA	-	complementary DNA
cPR	-	Complete Pathological Response
CM	-	Conditioned Media
Ct	-	Comparative Threshold
DDR2	-	Discoidin Domain-containing Receptor 2
DFS	-	Disease-Free Survival
DISC	-	Death Inducing Signalling Complex
DMEM	-	Dulbecco's Minimum Essential Medium
DMSO	-	Dimethyl Sulfoxide
DNA	-	Deoxyribonucleic Acid
dNTP	-	Deoxynucleotide Triphosphate
ECM	-	Extra-Cellular Matrix
EDTA	-	Ethylenediaminetetraacetic Acid
EMT	-	Epithelial to Mesenchymal Transition
ER	-	Estrogen Receptor

ER	-	Endoplasmic Reticulum
ERK	-	Extracellular Signal-regulated Kinases
FAK	-	Focal Adhesion Kinase
FADD	-	Associated Death Domain
FAP	-	Fibroblast Activation Protein
FC	-	Fold Change
FCS	-	Fetal Calf Serum
FLIP	-	FLICE-inhibitory Protein
GAPDH	-	Glyceraldehyde-3-Phosphate Dehydrogenase
GFP	-	Green Fluorescent Protein
HER2	-	Human Epidermal Growth Factor Receptor 2
HIF	-	Hypoxia Inducible Factor
HMEC	-	Human Mammary Epithelial Cell
hPSC	-	human Pancreatic Stellate Cell
HSC	-	Hepatic Stellate Cell
HuR	-	Human Antigen R
IAP	-	Inhibitor of Apoptosis
IGFBP	-	Insulin-like Growth Factor Binding Protein
IHC	-	Immunohistochemistry
IM	-	Immunomodulatory
IMS	-	Industrial Methylated Spirits
ILK	-	Integrin-linked Kinase
kDa	-	Kilo Daltons
KM	-	Kaplan-Meier
LAR	-	Luminal Androgen Receptor
M	-	Mesenchymal
miR	-	microRNA
miRNA	-	microRNA

MMP	-	Matrix Metalloproteinase
mRNA	-	messenger RNA
MSL	-	Mesenchymal Stem-like
NC	-	Negative control
No RT	-	No Reverse Transcriptase
NSCLC	-	Non-Small Cell Lung Cancer
OD	-	Optical Density
OMM	-	Outer Mitochondrial Membrane
OS	-	Overall Survival
OV	-	Overexpression
PBS	-	Phosphate Saline Buffer
PCR	-	Polymerase Chain Reaction
PDAC	-	Pancreatic Ductal Adenocarcinoma
PDGFRα	-	PDGF receptor-α
PDGFRβ	-	PDGF receptor-β
PET	-	Pancreatic Endocrine Tumour
PI3K	-	Phosphoinositide 3-kinase
Pre-miRNA	-	Preliminary microRNA
Pri-miRNA	-	Primary microRNA
PR	-	Progesterone Receptor
PSC	-	Pancreatic Stellate Cell
q-RT-PCR	-	quantitative Reverse Transcriptase PCR
RB1	-	Retinoblastoma Protein 1
RFP	-	Red Fluorescent Protein
RFS	-	Relapse Free Survival
RISC	-	RNA-induced Silencing Complex
RNA	-	Ribonucleic Acid
RNAi	-	RNA interference

RNase	-	Ribonuclease
RNA pol	-	RNA Polymerase
rpm	-	Revolutions Per Minute
RPMI	-	Roswell Park Memorial Institute Medium
shRNA	-	short hairpin RNA
siRNA	-	short interfering RNA
Smac/DIABLO	-	Second Mitochondrial-derived activator of caspases/direct IAP binding protein
Spg	-	Sponge
TAF	-	Tumour-associated Fibroblast
TIMP	-	Tissue Inhibitor of Metalloproteinase
TNBC	-	Triple Negative Breast Cancer
TNF	-	Tumour Necrosis Factor
TRBP	-	TAR Binding Protein
Un	-	Untransfected
UPR	-	Unfolded Protein Response
UTR	-	Untranslated Region
v/v	-	volume/volume
XIAP	-	X-linked Inhibitor of Apoptosis

Conference Presentations

- **Poster presentation.** **Gemma Moore**, Fiona O'Neill, Sinead Aherne, Gerard McVey, Michael Moriarty, Laura Breen and Martin Clynes. **Investigating the role of the tumour microenvironment in the behaviour of pancreatic cancer cells using indirect co-culture**. Cambridge Pancreatic Cancer Symposium, Cambridge, England, 2017.
- **Oral presentation.** **Gemma Moore**, Fiona O'Neill, Sinead Aherne, Gerard McVey, Michael Moriarty, Laura Breen and Martin Clynes. **Investigating the role of the tumour microenvironment in the behaviour of pancreatic cancer cells using indirect co-culture**. School of Biotechnology 8th Annual Research Day, DCU, 2016.
- **Flash 5 Oral presentation.** **Gemma Moore**, Fiona O'Neill, Sinead Aherne, Gerard McVey, Michael Moriarty, Laura Breen and Martin Clynes. **Investigating the role of the tumour microenvironment in the behaviour of pancreatic cancer cells using indirect co-culture**. School of Biotechnology 8th Annual Research Day, DCU, 2016.
- **Poster presentation.** **Gemma Moore** and Fiona O'Neill*. **Investigating the role of the tumour microenvironment and its role in radiation therapy in pancreatic cancer**. AACR, The Function of the Tumor Microenvironment in Cancer Progression in San Diego, CA, 2016. *Presenting author
- **Poster presentation.** **Gemma Moore**, Fiona O'Neill, Sinead Aherne, Gerard McVey, Michael Moriarty, Laura Breen and Martin Clynes. **Investigating the role of the tumour microenvironment in the behaviour of pancreatic cancer cells using indirect co-culture**. Pancreatic Cancer Symposium, Marseille, France, 2015.
- **Poster presentation.** **Gemma Moore**, Fiona O'Neill, Sinead Aherne, Laura Breen and Martin Clynes **Investigating the role of the tumour microenvironment in the behaviour of pancreatic cancer cells using indirect co-culture**. Cambridge Pancreatic Cancer Symposium, Cambridge, England, 2015.
- Annual BioAT Research Day, poster and oral presentations 2012-2015.
    - June 2012 – Poster – **Mechanisms of Anoikis Resistance in Human Cancer Cells**
    - June 2013 – Oral presentation – **Mechanisms of Anoikis Resistance in Breast Cancer Cells**
    - June 2014 – Poster – **The effects of pancreatic cancer cell & pancreatic stellate cell interactions**
    - June 2015 – Oral presentation – **Investigating the role of the tumour microenvironment in the behaviour of pancreatic cancer cells using indirect co-culture**.

Abstract

Investigation into mechanisms of metastasis in breast cancer and pancreatic cancer

Gemma Moore

The aim of this project was to investigate mechanisms of metastasis in triple negative breast cancer (TNBC) and pancreatic cancer. Metastasis is the ability of a cell to spread to another location colonising a secondary site, which contributes to approximately 90% of cancers fatalities. Both TNBC and pancreatic cancer possess poor prognosis, limited therapeutic options and the risk of each becoming metastatic remains a major risk. This body of work aimed to investigate unique influences on the metastatic capabilities of both TNBC and pancreatic cancer cells. Three critical metastatic phenotypes were investigated, specifically anoikis resistance (anchorage independence), colony formation, proliferation and invasion. Metastasis was investigated through three approaches: i) microarray profiling was used to investigate genes that were differentially expressed in anoikis resistant conditions, ii) an indirect co-culture model that mimicked the tumour microenvironment was used to assess critical metastatic phenotypes in pancreatic cancer and iii) miRNA expression profiling and a range of methods for altering miRNA expression in cell culture were deployed to assess the effect of altered miRNA expression on the metastatic phenotypes of pancreatic cancer.

Through microarray profiling 26 genes were identified as differentially expressed in anoikis resistant conditions. Specifically, GRP78 was identified as a regulator of growth in TNBC through proliferation and colony formation, with GRP78 acting as an oncogene. The development of an indirect co-culture model allowed insight into the complicated role of the tumour microenvironment in pancreatic cancer. This investigation led to the observation that the stroma can act to inhibit and restrain the progression of pancreatic cancer. Altering miRNA expression led to the identification of a range of tumour suppressor miRNA including miR-7a, miR-204 and miR-378. Each induced different changes in metastatic phenotypes including a reduction proliferation, colony formation and an extreme increase in invasion. A highly novel finding is the validity of using sponge knockdown vectors as a valuable research tool in pancreatic cancer. In conclusion, anoikis, proliferation, colony formation and invasion were greatly influenced by gene expression, the tumour microenvironment and miRNA expression. Using these three approaches a greater understanding of metastasis and consequently of how both TNBC and pancreatic cancer progress has been gained. With this greater understanding comes a greater possibility of developing effective therapies.

1. Introduction

1.1. Cancer

Cancer is the second leading causes of death worldwide, accounting for 8.2 million deaths in 2012 (Ferlay et al. 2013). There are over 200 different types of cancer, each with different characteristics, prognosis and treatments. Two different cancer types are the focus of this investigative project, triple negative breast cancer and pancreatic cancer. Both of these malignancies possess poor prognosis and poor treatment options.

Metastasis is a process which contributes to the high mortality rate in cancer (Jiang et al. 2015). In fact, without metastasis 90% of cancers would not be fatal (Hu et al. 2016). Metastasis is the ability of a cell to spread to another location in the body not only surviving in this foreign site, also surviving the journey and establishing further growth in this new location (Kozlowski, Kozlowska and Kocki 2015). Gaining a greater understanding of metastasis is required to further understand the progression of cancer and with this comes a greater possibility of developing effective targeted therapies. Metastasis occurs through a cascade of processes, signals and functions. This body of work aims to investigate metastasis through several metastatic characteristics, specifically anoikis, invasion, miRNA and the tumour microenvironment. Each of these aspects of metastasis (which are explained in further detail below) are critical steps in the metastatic cascade.

This project aimed to investigate the metastatic process through anoikis, growth and invasion in both triple negative breast cancer and pancreatic cancer. The effect of the tumour microenvironment and altered miRNA expression on the metastatic phenotypes mentioned was assessed in pancreatic cancer.

1.2. Breast Cancer

Breast cancer, a cancer of the tissues of the breast, is the second most common cancer in women in Ireland, affecting approximately 3,000 women every year (National Cancer Registry Ireland 2016). Investigation of the genes expressed in breast cancer cells has been performed in recent years using DNA Microarrays; this work has led to identification of four main molecular classes of breast cancer (Sotiriou et al. 2003). These classes are Luminal A, Luminal B, HER2 and triple negative (Sotiriou, Phil and Pusztai 2003) and are known as the intrinsic subtypes of breast cancer. These classes differ due to the receptors expressed on the cell surface. The receptors include the estrogen receptor (ER), the progesterone receptor (PR) and the HER2 receptor. Luminal A and B both are ER positive (ER+) with luminal A being HER2 positive and luminal B being HER2 negative (Carey et al. 2006). Luminal B can in some instances be HER2 positive this is associated with high expression of Ki67 (a proliferative marker) which luminal A expresses lowly (Voduc et al. 2010).

The HER2 subtype of breast cancer is ER-, PR- and HER2 positive (Hugh et al. 2009). Triple negative breast cancer (TNBC) is negative for all these receptors and is also known as basal-like breast cancer. Prior to these molecular classifications breast cancer was classified based on tumour size, presence of lymph node metastasis and histological grade (Reis-Filho and Pusztai 2011). TNBC tumours are generally larger, of higher grade than in other forms of breast cancer and TNBCs have lymph node involvement at diagnosis (Lehmann et al. 2011). Over the last decade breast cancer has become much more treatable with the advances in using hormone and targeted therapies. These therapies are applicable to Luminal A, Luminal B and HER2 classes of breast cancer (Sotiriou, Phil and Pusztai 2003) as the therapies are effective on the receptors on the cell surface. TNBC cannot be treated with these therapies due to the lack of these receptors on its cell surface. As a result, triple negative breast cancers have limited treatment options (Foulkes, Smith and Reis-Filho 2010) and poor prognosis (Ressler, Mlineritsch and Greil 2010). Unfortunately, the risk of TNBC becoming metastatic i.e. spreading to other areas of the body, remains a genuine risk and concern. A major factor

in the success of metastasis is the ability to resist anoikis. Anoikis is a form of cell death due to detachment of a cell from the extra-cellular matrix (ECM) (Frisch and Francis 1994). This aspect of metastasis in TNBC was investigated through microarray analysis in this research. A better understanding of how TNBC spreads through the body may lead to development of new and efficient treatment for TNBC.

Figure 1-1. Anoikis sensitivity and anoikis resistance in metastasis

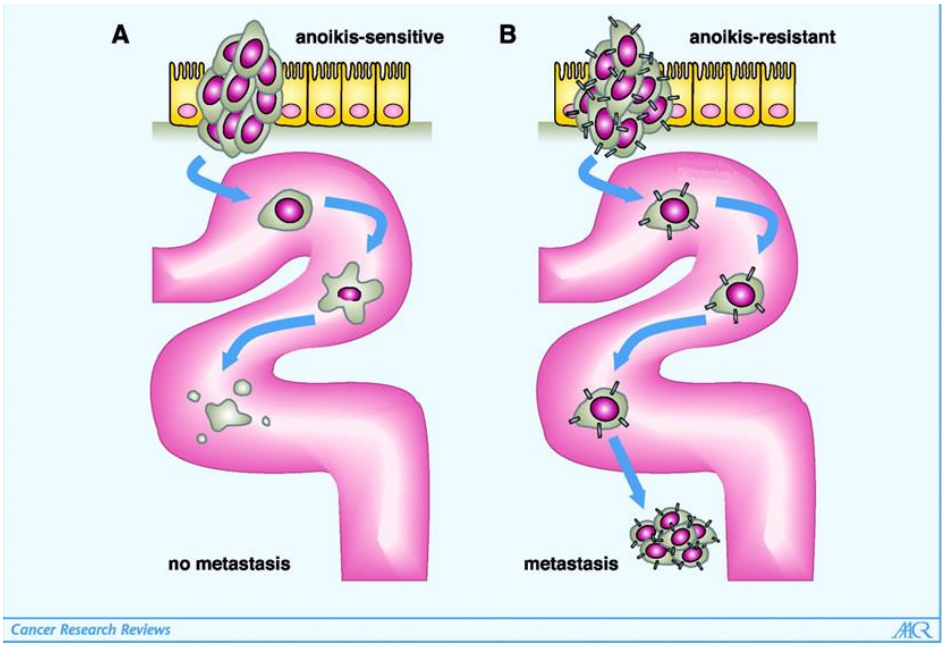

(A) shows anoikis-sensitive cells separating from a primary tumour and undergoing anoikis upon entering the blood stream. (B) shows anoikis resistance protecting circulating tumour cells from undergoing anoikis, thereby facilitating metastasis (Geiger and Peeper 2005).

1.3. Triple Negative Breast Cancer

Triple negative breast cancer constitutes 10-20% of breast cancer cases (Carey et al. 2010). This form of breast cancer affects younger people i.e. premenopausal women, more frequently and has a higher prevalence in African-American and Hispanic women (Carey et al. 2006, Amirikia et al. 2011). TNBC is biologically more aggressive than the other breast cancer subtypes; it has a higher rate of early recurrence and metastasis, with this metastasis being more often to the central nervous system, specifically the brain and the lungs compared to the other subtypes (Elsamany and Abdullah 2014). This

higher rate of early metastasis is shown by a study of 1601 breast cancer patients between the years of 1987 and 1997 in Toronto. This study showed the median time to death of TNBC patients was 4.2 years compared to 6 years for the other breast cancer types. Also, all TNBC patients died within 10 years of diagnosis with deaths of patients with other breast cancer types occurring over 18 years (Dent et al. 2007). This group also observed that there was no correlation between tumour size and nodal status in TNBC while a correlation was present in other breast cancer types. In TNBC even small tumours had a high rate of positive nodal status with 55% of women with tumours ≤1cm possessing at least one positive lymph node (Dent et al. 2007). This observation displays how early the metastasis occurs in TNBC, before the tumour has even reached a substantial size the cancer has begun to spread. This is confirmed by the observation that the mean time to distant recurrence in TNBC was only 2.6 years compared to 5 years in the other breast cancer patients (Dent et al. 2007). This early recurrence and metastasis has been observed by many other studies (Kennecke et al. 2010, Radosa et al. 2016, Lai et al. 2016, Chen, Ding and Wang 2015, Kümmel et al. 2015). It is due to this startlingly early recurrence and metastasis, that greater understanding of the mechanisms of metastasis in TNBC is required. To successfully treat a cancer with such early metastasis is near impossible.

TNBC has a compelling association with BRCA mutational status, with the triple negative subtype being diagnosed significantly more frequently in women with BRCA mutations in comparison with BRCA-negative patients (Pellegrino et al. 2016). Patients carrying BRCA mutations carry an 80% lifetime risk of developing breast cancer (Anders and Carey 2009). Chemotherapy is the current standard therapy available for TNBC, either individually or in combination with surgery and/or radiotherapy. Despite having higher rates of initial clinical response to neo adjuvant chemotherapy compared to other intrinsic subtypes, most TNBC cases relapse within 3 years (Kleivi Sahlberg et al. 2015). This chemotherapy treatment focuses on cytotoxic agents such as anthracyclines and taxanes but in recent years an interest has developed in platinum compounds. This interest developed due to the association of BRCA mutation and TNBC. Platinum drugs produce DNA double-strand breaks, while BRCA mutations cause dysfunction of the DNA

repair process (Hastak, Alli and Ford 2010). Therefore, a treatment inducing double-strand DNA breaks in a BRCA mutated TNBC which has inhibited DNA repair function may prove to be highly effective (Staudacher et al. 2011). Several studies and clinical trials are investigating this hypothesis currently (Tutt et al. 2015, Karginova et al. 2015). Another developing treatment for TNBC, poly (ADP-ribose) polymerase (PARP) inhibitors also act to block DNA repair mechanisms and therefore may be a promising treatment in BRCA mutated TNBC patients (O'Shaughnessy et al. 2011). There are several PARP inhibitors at different stages of clinical development (Audeh 2014) and studies are now showing a greater efficacy using PARP inhibitors in combination with chemotherapeutics (O'Shaughnessy et al. 2011, Sun et al. 2014).

1.3.1. Triple Negative Breast Cancer Subtypes

TNBC is a diverse heterogenous collection of breast cancers which show a range of histological patterns and pathological features. In recent years, the TNBC subtype has been analysed using gene expression profiles and has been further divided into subtypes within TNBC. There is some ambiguity in the literature on these subtypes as different groups have identified different subtypes and some have identified similar subtypes but titled them differently. The following sections address this ambiguity, settling on one form of classifications and giving some insight into the crossover of other classifications.

1.3.2. TNBC or Basal-like?

There is a crossover in use of the terms of TNBC and Basal-like breast cancer with many believing the two are relatively synonymous but just as many believe this to be untrue. Basal-like subtype is described as possessing characteristics of normal myoepithelial cells of the breast ductal and lobular system, such as expressing keratin 5/6 and 17 (Van De Rijn et al. 2002, Perou et al. 2000). The title basal-like comes from the fact that these cytokeratins are typically found in the basal epithelium layer of the skin and airways (Perou 2010). These tumours are highly proliferative whether measured by Ki-67 staining, proliferating cell nuclear antigen, immunohistochemistry (IHC) or gene

expression (Perou 2010, Cheang et al. 2009, Hugh et al. 2009). This high rate of proliferation may be due to a non-functional RB1 protein which is a critical cell cycle regulator (Perou 2010). As well as being RB1 deficient these tumours are p53 deficient and are associated with BRCA1 mutation (Chiche et al. 2016). Interestingly, the majority of BRCA1 mutation carriers who develop breast cancer develop the basal-like form of breast cancer (Perou 2010). The relationship between TNBC and basal-like is difficult. Some reports show 90% of TNBC to be basal-like (Kreike et al. 2007). More recently gene expression analysis identifying subtypes within TNBC observed only 47% of TNBC cases to be basal-like (Lehmann et al. 2011). There is still no internationally accepted definition or distinction for Basal-like and Triple Negative breast cancer.

1.3.3. Triple Negative Breast Cancer Subtypes

Lehmann *et al.,* performed gene expression profiling on 21 breast cancer data sets which identified 587 TNBC cases. Cluster analysis on these TNBC cases resulted in 6 subtypes of TNBC but this has recently been refined to just four subtypes (Lehmann et al. 2016). The original six subtypes were Basal-like 1 (BL-1), Basal-like 2 (BL-2), Immunomodulatory (IM), Mesenchymal (M), Mesenchymal stem-like (MSL) and Luminal androgen receptor (LAR). The four refined subtypes and their relative frequencies are:

- Basal-like 1 (BL-1) – 35%
- Basal-like 2 (BL-2) – 22%
- Mesenchymal (M) – 22%
- Luminal androgen receptor (LAR) – 16%

2% of cases were unclassified with the Immunomodulatory and Mesenchymal stem-like subtypes being removed. These subtypes were determined to represent tumours with substantial infiltrating lymphocytes and tumour-associated mesenchymal cells respectively (Lehmann et al. 2016). These subtypes were identified using publicly available gene expression datasets from 587 TNBC tumours with the four subtypes being distributed as follows: 35% BL-1, 22% BL-2, 25% M, 16% LAR and 2% unclassified (Lehmann et al. 2016). Comparison of the four TNBC subtypes with the intrinsic subtypes

of breast cancer found BL-1, Bl-2 and M subtypes are largely composed of genes associated with basal-like breast cancers while the LAR subtype is mainly comprised of genes associated with luminal and HER2 subtypes (Lehmann et al. 2016). This finding agrees with a study from North Carolina. This study also used DNA microarray profiling to subtype TNBC, identifying that each of the four intrinsic breast cancer subtypes are present within the TNBC subtype (Perou 2010). The four refined subtypes identified by Lehmann *et al.*, as well as some crossover of these subtypes with subtypes identified through other studies are detailed below.

1.3.3.1. Basal-like subtypes

These TNBC subtypes are highly proliferative showing high staining (70%) of Ki-67 which is a proliferation marker (Elsamany and Abdullah 2014). The basal-like TNBCs are highly sensitive to antimitotic chemotherapeutic agents e.g. taxanes, with BL-1 patients showing a pathological complete response (pCR) of 41% compared to 18% in BL-2 patients and 29% in LAR (Lehmann et al. 2016). Tumours in BL-1 patients were found to be of the highest grade compared to all other subtypes but interestingly were of the lowest clinical stage with only 6% determined as stage 3 (Lehmann et al. 2016). The BL-2 subtype possessed the highest clinical stage with 30% of BL-2 tumours being stage 3 (Lehmann et al. 2016). While both Basal-like subtypes share several characteristics, there are differences present. The BL-1 class displays high expression of genes associated with cell cycle and cell division while the gene expression profile of the BL-2 class is enriched for genes involved in growth factor signalling, glycolysis and gluconeogenesis as well as growth factor receptors (Lehmann et al. 2011). BL-1 patients showed a significantly better overall survival compared to all other refined subtypes combined (Lehmann et al. 2016). The BL-1 subtype also displayed a better relapse-free survival (RFS) with near 60% survival at 10 years (Lehmann et al. 2016). There is some cross-over of characteristics and similarities between the BL1 and BL2 subtypes. Both classifications show high levels of proliferation and an overall basal-like profile. These subtypes are most likely subtypes of each other with BL1 and BL2 being further subtyping of the Basal-like subtype described in section 1.3.2.

1.3.3.2. Mesenchymal

The gene expression profile of the M subtype shows enrichment for genes involved in cell motility, cell differentiation pathways, growth pathways and genes associated with ECM receptor interaction (Lehmann et al. 2011). The signalling pathway components present in the expression profile of the M subtype are also found in the profile of metaplastic breast cancer (Gibson et al. 2005). Metaplastic breast cancer is a rare form which occurs in between 0.02% to 5% of breast cancer patients (Hu et al. 2013). This form of cancer is characterised by mesenchymal and epithelial components and is known to be chemoresistant (Hu et al. 2013). The M subtype is described as having a low level of lymph node involvement as only 21% of cases had lymph node disease but displayed a significantly higher frequency of lung metastasis (46%) compared to all other subtypes (25%) (Lehmann et al. 2016).

1.3.3.3. Luminal androgen receptor

The gene expression profile of this subtype is the most varied among the TNBC subtypes. While the TNBC subtypes are ER negative, the luminal androgen receptor (LAR) subtype is heavily enriched for genes found in hormonally regulated pathways such as steroid synthesis, porphyrin metabolism and androgen/estrogen metabolism (Lehmann et al. 2011). Interestingly, this LAR subtype displayed high expression of androgen receptor (AR) mRNA which is known to be highly expressed in ER-negative breast cancer subtypes (Hayes et al. 2008). The level observed was 9-fold greater than the other TNBC subtypes (Lehmann et al. 2011). Using IHC methods the level of AR protein was investigated across an array of TNBC tumours. The LAR subtype displayed a higher percentage of tumours with nuclear staining and higher intensity of staining compared to the other TNBC subtypes (Lehmann et al. 2011). Diagnosis of the LAR subtype occurred more often in older women, with these tumours being of the lowest grade, compared to all other subtypes (Lehmann et al. 2016). Cases of the LAR subtype presented with a significant level (nearly half (47%) of patients) of lymph node metastasis as well as a significantly

higher incidence of bone metastasis (46%) compared to all other subtypes (16%) (Lehmann et al. 2016).

1.3.4. Other classifications

Other publications divide TNBC into several other subtypes:

- Claudin-low
- Molecular Apocrine

1.3.4.1. Claudin-low

The claudin-low subtype recently identified has been characterised by loss of tight junction markers (notably claudins), high expression of EMT markers and enrichment of mammary stem cell markers. This is similar to the MSL subtype previously identified by the Lehmann study but which was recently shown to be due to tumour-associated mesenchymal cells (Jiao et al. 2014, Lehmann et al. 2016). Hierarchical clustering using the claudin-low predictor set identified a portion of the M and MSL subtypes with low claudin, cytokeratin and CD24 expression (Lehmann et al. 2011). The MSL subtype displayed low expression of claudins 3, 4 and 7 which indicates there may be a relationship between the MSL subtype and this Claudin-low subtype, the claudin-low subtype may also be due to tumour-associated mesenchymal cells as was the case with the MSL subtype.

1.3.4.2. Molecular Apocrine

In 2005 Farmer *et al.*, subtyped breast cancer into three subtypes: luminal, basal and molecular apocrine (Farmer et al. 2005). This group performed a microarray study on large operable and locally advanced breast cancers. The molecular apocrine subtype observed had increased androgen signalling, a ‘molecular apocrine’ gene expression profile and possessed some apocrine morphological features. These gene expression

and morphological features were similar to the apocrine tissue of the breast, hence the name. Apocrine tissue in the breast is a benign fibrocystic change (Farmer et al. 2005). All of the tumours classified as molecular apocrine were ER negative and represented 8-14% of the tumours tested (Farmer et al. 2005). Using the classifications of Lehmann *et al.*, this molecular apocrine subtype is similar to the LAR subtype as both express the androgen receptor and are ER negative. In the study of the LAR subtype all 6 apocrine tumours strongly correlated with the LAR subtype and the Lehmann study concluded that the LAR subtype is composed of AR-driven tumours which include the molecular apocrine subtype (Lehmann et al. 2011).

The topic of breast cancer subtypes and the subtypes within triple negative breast cancer can be ambiguous. Many papers describe different subtypes or describe similar subtypes divided in different ways. While the area can be indistinct the subtypes described above aim to give a clear insight into one way of subtyping TNBC identified by Lehmann *et al.*, The four refined subtypes identified by this group have been discussed above as well as the crossover between papers, authors and other subtypes so as to give a clear and concise view. The four refined subtypes identified by Lehmann *et al.*, were the accepted and used subtypes for the purpose of this study.

1.4. Pancreatic cancer

The pancreas is an organ that produces digestive enzymes and hormones. This organ has 3 sections: head, body and tail. There are two distinct pancreatic cell types. The endocrine component is composed of islet cells which are found in the body and the tail of the pancreas and produce hormones such as insulin that regulate carbohydrate metabolism (Omary et al. 2007). The exocrine component consists of clusters of acinar cells which are found throughout the organ and represent 95% of the cells in the pancreas. This cell type is responsible for secreting digestive enzymes into the duodenum (Omary et al. 2007).

Pancreatic cancer is one of the most lethal cancers worldwide. The 5-year survival rate is approximately 6%, due to late diagnosis by which time usually metastasis has occurred (Rucki and Zheng 2014). Over the last 40 years there has been very few advances in pancreatic cancer treatment and no change in the survival rate as shown by Figure 1-2. In Ireland 500 people are diagnosed each year (National Cancer Registry Ireland 2016), this number is expected to increase in coming years due to changes in lifestyle. In a report, The 2014 Euro Pancreatic Cancer Index, published by Swedish based research organisation Health Consumer Powerhouse, Ireland was ranked 4th out of 30 countries in a comparison of pancreatic cancer treatment (Yazbeck and Bjornberg 2014). This indicates Ireland has the 4th highest level of pancreatic cancer treatment out of the 30 countries investigated.

95% of pancreatic cancers are cancer of the exocrine cells. These cancers are classified as adenocarcinomas and usually originate in the head of the pancreas. The cancers of the endocrine pancreatic component, pancreatic endocrine tumours (PET), are quite different. These tumours are known as islet cell tumours or neuroendocrine tumours. They are slow growing with a different prognosis and treatment to the adenocarcinomas. Pancreatic adenocarcinomas are the focus of this project. Less than 20% of pancreatic cancer adenocarcinoma patients are eligible for surgical resection at time of diagnosis due to the high level of metastasis (Rucki and Zheng 2014). Therefore, approximately 80% of patients present with locally advanced or distant disease at diagnosis. Even after surgery of the 20%, the 5-year survival of the patients eligible for resection is only 18-27% (Katz et al. 2009). The 5-year survival rate differs based on the stage of the disease at diagnosis, with patients with localised disease having a 5-year survival rate of 25%, regional disease 10% and distant disease 2% with only 10% of pancreatic cancer patients presenting with localised stage I and II disease (Siegel, Miller and Jemal 2015). The lack of improvement in pancreatic cancer survival rates over the past 40 years is largely due to the advanced disease level present at diagnosis. Once a disease becomes systemic the possibility of complete recovery is infinitely smaller. Therefore, early detection is highly important in further advancing pancreatic cancer treatment. This has proven quite difficult so far, however a greater understanding of the

mechanisms of this early metastasis may play an important role in the development of early detection strategies, as well advanced treatment options.

Figure 1-2. Trends in cancer survival by tumour site 1971-2011 (Pancreatic Cancer Action 2017)

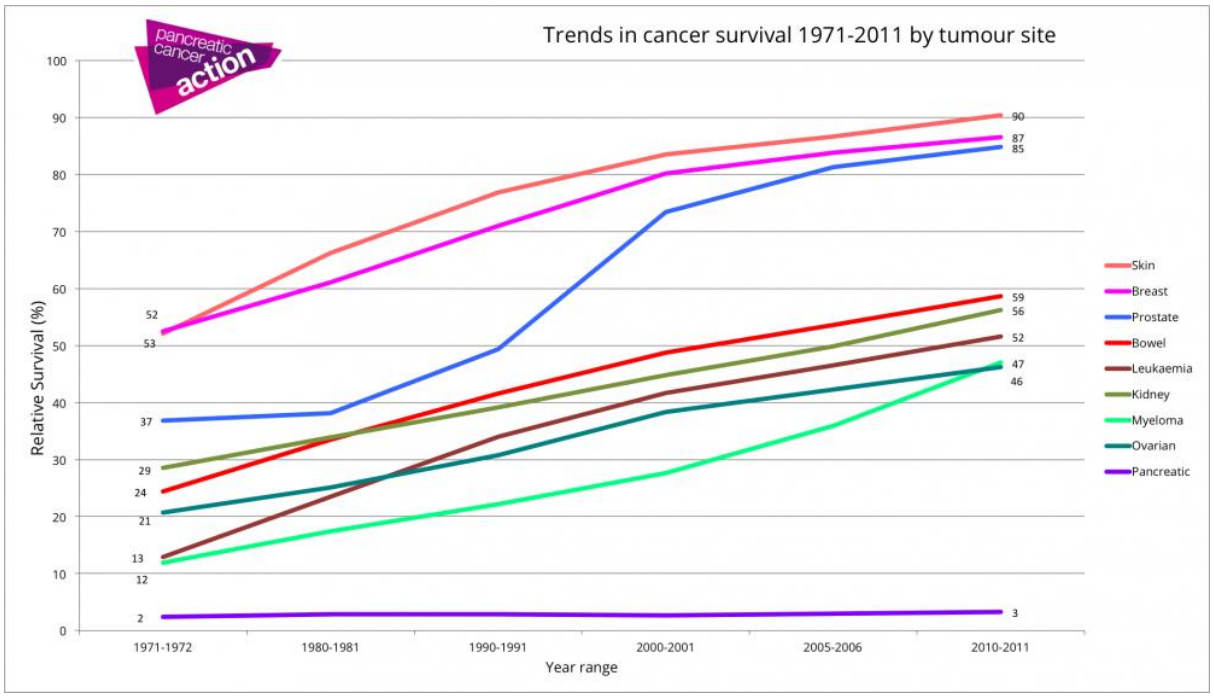

Relative survival (1971-2011) across a range of cancer types based on tumour site. Very little change in the survival of pancreatic cancer is present across the 40-year period.

1.4.1. Fibrosis

A hallmark of pancreatic cancer is a high level of stroma in the tumours, as seen in Figure 1-3, which is due to fibrosis also known as desmoplasia. Fibrosis is defined as an accumulation of extracellular matrix (ECM) proteins due to the loss of balance between the manufacture and degradation of ECM (Apte, Pirola and Wilson 2012), as seen in Figure 1-4. When an injury or insult causes damage to the pancreas, this tissue damage causes our body to induce inflammation as a part of our immune response to repair the tissue. This inflammation in turn activates pancreatic stromal cells, which once activated produce scores of ECM proteins. Over a period of time if repetitive cycles of damage and repair occur, this leads to a build up a fibrous tissue surrounding the pancreas. The

progressive replacement of pancreatic tissue with ECM-rich connective tissue leads to exocrine and endocrine insufficiency i.e. the levels of exocrine and endocrine tissue are reduced causing a reduction in pancreatic function (Jaster 2004). This fibrosis plays a major role in the development and progression of chronic pancreatitis and pancreatic cancer. This dense stroma surrounding the pancreas is reported to give some protection to pancreatic tumours from anti-cancer drugs and furthermore stromal cells may induce progression of the cancer through promotion of migration and invasion in the pancreatic cancer cells (Hwang et al. 2008).

Figure 1-3. Abundance of stroma in pancreatic cancer tumours

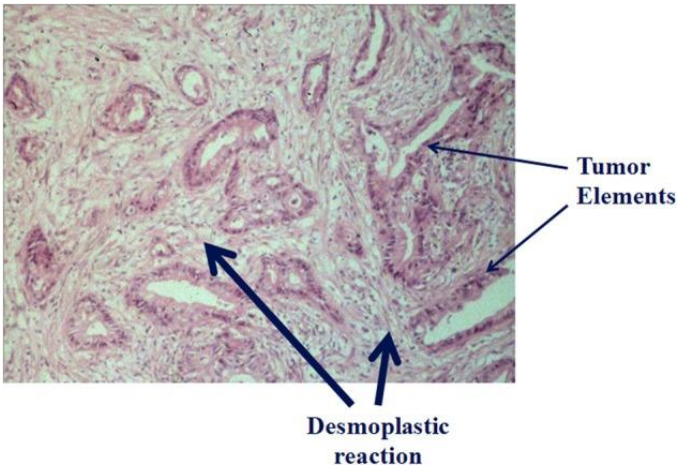

Pancreatic tumour section with H and E stain showing tumour elements embedded in abundant stroma (Wilson, Pirola and Apte 2014).

Pancreatic stellate cells (PSCs) along with pancreatic fibroblasts play a key role in ECM turnover in the healthy pancreas. As well as producing ECM the stromal cells are also a source of matrix degrading enzymes (MMPs) and their inhibitors tissue inhibitors of metalloproteinases (TIMPS) (Jaster 2004). Stromal cells are responsible for the maintenance of normal pancreatic architecture by maintaining a balance in production and degradation of ECM proteins as shown in Figure 1-4. They are also responsible for the fibrosis which plays a major role in the development and progression of chronic pancreatitis and pancreatic cancer.

Figure 1-4. The fine balance of production and degradation of ECM in the pancreatic microenvironment in both healthy and desmoplastic pancreas

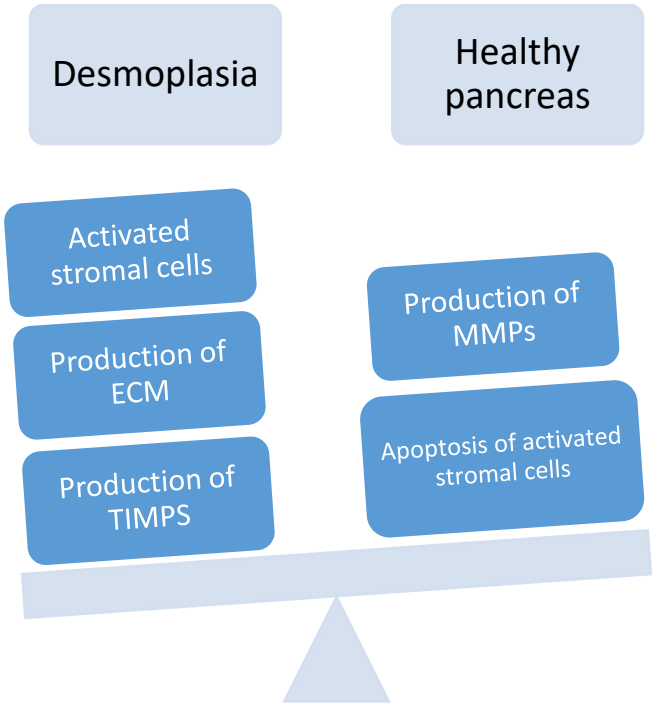

As seen in Figure 1-5, when an injury occurs in the pancreas the stromal cells become activated through inflammation. Once activated, stromal cells produce ECM proteins which provide a scaffold for epithelial cell regeneration. This regeneration resolves the injury. The stromal cells then secrete matrix metalloproteinases (MMPs) which function to degrade the excess ECM. Following this, the activated stromal cells then undergo apoptosis and normal pancreatic histology is resumed.

Figure 1-5. The role of ECM in the recovery from injury in a healthy pancreas (information adapted from (Phillips 2012))

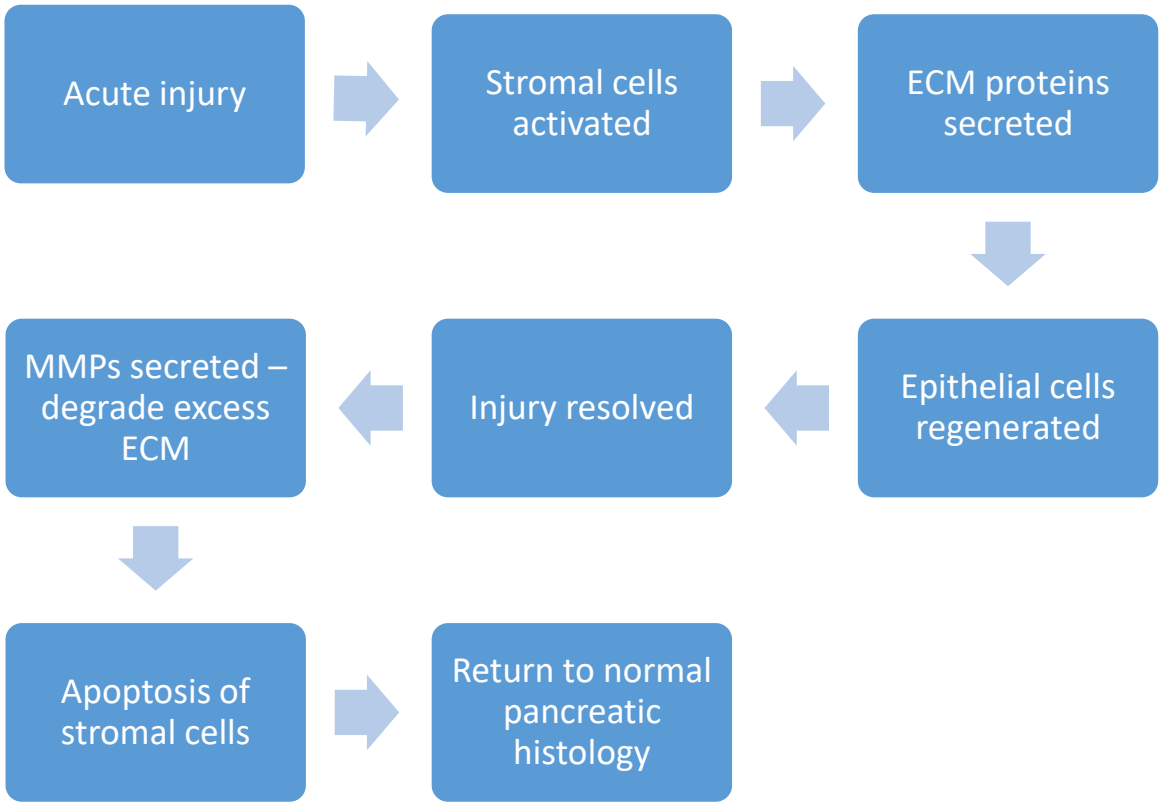

In the pancreatic tumour microenvironment the stromal cells become perpetually activated. As seen in Figure 1-6, when the pancreatic injury is resolved the activated stromal cells continue in the activated state. The stromal cells have the ability to secrete their own cytokines and growth factors maintaining this constant activation. MMPs are not secreted meaning the excess ECM proteins are not degraded and the activated stromal cells do not undergo apoptosis. The stromal cells continue to produce ECM proteins leading to fibrosis as seen in Figure 1-6. This fibrosis contributes to the progression of pancreatic cancer. This role of the tumour microenvironment in the progression of pancreatic cancer is becoming the focus of more and more pancreatic cancer research. This in part is due to the realisation that the stromal cells surrounding tumours play an important role in the progression and metastasis of this cancer.

Figure 1-6. Loss of balance in ECM production by stromal cells leads to fibrosis (information adapted from (Phillips 2012))

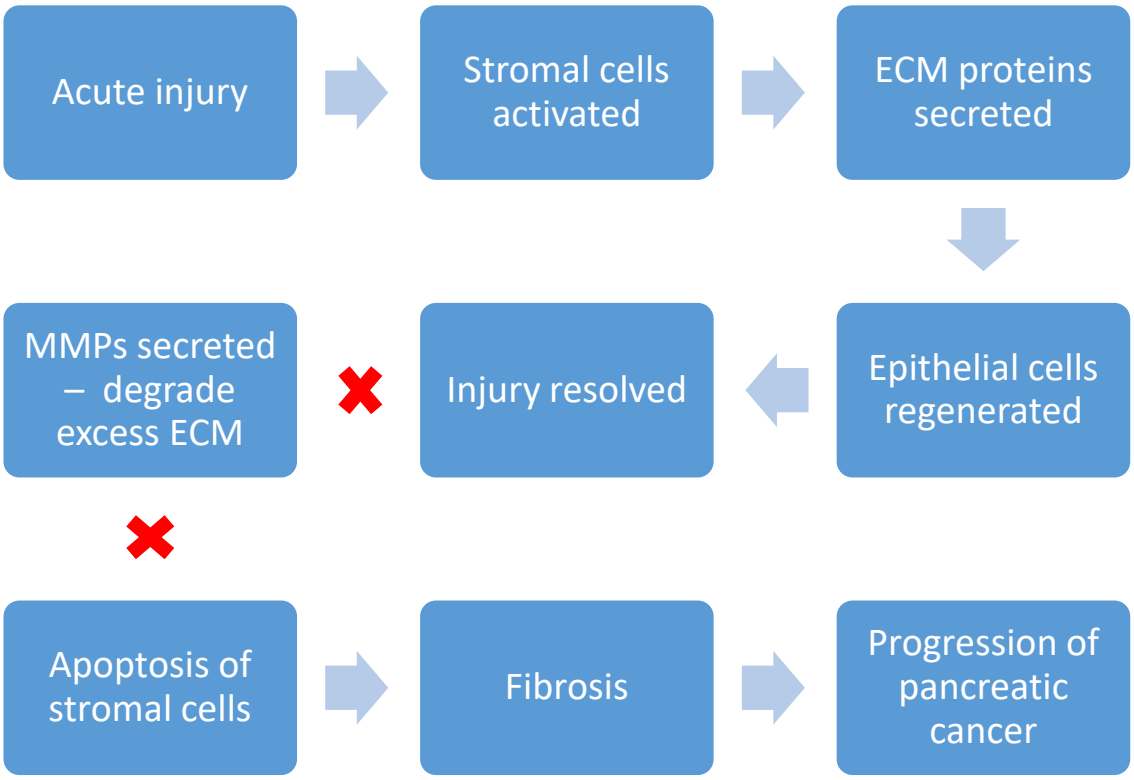

1.4.2. Pancreatic Microenvironment

The pancreatic microenvironment consists of two components. The cellular component contains fibroblasts, stellate cells, immune cells, endothelial cells, nerve cells and epithelial cells. The acellular component is made up of enzymes, growth factors and the extracellular matrix (ECM). The ECM provides structural and biochemical support to the surrounding cells. This means the ECM acts as a physical structure for the acellular component to build around but also has a chemical influence on the cells behaviour by secreting enzymes and growth factors. Proteins such as collagen, fibrinogen, hyaluronan and fibrin make up the pancreatic ECM. In a healthy pancreas, the pancreatic microenvironment is responsible for the fine balance in production and degradation of ECM.

1.4.3. Pancreatic Stromal Cells

As previously mentioned the cellular component of the pancreatic microenvironment contains a range of cell types. Two stromal cell types are the focus of this investigation, patient tumour derived fibroblasts and pancreatic stellate cells. Both cell types are responsible for the balance in production and degradation of ECM. When this balance is lost, ECM builds up and this is due to both pancreatic fibroblasts and stellate cells. This build up, known as fibrosis plays a role in the progression of pancreatic cancer.

Fibroblasts have been called the cockroaches of the human body due to their extreme resilience (Kalluri 2016). They survive severe stress lethal to other cell types. They are the only normal cell type that can be live-cultured from post-mortem and decaying tissue, and they are undoubtedly the most versatile cell type owning to their ease of isolation and culture which has led to fibroblasts being the most extensively studied cell type *in vitro* (Bliss et al. 2012, Kalluri 2016). Fibroblasts are usually quiescent and become activated in a wound healing response. Fibroblasts associated with cancer have several terms including cancer-associated fibroblasts (CAFs), tumour-associated fibroblasts (TAFs), activated fibroblasts, activated myofibroblasts. In terms of this project, fibroblasts are referred to as patient tumour derived fibroblasts. The patient tumour derived fibroblasts were developed in house. Tumour samples, received from St. Vincent's University Hospital, were enzymatically digested using hyaluronidase and collagenase. Following this digestion, the samples were then explanted into culture and outgrowth used to develop fibroblasts.

Pancreatic stellate cells (PSCs) are a relatively new cell type isolated from human pancreas tissue. PSCs are myofibroblast-like cells and comprise approximately 4-7% of the total mass of pancreatic tissue (Apte, Pirola and Wilson 2012). The presence, role and functions of PSCs have come to light over the last 20 years but a large amount is still to be determined. This is principally due to the lack of an isolation method for PSCs which was not developed until 1998 (Bachem et al. 1998). Pancreatic stellate cells are a

part of the exocrine component of the pancreas. They can be found in the periacinar space, the perivascular and periductal regions of the pancreas and show a periacinar distribution i.e. the cells are found in the space surrounding the acinar cells and also surrounding blood vessels and ducts as can be seen in Figure 1-7 (Omary et al. 2007, Jaster 2004).

Figure 1-7. Pancreatic stellate cells in the pancreatic tumour microenvironment

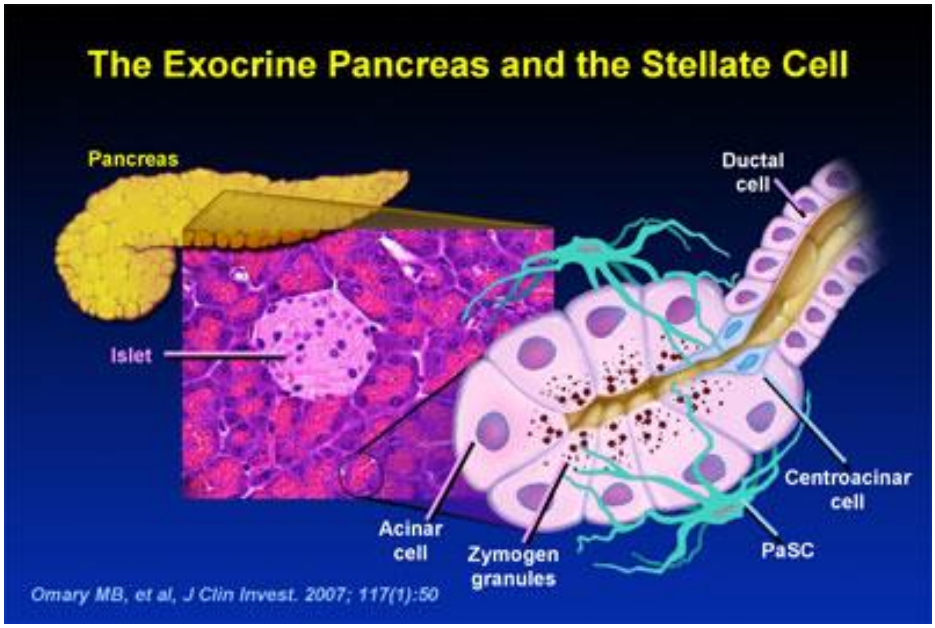

This figure shows the exocrine component of the human pancreas. The quiescent PSCs are located in the periacinar space and encircle the base of the acinus (Omary et al. 2007).

PSCs are so called due to their star like shape *in situ* (*stella* means star in Latin) and also after their liver counter-parts hepatic stellate cells (HSCs) (Apte, Pirola and Wilson 2012). Like HSCs, the major role of PSCs is in fibrosis. In a healthy pancreas, PSCs are in a non-activated state known as quiescent state. Quiescent PSCs have a polygonal shape and contain large numbers of vitamin A droplets in their cytoplasm; the presence of these droplets is a key aspect to distinguish active and non-active PSCs (Apte, Pirola and Wilson 2012). The activated PSC state is recognisable by a change to a myofibroblast-like phenotype, the loss of vitamin A droplets and by the expression of α smooth muscle actin (α-SMA) and ECM proteins such as fibronectin and collagen I and III (Omary et al.

2007). It is in this activated state that PSCs cause pancreatic fibrosis by producing ECM proteins and cytokines. The key step in development of pathogenesis of pancreatic cancer is the disruption of the balance between the quiescent and active PSCs along with the loss of elimination of activated PSCs (Jaster 2004).

1.4.3.1. Fibroblasts vs Stellate cells

Despite similarities at a cell biology level between fibroblasts and stellate cells, functional differences, if any, are yet to be clearly defined at a molecular level. There is a large crossover in terms of function, expression markers and morphology in both healthy and malignant pancreas. The shared expression markers are summarised in Table 1-1. One unshared characteristic, unique to quiescent PSCs is the presence of vitamin A droplets in their cytoplasm which determines there are differences between the two cell types but the extent and functional effects of these differences have yet to be determined. Due to this, this body of work investigated the interactions of pancreatic cancer cells with both tumour derived fibroblasts and PSCs to elucidate if any functional differences were present.

Table 1-1. Expression markers of fibroblasts and stellate cells

Marker	Fibroblasts	Stellate cells	References
αSMA	✓	✓	(Haag et al. 2010, Bachem et al. 1998)
Desmin	✓	✓	(Haag et al. 2010, Bachem et al. 1998, Lardon, Rooman and Bouwens 2002)
FAP	✓		(Haag et al. 2010)
FSP-1	✓		(Haag et al. 2010)
GFAP	✓	✓	(Bachem et al. 1998, Hainfellner et al. 2001, Lardon, Rooman and Bouwens 2002)
Nestin	✓	✓	(Bachem et al. 1998, Lardon, Rooman and Bouwens 2002, Janmaat et al. 2015)
Synemin		✓	(Zhao and Burt 2007)
Vimentin	✓	✓	(Bachem et al. 1998, Lardon, Rooman and Bouwens 2002, Cheng et al. 2016a)

1.4.3.2. Activated vs Quiescent stromal cells

The activation state of stromal cells is an area of research gathering a lot of attention. Whether the stromal cells in the pancreatic tumour microenvironment are activated or quiescent has a major impact on the influence the stromal cells have on the pancreatic cancer cells. There are a wide range of markers published to distinguish between activated and quiescent stromal cells, these include fibroblast-specific protein (FSP1), vimentin, αSMA, fibroblast activation protein (FAP), PDGF receptor-α, (PDGFRα), PDGFRβ, desmin and discoidin domain-containing receptor 2 (DDR2) (Sugimoto et al. 2006, Haag et al. 2010). A small number of quiescent stromal cells are present in the stroma of healthy organs, embedded in the ECM. In tumour stroma, there is an increased number of activated stromal cells expressing activation markers such as αSMA or desmin. These stromal cells deposit increased levels of collagen fibrin and other ECM components compared to quiescent fibroblasts (Kalluri and Zeisberg 2006, Hanahan and Coussens 2012, Marsh, Pietras and McAllister 2013). Research focusing on the role of stromal cells is now including examinations of the activation state of the stromal cell populations. Several such studies have investigated new activation markers including palladin and podoplanin. A 90 kDa isoform of palladin has been shown to be overexpressed in CAFs of several different cancer types including pancreas (Goicoechea et al. 2010). One such study analysed palladin expression during the activation process of fibroblasts and found upregulated expression during activation and that palladin expression is required for αSMA upregulation in CAFs (Brentnall et al. 2012). A related study observed that palladin expression in CAFs enhanced the invasive capabilities of pancreatic cancer cells both *in vitro* and *in vivo* (Goicoechea et al. 2014). A similar study investigated podoplanin, a 17 kDa transmembrane glycoprotein, as an activation marker in CAFs. This study observed that CAFs positive for podoplanin expression enhanced the invasive capabilities of the pancreatic cancer cells compared to CAFs with no podoplanin expression (Shindo et al. 2013). More and more studies are emerging studying the activation status of stromal cells populations but as of yet no distinct marker or characteristic has been established which undoubtedly, uniquely distinguishes cultured activated stromal cells from quiescent stromal cells.

1.5. Metastasis

Metastasis is a process which contributes to the high mortality rate in cancer (Jiang et al. 2015). In fact, without metastasis 90% of cancers would not be fatal (Hu et al. 2016). Metastasis is the ability of a cell to spread to another location in the body not only surviving in this foreign site, also surviving the journey and establishing further growth in this new location (Kozlowski, Kozlowska and Kocki 2015). Gaining a greater understanding of metastasis is required to further understand the progression of both triple negative breast cancer and pancreatic cancer. With this greater understanding comes a greater possibility of developing effective therapies. Metastasis occurs through a cascade of processes, signals and functions. This body of work aims to investigate metastasis through several metastatic characteristics, specifically anoikis, invasion, miRNA and the tumour microenvironment. These metastatic phenotypes are major factors in the success of metastasis. Each of these aspects of metastasis (which are explained in further detail below) are critical steps in the metastatic cascade.

1.5.1. Anoikis

Anoikis is a form of programmed cell death due to detachment of cells from the extra-cellular matrix (ECM), first identified in by Frisch and Francis in 1994 (Frisch and Francis 1994). Usually when a cell detaches from its natural location it dies, this death process is called anoikis, which is a Greek word meaning 'homelessness' (Chiarugi and Giannoni 2008). Anoikis is induced by loss of cell adhesion or inappropriate cell adhesion (Chiarugi and Giannoni 2008). This process is important for the homeostasis of the living organism. Without anoikis, cells could freely travel around the body, attach and grow in foreign locations. Therefore, anoikis prevents detached epithelial cells from surviving and colonizing other locations or attaching to an incorrect ECM (Kim et al. 2012). Standard epithelial cells require adhesion to the ECM through cell surface receptors known as integrins (Kim et al. 2012). Cells may be anoikis resistant i.e. these cells do not require adhesion to the ECM to proliferate or survive (Chiarugi and Giannoni 2008). A small number of cell types have the ability to avoid anoikis, e.g. blood cells are naturally

anoikis resistant. However, in the cancer setting the ability of a cancer cell to resist anoikis is associated with a metastatic phenotype. Metastatic cancer cells lack sensitivity to anoikis unlike normal epithelial cells, meaning the cancer cells have developed the ability of anchorage independence. This ability is important in metastasis; it is a requirement for cancer cells to successfully spread.

Anoikis, in the same way as apoptosis, is initiated by either of two pathways; one being the intrinsic pathway and the second being the extrinsic pathway. Both pathways progress differently but merge at the point of activation of caspases and lead to activation of endonucleases, DNA fragmentation and ultimately cell death (Chiarugi and Giannoni 2008). Both pathways rely on and require a family of proteins known as the Bcl-2 family.

1.5.1.1. The Intrinsic Pathway

The intrinsic pathway as seen in Figure 1-8 is triggered by cellular signals such as DNA damage, endoplasmic reticulum stress (Paoli, Giannoni and Chiarugi 2013). This pathway initiates anoikis through caspase activation which is induced due to perturbation of the mitochondria. This permeabilization of the mitochondria causes activation of caspases. The intrinsic pathway is initiated by BH3-only activator proteins Bid and Bim which become activated following detachment of cells from the ECM (Chiarugi and Giannoni 2008). These activators promote the formation of oligomers of the pro-apoptotic proteins Bax and Bak within the OMM. Together these proteins translocate from the cytosol to the outer mitochondrial membrane where they form oligomers which create channels in the OMM (Kim et al. 2012). These channels or pores result in membrane permeability. This process is known as intrinsic pore forming activity. There is a suggestion that this pore forming activity may not be wholly due to Bax proteins but also due to the interaction of these proteins with mitochondrial channel proteins for example, VDACs (voltage-dependent anion channels) (Taddei et al. 2012). However, work carried out by Baines *et al.* appears to dispute this suggestion (Baines et al. 2007). The disruption of the OMM occurs along with release of cytochrome c leading to the

formation of the apoptosome (Wazir et al. 2015). Smac/DIABLO is also released; it acts to impede the function of inhibitor of apoptosis proteins, IAP and XIAP (Mawji et al. 2007). The apoptosome is composed of caspase-9, the cofactor Apaf (apoptosis protease activating factor) and cytochrome c, this leads to activation of the effector capsase-3 and execution of apoptosis (Wazir et al. 2015). The BH3-only sensitizer proteins also play a role in the intrinsic pathway of anoikis. These proteins compete for the BH3-only binding site on Bcl-2 proteins which inhibits the anti-apoptotic actions of Bcl-2 (Paoli, Giannoni and Chiarugi 2013). This then allows the activator BH3-only proteins to induce Bax-Bak formation as Bim and Bid are no longer being sequestered by the Bcl-2 proteins.

Figure 1-8. Schematic of the intrinsic and extrinsic pathways

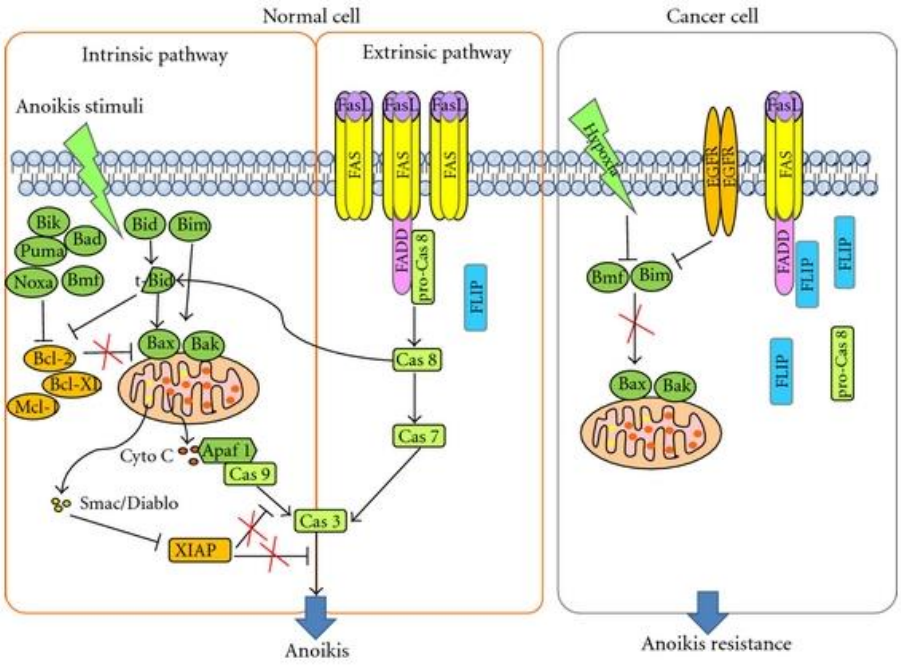

Schematic of the intrinsic and extrinsic pathways that lead to anoikis in a normal cell. Also shown is the process in which neither of these pathways occurs, leading to anoikis resistance in a cancer cell (Kim et al. 2012).

1.5.1.2. The Extrinsic Pathway

The extrinsic pathway triggers cell surface death receptors to activate anoikis. This pathway, shown in Figure 1-8, is initiated by the binding of members of the TNF receptor superfamily e.g. Fas Ligand and TNF-α; to their transmembrane death receptors e.g. Fas and TNF-α receptor (TNFR) (Taddei et al. 2012). This results in the assembly of the Death-Inducing Signalling Complex (DISC). The role of DISC is to recruit adaptor proteins e.g. Fas-associated death domain (FADD); which engages and aggregates molecules of caspase-8 (FLICE), promoting its activation and autoprocessing (Chiarugi and Giannoni 2008). Active caspase-8 is released into the cytoplasm where it proteolytically processes and cleaves caspase-3 and caspase-7 causing their activation (Taddei et al. 2012). This causes more caspase activation and results in substrate proteolysis and cell death. FLIP (FLICE-inhibitory protein) is an inhibitor of caspase-8, many malignant cells overexpress FLIP to avoid anoikis (Kim et al. 2012). Upregulation of FLIP plays a role in developing anoikis resistance, as shown in Figure 1-8.There are two classes of cells that respond to extracellular death cells:

- Type I: activation of caspase-8 is sufficient to cleave effector caspases leading to cell death
- Type II: caspase-8 cannot initiate apoptosis itself. The extrinsic death signals crosstalk with intrinsic pathway.

Both pathways converge on the activation of the effector caspase-3. This initiates a downstream proteolytic cascade which is a central event in programmed cell death. The cleavage of signalling molecules such as focal adhesion-kinase, Cas and paxillin are particularly important for the progression of this cascade (Chiarugi and Giannoni 2008). FAK is one of the key players in integrin-mediated signal transduction leading to anoikis, along with integrin-linked kinase (ILK), Src tyrosine kinase, PI3K, ERK and the adaptor protein Shc. Over expression of FAK or ILK blocks anoikis despite loss of cell anchorage, showing the role of these kinases in anoikis regulation.

1.5.1.3. Bcl-2 Family of Proteins

This family of proteins consists of 3 groups: Anti-apoptotic proteins, Multidomain Pro-apoptotic proteins, and Pro-apoptotic BH3-only proteins.

1.5.1.3.1. Anti-apoptotic proteins

The proteins in this group, which include Bcl-2, Bcl-XL and Mcl-1 (Myeloid Leukaemia Cell Differentiation Protein 1), prevent and inhibit apoptosis. These proteins prevent apoptosis by avoiding outer mitochondrial membrane disruption, pore formation and maintaining membrane integrity (Chiarugi and Giannoni 2008). Anti-apoptotic proteins are structurally related to pro-apoptotic proteins Bax and the BH3-only family (Chiarugi and Giannoni 2008). Inhibition of apoptosis can also be carried out due to sequestering of BH3-only proteins, mainly Bid and Bim therefore preventing formation of an oligomer of Bax and Bak which is essential for anoikis (Chiarugi and Giannoni 2008).

1.5.1.3.2. Multidomain Pro-apoptotic proteins

The role of these proteins is to encourage apoptosis by regulating the intrinsic pathway of anoikis activation. The major members are Bax, Bak and Bok (Tan et al. 2013). Bax and Bak form oligomers resulting in pore channels in the outer mitochondrial membrane (OMM) (Chiarugi and Giannoni 2008). These pores cause permeability of the membrane, which therefore leads to cell death (Taddei et al. 2012). The role Bax and Bak play in anoikis is key. For the successful formation of OMM pores multidomain pro-apoptotic proteins require assistance from the BH3-only proteins (Danial 2007).

1.5.1.3.3. Pro-apoptotic BH3-only proteins

BH3-only proteins initiate the intrinsic pathway to cause cell death. This is the largest group in the family with members including Bid, Bad, Bim, Bik, Bmf, Noxa, Puma and Hrk

(Taddei et al. 2012). These proteins are further subdivided into activators and sensitizers. Bid and Bim are known as activators. Following detachment of the cell from the ECM, Bid and Bim are activated and then cause formation of Bax-Bak oligomers in the OMM (Taddei et al. 2012). This is a key step in the anoikis process. Investigations have shown that siRNA knockdown of Bid inhibits anoikis in several cell types (Gilmore 2005). Bad, Bik, Bmf, Noxa, Puma and Hrk are the sensitizers in the group. These proteins compete for the BH3-only binding site on Bcl-2 proteins thus inactivating Bcl-2's anti-apoptotic actions (Chiarugi and Giannoni 2008). This then allows the activator BH3-only proteins to induce Bax-Bak formation. Sensitizer proteins are unique in that they do not directly regulate anoikis; they sensitize cells to the effects of apoptosis (Paoli, Giannoni and Chiarugi 2013). There is some evidence that in certain cell lines overexpression of Bad does not induce apoptosis but only sensitizes cells to the effects of anoikis (Idogawa et al. 2003).

- Noxa and Puma are transcriptionally regulated by p53 and are shown to be involved in fibroblast anoikis
- Bim and Bad can be controlled by PI3K and ERK pathways. Bid may also be cleaved in the extrinsic pathway. Bim is contained in the dynein complex until it is released due to loss of integrin attachment; Bim then relocates to the mitochondria. Here it interacts with Bcl-XL neutralizing the Bcl-XL pro-survival function (Paoli, Giannoni and Chiarugi 2013).
- Loss of ECM contact leads to an accumulation of Bim as usually integrin engagement means ERK and PI3K phosphorylate Bim and cause proteasome-dependent degradation of Bim. The loss of ECM contact means no integrin engagement and therefore the above degradation does not occur (Paoli, Giannoni and Chiarugi 2013).
- Bmf (Bcl-2 Modifying Factor) plays a role in anoikis due to its interaction with the myosin V motor complex. Bmf is usually sequestered in these complexes but upon detachment from the ECM Bmf is released. Similar to Bim, Bmf counteracts the activity of the anti-apoptotic Bcl-2 protein when cell adhesion is disrupted. Suppression of Bim and Bmf may confer anoikis resistance (Kim et al. 2012).

Expression of these proteins can be decreased with hypoxia which blocks anoikis in mammary epithelial cells (Kim et al. 2012).

1.5.2. Anoikis resistance

Anoikis resistance, a hallmark of cancer progression, is a critical step in tumour metastasis (Kim et al. 2012, Attwell, Roskelley and Dedhar 2000). Cells which have become anoikis resistant can detach from their appropriate ECM, survive and travel through the vascular system to a secondary site where they can reattach and begin to grow a new colony. There are many strategies involved in malignant cells developing anoikis resistance. One such strategy is a change in the pattern of integrin expression. As previously stated integrins play an important role in determining if a cell is going to survive (Kim et al. 2012). Cancer cells have the ability to change the integrin expression on their surface to signal cascades that can enhance cell survival. (Taddei et al. 2012). There is large amount of evidence to support this finding; many different cancer cell types have been shown to have altered integrin expression, with this new expression improving survival while detached (Huang et al. 2016b, Puchsaka, Chaotham and Chanvorachote 2016, Mizejewski 1999). Another process in development of anoikis resistance is inducing cell survival pathways to become constitutively activated e.g. prosurvival pathways induced by PI3K, MEK/ERK and NF-κB (Chiarugi and Giannoni 2008). Hypoxia has been shown to induce anoikis resistance by decreasing expression of pro-apoptotic BH3-only proteins Bim and BMF (Kim et al. 2012). Epithelial-mesenchymal transition (EMT) also plays a role in gaining anoikis resistance (Tiwari et al. 2012). EMT is a fast, reversible change of cell phenotype (Savagner 2010). Through EMT epithelial cells loosen cell-cell adhesion structures, become isolated, motile and anoikis resistant. Cells also acquire several mesenchymal characteristics, hence the name; the process is a transition from epithelial cell type towards mesenchymal (Chunhacha, Sriuranpong and Chanvorachote 2013). Cells undergoing EMT dissolve their adherent and tight junctions resulting in a loss of cell-cell junctions (Tiwari et al. 2012). Cells undergoing EMT lose several proteins involved in adhesion such as E-cadherin, β-catenin, and γ-catenin (Kim et al. 2012). This loss of junctions and proteins involved in adhesion are

important steps in cells detaching from their primary site and becoming anoikis resistant.

Many processes contribute to the development of anoikis resistance but how the extrinsic pathway of anoikis is actually blocked is shown in Figure 1-8. FLIP, a caspase-8 inhibitor, is overexpressed in anoikis resistant cancer cells. FLIP inhibits the extrinsic pathway of anoikis by blocking activation of caspase-8. Anisomycin, an antibiotic, has been shown to sensitize cells to anoikis by decreasing FLIP levels and also inhibited distal tumour formation in a mouse model of prostate cancer (Kim et al. 2012). Figure 1-8 also shows the role of hypoxia by downregulating Bim and Bmf resulting in inhibition of the mitochondrial pathway (Kim et al. 2012). While a large amount is known about the pathways inducing anoikis resistance, the way the pathways especially the intrinsic pathways are actually blocked still needs to be explained. This body of work investigated anoikis resistance in TNBC through microarray analysis, in pancreatic cancer the effects of indirect co-culture and altered miRNA expression on anoikis were examined.

1.5.3. Invasion

A hallmark of both triple negative breast cancer and pancreatic cancer is the level of metastasis present at diagnosis. Both have the ability to metastasise early on soon after the development of the cancer. This metastasis usually occurs before symptoms are present. Less than 20% of pancreatic cancer patients are eligible for surgical resection at time of diagnosis due to the high level of metastasis (Rucki and Zheng 2014). Invasion is a key process in metastasis i.e. the development of cancer at a secondary location. Invasion is the process which transforms a locally growing tumour into a metastatic systemic disease. Invading tumour cells engage the blood and lymph vessels; penetrate through the basement membrane and endothelial walls to then disseminate through the vessel lumen allowing colonisation of distant sites to occur (Friedl and Alexander 2011). Tumours can use different cellular and molecular modes of invasion depending on specific cell-type, autonomous mechanisms and also the surrounding

microenvironment which can induce changes in invasion level or mechanism (Friedl et al. 2012). The process of invasion can occur in several different ways. These include single-cell invasion, multi-cellular streaming and collective invasion, a schematic diagram of these different forms can be seen in Figure 1-9 below.

Figure 1-9. Schematic of different forms of invasion

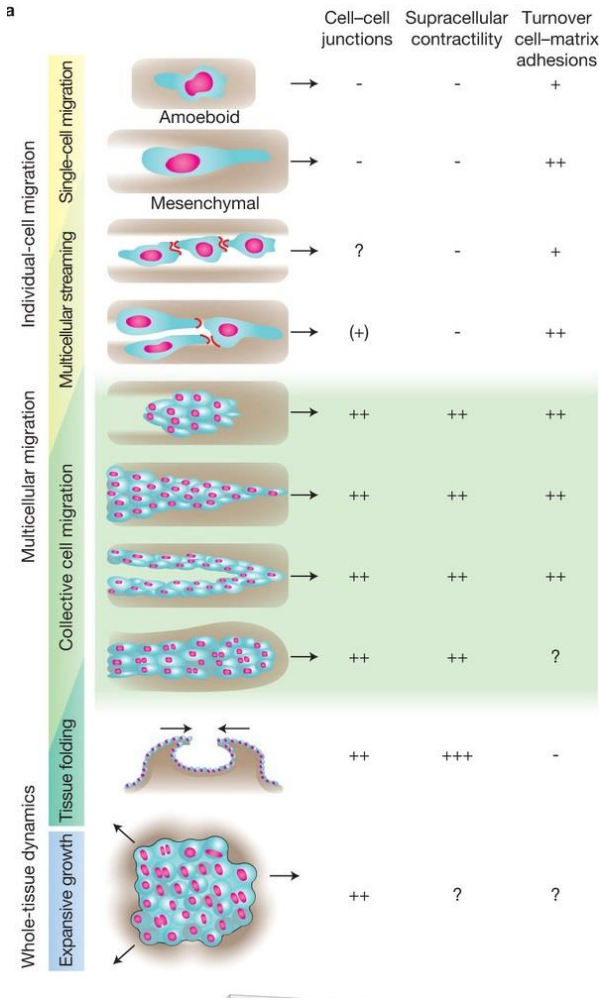

A schematic diagram showing different forms of invasion including amoeboid and mesenchymal single cell invasion, multicellular streaming and collective invasion (Friedl et al. 2012).

1.5.3.1. Single-cell invasion

Individual cells invade singly – shown in Figure 1-10 A. Single cell invasion occurs through a five-step process which changes the cell shape, position & structure (Friedl and Alexander 2011).

- Step 1: Actin polymerisation causes the cytoskeleton to polarise causing a leading protrusion to form.
- Step 2: The leading protrusion engages with the extracellular matrix causing recruitment and adhesion of cell surface receptors. This extracellular adhesion causes intracellular signalling leading to the generation of traction force.
- Step 3: Several micrometres back from the tip of the leading protrusion proteases engage with extracellular scaffold proteins causing proteolysis (Friedl and Alexander 2011). This causes the surrounding tissue properties to change allowing space for the advancing cell body.
- Step 4: Tension is created inside the cell through contraction mediated by actomyosin (Friedl and Alexander 2011).
- Step 5: The adhesion bonds at the trailing edge of the invading cell are gradually turned over causing the trailing edge to slide forward as the leading edge protrudes further

This five-step process can vary depending on which form of single cell invasion is occurring. There are two forms, mesenchymal like and amoeboid invasion. Mesenchymal like invasion is a slow, mesenchymal like process in which cells are spindle shaped, elongated and require high levels of cell-matrix adhesion and proteolysis (Wolf et al. 2007). This form of invasion is dependent on proteases, integrins and stress-fibers (Valastyan and Weinberg 2011). 3D models have shown this invasion to have quite slow velocities of 0.1-2μm/min (Friedl and Wolf 2003). Amoeboid invasion is the faster form that resembles an amoeboid action in which the cells are rounded. The velocities of this action have been shown to be 10-30 times faster than mesenchymal invasion (Friedl and Wolf 2003). Amoeboid invasion requires no proteolytic ECM remodelling with little cell-

matrix adhesion but relies on cortical actomyosin contractility (Geiger and Peeper 2009) (Friedl et al. 2012). This form is independent of proteases, integrins and stress-fibers (Valastyan and Weinberg 2011).

Figure 1-10. Representative images of two different forms of invasion

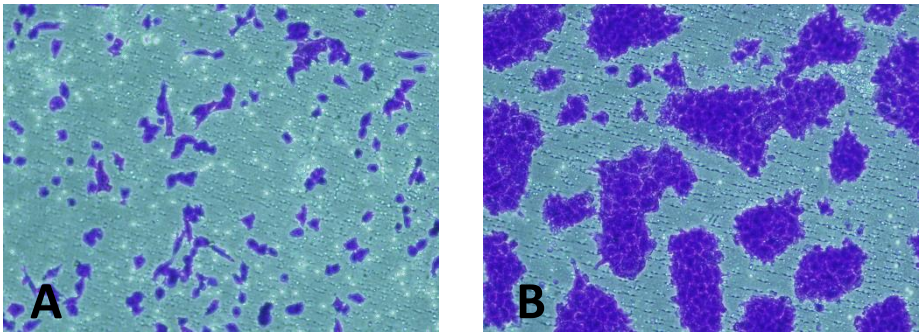

Representative images of two different forms of invasion – (A) Individual invasion and (B) Collective invasion.

1.5.3.2. Multi-cellular streaming

This form of invasion involves cells moving individually but as one, in multi-cellular strands or in small strands of cells (Friedl et al. 2012). The cells move individually as the cytoskeleton of each cell acts independently to generate traction on the ECM while the cells form only weak cell-cell adhesions (Friedl et al. 2012). These strands of cells are directed in their movement through the guidance of external sources such as a chemokine gradient or extracellular tissue structures (Friedl et al. 2012). Due to the transient cell-cell adhesions and the ability of each individual cell to generate traction force which is a key feature of this invasion process, this multi-cellular streaming permits rapid migration (1 µm min^{-1}, or faster) (Friedl et al. 2012).

1.5.3.3. Collective invasion

Collective invasion – shown in Figure 1-10 B, is the form of invasion seen most often in carcinomas. Cells invade as a cohesive, multicellular group maintaining cell-cell adhesions and multi-cellular coordination is also required (Friedl and Alexander 2011). Collective invasion can possess several different morphologies which depend on the cell type, number of cells and the tissue structure being invaded (Friedl and Alexander 2011). These morphologies are:

- Small clusters
- Solid strands
- Cells files
- Presence of a lumen, which can be formed if polarity is retained (Friedl and Gilmour 2009)

The morphology of the collective invasion structure is determined by the specific combinations of cell-cell adhesions, cell-matrix adhesions and proteolysis involved (Friedl et al. 2012). Usually in collective invasion the tip of the strand is formed by several leading cells known as the leading edge. These leader cells generate traction and proteolysis of the surrounding tissue (Khalil and Friedl 2010). This traction force is generated by actomyosin-mediated protrusion and contractility; often cells at the lateral regions join in as a part of this action (Friedl et al. 2012). The energy for this traction is provided by substrate binding integrins. The leading cells express several different integrins to connect to ECM components such as fibronectin, collagen and fibrin-rich surfaces (Alizadeh, Shiri and Farsinejad 2014). The structure of the leading edge can vary, it is determined by several factors including level of proteolysis, protrusion, expansion and the type of tissue encountered (Friedl et al. 2012). Cancer cell models have shown the leading cells in collective cancer invasion to have mesenchymal characteristics as well as actin-rich protrusions (Friedl and Alexander 2011). These protrusions generate adhesive traction for forward movement and matrix proteolysis. This results in a zone of re-aligned, partially proteolysed ECM which guides the group (Wolf et al. 2007). The remainder of the collection reinforce this alignment and increase

the diameter of the invading strand (Friedl et al. 2012). It has been shown in collective cancer invasion that cancer-associated fibroblasts perform a similar function to this (Gaggioli et al. 2007). In collective invasion, the cells inside the group have no direct access to the ECM unlike the cells at the border of the group. These interior cells only have contact with neighbouring cells and intercellular matrix that may be present along cell-cell junctions (Friedl et al. 2012).

1.5.4. Indirect Co-culture

As the significance of the tumour microenvironment has been realised in recent years the role of stromal cells in the progression of pancreatic cancer has become the centre of a great deal of pancreatic cancer research. It has become clear that the interaction between pancreatic tumour cells with the surrounding stromal cells is critical to the progression of pancreatic cancer. Due to the heterogeneity of the stroma an exact understanding of these interactions and how they contribute to the progression of pancreatic cancer is still to be determined. A small number of publications to date have investigated the interaction between the stroma and pancreatic tumour cells, each focusing on different hallmarks of cancer progression. In this current project these interactions were investigated using an indirect co-culture system. The type of interaction studied in this work was based on the hypothesis that soluble factors produced by stromal cells & secreted into the media of the pancreatic cancer cells may stimulate signalling pathways related to metastatic phenotypes. This type of interaction represents the indirect contact between stromal cells & pancreatic cancer cells i.e. soluble factors are investigated without physical contact between the two cell types. Co-culture which investigates the physical contact of different cell populations is known as direct co-culture. The indirect co-culture system used in this work uses co-culture inserts similar to invasion inserts but with a smaller pore. The insert contains a polyester membrane with a pore size of 3.0µm, too small to allow cells to pass through. This membrane allows secretions to pass from the stromal cells into the pancreatic cancer cells without the cells ever being in direct contact (Fujita et al. 2009). As seen in Figure 1-11, the pancreatic cancer cells are seeded in a 6 well plate with a co-culture insert

placed above which contains the stromal cell population. The effects of this co-culture on anoikis, proliferation, colony formation and invasion were examined across a panel of pancreatic cancer cell lines.

Figure 1-11. A schematic of the indirect co-culture model used to investigate the pancreatic tumour microenvironment

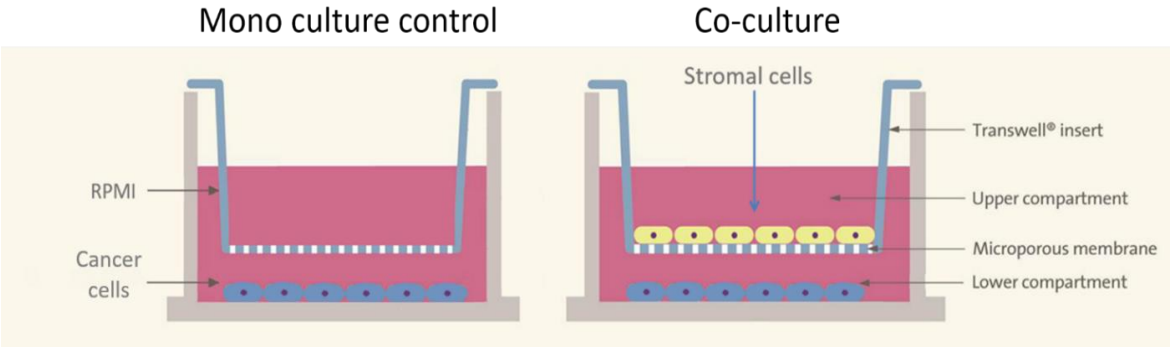

Schematic of the indirect co-culture model set up. Pancreatic cancer cells are seeded in a 6 well plate with the stromal cell population above in a co-culture insert. The insert contains a polyester membrane with a 3.0µm pores which allow secretions to pass between the two cell types (Crosson 2014).

1.5.5. miRNA

MicroRNA (miRNA) are short, naturally occurring non-coding RNA molecules, typically 19-24 nucleotides in length. They play a major role in regulating gene expression at a post-transcriptional level. These small RNA molecules are vital to the appropriate function of the organism and due to this they are highly conserved across a wide range of species. miRNA target messenger RNA (mRNA) of protein-coding genes. it is predicted 30% of protein-coding genes in mammals are regulated by miRNA (Rachagani et al. 2015). miRNA act to downregulate gene expression of target mRNA through one of two actions which both induce gene silencing. The first being degradation of the target mRNA, the second is inhibition of translation of the target mRNA resulting in effective expression inhibition. This repression is a result of the miRNA binding through direct base-pairing interactions to the 3'-untranslated region (3'-UTR) leading to degradation or translational arrest of the target mRNA (Tay et al. 2015). Target degradation occurs when perfect complementarity exists between the miRNA and the mRNA target. This type of repression is very rare in mammals; it occurs most often in plants (Pasquinelli

2012). Usually in mammals incomplete complementarity exists between the miRNA and the mRNA target which leads to inhibition of translation. This incomplete complementarity is due to mismatches present in the miRNA sequence which cause bulges to form when the miRNA and mRNA interact (Hibio et al. 2012). The specificity of a miRNA is determined by nucleotides 2-8 at the 5' end, this is known as the seed region (Bartel 2009). This short sequence is common in the 3'UTR of many mRNA transcripts, it is this which allows miRNA to target multiple mRNAs, in fact each miRNA has the potential to regulate thousands of genes (Lewis, Burge and Bartel 2005). In line with this, the expression of each protein-coding gene may be controlled by multiple miRNA. Through this gene silencing miRNA play a role in virtually all biological functions such as development, growth, differentiation and apoptosis.

1.5.5.1. Biogenesis

The biogenesis of miRNA, explained visually in Figure 1-9, is tightly controlled, both temporally and spatially (Ha and Kim 2014). miRNA begin in the nucleus where it is transcribed by RNA polymerase II, resulting in a long hairpin loop structure known as a primary miRNA (pri-miRNA) (Romero-Cordoba et al. 2014). These pri-miRNA structures have a 5'-cap and a 3'-poly A tail (Hawa et al. 2016). A microprocessor consisting of Drosha and DGCR8 cleave this pri-miRNA into a shorter, ~60-100 nucleotide hairpin structure called a precursor-miRNA (pre-miRNA) (Hawa et al. 2016). Following these steps of processing the pre-miRNA is transported from the nucleus into the cytoplasm for further processing. This transportation occurs through an interaction of the pre-miRNA with the nuclear transport receptor Exportin-5 and the nuclear protein Ran-GTP (Chitkara, Mittal and Mahato 2015). The next step in the process is performed by an RNase III endonuclease protein, Dicer, together with TAR-binding protein (TRBP) which acts as a catalytic partner (Baumann and Winkler 2014). This duo removes the hairpin loop from the transcript, cleaving the pre-miRNA into a short double stranded RNA molecule (Pai et al. 2013). This duplex is then loaded into the RNA-induced silencing complex (RISC). The RISC complex consists of TRBP, Dicer and Argonaute-2 (Ago-2) (Hawa et al. 2016). One of the loaded strands known as the guide strand is destined to

be the mature miRNA, while the other, the passenger strand will be degraded. The passenger strand is cleaved by Ago-2 of the RISC complex leaving the guide strand to function as a mature miRNA i.e. binding an mRNA target to either degrade the transcript or inhibit translation (Romero-Cordoba et al. 2014).

Figure 1-12. miRNA biogenesis and processing

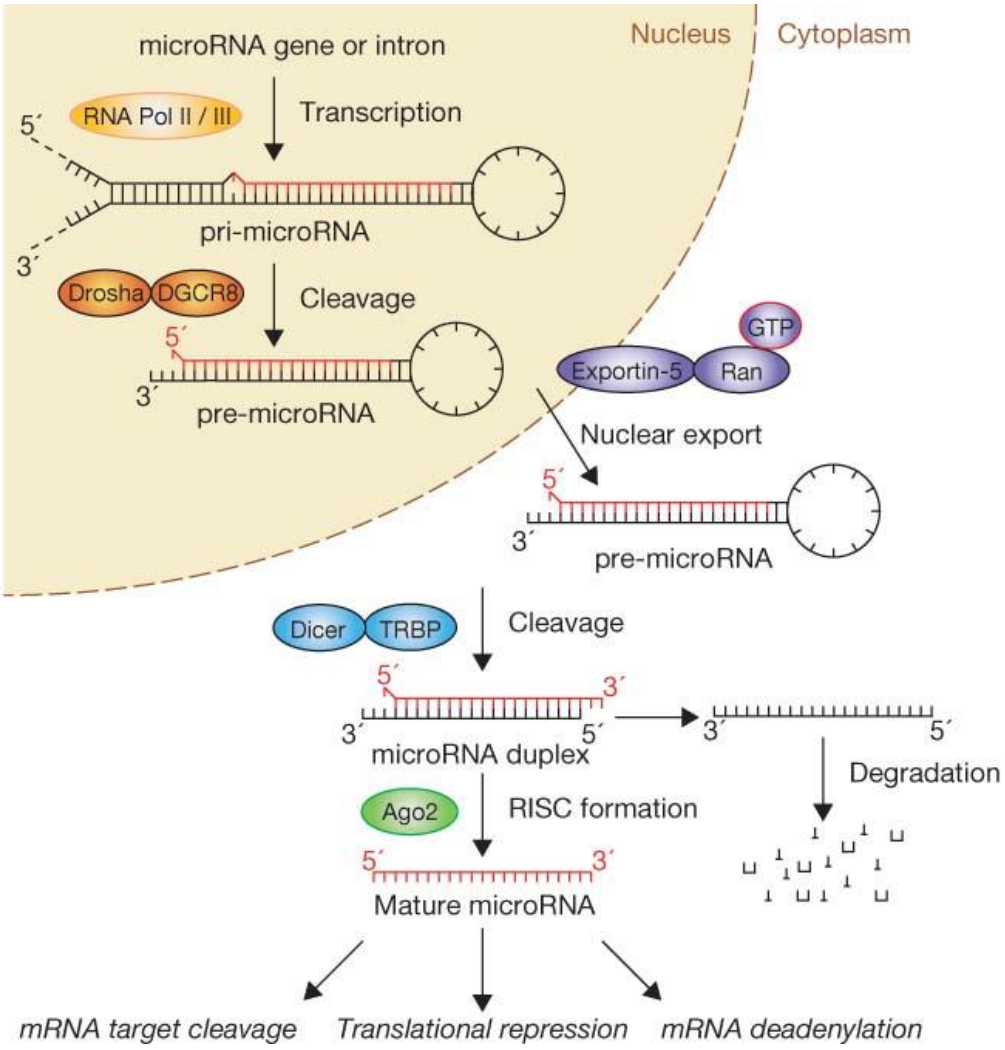

miRNA are transcribed in the nucleus by either RNA Pol II or III producing a pri-miRNA. Drosha and DGCR8 cleave this pri-miRNA into a shorter, ~60-100 nucleotide hairpin structure, a pre-miRNA. The pre-miRNA is transported through Exportin-5 with Ran-GTP. Dicer, together with TAR-binding protein (TRBP) removes the hairpin loop, producing a short double stranded RNA molecule. This duplex is then loaded into the RNA-induced silencing complex (RISC). The RISC complex consists of TRBP, Dicer and Argonaute-2 (Ago-2). The passenger strand is cleaved by Ago-2 of the RISC complex leaving the guide strand to function as a mature miRNA (Winter et al. 2009).

1.5.5.2. Nomenclature

There are several different forms of miRNA names, some of which can be seen in Table 1-2. During the biogenesis of miRNA which has been discussed previously, the immature miRNA is double stranded. The mature miRNA can result from either of these strands. The two strands of miRNA are termed 5p, produced from the 5' strand and 3p, produced from the 3' strand (Ha and Kim 2014). This form of naming is used when it is not possible

to determine which sequence is the predominant one. In some instances, one of the strands is prevalently expressed over the other. In this instance the mature miRNA produced from the less commonly expressed strand is assigned the term * after the miRNA number e.g. miR-21* (Ha and Kim 2014). Another adjustment in naming miRNA include the addition of a letter after the number, e.g. miR-200a, miR-220b. These letters are used to distinguish two miRNA which are almost identical but differ by just one or two nucleotides (Ambros et al. 2003). miRNA names can also include a number preceded by a dash after the miRNA number, e.g. miR-121-1 and miR-121-2, these mature miRNA are identical but originate from different locations in the genome (Lagos-Quintana et al. 2001).

Table 1-2. miRNA nomenclature, different forms of miRNA titles

Nomenclature	Meaning
hsa/mmu/rno – miR-XX	Mature sequence designated miR-XX (hsa – homo sapiens; mmu – mouse; rno – rat)
miR-XX	Refers to miR XX gene
miR-XX-1; miR-XX-2	Refers to mature identical sequences that come from different genes (i.e. distinct hairpin pre-miRNA loci)
miR-XXa/b	Closely related mature sequences (differ at only one or two positions)
miR-XX-5p; miR-XX-3p	From 5'- and 3'-arms (i.e. two different mature miRNA sequences are excised from opposite arms of the same precursor). N.B. This will become the new uniform nomenclature for the next version of miRBase instead of miR*.
miR-XX*	"Passenger" strand of the mature miRNA. Usually thought to be degraded but in some instances also shown to be functional.

1.5.5.3. miRNA in cancer

Due to the range of biological functions regulated by miRNA, miRNA have been shown to be important in regulating many disease states. As such important regulators of gene expression, the involvement of miRNA in cancer has been a topic of a large amount of research over the past decade and it has become apparent that miRNA are key in the development and progression of cancer. miRNA influence many cancers related processes, such as proliferation, cell cycle control, apoptosis, migration and metabolism. In fact, miRNA have been shown to affect all six hallmarks of cancer. The six hallmarks of cancer being:

1. Sustaining proliferative signalling
2. Evading growth suppressors
3. Tissue invasion and metastasis
4. Limitless replicative potential
5. Inducing angiogenesis
6. Evading apoptosis

As a single miRNA can target hundreds of mRNAs, altered expression of a miRNA can have a vast affect. This may cause a range of genes to be silenced therefore allowing miRNA to majorly influence a condition such as cancer. This has been established by the observation of wide dysregulation of miRNA across various cancers. Further evidence of the importance of miRNA in cancer is found in that approximately 50% of the annotated miRNA are found to be in fragile chromosomal sites (sites that are deleted, amplified, translocated) or cancer-associated loci in the genome (Calin et al. 2004).

miRNA in cancer can be considered oncogenic or tumour suppressive in cancer (Baumann and Winkler 2014). Oncogenic miRNA are upregulated and therefore silence, tumour suppressor genes allowing further progress of the cancer. miRNA with upregulated expression in cancer i.e. oncogenes, include miR-21 and miR-155 (Farazi et al. 2011). miRNA targeting oncogenic genes are considered tumour suppressive as they inhibit the translation of an oncogenic target. Tumour suppressor miRNA i.e. miRNA with

downregulated expression in cancer include miR-10b, miR-125b and miR-145 (Farazi et al. 2011). Interestingly however, in the majority of cases miRNA expression is supressed in cancer cells and tissues in comparison to normal cells and tissue, meaning that in the presence of cancer, tumour suppressive miRNA are usually downregulated allowing the oncogene to be translated and expressed (Volinia et al. 2006, Lu et al. 2005). This is unsurprising due to the important roles miRNA play in maintaining homeostasis of the organism. This global downregulation may indicate the miRNA bioprocessing machinery to be inhibited in malignancy formation. Convincing evidence of this has been shown, genetic deletion of the miRNA processing machinery e.g. DICER, resulted in cell transformation and tumourigenesis *in vivo* (Lambertz et al. 2010, Kumar et al. 2009). Downregulated expression of the machinery members Dicer and Drosha has been observed in a wide range of cancer types (Allegra et al. 2014, Guo et al. 2012, Dedes et al. 2011, Torres et al. 2011). This lowered expression has also been associated with advanced stage and poor clinical outcome. Downregulation of miRNA can occur due to several mechanisms such as deletion of the genomic region which encodes the miRNA, genetic mutation, epigenetic silencing or alterations to the miRNA processing machinery. The downregulation of miRNA can be a causative step in the development of cancer, these tumour suppressor miRNA once inhibited allow oncogenes to be expressed and aberrant control of cellular processes to occur.

However, it is important not to classify any specific miRNA as either oncogenic or tumour suppressive as the miRNA may behave differently in different cancer types. The genetic diversity of tumours and cancer cell lines means an upregulated and therefore considered an oncogenic miRNA in one cancer may be downregulated and considered tumour suppressive in another. For example, miR-26a is downregulated in hepatocellular carcinoma and its reintroduction induces apoptosis, in this instance miR-26a plays a tumour suppressive role (Kota et al. 2009). However, miR-26a is overexpressed in gliomas and non-small cell lung cancer, in NSCLC overexpression of miR-26a promotes a metastatic phenotype (Liu et al. 2012, Huse et al. 2009).

As well as investigations into the miRNA bioprocessing machinery in malignant situations, the role of specific miRNA in a range of cancer types has received a large amount of interest and research over the past 15 years since their regulatory function was discovered. Among the first miRNA identified to have a functional role in cancer, were miR-15 and miR-16. Studies have shown the loci for miR-15 and miR-16 are absent in the majority of samples from B cell chronic lymphocytic leukaemia (B-CLL) patients. There is a homozygous loss of the 13q14 region which is associated with the deletion of miR-15 and miR-16, reported in 68% of B-CLL cases (Calin et al. 2002). The target of these miRNA is an anti-apoptotic gene, BCL2. These miRNA act as tumour suppressors to negatively regulate the BCL2 gene therefore their deletion leads to overexpression of this target which results in uninhibited proliferation of the cancer cells (Lin et al. 2014b). Due the large amount of data available regarding the role of miRNA in cancer, Table 1-3 and Table 1-4 below give an insight into the different roles and targets of specific miRNA in different cancers. These tables show the function of miRNA as tumour suppressors and oncogenes.

Table 1-3. List of tumour suppressor miRNAs, their targets and functions in different cancer types (Di Leva, Garofalo and Croce 2014)

miRNA	Tumour/Cell line	Target	Notes
miR-15/16	Chronic lymphocytic leukaemia	BCL2	miR-15 and miR-16 target BCL2, inducing apoptosis in a leukemic cell line model
	Colon cancer	COX-2	miR-16 targets COX-2; elevated levels of HuR antagonize miR-16 function
	Fibroblast	CEBPβ, CDC-25a, CCNE1	Upon cell-cycle re-entry, rapid decay of miR-16 alleviates repression of target genes, allowing proper resumption of the cell cycle
	Fibroblast	VEGF, VEGFR2, FGFR1	miR-16 plays important roles in regulating cell-intrinsic angiogenic activity of endothelial cells
	CAFs	FGF2, FGFR1	Downregulation of miR-15 and miR-16 in cancer-associated fibroblasts promotes tumour growth and progression
	Multiple Myeloma	FGFR1, PI3KCA, MDM4, VEGFα	Deletion of miR-15/16 is observed in early stages of multiple myeloma
	Breast Cancer	WIP1	miR-16 regulates WIP1 phosphatase in the DNA-damage response and mammary tumorigenesis
	Ovarian Cancer	BMI-1	miR-15a and miR-16 target BMI-1, leading to low proliferation and clonal growth
	Lung Cancer	CCND1, CCND2, CCNE1	Overexpression of miR-15/16 induces arrest in G1-G0
	Colon Cancer	SIRT1	miR-34 targets SIRT1, leading to apoptosis only in the context of wild-type p53
	Gastric cancer	BCL2, NOTCH, HMGA2	miR-34 targets BCL2, NOTCH, and HMGA2

miR-34	Fibroblast	MYC	During senescence, miR-34a targets MYC and controls a set of cell-cycle regulators
	Lung Cancer	AXL	miR-34a and miR-199a/b target the AXL receptor; both miRNAs are silenced by promoter methylation
	Ovarian Cancer	MET	miR-34 targets MET
	Colon cancer	SNAIL1	A new link was found between p53, miR-34, and SNAIL1 in the regulation of cancer cell epithelial-to-mesenchymal transition programs
	Lung Cancer	KRAS	The let-7 family negatively regulates let-60/KRAS in *Caenorhabditis elegans* and lung tumours
	Burkitt lymphoma	MYC	Dysregulation of let-7 participates in genesis and maintenance of Burkitt lymphoma and other MYC-dysregulated cancers
	Fibroblast	CDC-34	let-7 represses CDC-34, stabilizesWEE1 kinase, and increases the fraction of cells in G2-M in primary fibroblasts
let-7 family	Breast Cancer	IL-6	Inflammation activates a positive feedback loop that maintains the epigenetic transformed state
	Prostate cancer	E2F2, CCND2	let-7a targets E2F2 and CCND2, acting as a tumour suppressor in prostate cancer
	Liver cancer	BCL-XL	let-7 targets BCL-XL and potentiates sorafenib-induced apoptosis
	Breast Cancer	ZEB1, ZEB2	Downregulation of the miR-200 family may be an important step in tumour progression
	Bladder cancer	ERRFI-1	miR-200 restores EGFR dependency

	Nasopharyngeal carcinoma	ZEB1, CTNNB1	miR-200a inhibits cell growth, migration, and invasion
	Pancreatic cancer	BMI-1	ZEB1 links epithelial-to-mesenchymal transition and stemness maintenance by suppressing the miR-200 family and thereby promotes migration
	Breast Cancer	PLCγ1	miR-200 negatively regulates EGF-driven invasion, viability, and cell-cycle progression
	Breast Cancer	SUZ12	miR-200b–Suz12–cadherin pathway sustains cancer stem cell growth and invasiveness
miR-200 family	Lung Cancer	FLT1, VEGFR1	miR-200 suppresses metastasis by targeting FLT1
	Breast and endometrial cancer	FN1, LEPR, NTRK2, ARHGAP19	miR-200c inhibits cell motility and anoikis resistance
	Ovarian Cancer	p38α	miR200a-dependent stress signature correlates with improved survival and response to treatment

Table 1-4. List of oncogenic miRNAs, their targets and functions in different cancer types (Di Leva, Garofalo and Croce 2014)

miRNA	Tumour/Cell line	Target	Notes
miR-17/92	Colon	TSP-1, CTGF	Upregulated in colonocytes that co-express KRAS, c-Myc, and a non-functional p53
	Prostate cancer, Burkitt lymphoma, testis carcinoma	E2F2, E2F3	Auto-regulatory feedback loop exists between E2F factors and miR-17/92
	Myc-induced lymphoma	BIM, PTEN	Transgenic mice have higher expression of miR-17/92 in lymphocytes
	Lung cancer	HIF1α	Intricate and finely tuned circuit involving c-Myc, miR-17/92, and HIF1α

	Cervix tumour cell line	PTPRO	E2F1 and miR-17/92 control PTPRO
	Myeloid cell	p63	miR-92 increases cell proliferation by repressing p63
	T cell acute lymphoblastic leukaemia	BIM, PTEN, PRKAA1, PPP2R5e	Functional genomics reveals a repression of regulators of PI3K survival signals by miR-19
	Endothelial cell	JAK1	miR-17/92 family provides a therapeutic perspective to enhance therapeutic angiogenesis
	Breast cancer	HBP1	miR-17/92 family inhibits HBP1 and regulates invasion by activating Wnt/β-catenin
	Ras-induced senescent fibroblast	$p21^{WAF1}$	miR-17/92 family disrupts senescence
	Glioblastoma	TGF-BII	miR-17/92 family suppresses TGF-β, stimulating angiogenesis and tumour cell growth
	Prostate cancer	MnSOD, GPX2, TRXR2	miR-17/92 family suppresses tumourigenicity by inhibiting mitochondrial antioxidant enzymes
miR-222/221	Glioblastoma, prostate and thyroid carcinoma	$p27^{Kip1}$	High miR-222/221 maintains low p27Kip1 and stimulates proliferation
	Normal fibroblast	$p57^{Kip2}$	Upregulation initiates S phase with growth factor signalling pathways that stimulate cell proliferation
	Non-small cell lung cancer and hepatocellular carcinoma	PTEN, TIMP3	Target PTEN and TIMP3, induce TRAIL resistance, and enhance cellular migration; MET oncogene activates miR-222/221 through the c-Jun transcription factor
	Breast cancer	FOXO3A	Target FOXO3A to suppress p27Kip1 at a transcriptional level
	Endothelial cell	KIT	miR-222 targets c-Kit, controlling the ability of endothelial cells to form new capillaries

	Breast cancer	ESR1	Modulation of ERαis associated with anti-estrogen therapy
	Glioblastoma	PUMA	Directly regulate apoptosis by targeting PUMA
	Breast cancer	TRSP1	Promote epithelial-to-mesenchymal transition, contributing to the more aggressive clinical behaviour of basal-like breast cancers
	Glioblastoma	PTPμ	Target PTPμ and regulate glioblastoma tumorigenesis
	Breast cancer	DICER	Repress DICER in ERα-negative breast cancers
	Non-small cell lung cancer	APAF1	Activated by EGFR and MET; by targeting APAF1, responsible for gefitinib resistance
miR-21	Cholangiocarcinoma	PTEN	Modulates gemcitabine-induced apoptosis by PTEN-dependent activation of PI3K
	Breast cancer	TPM1	Suppression inhibits tumour growth
		PDCD4	Suppresses PDCD4 to control apoptosis
	Glioblastoma	RECK, TIMP3	Inhibition provides a novel therapeutic approach for physiological modulation of multiple proteins whose expression is deregulated in cancer
		p63, JMY, TOPORS, TP53BP2, DAXX, HNRPK, TGF-βRII	Targets multiple important components of p53, TGF-β, and mitochondrial apoptosis tumour-suppressive pathways
	Prostate cancer	MARKS	Promotes apoptosis resistance, motility, and invasion
	Breast cancer	SOCS1	May serve as a bridge between inflammation and cancer
miR-155	Acute Myeloid Leukaemia	CEBPB, PU.1, CUTL1, PICALM	Contributes to physiological granulocyte/macrophage

			expansion during inflammation and to certain pathological features associated with acute myeloid leukaemia
	Lymphocyte	C-MAF	BIC/miR-155 plays a key role in the homeostasis and function of the immune system
	Diffuse large B cell lymphoma	HGAL	Cell dissemination and aggressiveness are a phenotype of diffuse large B cell lymphoma, typically with high levels of miR-155 expression and no HGAL expression
	Nasopharyngeal carcinoma	JMJD1A	LMP1 and LMP2A activate miR-155 to repress JMJD1A
	Breast cancer	WEE1	Targets WEE1 and enhances mutation rates by decreasing the efficiency of DNA safeguard mechanisms
	Pancreatic cancer	TP53INP1	-
	Breast cancer	FOXO3A	Molecular links between miR-155 and FOXO3A affect cell survival and response to chemotherapy
	Colon cancer	hMSH2, hMSH6, hMLH1	Inactivates mismatch repair

1.5.5.4. miRNA in Pancreatic Cancer

Despite an influx of research in pancreatic cancer in recent years very little progress has been made and the development of new, more effective therapies is needed. One such area which shows promise for these new developments is the area of miRNA in pancreatic cancer. Investigations of miRNA in pancreatic cancer have covered several topics from large studies aiming to profile pancreatic cancer through both cell lines and tumour samples, to studies of miRNA as biomarkers and the therapeutic potential of miRNA.

Many studies have investigated the impact miRNA have on pancreatic cancer, with some miRNA being involved in progression of the disease, some inhibiting its development or treatment, among many other cellular functions. Below in Table 1-5 and Table 1-6 is a summary of a range of findings about the role of miRNA in pancreatic cancer. These tables give a glimpse into what is already known about miRNA in pancreatic cancer. The therapeutic potential of miRNA in pancreatic cancer is vast. Considering the fact that each miRNA can target hundreds of mRNA transcripts, targeting a single miRNA using RNAi can yield dramatic results.

Table 1-5. List of oncogenic i.e. upregulated miRNA in pancreatic cancer

miRNA	Impact	Target	Reference
miR-10a	↑ invasive/metastatic behaviour	HOXA1, HOXB1, HOXB3	(Weiss et al. 2009)
miR-21	↑ proliferation ↑ drug resistance	PTEN	(Song et al. 2013, Wei et al. 2016)
miR-155	↓ apoptosis	TP53INP1	(Seux et al. 2011)
miR-192	↑ cell cycle progression	SIP1 and cell cycle regulatory genes	(Zhao et al. 2013)
miR-208	↑ EMT	E-cadherin	(Liu et al. 2014)
miR-221	↑ EMT	TRPS1	(Sarkar et al. 2013, Su et al. 2013)
miR-424-5p	↑ proliferation and invasion	SOCS6	(Wu et al. 2013)

List of oncogenic i.e. upregulated (red indicates upregulation) miRNA in pancreatic cancer, the impact this expression has on cellular processes and the targets affected.

Table 1-6. List of tumour suppressor i.e. downregulated miRNA in pancreatic cancer

miRNA	Impact	Target	Reference
miR-34a	↑ cell cycle progression and angiogenesis ↓ apoptosis and DNA repair	P53	(Chang et al. 2007)
miR-124	↑ proliferation, invasion and metastasis	RAC1	(Wang et al. 2014)
miR-126, let-7d	↑ proliferation	KRAS	(Jiao et al. 2012)
miR-143	↑ growth, invasive and migration	GEF1, GEF2, KRAS	(Hu et al. 2012)
miR-146a	↑ invasive	EGFR	(Ali et al. 2014)
miR-200 family	↑ EMT	ZEB1	(Lu et al. 2014, Burk et al. 2008)
miR-203	↑ EMT, cell cycle progression ↓ apoptosis	BIRC5 (Survivin), CAV1	(Xu et al. 2013, Miao et al. 2014)

List of tumour suppressor i.e. downregulated (green indicates downregulation) miRNA in pancreatic cancer, the impact this expression has on cellular processes and the targets affected.

1.5.5.5. RNAi

There are several methods to alter miRNA expression in cell culture. These methods can be used to induce over expression of the target miRNA or reduce expression of the target miRNA. The change in expression can be transient, meaning a short-term change or stable, meaning a permanent, long lasting effect. A schematic of the four methods used in this project and summarised below is shown in Figure 1-13.

Figure 1-13. Schematic of RNAi methods used to alter miRNA levels

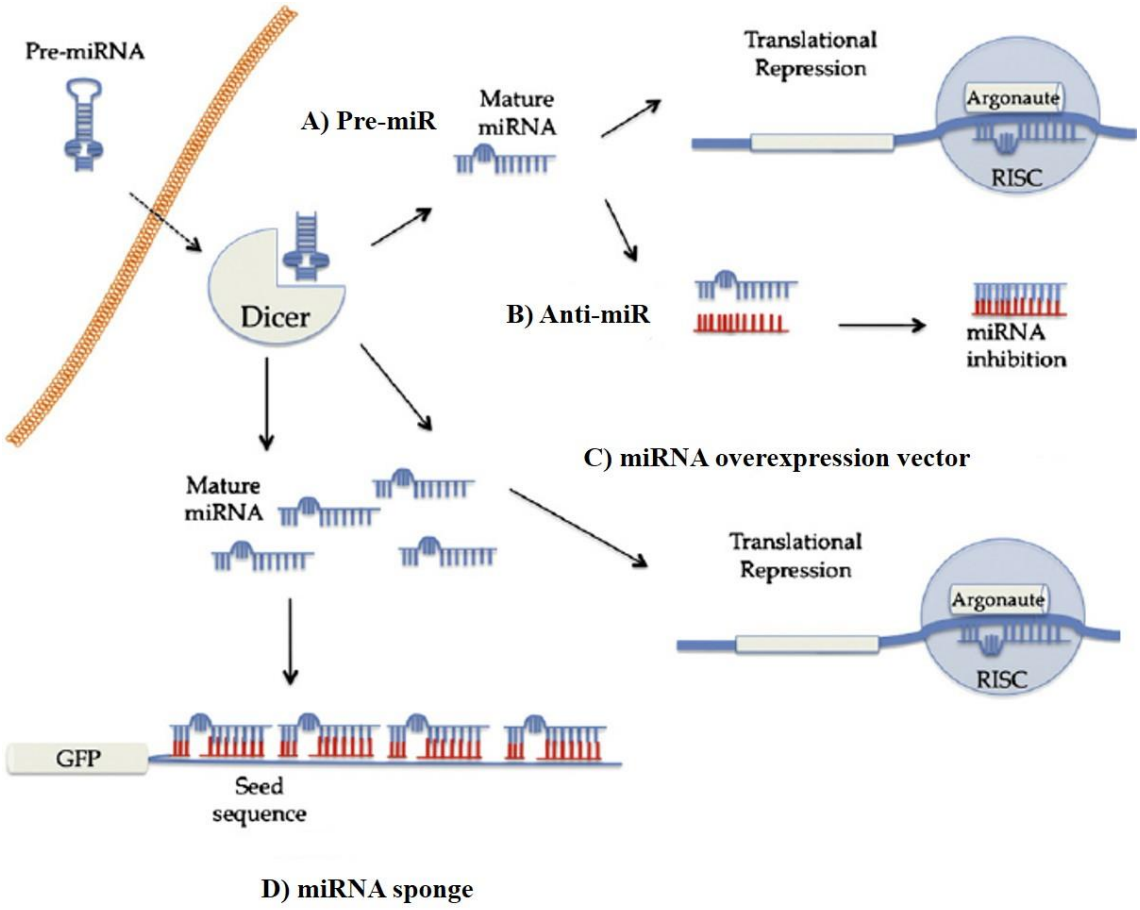

Schematic of RNAi methods used to alter miRNA levels. A) Pre-miR technology induces transient overexpression of the target miRNA and inhibits translation of the target mRNA. B) Anti-miR technology binds the target miRNA, transiently inhibiting its function and allowing translation of the target mRNA. C) miRNA overexpression vectors induce stable overexpression of the target miRNA and translation inhibition of the target mRNA. D) miRNA sponges bind the target miRNA at multiple sites, stably inhibiting its function and allowing translation of the target mRNA (Ruberti, Barbato and Cogoni 2012).

Transient transfections of cells are with either Pre-miRs or Anti-miRs for a target miRNA. These tools are synthetic oligonucleotides, used to alter the level of expression of the chosen miRNA to then allow for assessment of phenotypic changes. These tools do not alter the miRNA expression or stability, rather they intervene by increasing (Pre-miR) or preventing (Anti-miR) the translational repression of the target mRNA by the specific miRNA. Pre-miR or mimic miRNA are used to restore miRNA levels to induce a loss of function (Bader et al. 2011). Pre-miR technology is used to increase the level of the

target miRNA in the cell, i.e. they act in the same way as endogenous miRNA resulting in the translation of the target mRNA being repressed therefore reducing expression, shown in Figure 1-13. However, they are structurally different in that they are double stranded 22 nucleotide duplexes, double stranded duplexes were shown to be 100-1000 fold more effective than single stranded (Martinez et al. 2002). They are structured and act in a similar fashion to siRNA in that the guide stand is loaded into the RISC complex to inhibit translation. Pre-miR molecules have, at the 5' end, a partial complementary motif to the 3'UTR of the target mRNA (Robertson, Amand and Vermeulen). As previously stated mRNA transcripts share common sequences in their 3'UTRs which allows them to be regulated by the same miRNA. Due to this Pre-miRs are designed to be partially complementary to a unique motif in the 3'UTR of the target mRNA this should ensure a gene-specific action (Zhang et al. 2013). Pre-miRs have potential as therapeutic tools in cancer, as previously stated miRNA expression is overall downregulated in cancer (Lu et al. 2005). miRNA downregulated in cancer are considered tumour suppressor miRNA and target oncogenes. The overexpression of oncogenes induced by decreased expression of tumour suppressor miRNA contributes to the development and progression of the cancer. Pre-miRs can be used to restore expression of the tumour suppressor miRNA therefore inhibit the expression of these oncogenes and possibly reduce the cancer progression. A Pre-miR known as MRX34 entered clinical testing in 2013. miR-34a, a tumour suppressor, has little to no expression across a variety of cancers including lung, breast, liver and colon. This miRNA is involved in the p53 and Wnt/β-catenin pathways and restoration of its expression through Pre-miR transient transfection has been shown to inhibit tumour growth and progression (Liu et al. 2011). Unfortunately, as of September 2016, this clinical trial was halted due to immune related adverse effects. Pre-miR technology shows huge promise especially as an insight into the role of specific miRNA in cancer but to translate this technology to the clinic has yet to be achieved.

An anti-miR is an antagonistic oligonucleotide which acts to inhibit the action of endogenous miRNA by intercepting, binding and degrading the target miRNA therefore allowing expression of the target mRNA, allowing for a gain of function (Baumann and

Winkler 2014). These are single stranded antisense-like molecules which bind efficiently to the target miRNA inhibiting their ability to function as translation inhibitors, displayed in Figure 1-13. Anti-miRs are fully complementary to the target miRNA and function by either possessing a higher binding affinity to the target miRNA then the complementary mRNA sequence or are present in greater abundance than the mRNA target (Kasinski and Slack 2012). Anti-miRs are considered a more favourable tool to use than Pre-miRs for several reasons. One being that it is not necessary to find a gene-specific sequence in the 3'UTR as there is when using Pre-miRs as the Anti-miR is designed to be specific to the miRNA of choice (Krützfeldt et al. 2005). Another advantage Anti-miRs have over Pre-miRs is their pharmacokinetic properties. These properties consist of chemical modifications which grant a greater stability to Anti-miRs against degradation and rapid elimination (Pai et al. 2013). Studies have shown that using anti-miR technology it is possible to reduce miRNA level to virtually zero. Since the invention of the technology in 2004, ~90% of publications investigating the effects of miRNA loss of functions studies have used this technology in some form. A disadvantage of Anti-miRs is that while they are miRNA specific they are not gene specific meaning that when the miRNA is inhibited and gene expression increases, the expression of multiple genes may increase. This is due to the fact that one miRNA can target multiple mRNA transcripts so if a phenotype is observed it may be due to the increased expression of multiple protein-coding genes. It is also important to be aware that while Anti-miRs are designed to be specific there may be cross-reactivity amongst families of miRNA, meaning miRNA that have similar sequences. With families of closely sequenced related miRNA non-specific effects may be present. The use of anti-miRs *in vivo* has been attempted such as miR-122 in mouse liver. In this case a relatively high dose (80mg/kg) was required to illicit downregulated expression, this led to it being unsuitable for therapeutic applications (Thakral and Ghoshal 2015).

Another potential therapeutic agent for cancer is a plasmid miRNA vector, which aims to achieve efficient and long-term gene silencing. These vectors overcome some of the disadvantages of transient transfections specifically the short half-life. Plasmid vectors once introduced induce a virtually permanent change in expression as the plasmid stably

integrates into the host genome. This technology has long been used to alter gene expression but in more recent times has been utilised to alter miRNA expression. Once inserted these vectors act to produce the mature target miRNA therefore increasing the levels of endogenous miRNA and inhibiting translation of the target mRNA, seen in Figure 1-13. Post transfection the cells undergo a selection process; this involves exposing the cells to an antibiotic. The resistance gene for the selection marker is included into the plasmid vector therefore successfully transfected cells can survive the antibiotic treatment. This aims to remove untransfected cells from the cell population, thus allowing for a greater examination of functional changes due to the miRNA expression alteration. A reporter gene, such as Green Fluorescent Protein (GFP), can be included in the vector to allow for identification of cells containing the plasmid. The vectors used in this project consist of short hairpin RNA (shRNA) sequences using an RNA Pol II promoter to reduce expression of the target mRNA (Rossi 2008). shRNA, which consists of short inverted repeats linked by small loop sequences are processed into 19-22nt sequences and act in a similar fashion to siRNA to suppress target mRNA expression (Xu et al. 2009). However, using plasmid vectors for miRNA overexpression can lead to the processing machinery, for example, exportin 5 and RISC becoming saturated, then affecting the processing of endogenous miRNA in the cell i.e. potential side effects of inhibiting unrelated endogenous miRNA functions (Yi et al. 2005, Zeng, Wagner and Cullen 2002). The vectors in this project are inducible vectors, meaning that the action of the vector can be controlled to a certain extent. The transcription of the vector is controlled through treatment with an inducement agent. Whether a sponge or overexpression vector, the alteration of the miRNA expression level does not occur until the inducer is added. Doxycycline Hyclate is the inducer for the vectors used. This is an antibiotic which activates transcription of the sponge/overexpression miRNA.

miRNA sponges or decoys are plasmid constructs used to inhibit miRNA function by preventing binding of the miRNA to their mRNA targets. These plasmids are longer DNA structures which contain multiple miRNA binding sites for a specific miRNA (Ebert and Sharp 2010). This miRNA will then be sequestered by the sponge inhibiting it from functioning to silence gene expression, shown in Figure 1-13. This technology was

developed by Sharp's laboratory and published in 2007 in "MicroRNA sponges: competitive inhibitors of small RNAs in mammalian cells" by Ebert *et al.,* A typical sponge construct consists of an RNA Pol II promoter (Pol III is sometimes used) containing a reporter gene and multiple tandem miRNA binding sites in the 3'UTR (Ebert, Neilson and Sharp 2007). The miRNA multiple binding sites, typically four to ten sites, are present in the 3'UTR of the reporter gene. When the mRNA for this reporter gene is transcribed so is the miRNA sponge (Jung et al. 2015). Sponge vectors, in the same way as overexpression vectors, require a selection process to remove untransfected cells from the population. miRNA sponges are not fully complementary for the target miRNA. They contain a mismatch in the seed region, specifically at positions 9-12 which creates a bulge when the sponge is bound to its target. This bulge functions to inhibit cleavage and degradation of the sponge by Argonaute 2 through endonucleolytic cleavage (Ebert, Neilson and Sharp 2007). This cleavage is inhibited as the bulge is positioned at the site normally cleaved by Argonaute 2 (Ebert, Neilson and Sharp 2007). Inhibition of this cleavage impedes quick turnover of the sponge allowing a longer time of inhibition of the target miRNA through sequestering. Sponges are similar to anti-miRs in that they are antisense, base-pair to their target miRNA and that the transcripts are present in a higher abundance than the target mRNA allowing them to bind the majority of the endogenous miRNA. This results in more of the target mRNA being translated into functional protein. miRNA sponges differ from anti-miRs in that they are not fully complementary to the target miRNA. Unlike anti-miRs, miRNA sponges do not cause the target miRNA to be degraded they only sequester the miRNA and inhibit it from binding its target mRNA.

1.6. Aims

The aim of this thesis was to investigate the mechanisms of metastasis in breast cancer and pancreatic cancer utilising a variety of techniques listed below.

1. Investigate the role of anoikis resistance in the metastatic phenotype of TNBC using microarray analysis
    a) Gene expression profiling of two anoikis resistant TNBC cell lines (MDA-MB-231 and MDA-MB-468) and two anoikis sensitive TNBC cell lines (HCC1954 and HS578T).
    b) Identify targets contributing to anoikis resistance
    c) Induce downregulated expression of selected targets
    d) Assess functional changes of this downregulation on metastatic phenotypes

2. Investigate the role of the tumour microenvironment in the metastatic phenotype of pancreatic cancer
    a) Develop a co-culture model to mimic the tumour microenvironment *in vitro*.
    b) Optimise this model to assess a range of metastatic phenotypes including anoikis, invasion, proliferation and colony formation
    c) Assess phenotypic changes in metastatic cellular functions due to co-culture of PDAC cells with human pancreatic stromal cells

3. Investigate the role of altered miRNA expression in the metastatic phenotype of pancreatic cancer
    a) Alter the expression of selected miRNA targets, both transiently and stably.
    b) Compare transient and stable alteration of selected miRNA target
    c) Validate if sponge knockdown technology can successful induce phenotypic changes in pancreatic cancer
    d) Assess the effect of altered miRNA expression on the metastatic phenotypes of pancreatic cancer

2. Materials and Methods

2.1. Cell culture

All cell culture work was carried out in a class II laminar air-flow cabinet (Nuaire). The laminar was turned on and the air flow was allowed to acclimatize for 15 min before use. Both before and after use the laminar air-flow cabinet was cleaned with 70% industrial methylated spirits (IMS). Any items brought into the laminar were also swabbed down with IMS and regular cleaning of gloved hands with IMS was carried out to insure the prevention of contamination. At any time, only one cell line was used in the laminar air-flow cabinet and upon completion of work with any given cell line, the laminar airflow cabinet was allowed to clear for at least 15 minutes before further use. This was to eliminate any possibilities of cross-contamination between the various cell lines. The cabinet was cleaned weekly with Virkon (Antech International, P0550) followed by water and IMS. Each laminar air-flow cabinet was validated by annual inspection by a certified contractor. Details pertaining to the cell lines used in this body of work are provided in Table 2-1. All cells were incubated at 37°C and where required, in an atmosphere of 5% CO_2. Cells were fed with fresh media or sub-cultured (see section 2.1.3) every 2-3 days or as required in order to maintain active cell growth. Cell lines were used within a range of 10 passages from thaw at which point fresh stocks were revived, see section 2.1.6. All the cell lines listed in Table 2-1 are anchorage-dependent cell line

2.1.1. Cell Lines

Table 2-1. Cell lines with culture media details as well as histology information

Cell Line	Culture media	Histology	Source
MDA-MB-231	Leibovitz L-15 media supplemented with 10% FBS Non-CO_2 conditions (Gibco 11415064)	Derived from a pleural effusion of a breast adenocarcinoma	NICB
MDA-MB-468	Leibovitz L-15 media supplemented with 10% FBS Non-CO_2 conditions	Derived from a pleural effusion of a breast adenocarcinoma	NICB
HS578T	DMEM media supplemented with 10% FBS and 2mM L-glutamine (Sigma D5671)	Derived from a carcinoma of the breast.	NICB
HCC1954	RPMI media supplemented with 10% FBS (Sigma R8758)	Derived from a primary stage IIA, grade 3 invasive ductal carcinoma with no lymph node metastases	NICB
DLKP-M	DMEM:F12 media supplemented with 5% FBS (D8437)	Mesenchymal-like subpopulation of DLKP, a non-small cell lung cancer	NICB
AsPc-1	RPMI media supplemented with 10% FBS	Derived from nude mouse xenografts initiated with cells from an ascites site in a patient. Produce abundant mucin.	NICB
BxPc-3	RPMI media supplemented with 10% FBS	Obtained from a patient with cancer of the body of the pancreas. No metastasis had occurred	NICB
Mia PaCa-2	DMEM media supplemented with 10% FBS and 2mM L-glutamine	Developed from a tumour involving the body and tail of the pancreas and had infiltrated the periaortic area	NICB
Panc-1	DMEM media supplemented with 10% FBS and 2mM L-glutamine	Originated from a tumour in the head of the pancreas which invaded the duodenal wall	NICB
Pt-102	RPMI media supplemented with 10% FBS	Fibroblasts derived from a poorly differentiated cholangiocarcinoma diagnosed in a 61-year-old Irish male.	NICB Developed in-house
Pt-127	RPMI media supplemented with 10% FBS	Fibroblasts derived from an invasive, moderately differentiated adenocarcinoma diagnosed in a 72-year-old Irish male.	NICB Developed in-house
hPSC24	RPMI media supplemented with 10% FBS	Pancreatic stellate cells were a kind gift from Dr. Atsushi Masamune in Tohoku University, Japan and were isolated as previously described (Bachem et al. 2005)	Tohoku University, Japan

The patient tumour derived fibroblasts were developed in house by Dr. Sinéad Aherne. Tumour samples, received from St. Vincent's University Hospital, were enzymatically digested using hyaluronidase and collagenase. Following this digestion, the samples were then explanted into culture and outgrowth used to develop fibroblasts. As these fibroblast cell lines were primary cultures, a high level of confluency in culture was always maintained as low cell densities led to a halt in growth. The cells were also used within a range of 10 passages from thaw at which point fresh stocks were revived, see section 2.1.6, to ensure the cells did not become senescent. While both fibroblast primary cell lines were developed in the same way, they have differences. Pt-102 fibroblasts were derived from a Whipple surgery performed on an Irish male diagnosed at 61 years of age. This tumour measured 23mm at the time of surgery and was later characterised as a poorly differentiated cholangiocarcinoma. A cholangiocarcinoma is a cancer of the bile duct, patient 102 was diagnosed with a tumour of the distal common bile duct. This tumour was staged as T3 N1, meaning the cancer had grown into nearby structures such as the gallbladder, duodenum and pancreas, the cancer had also spread to the nearby lymph nodes (N1). There is a strong link between cholangiocarcinoma and pancreatic cancer as both are cancers of the ducts but also several other links. One being that the common bile duct passes through part of the pancreas before joining with the pancreatic duct which empties into the duodenum. Also, both conditions have the peribiliary glands in common, cholangiocarcinoma of the common bile duct arises in these glands and these glands have been shown to be interspersed with pancreatic acini (Terada, Nakanuma and Kakita 1990, Cardinale et al. 2012). Table 2-2 summaries the similarities between cholangiocarcinoma and pancreatic cancer (Schmuck et al. 2016). While pathology analysis of the Pt-102 tumour unexpectantly showed it to be a cholangiocarcinoma, these fibroblasts may still have relevance in the pancreatic cancer microenvironment shown by the strong relationship between pancreatic cancer and cholangiocarcinoma. Pt-127 fibroblasts were derived from a Whipple surgery performed on an Irish male diagnosed at 72 years of age. This tumour measured 48mm at time of surgery and was later characterised as an invasive, moderately differentiated adenocarcinoma. The tumour derived fibroblasts (Pt-102) underwent STR profiling to be used as a reference for future STR profiling to determine if any genetic drift is occurring.

This STR profile is displayed in . The pancreatic cancer cell lines also underwent STR profiling shown in Table 2-4.

Table 2-2. Similarities and differences between cholangiocarcinoma of common bile duct and pancreatic cancer (Schmuck et al. 2016)

	Cholangiocarcinoma	Pancreatic cancer
Development origin	Ventral part of forgut forms main extrahepatic bile ducts	Ventral part of forgut forms main pancreatic duct
Tumourigenesis	Ductal system or periductal glands	Ductal system or periductal glands
Premalignant lesion	Biliary intraepithelial neoplasia (BilIN)	Pancreatic intraepithelial neoplasia (PanIN)
Precursor lesions with malignant potential	Intraductal papillary mucinous neoplasms (IPMN)	Intraductal papillary neoplasm of the biliary tract (IPNB)
Molecular pattern	KRAS+, p53+	KRAS+, p53+
Phenotype	CK20+, MUC1+, S100P+	CK20+, MUC1+, S100P+
Surgery	PPPD/Kausch-Whipple, extended hemihepatectomy for Klatskin tumours	PPPD/Kausch-Whipple
Response to Chemotherapy	5-FU + Gemcitabine + CapOx + Gemcitabine + cisplatin + nab-Paclitaxel	- Gemcitabine + CapOx + Gemcitabine + cisplatin - nab-Paclitaxel

Table 2-3. STR profiling of Pt-102 tumour derived fibroblasts

Marker	Allele 1	Allele 2
AMEL	X	Y
CSF1PO	12	12
D13S317	10	12
D16S539	11	11
D18S51	10	12
D21S11	29	29
D3S1358	15	16
D5S818	11	11
D7S820	9	10
D8S1179	10	14
FGA	22	24
Penta D	9	10
Penta E	7	12
TH01	6	7
TPOX	8	11
vWA	14	18

Table 2-4. STR profiling of the pancreatic cancer cell lines

	Amelogenin	CSF1PO	D13S317	D16S539	D5S818	D7S820	TH01	TPOX	vWA
AsPc-1	✓	✓	✓	✓	✓	✓	✗	✓	✓
BxPc-3	✓	✓	✓	✓	✓	✓	✓	✓	✓
Mia PaCa-2	✓	✓	✓	✓	✓	✓	✓	✓	✓
Panc-1	✓	✓	✓	✓	✓	✓	✓	✓	✓

The STR profiling or DNA fingerprinting of the pancreatic cancer cell lines and the Pt-102 tumour derived fibroblasts was carried out by Source BioScience UK Limited. The method used looked at STR profiling of 16 polymorphic regions. These markers include those as used by the ATCC such as Amelogenin, CSF1PO, D135317 and TH01. Using gene amplification technologies, the genomic DNA was mapped and analysed resulting in the genomic fingerprint of each cell line which was then compared to that provided by the ATCC. All cell lines matched perfectly to the ATCC profile with the exception of the AsPc-1 cell line which had one deviation in the TH01 marker. ATCC states that the AsPc-1 cell line should have one allele of 7 and a second of 9.3 for the TH01 marker but the AsPc-1 cell line used in this body of worked had two alleles of 9.3. As there was only one alteration out of 9 markers and it was not extremely different from the ATCC profile this cell line was deemed suitable to use in the current research project.

2.1.2. Monitoring of sterility of cell culture solutions

Sterility testing was performed on all cell culture media and related culturing solutions. Samples of complete basal media were added to Tryptone Soya Broth and Thioglycollate broth and incubated at 37°C for a period of seven days. This ensured that no bacterial or fungal contamination was present in the media.

2.1.3. Sub-culturing of adherent cell lines

Spent cell culture medium was removed from the tissue culture flask and discarded into a sterile bottle. The flask was then rinsed out with autoclaved/sterile PBS solution in order to remove any residual media. Depending on the size of the flask, 2-5mL of trypsin solution (0.25% (v/v) of trypsin (Gibco, 043-05090) and 0.01% (v/v) of EDTA (Sigma, E9884) solution in PBS) was then added. The flask was incubated at 37°C for the required period of time until all cells were detached from the surface of the culture flask. The trypsin was deactivated with an equal volume of complete media. The cell suspension was removed from the flask and placed into a 30mL sterile universal container and centrifuged at 1000 rpm (Thermo Electron Jouan C3i Multifunction centrifuge) for 5 minutes. The supernatant was discarded from the universal and the pellet was re-suspended in fresh complete media. A cell count was performed using a haemocytometer and an aliquot of cells was then used to re-seed a flask at the required cell density with fresh media. All cell waste or media exposed to cells was autoclaved before disposal.

2.1.4. Assessment of cell number and viability

Prior to cell counts, cells were prepared by sub-culturing as detailed in section 2.1.3 An aliquot of the cell suspension was then added to trypan blue (Gibco, 525) at a ratio of 1:1 (v/v). The mixture was incubated for 2-3 minutes at room temperature. An aliquot (20µL) was then applied to the chamber of a glass coverslip-enclosed haemocytometer. Viable cells exclude the Trypan Blue dye as their membranes remain intact and therefore

remain unstained while non-viable cells stain blue. For each of the four corner grids of the haemocytometer (see Figure 2-1), cells in the 16 squares were counted using an inverted light microscope. The average of the four grids was multiplied by a factor of 10^4 (Volume of the grid) and the relevant dilution factor to determine the average cell number per mL of the cell suspension. Using the data for viable and non-viable cells, percentage viability was calculated.

Figure 2-1. Haemocytometer grid layout

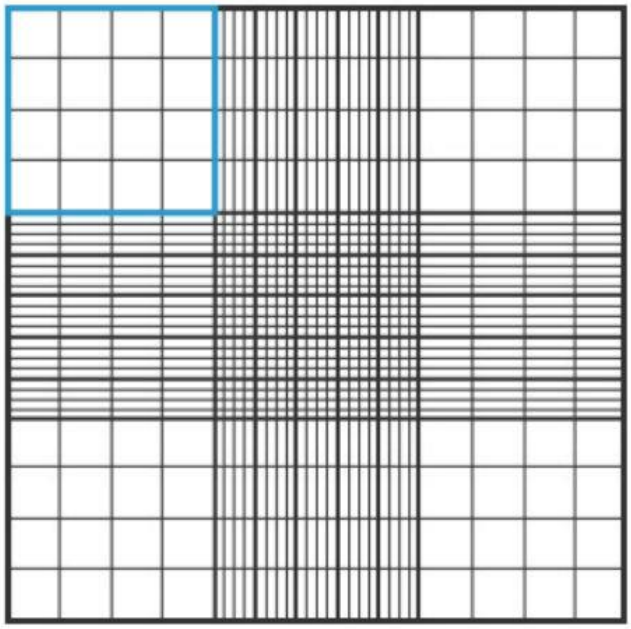

2.1.5. Cryopreservation of cells

Cells for cryopreservation were harvested in the mid-log phase of growth and counted as described in section 2.1.4. Cells were frozen down at a cell density of 1.5-3.0 $x10^6$ cells/mL depending on the cell size (smaller size, higher cell number). Cell pellets were re-suspended in a suitable volume of warm fetal calf serum (FCS) and aliquoted in 500µL volumes into cryovials (Greiner, 122278). A solution of fetal calf serum containing 10% (v/v) DMSO (Sigma D5879) was prepared, filter sterilised and cooled to 4°C. 500µL of

this solution was added in a dropwise fashion to each cell suspension. Cryovials were immediately placed in a -20°C freezer overnight and then transferred to a -80°C freezer for long term storage.

2.1.6. Thawing of cryopreserved cells

A volume of 5mL of fresh warmed growth media was added to a sterile universal. The cryopreserved cells were removed from the -80°C freezer and slightly thawed, rapidly at 37°C. The cells were removed from the vials and transferred to the aliquoted media using a Pasteur pipette. The resulting cell suspension was centrifuged at 1000 rpm for 5 minutes to remove the toxic DMSO. The supernatant was removed and the pellet re-suspended in fresh culture medium. Certain cell lines, e.g. BxPc-3, did not respond well to centrifugation post thaw, for these cell lines this step was skipped. Thawed cells were then added to an appropriately sized tissue culture flask with a suitable volume of growth medium and allowed to attach overnight. The following day, flasks were fed with fresh media to remove any non-viable cells.

2.1.7. *Mycoplasma* analysis of cell lines

Mycoplasma testing was carried out quarterly for all cell lines for possible *Mycoplasma* contamination in house by a technician at the NICB, according to the SOP 007-01 using the in-direct test. All cell lines are found to be *Mycoplasma* free.

2.2. Anoikis Assay Optimisation

The anoikis assay previously used and the method which most often published involves coating tissue culture plates with polyhema (Frisch and Francis 1994). Polyhema (Sigma P3932) is a polymer that forms a hydrogel which inhibits cell attachment, therefore coating plates with polyhema causes the cells to be in suspension. A concentration of 20mg/mL was used and dissolved in 95% ethanol overnight at 50°C (Yu et al. 2013). A volume of 200µL was used to coat a well in a 24 well plate and allowed to dry at room

temperature overnight (Chunhacha, Sriuranpong and Chanvorachote 2013). Once dried a second coating of 200µL was added and allowed to dry. The control used was non-coated wells on a tissue culture plate i.e. the cells attach and grow as a monolayer. When all coatings had dried $1x10^5$ cells were seeded and incubated for 24hr. The metabolic activity was then assessed using a dye, Alamar blue, which measures metabolic activity. The levels of activity between the control (attached) and coated (suspension) wells were then compared allowing the level of anoikis in the suspension wells to be calculated.

Unfortunately, a successful smooth coating was rarely achieved using this method. The coatings appeared cloudy instead of clear and cells were able to attach to them in some instances. Sigma Aldrich, the company which produce the polyhema were first contacted to report the problems incurred. Sigma provided a new protocol which the company uses for quality control (QC) of the polyhema product. This method dissolved the polyhema (120mg/mL) in 95% isopropanol as opposed to the ethanol used in other methods. The QC protocol also dissolved the polyhema at a lower temperature, 37°C overnight, instead of the 50°C previously used. Both of these new conditions were used in the further steps to optimise the assay. Many different conditions were then investigated in an attempt to achieve a clear coating. These conditions included:

- A range of polyhema concentrations (10, 12.5, 20, 120mg/mL)
- A range of drying conditions (in the incubator, laminar, air tight container)
- Varied number/volume of polyhema coatings (1-2 coats, volumes of 200/400uL)

Taking all these conditions into account the most consistent coatings within a reasonable drying time was two coatings of 200µL of polyhema dried in its original packet in the press. 20mg/mL was chosen as the optimal concentration as it achieved a clear coating and the cost and usage of polyhema was taken into account. The plates required 48hr to dry with the second coat being added on the second day. Using these new optimum conditions, smooth coatings were achieved and the anoikis assay was successfully carried through until completion, although a small number of cells (≤5%) still attached to the coating, a problem observed from all coating methods investigated.

Following determination of the optimum coating conditions the reproducibility of the assay was investigated. To determine this, the cell line DLKP-M which was anoikis sensitive was used. This cell line was chosen as it displays a moderate level of anoikis of 50% (Keenan et al. 2012). The next step was to optimise the assay using the two TNBC cell lines, MDA-MB-231 and MDA-MB-468. Minor optimisation had to be completed on the cell number used to ensure that optimal cell confluency at the end of the assay was achieved. Following this optimisation in cell number, replicate anoikis assays were performed and it was determined the assay was not reproducible as there was a large amount of variability present between biological replicates. This optimised assay could not be used due to large variability, therefore a new technique to assess anoikis was required. This led to the purchase of Corning® Costar® Ultra-Low attachment multiwall plates. These plates offered much less variability due to the consistency of the coatings and the results from each cell line showed consistent levels of anoikis. Therefore, going forward these plates were used as opposed to using Polyhema coated plates to induce anoikis.

2.3. Anoikis Assay

For this assay two types of 24 well plates were required. One a regular tissue culture plate which acted as the control as the cells attached and the other a Corning® Costar® Ultra-Low attachment plate (Sigma CLS3473) which induced suspension conditions. The cells were trypsinised and counted according to sections 2.1.3 and 2.1.4. A 1mL volume of cell suspension at a concentration of $1x10^5$ cells/mL was added to each plate (attachment & suspension). The plates were then incubated for 24 hours at the appropriate culture conditions for each cell line. Four hours prior to the end of the assay, 100µL ($1/10^{th}$ volume of media in the well) Alamar Blue (LifeTech DAL1100), an indicator dye was added. Cells in suspension were mixed at this point to break up clumps. At the 24hr time point, the colour development was measured on a Bio-Tec plate reader at 570nm with reference wavelength of 600nm. Before reading the wells

were mixed thoroughly to ensure break up of clumps as these clumps cause variation between wells.

Alamar blue is a cellular health indicator that uses the natural reducing power of living cells to convert resazurin to the fluorescent resorufin (O'Brien et al. 2000). It incorporates a fluorometric/colorimetric growth indicator based on detection of metabolic activity. Alamar blue specifically incorporates a REDOX indictor that both fluoresces and changes colour in response to chemical reduction of the growth medium resulting from cell growth (Lancaster and Fields 1996). The innate metabolic activity of viable, growing cells induces a chemical reduction of the Alamar blue, while a lack of growth i.e. a lack of metabolism, maintains the oxidised environment. The oxidised form of the REDOX indicator is a non-fluorescent, blue, the metabolic change of the Alamar blue induces a reduced, fluorescent, red form (Lancaster and Fields 1996). Using a microtiter plate reader, these absorbance (570 and 600nm) or fluorescent (excitation 530-560nm, emission 590nm) readings are quantitative of the cellular activity of the cells (Rampersad 2012). The amount of fluorescence or absorbance is proportional to the number of living cells and corresponds to the cells metabolic activity (Al-Nasiry et al. 2007). In relation to the above anoikis assay, Alamar blue was used as an indicator of cellular health through metabolic rate. Cells undergoing anoikis displayed a reduced metabolic rate and therefore induced less reduction of the Alamar blue resulting in little to no colour change. This lack of colour change was detected by the microtiter plate reader and expressed as a percentage survival. This survival was calculated using the control sample in attached conditions as a comparison, meaning the control in attached conditions was expressed as 100% survival with everything else relative to this. Therefore, samples which reduced the Alamar blue to a greater or lesser extent than the control were displayed as having a greater or lesser percentage survival.

2.4. Microarray Profiling

All microarray profiling was performed in-house by Dr. Sinéad Aherne.

2.4.1. Microarray GeneChip® Human Gene 1.0 ST Array processing and hybridization

This microarray featured 28,869 well-annotated genes with 764,885 distinct probes. Preparation of cRNA, hybridization, and scanning of microarrays was performed according to the manufacturer's protocol (Affymetrix). In brief, 300ng of total RNA was converted into double-stranded cDNA by reverse transcription. Biotin-labelled cRNA was generated by converting the cDNA sample using the Genechip WT plus reagent kit (Affymetrix). Labelled cRNA was hybridized to the Affymetrix GeneChip® Human Gene 1.0 ST Array while rotating at 60 rpm for 16 hours at 45°C. After hybridization, the microarray was washed using the Affymetrix Fluidics Station according to the manufacturer's protocol. The chips were scanned in an Affymetrix 3000 7G scanner.

2.4.2. Microarray miRNA 3.0 processing and hybridization

The GeneChip® miRNA 3.0 Array was a single array comprised of 179,217 probes that represent 19,913 mature microRNA. The Flash Tag Biotin HSR kit (Affymetrix) was used according to manufacturer's protocol to label the miRNA. In brief, the process started with total RNA containing low molecular weight RNA and the procedure began with a brief tailing reaction followed by ligation of the biotinylated signal molecule to the target RNA sample. The labelled sample was then hybridized to the Affymetrix miRNA GeneChip while rotating at 60 rpm for 16 hours at 48°C. After hybridization, the microarray was washed using the Affymetrix Fluidics Station according to the manufacturer's protocol. The chips were scanned in an Affymetrix 3000 7G scanner.

2.5. Western Blotting

2.5.1. Whole cell extract preparation

Cells were grown to 80-90% confluency, spent cell culture medium was removed from the tissue culture plate/flask and cells were washed twice with PBS in order to remove any residual media. All procedures from this point forward were performed on ice. Cells were lysed in 100-200µL of NP-40 lysis buffer and incubated on ice for 30 minutes with regular agitation, to ensure complete cell lysis of the cell culture monolayer by the lysis buffer. Table 2-5 below provides the details of the NP-40 lysis buffer.

Table 2-5. NP-40 Lysis Buffer Recipe

Component	Volume (µL)
DTT 100mM	10
PMSF 100mM	10
Protease Inhibitors 25x	40
NP-40 Lysis Buffer	940
Total	1000

After incubation on ice, lysates were transferred to a microcentrifuge tube and centrifuged on a bench centrifuge at 14000 rpm for 15 minutes at 4°C. Supernatant containing extracted protein was transferred to a fresh chilled microcentrifuge tube. Protein concentration was quantified using the Biorad assay as detailed in section 2.5.2. Samples were then stored in aliquots at -80°C.

2.5.2. Protein Quantification

Protein levels were determined using the Bio-Rad protein assay kit (Bio-Rad, 500-0006) as follows. A 2mg/mL bovine serum albumin (BSA) solution (Sigma, A9543) was prepared fresh in lysis buffer. A protein standard curve (0, 0.2, 0.4, 0.6, 0.8 and 1.0 mg/mL) was prepared from the BSA stock with dilutions made in lysis buffer. The Bio-Rad reagent was diluted 1:5 in UHP water. A 20µL volume of protein standard dilution or sample

(diluted 1:10) was added to 980µL of diluted dye reagent and the mixture vortexed. After 5 minutes' incubation, absorbance was assessed at 570nm on the BioTek plate reader. The concentration of the protein samples was determined from the plot of the absorbance at 570nm versus concentration of the protein standard.

2.5.3. Immunoblotting

Protein (30µg) was electrophoretically resolved on 4-12% Bolt™ Bis-Tris Plus (Invitrogen NW04120BOX) denaturing polyacrylamine gels. The resolved proteins were then transferred to nitrocellulose membranes (Invitrogen, IB3010-01) using the iBlot® 2 transfer system (Invitrogen, IB21001). Protein transfer was visually confirmed using Ponceau S staining (Sigma, P7170). Membranes were blocked with 2.5% skimmed milk powder in PBS and incubated overnight at 4°C with primary antibodies, listed in Table 2-6. Membranes were washed with 0.1% PBS-tween 3 times for 10 minutes each, both prior to and following incubation with secondary antibodies, listed in Table 2-6. Following the final washing, the membranes were exposed to ECL Prime reagent (GE Healthcare, RPN 2232) in the dark room and the membrane was exposed to autoradiographic film (Kodak,) for various times (from 10 seconds to 30 minutes depending on the signal). The exposed autoradiographic film was developed for 3 minutes in developer (Kodak, LX-24). They were then washed in water and transferred to fixative (Kodak FX-40) for 5 minutes. The film was then washed with water and allowed to dry at room temperature.

Table 2-6. Details of Primary and Secondary antibodies.

Antibody	Dilution	Cat. No.
Purified Mouse Anti-BiP/GRP78	1:1000	BD Biosciences (610978)
Rabbit Anti-Podoplanin/GP36	1:1000	Abcam (ab128994)
Goat Anti-Mouse HRP	1:3000	Bio-Rad (170-6516)
Goat Anti-Rabbit HRP	1:3000	Bio-Rad (170-6516)

2.6. Transfection

2.6.1. siRNA Transfection Optimisation

Before beginning alteration of expression of target genes it was necessary to determine the optimum transfection conditions for both triple negative breast cancer cell lines. GAPDH was chosen as a positive control and as the gene to use for the optimisation process as it is expressed at a relatively constant level in both the TNBC cell lines.

The efficiency of each transfection was determined using q-RT-PCR to assess the expression of GAPDH post transfection using B2M as an endogenous control. The transfection parameters optimised included:

- Transfection direction i.e. forward or reverse transfection
- Cell number
- Transfection reagent
- Concentration of transfection reagent
- siRNA concentration

The optimisation of transfecting MDA-MB-231 and MDA-MB-468 has shown the optimal conditions to result in sufficient gene knockdown while maintaining cell viability to be the following:

- Reverse transfection
- Cell number of 1 x 10^5/mL
- Lipofectamine® 2000 as the transfection reagent
- Lipofectamine® 2000 at a concentration of 1ul per well in a 24 well plate
- siRNA at a concentration of 3nM per well in a 24 well plate

2.6.2. siRNA Transfection Protocol - 24 well plate format

Lipofectamine® 2000 (Invitrogen 11668027) and Opti-MEM® (Gibco 31985062) were brought to room temperature before use. Lipofectmine® 2000 was diluted to the optimum concentration (1µL/well) using Opti-MEM® with a total volume of 50µL per

well in a 24 well plate. This was incubated for 5min at room temperature. siRNA (Ambion) were diluted to the optimum concentration previously determined, using Opti-MEM® with a total volume of 50µL per well. siRNA used are detailed in Table 2-7. This was incubated for 5min at room temperature. Next 50µL of the Lipofectamine® 2000 dilution was mixed with the 50µL of siRNA dilution and incubated for 20min at room temperature. In each transfection, an untransfected control and negative control were included. As an untransfected control 100µL of Opti-MEM® was added to a well in place of siRNA/Lipofectamine® solution. A negative control was also included. This negative control was *Silencer*® Select Negative Control No. 2 (Ambion 4390846) and is an siRNA sequence which does not target any known gene. According to the manufacturer, these negative control siRNA are carefully designed and extensively tested to have no significant sequence similarity to mouse, rat or human. Testing has also shown that these negative controls have minimal effect on global gene expression and no significant effect on cell proliferation, viability or morphology. This negative control was transfected at the same concentration as the target being transfected in order to represent a true negative control. After 20min incubation at room temperature, 100µL of each siRNA/Lipofectamine® solution was added to a well in a 24 well plate. A cell concentration of $1x10^5$/mL was used with 500µL of this cell suspension added on top of the 100µL siRNA/Lipofectamine® 2000 solution or Opti-MEM® control. The cells were then incubated for 48hr.

Table 2-7. Details of Ambion® *Silencer*® Select siRNA used through transfection

siRNA	Ambion® Cat. No.
Silencer® Select GAPDH Positive Control	4390849
Silencer® Select Negative Control No. 2	4390846
Silencer® Select GRP78 siRNA	4392420 – s6979

2.6.3. Pre/Anti-miR Transfection Protocol

Lipofectamine® 2000 and Opti-MEM® were brought to room temperature before use. Lipofectmine® 2000 was diluted to the optimum concentration (3µL/well) using Opti-MEM® with a total volume of 150µL per well in a 6 well plate. This was incubated for 5min at room temperature. Pre/Anti-miR was diluted to the 25nM per well using Opti-MEM® with a total volume of 150µL per well. This was incubated for 5min at room temperature. Pre-miRs and Anti-miRs used are detailed in Table 2-8. Next the 150µL of Lipofectamine® 2000 dilution was mixed with the 150µL of Pre/Anti-miR dilution and incubated for 20min at room temperature. In each transfection, an untransfected control and negative control were included. As an untransfected control 300µL of Opti-MEM® was added to a well in place of Pre/Anti-miR /Lipofectamine® solution. The negative controls were Anti-miR miRNA Inhibitor Negative Control #1 (AM17010) and Pre-miR miRNA Precursor Negative Control #1 (AM17110). According to the manufacturer, the Anti-miR negative control is a random sequence, designed in the same way as Anti-miRs which specifically bind to and inhibit endogenous miRNA, except the negative control has been extensively validated to have no effects on known miRNA function. Similarly, the manufacture states that the Pre-miR negative control is a random sequence, designed in the same way as Pre-miRs which mimic endogenous, mature miRNA, except the negative control has been extensively validated to have no effects on known miRNA function. After 20min incubation at room temperature, 300µL of each Pre/Anti-miR /Lipofectamine® solution was added to a well in a 6 well plate. A cell concentration of $2x10^5$/mL was used with 1.5mL of this cell suspension added on top of the 300µL Pre/Anti-miR/Lipofectamine solution or Opti-MEM® control. The cells were then incubated for 48hr.

Table 2-8. Details of Pre-miR and Anti-miRs used through transfection

miRNA	Ambion® Cat. No.
Pre-miR Negative Control #1	Ambion® (AM17110)
Anti-miR Negative Control #1	Ambion® (AM17010)
Pre-miR-204	Shanghai Gene Pharma (B02003)
Pre-miR-224	Ambion® (PM12571)
Anti-miR-224	Ambion® (AM12571)
Pre-miR-320a	Shanghai Gene Pharma (B02003)
Anti-miR-320a	Shanghai Gene Pharma (B03001)
Anti-miR-378	Shanghai Gene Pharma (B03001)

2.6.4. Plasmid Transfection Protocol

The Mirus TransIT-X2 (Mirus MIR 6000) transfection reagent was used to transfect plasmid DNA. 24hr prior to transfection cells were seeded at a density of $3x10^5$ in 2mL in a 6 well plate. The following day the TranIT-X2 reagent was brought to room temperature. 250µL of Opti-MEM® was mixed with 5µg of plasmid DNA and 7.5µL of TransIT-X2, these conditions were optimised, see section 7.2.3. The solution was mixed gently and incubated at room temperature for 30min. The solution was then added in a dropwise fashion to the cells seeded the previous day. The cells were incubated for 48hr.

2.6.5. Selection of stably transfected cells

48hr post transfection with plasmid DNA the cells were fed with complete media containing the selection agent, Hygromycin B (Roche 10843555001) at a concentration of 400µg/mL. This concentration was optimised, see section 7.2.3.1. Cells were under selection until their growth profile matched that of the parental cell line, at this point they were determined to be resistant and selected.

2.7. RNA Extraction

Total RNA was extracted from cells in the mid-log phase of growth using TRIzol® Reagent (Ambion 15596026) and according to the manufacturer's isolation protocol. Spent cell culture medium was removed from the tissue culture plate/flask and cells were washed twice with PBS in order to remove any residual media. Depending on the culture vessel, 1-3mL of TRIzol® Reagent was added. TRIzol® is a mixture of guanidine thiocyanate and phenol in a monophase solution. It effectively dissolves DNA, RNA and protein on lysis of cell culture samples. The flask was incubated at room temperature for 5min to allow full lysis of the cells. Samples were then mixed well by pipetting and transferred to a microcentrifuge tube. Samples were allowed to stand for 5 min at room temperature to allow complete dissociation of nucleoprotein complexes. Phase separation was achieved with the addition of 200µL of Chloroform (Sigma C2432) to the cell lysate per 1mL of TRIzol® used. Samples were shaken by hand for 15sec and incubated for 2-3 min at room temperature. Samples were centrifuged at 12,000 x g for 15min at 4°C which resulted in phase separation. The three distinct phases were 1) red organic phase containing protein, 2) intermediate phase containing DNA and 3) an upper aqueous colourless phase containing RNA. The aqueous phase (upper-clear layer) was transferred to a fresh microcentrifuge tube and 500µL of isopropanol (Sigma I9516) was added per 1mL of TRIzol® used. This sample was then mixed vigorously by vortexing at high speed for 15 seconds and allowed to stand at room temperature for 10 min. Following this the sample was centrifuged at 12,000 x g for 10 min at 4°C. The supernatant was removed and the pellet (RNA precipitant) washed with 1mL of 75% ethanol per 1mL of TRIzol® used. The samples were vortexed briefly and centrifuged at 7,500 x g for 5min at 4°C. Following this, as much ethanol as possible was removed without disturbing the RNA pellet which was then air dried. The pellet was then suspended in 20µL of nuclease-free water which had been heated to 60°C, this helps to re-suspend the RNA pellet. The extracted RNA was stored at -80°C until required for PCR analysis.

2.8. RNA quantification using the Nanodrop spectrophotometer

RNA samples were quantified using the Nanodrop® ND-1000 spectrophotometer (NanoDrop Technologies). Before applying the RNA sample, the pedestal was wiped down using a lint-free tissue. A volume of 1µL of nuclease-free water was then loaded onto the lower measurement pedestal to initialise the instrument. 1µL of nuclease-free water was used to blank the instrument. RNA was quantified spectrophotometrically at 260nm and 280nm with the ratios of A260/A280 was used to indicate the purity of the RNA A A260/A280 ratio ~2 and an A260/A230 of ~1.8-2.2 is indicative of a pure RNA/DNA sample with an absorbance considerably above or below these values indicating the presence of contaminants such as protein or phenol. The concentration of RNA was calculated by software using the following formula:

OD260nm x Dilution factor x 40 = ng/µL RNA

An optical density of 1 at 260nm is equivalent to 40mg/mL RNA. The range of accurate quantification of RNA is 10ng/µL minimum to 3000ng/µL maximum.

2.9. Reverse Transcription PCR

2.9.1. cDNA synthesis

The High Capacity cDNA Reverse Transcription Kit (Applied Biosystems 4368814) was used to synthesise cDNA from total RNA according to the manufacturers protocol. The RT and No RT master mixes were prepared as described in Table 2-9, No RT samples lacked the Reverse Transcriptase enzyme to act as a control.

Table 2-9. RT and No RT master mixes made using the High Capacity cDNA RT Kit

Master Mix component	x1 (µL)	No RT x1 (µL)
RT Buffer	2	2
dNTP Mix	0.8	0.8
Random Primers	2	2
Reverse Transcriptase	1	-
RNase Inhibitor	1	1
H_2O	3.2	4.2
Total per Reaction	10	10

The maximum RNA allowed in each sample for PCR was 2µg diluted to 10µL in nuclease-free water in a 0.5mL PCR tube. To this 10µL of the appropriate master mix was added. The PCR was performed using the G-Storm thermocycler (Model GS1, Somerton Biotechnology Centre, Somerset, UK) and the conditions listed Table 2-10. Synthesised cDNA was stored at -20°C.

Table 2-10. Conditions used to perform PCR using the G-Storm thermocycler

Parameter	Step 1	Step 2	Step 3	Step 4
Temp (°C)	25	37	85	4
Time	10min	120min	5min	∞

2.9.2. miRNA Reverse Transcription

The Taqman® miRNA Reverse Transcription Kit (Applied Biosystems 4366597) was used to synthesise miRNA from total RNA according to the manufacturer's protocol. The master mix was prepared as stated Table 2-11.

Table 2-11. Master mix used to synthesise miRNA using the Taqman® miRNA RT Kit

Master Mix component	x1 (µL)
100mM dNTPs	0.15
MultiScribe™ RT	1
RT Buffer	1.5
RT Primer	3
RNase Inhibitor	0.19
H_2O	4.16
Total per Reaction	10

10ng of RNA was used in each sample diluted to 5µL with nuclease-free water in a 0.5mL PCR tube. Each reaction has a total volume of 15µL, 10µL of master mix with 5µL of the RNA sample added. The PCR was performed using the G-Storm thermocycler (Model GS1, Somerton Biotechnology Centre, Somerset, UK) and the conditions listed below. Synthesised miRNA was stored at -20°C.

Table 2-12. Conditions used to perform PCR using the G-Storm thermocycler

Parameter	Step 1	Step 2	Step 3	Step 4
Temp. (°C)	16	42	85	4
Time	30min	30min	5min	∞

2.10. Quantitative Reverse Transcription PCR

2.10.1. Gene expression Assays

Taqman® qPCR was used to assess gene expression. Taqman® qPCR involved using individual Taqman® gene expression assays (Applied Biosystems 4453320) for each gene, these assays contain the individual primers and probe for each gene and are listed in Table 2-13. These assays were used with Taqman® Fast Advanced Master Mix (Applied Biosystems 4444556) and MicroAmp® Fast Optical 96 well reaction plates (Applied

Biosystems 4346907). cDNA sample was diluted between 1pg to 100ng per reaction. The cDNA was diluted using nuclease-free water and 1µL was loaded per well with 1µL of Taqman® assay and 10µL of Taqman® Master Mix. The plate was then sealed using MicroAmp® Optical Adhesive Film (Applied Biosystems 4311971) and the cycles listed in Table 2-14 were performed in Applied Biosystems 7900 Real-Time PCR System.

Table 2-13. Details of Taqman Gene Expression assays used

Assay Name	Assay ID
B2M	Hs00984230_m1
GAPDH	Hs03929097_g1
HSPA5 (GRP78)	Hs00607129_gH

Table 2-14. Conditions used to perform qPCR using the Applied Biosystems 7900 Real-Time PCR System

Parameter	Hold	Hold	40 cycles	
Temp. (°C)	50	95	95	60
Time	2min	20sec	1sec	20sec

2.10.2. miRNA expression Assays

Taqman® qPCR was used to assess miRNA expression. Taqman® qPCR involved using individual Taqman® miRNA expression assays (Applied Biosystems 4427975) for each miRNA, these assays contain the individual primers and probe for each miRNA and are listed in Table 2-15. These assays were used with Taqman® Fast Advanced Master Mix and MicroAmp® Fast Optical 96 well reaction plates. 1.33µL of each miRNA cDNA sample loaded per well with 1µL of Taqman® assay, 10µL of Taqman® Master Mix and 7.67µL of nuclease-free water. The plate was then sealed using MicroAmp® Optical Adhesive Film and the cycles listed in Table 2-16 were performed in Applied Biosystems 7900 Real-Time PCR System.

Table 2-15. Details of Taqman miRNA Expression assays used

miRNA Assay	Applied Biosystems Cat. No. 4427975
miR-7a	000386
miR-10a	000387
miR-23b	000400
miR-34a	000426
miR-144	002676
miR-204	000508
miR-206	000510
miR-338	002252
miR-378	002243
miR-409	002331
miR-451	001105
miR-455	001280
miR-497	001043
miR-505	002089

Table 2-16. Conditions used to perform qPCR using the Applied Biosystems 7900 Real-Time PCR System

Parameter	Hold	Hold	40 cycles	
Temp. (°C)	50	95	95	60
Time	2min	20sec	1sec	20sec

2.11. Proliferation Assay

Proliferation was measured using an acid phosphatase assay (Martin Clynes 1991). This colorimetric assay uses *p*-nitrophenyl phosphate to determine the percentage of live cells. $5x10^4$ cells were seeded in a 6 well plate in 2mL of complete medium. Following the incubation period of 7 days, media was removed from the plates. Each well on the plate was washed twice with 1mL PBS. This was then removed and 2mL of freshly prepared phosphatase substrate (10mM p-nitrophenyl phosphate (Sigma 1048) in 0.1M sodium acetate (Sigma, S8625) with 0.1% Triton X (BDH, 30632) at pH 5.5) was added to each well. The plates were then incubated in the dark at 37°C for 2 hours. Colour development was monitored during this time. The enzymatic reaction was stopped by

the addition of 1mL of 1M NaOH. The plate was read in a dual beam plate reader at 405nm with a reference wavelength of 620nm using the Synergy HT plate reader (BioTek, Winooski, Vermont, USA). Proliferation was calculated relative to the control samples, i.e. control samples were calculated as 100% with test samples made relative to this.

2.12. Invasion assay

Invasion assays were carried out in Boyden chambers with a pore size of 8µm (Sigma CLS3463) using the method of Albini (Albini 1998). Matrigel® (Sigma E-1270)) which is a basement membrane matrix diluted to 1 mg/mL in serum-free DMEM medium was defrosted overnight at 4°C. Matrigel® was kept cold at all times. Each transwell insert was coated in 100µL of Matrigel® and incubated over-night at 4 °C. The inserts and the plate were incubated at 37°C for 1 hour prior to use to allow the gel to polymerise. Cells were harvested and re-suspended in complete culture media at a concentration of $1x10^6$ cells/mL. Before use excess un-polymerised Matrigel® was removed and 100µL of complete medium added to each insert. Cell suspensions were prepared in complete basal media. A volume of 100µL of the cell suspension was added into the insert. 500µL of complete media was added to the lower chamber of the insert in the 24-well plate. The invasion assays were incubated for 24-48 hours depending on the cell line, at 37 °C and 5% CO2. After incubation, the media from inside the insert was removed and the non-invading cells were removed by wiping the apical side of the insert with a PBS soaked cotton swab. The insert was dipped in PBS to remove any media from the basolateral side of the insert. The insert was then submerged in 0.25% (w/v) crystal violet dye for 5-10min to stain the invaded cells. Three washes with sterile water were used to remove excess stain. The inserts were allowed to dry. The inserts were viewed and counted under a microscope with a graticule at 40X magnification. The number of cells per field in 14 fields were counted and used to calculate the average number of invading cells per field of view.

2.13. 2D Colony Formation

Cells were seeded at 250-2000 cells/well in 2mL in a 6 well plate. Cells were incubated and allowed to form colonies for ~14 days. Colony formation was visually assessed regularly under the microscope to ensure colonies had not joined together, at this point the assay must be stopped to allow for analysis of individual colonies. At the assay end point, the cells were washed gently with PBS and fixed in cold Methacare (75% v/v methanol, 25% v/v acetic acid) for 15 minutes. Methacare fixative was removed and fixed colonies were washed twice with PBS. The colonies were then stained using 1% Crystal Violet for 30 minutes then washed three times with UHP and allowed to dry. The plates were then scanned and MetaMorph software was used to analyse colony formation.

2.14. 3D Colony formation – Soft Agar Assay

This assay involved a high concentration of agar, dissolved in cell culture media which formed a solid layer. This solid layer was used as a base for a semi-solid, lower concentration layer of agar dissolved in media which contained the cell population. The cells were seeded at a low cell density in the semi-solid layer and could not attach therefore they formed colonies. The agar stock was set up with 1.5g of powder agar added to 50mL of water which was autoclaved to ensure sterility. Agar was heated in a water bath to 55°C along with a small volume of media. The media was heated so as to avoid clumping when the agar is added to the media. If the media was much cooler than the agar a homogenous mixture could not be formed. A 24 well plate format was used. The solid bottom layer of agar was 20% agar- media solution. A total bottom layer volume of 500µL was used; therefore, 100µL of solution agar was added to 400µL of pre-heated media for each well. This 500µL solution was added to a well in a 24 well plate and allowed to solidify. The semi-solid top layer was a 15% agar- media solution. A total top layer volume of 500µL was used. Therefore, 75µL of solution agar was added to 425µL of pre-heated media for each well. This solution was returned to the water bath

to inhibit the agar solution from solidifying. The cells were trypsinised and counted according to sections 2.1.3 and 2.1.4. A cell concentration of $5x10^3$ cells/well was used. The cells were centrifuged at 1000 rpm for 5min, during this 5min the agar solution was removed from the water bath and allowed to cool slightly. If the solution was at 55°C it would kill the cells but the agar would solidify ~35°C, therefore it was important to manage the temperature and the solidifying of the agar. The cell pellet was then re-suspended in 500µL of the agar-media solution and added on top of the solid bottom layer of agar. The assay was then incubated for 14 days with 200µL of fresh media added every 3-4 days to inhibit the agar layer from dehydrating. The colonies were then counted by eye under an inverted light microscope.

2.15. Indirect Co-culture

The indirect co-culture system used in this work uses Corning® Transwell cell culture inserts (Sigma 3452). The insert contains a polyester membrane with a pore size of 3.0µm. As seen in Figure 2-2, the pancreatic cancer cells were seeded in a 6 well plate with a co-culture insert placed above which contains the stromal cell population.

Figure 2-2. A schematic of the indirect co-culture model used to investigate the pancreatic tumour microenvironment

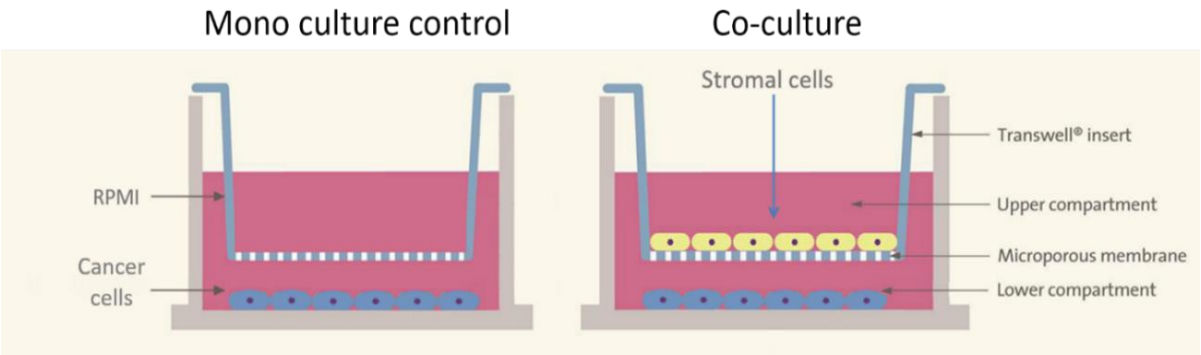

Schematic of the indirect co-culture model set up. Pancreatic cancer cells are seeded in a 6 well plate with the stromal cell population above in a co-culture insert above. The insert contains a polyester membrane with 3.0µm pores which allow secretions to pass between the two cell types (Crosson 2014).

The cells were trypsinised and counted according to sections 2.1.3 and 2.1.4. The pancreatic cancer cells were seeded at a density of $2.5x10^5$ in 2mL in a 6 well plate. The stromal cells were seeded at a density of $1x10^5$ in 2mL in a co-culture inserts. Both cell populations were allowed to attach for 4 hours before the co-culture began. After 4hr the insert was added into the well containing the pancreatic cancer cells. The co-culture was incubated for 48 hours.

2.16. Statistical Analysis

Statistical analysis performed on all experimental data used a two-tailed Student's t-test. A variation of t-tests containing equal and unequal variation were used, which to use was determined by carrying out an F-test on the data. With an F statistic of lower value than the critical F value indicating equal variance and conversely an F statistic of greater value than the critical F value indicating unequal variance. Data with a p-value of ≤ 0.05 was considered significant and the level of significance is shown in the Table 2-17 below.

Table 2-17. Significance and p-value representation

p-value ≤	Indicator	Significance
0.05	*	Lowly significant
0.01	**	Significant
0.001	***	Highly significant

3. Results – Microarray Analysis of Anoikis Resistance in Triple Negative Breast Cancer

3.1. Aim

Identify targets using microarray profiling, which contribute to anoikis resistance in triple negative breast cancer. Anoikis, a form of cell death was investigated due to the role anoikis plays in metastasis. Metastasis is the ability of a cell to spread to another location in the body, colonising this secondary site with tumour growth. TNBC has a higher rate of early metastasis than the other intrinsic breast cancer subtypes which contributes to the poor prognosis of TNBC. Anoikis is an important step in the metastatic cascade as the metastatic cells must be anoikis resistant to survive in suspension while travelling in the blood stream from the primary tumour to the secondary site. It is these three factors; metastasis, TNBC and anoikis which led to the experimental design. Microarray profiling of both anoikis resistant and anoikis sensitive cell lines in suspension and attached conditions, was used with the aim to identify targets which showed differential expression in the anoikis resistant cell lines while in suspension. The hypothesis was that targets upregulated in anoikis resistant cells in suspension may be genes which allow the cells to survive while detached. These targets were then investigated using siRNA knockdown for a change in anoikis resistance. Ultimately, the aim was to identify targets which contribute to anoikis resistance in TNBC.

3.2. Anoikis in metastasis

Anoikis is a form of programmed cell death due to detachment of cells from the extra-cellular matrix (ECM) (Frisch and Francis 1994). Usually when a cell detaches from its natural location it dies, this death process is known as anoikis, (Chiarugi and Giannoni 2008). Anoikis is induced by loss of cell adhesion or inappropriate cell adhesion (Chiarugi and Giannoni 2008). Anoikis prevents detached epithelial cells from surviving and colonizing other locations or attaching to an incorrect ECM (Kim et al. 2012). Cells may be anoikis resistant i.e. these cells do not require adhesion to the ECM to proliferate or survive (Chiarugi and Giannoni 2008). A small number of cell types have the ability to avoid anoikis, e.g. blood cells, metastatic cancer cells. These cells have developed anchorage independence. Metastatic cancer cells lack sensitivity to anoikis unlike healthy epithelial cells, meaning the cancer cells have developed the ability of anchorage

independence. This ability is important in metastasis; it is a requirement for cancer cells to successfully metastasise.

3.3. Microarray Analysis

The aim of this study was to investigate anoikis resistance in triple negative breast cancer (TNBC). Microarray analysis was used to evaluate differential expression in both anoikis sensitive and anoikis resistant triple negative breast cancer cells. Gene and miRNA expression profiling was performed on two anoikis resistant TNBC cell lines (MDA-MB-231 and MDA-MB-468) and two anoikis sensitive TNBC cell lines (HCC1954 and HS578T). The anoikis status of each cell line is shown in Figure 3-1. The TNBC subtypes of these cell lines using the classifications described in section 1.3.3 are as follows, HCC1954 is classified as basal which may be non-triple negative while the other three cell lines are identified as the mesenchymal subtype (Lehmann and Pietenpol 2014). This microarray profiling was performed in-house by a microarray technician, prior to the beginning of this Ph.D. project. The profiling was performed on the four cell lines in two different conditions:

- Cells in normal monolayer cell culture conditions i.e. attached
- Cells exposed to anoikis conditions i.e. in suspension

Anoikis was induced by exposing the cells to polyhema which induces suspension, for 4hr prior to microarray analysis. This time point for analysis was chosen as viability of the cells reduces over time while in anoikis conditions. However, this time point was not ideal for assessing expression changes due to attachment, as complete attachment can take longer than 4hr; also, significant changes in mRNA expression can be difficult to detect after 4hr. The experiment involved microarray profiling of all four TNBC cell lines (MDA-MB-231, MDA-MB-468, HS578T and HCC1954) in two conditions, anoikis conditions i.e. suspension and attached culture conditions.

Figure 3-1. Percentage anoikis across the range of TNBC cell lines

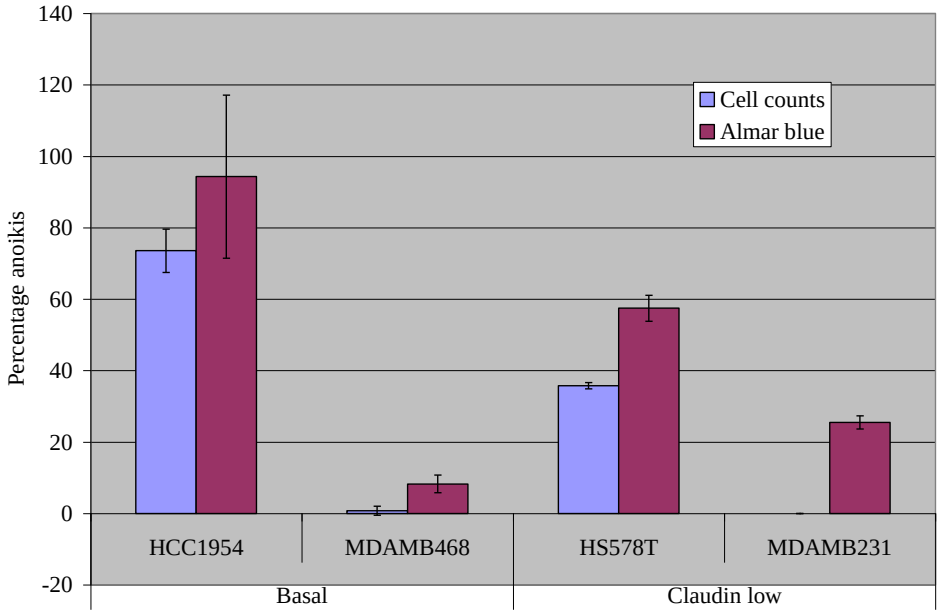

Characterisation of the anoikis status of a panel of TNBC cell lines at a 24hr timepoint, HCC1954, MDA-MB-468, HS578T and MDA-MB-231. Anoikis was assessed using an older Polyhema coating method (Keenan et al. 2012) *(this graph is a personal communication from Dr. Joanne Keenan, NICB)*.

3.4. Interrogation of microarray data

The analysis compared each of the four cell lines, both anoikis resistant and anoikis sensitive, in both attached conditions and suspension conditions. Analysis of the microarray data was carried out by an in-house Bioinformatician, Dr. Stephen Madden. The gene and miRNA expression profiles were used as the basis for further experimental analysis. This analysis identified genes and miRNA which showed differential expression in both the anoikis resistant cells lines in suspension compared to attached and showed no differential expression in the anoikis sensitive cell lines in suspension compared to attached. In simplistic terms the anoikis sensitive cell lines were used as a minus. In more detail the gene and miRNA expression profiles of the MDA-MB-231 cell line were analysed in the following way; the genes and miRNA expressed by the MDA-MB-231 cell line grown attached were compared to the genes and miRNA expressed when the MDA-MB-231 cell line was exposed to suspension conditions. The same analysis was

performed on the MDA-MB-468, HS578T and HCC1954 cell lines. This analysis focused on the genes and miRNA that were differentially expressed in both anoikis resistant cell lines in the same direction (upregulated/downregulated) when in suspension compared to attached and did not show differential expression in either anoikis sensitive cell line in suspension compared to attached. The aim was to identify a gene/miRNA which contributed to the ability of the anoikis resistant cells to survive in suspension. This profiling identified 26 significantly differentially expressed genes in the anoikis resistant cell lines when in suspension compared to attached and not differentially expressed in the anoikis sensitive cell lines, with significance being considered as an adjusted p value <0.05. These 26 genes and their fold changes can be seen in Table 3-1. No miRNA were identified as significantly differentially expressed.

Table 3-1. Differential expression of anoikis resistant cell lines

Gene	Log2 FC MDA-MB-231	Log2 FC MDA-MB-468	Gene	Log2 FC MDA-MB-231	Log2 FC MDA-MB-468
AHDC1	0.523	0.891	MAK	0.743	0.532
ALDH1A3	0.784	0.686	MEF2A	1.158	0.471
CRISPLD2	1.167	1.321	NPAS2	0.483	1.263
DNAH5	0.681	1.085	PXK	0.933	1.639
DUSP1	-1.489	-1.448	RAPH1	-0.598	-0.814
EDC3	0.565	0.791	RTP4	0.671	0.988
FOS	-1.673	-1.816	SECTM1	0.825	0.680
FZD7	0.700	0.852	SEMA3C	-0.598	-0.581
GADD45B	-0.673	-0.668	SGMS2	0.760	1.002
GNAO1	0.765	0.640	SLC25A45	0.555	0.785
GPR39	-0.782	-0.668	SLC7A5	1.155	0.783
HERPUD1	1.218	0.637	TNFRSF11A	1.023	0.776
HSPA5 (GRP78)	0.430	0.775	ZMIZ1	0.850	0.590

The log2 fold changes of the 26 significantly differentially expressed genes in the anoikis resistant cell lines, red indicates increased expression in suspension compared to attached while green indicates decreased expression in suspension compared to attached.

3.4.1. Literature Mining

The microarray profiling analysis identified 6 genes to be downregulated while the other 20 genes were upregulated in both anoikis resistant cell lines in suspension compared to attached conditions, with these targets showing no differential expression in the anoikis sensitive cells in suspension compared to attached conditions. Literature mining, utilising PubMed and Pathway Studios analysis software was performed on this list of 26 significantly differentially expressed genes. Pathway studios uses published scientific data to analyse a vast range of cellular characteristics including pathways, disease, functions etc., that are shared among the list of targets. A focus was placed on the targets that were found to be upregulated, as functional validation utilising siRNA knockdown was of interest. Figure 3-2 displays the diseases common among the list of targets from the profiling data, meaning the diseases that more than one target has been published as playing a role in. This figure also displays the effect the specific target has in that disease, either positive or negative, indicated by green or red respectively. For example, FZD7, a receptor, is displayed as having a positive effect (green) on metastasis. This data also indicates the protein classification of each target, for example SEMA3C is a ligand and is represented by a diamond shape. displays the cellular processes common among the list of targets from the profiling data, meaning the cellular processes that more than one target has been published as playing a role in. This figure also indicates the effect each target has on the specific cellular process, either positive or negative as described previously. For example, DUSP1, a protein phosphatase, is displayed as having a negative effect on cell migration meaning expression of DUSP1 inhibits cell migration. Using these tools and figures along with the p values and log2 fold change values from the microarray data analysis, a target gene was chosen.

Figure 3-2. Pathway Studios analysis of common priority diseases by effect

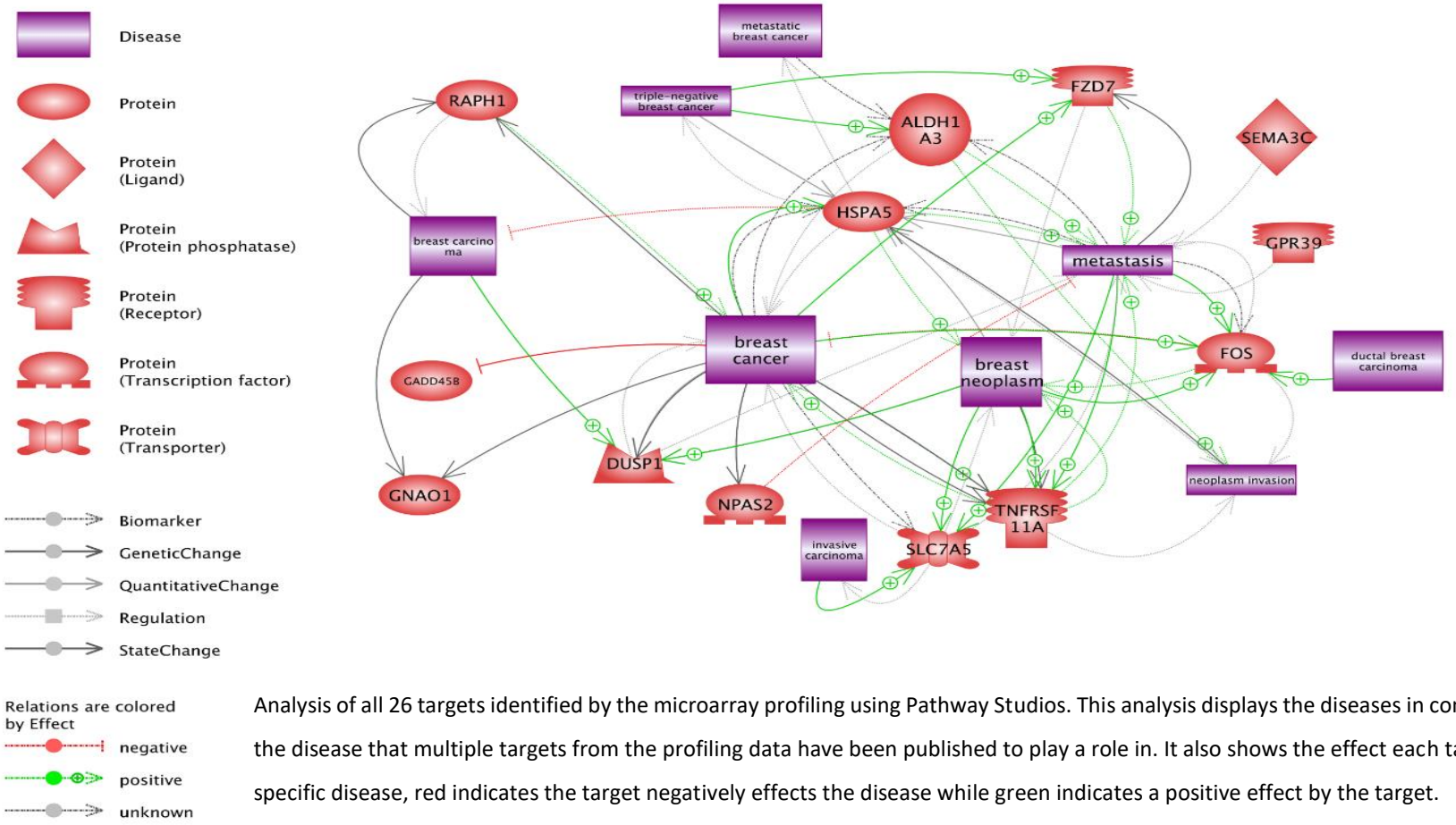

Analysis of all 26 targets identified by the microarray profiling using Pathway Studios. This analysis displays the diseases in common, meaning the disease that multiple targets from the profiling data have been published to play a role in. It also shows the effect each target has in that specific disease, red indicates the target negatively effects the disease while green indicates a positive effect by the target.

Figure 3-3. Pathway Studios analysis of common cellular processes

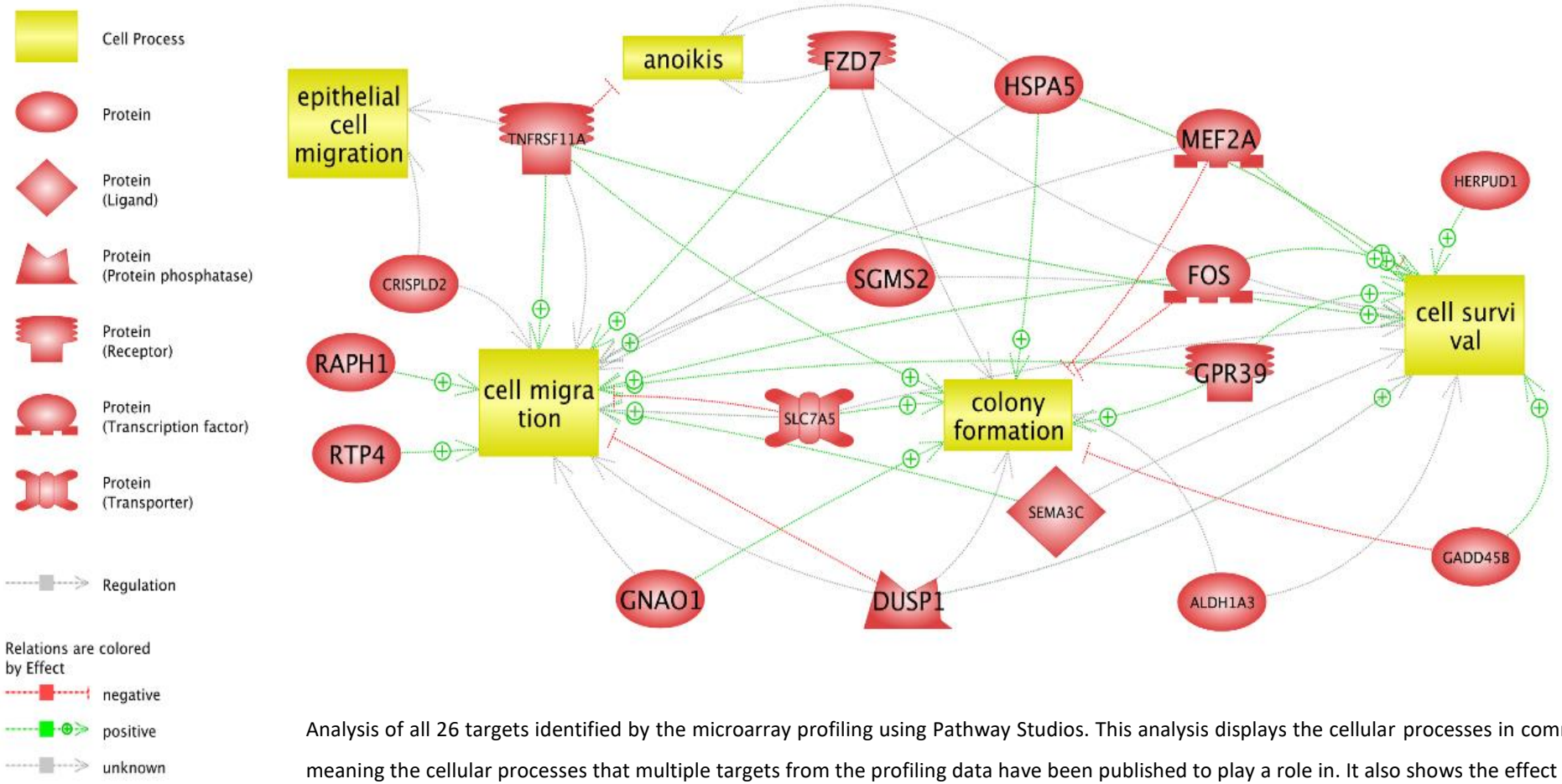

Analysis of all 26 targets identified by the microarray profiling using Pathway Studios. This analysis displays the cellular processes in common, meaning the cellular processes that multiple targets from the profiling data have been published to play a role in. It also shows the effect each target has on that specific process, red indicates the target negatively effects the process while green indicates a positive effect by the target.

3.4.2. Target gene – GRP78

Using the tools and data discussed previously, GRP78 (shown as HSPA5 in the microarray and Pathway Studios data) was chosen as a target to investigate further. GRP78 (also known as Bip and HSPA5) is a glucose regulated protein involved in the endoplasmic reticulum (ER) stress response (Lee 2007). From the literature mining using PubMed, many of the differentially expressed genes from the microarray profiling showed a role in the ER stress response which may indicate that stress response was highly important in the development of anoikis resistance. GRP78 is a member of the heat shock protein family, specifically the HSP70 protein family which is ubiquitously expressed in mammalian cells (Zhang and Zhang 2010). GRP78 is so highly conserved that its presence or the presence of a homologue are found in almost every organism from bacteria to man (Quinones, Ridder and Pizzo 2008). GRP78 plays an important part in cellular survival through several different functions including as a chaperone for folding, maturation and transport of proteins in the ER (Raiter, Yerushalmi and Hardy 2014). A major function is as part of the unfolded protein response (UPR) which is a response to stress conditions to protect the cell from apoptosis. When the protein level in the cell exceeds the folding capacity of the ER, the UPR is initiated in response to this stress (Lee 2007). This response activates several signalling pathways which result in attenuation of translation, upregulation of chaperones and folding enzymes as well enhanced degradation of misfolded proteins (Lee 2007). The other functions of GRP78 include inhibiting aggregation of protein intermediates, targeting misfolded proteins for degradation and Ca^{2+} binding to act as an ER stress signal regulator (Lee 2007).

Using the Pathway Studios data, GRP78 appeared to play a role in breast cancer, specifically triple negative breast cancer. This data also indicated a function of GRP78 in cell survival, cell migration, colony formation and anoikis. However, the literature mining did not show any evidence GRP78 played a part in anoikis in TNBC which vastly contributed to the decision to further investigate the part GRP78 had in anoikis resistance in TNBC. Additional Pathway Studios analysis was performed focusing on GRP78. Figure 3-4 shows the diseases GRP78 had been shown to play a role in and the

effect GRP78 played indicated by green or red as previously described. This data indicated a function of GRP78 in triple negative breast cancer, metastasis, invasion and carcinogenesis, as well as others, with GRP78 playing a positive part in the majority of these conditions. Figure 3-5 displays the cellular processes that GRP78 was known to play a part in and whether this part was positive or negative. GRP78 was shown to play a positive role in cell migration, invasion, survival and colony formation. Interestingly, GRP78 was shown to have both a positive and negative effect on survival. The effect GRP78 had in anoikis was unknown, indicated by the grey arrow and literature mining using PubMed showed no publications directly linking GRP78 with anoikis, this contributed to the interest in investigating the role GRP78 has in anoikis resistance.

While determining the potential of GRP78 as a functional target in TNBC, survival analysis was also performed. This analysis utilised software and data available through kmplot.com which yielded a Kaplan-Meier (KM) survival plot, shown in Figure 3-6. This database uses publicly available datasets integrated with clinical data of relapse free survival (RFS) and overall survival (OS) to analyse the prognostic value of a particular gene. The patient samples are split into two groups, according to various quantile expressions of the target. These cohorts are then compared by Kaplan-Meier survival analysis yielding a plot, hazard ratio and logrank P value. The KM plot of GRP78 expression was for the basal subtype of breast cancer as no triple negative subtype option was available in the analysis software. This plot displays GRP78 mRNA expression in terms of RFS of 618 patients over a period of 200 months (Szász et al. 2016). The KM survival analysis indicated that high expression of GRP78 was significantly (p value = 0.0308) associated with poorer RFS in basal breast cancer patients. The low expression cohort of patients possessed a median survival time of 24.05 months while the high expression cohort displayed a median survival time of 17.45 months. This high expression-poorer survival was in agreement with the original hypothesis in this body of work that high GRP78 expression may be significant in anoikis resistance. In the data from the microarray profiling, GRP78 showed a p value of 0.001 and a log2 fold change (FC) value of 0.43 in the MDA-MB-231 cell line and a p value of 0.000004 and a log2 FC value of 0.775 in the MDA-MB-468 cell line. These values along with the knowledge

gained from the Pathway Studios and Kaplan-Meier survival analysis led to GRP78 being chosen as a target to investigate in the development of anoikis resistance.

Figure 3-4. Pathway Studios analysis of HSPA5 effect in diseases

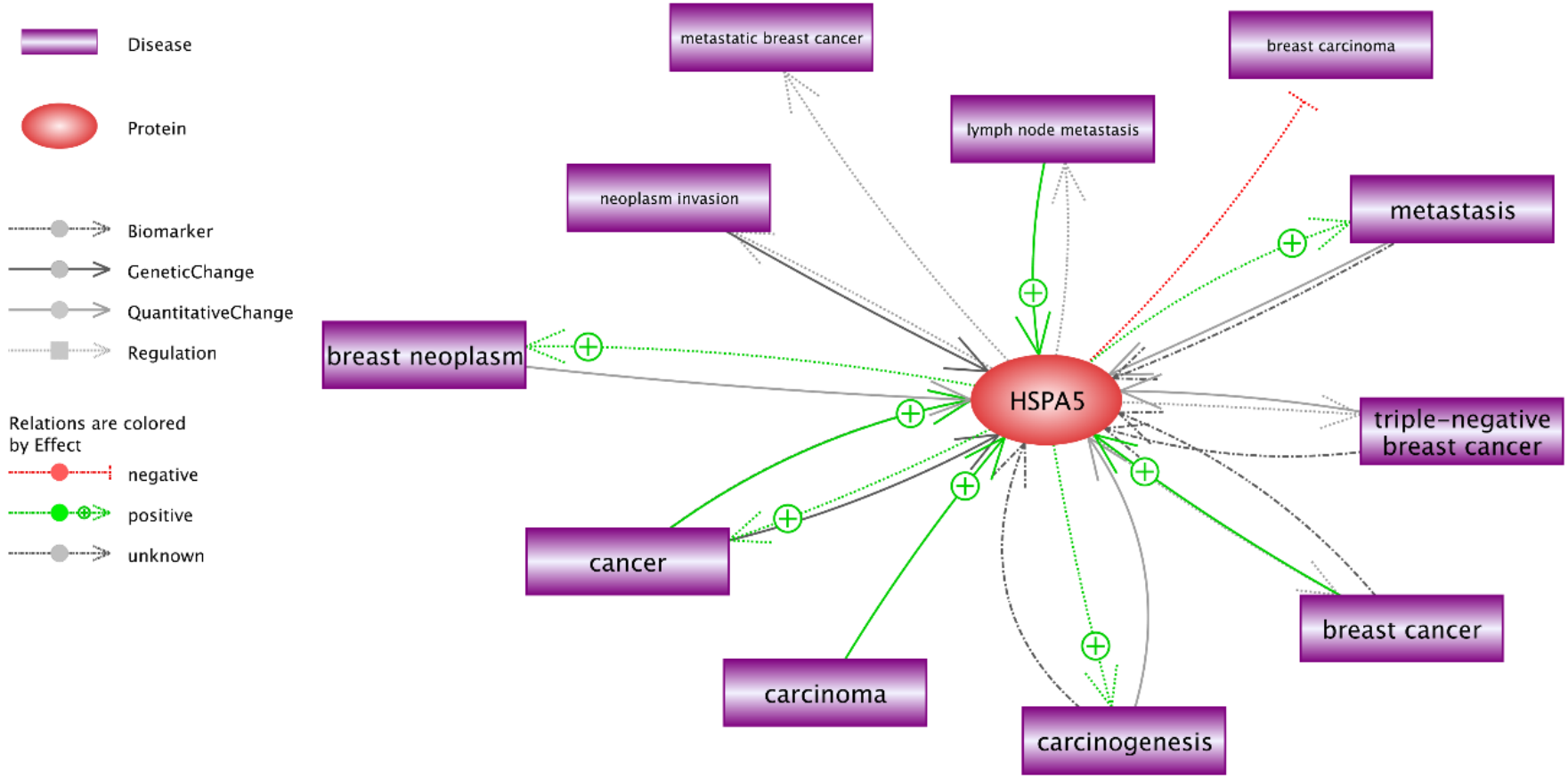

Analysis of HSPA5 using Pathway Studios. This analysis displays the diseases HSPA5 has been published to play a role in. It also shows the effect each target has in that specific disease, red indicates the target negatively effects the disease while green indicates a positive effect by the target.

Figure 3-5. Pathway Studios analysis of the role of HSPA5 in cellular processes

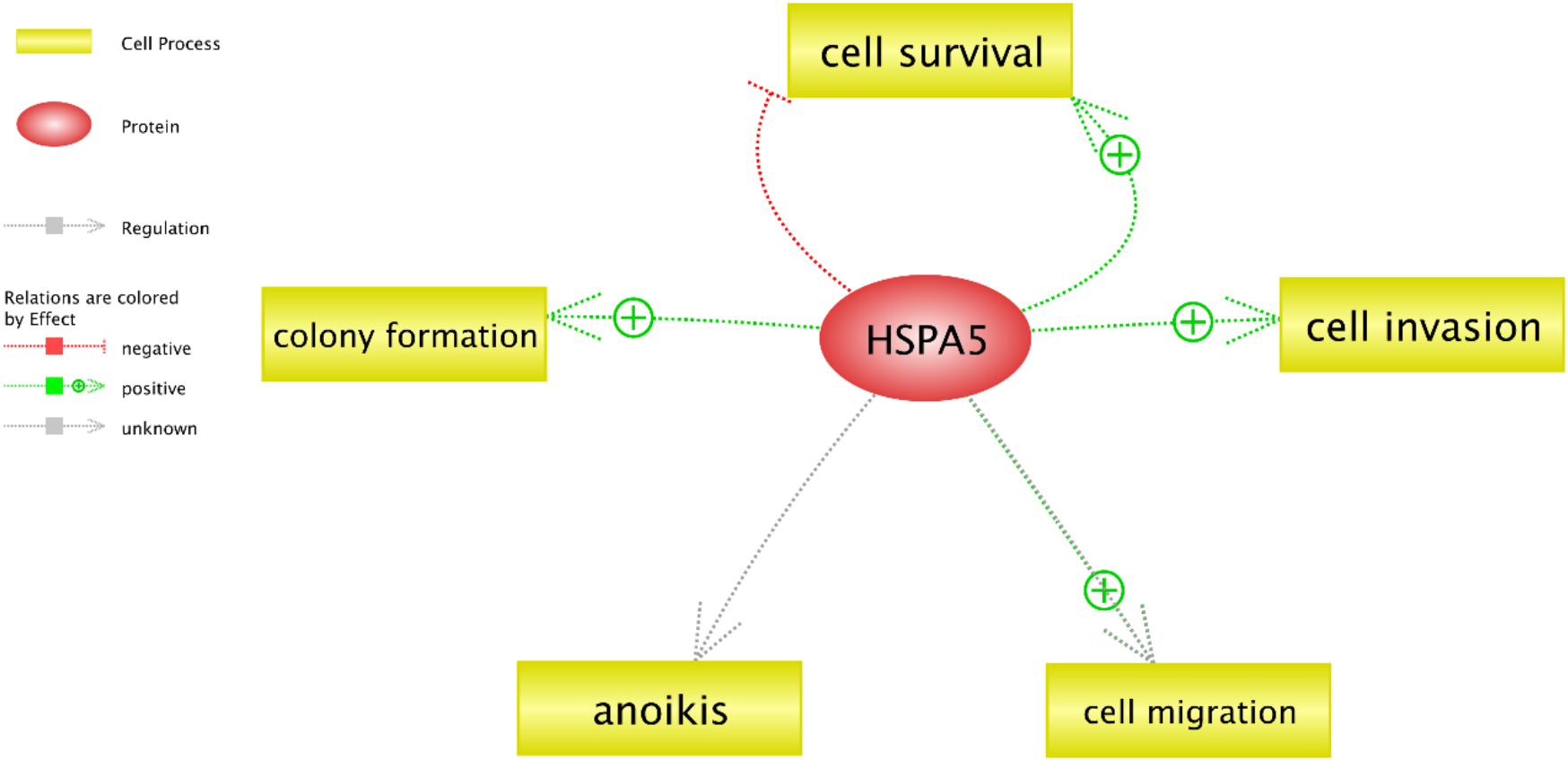

Analysis of HSPA5 using Pathway Studios. This analysis displays the cellular processes HSPA5 has been published to play a role in. It also shows the effect each target has in that specific disease, red indicates the target negatively effects the disease while green indicates a positive effect by the target.

Figure 3-6. Kaplan Meier plot showing the relationship of GRP78 expression with survival

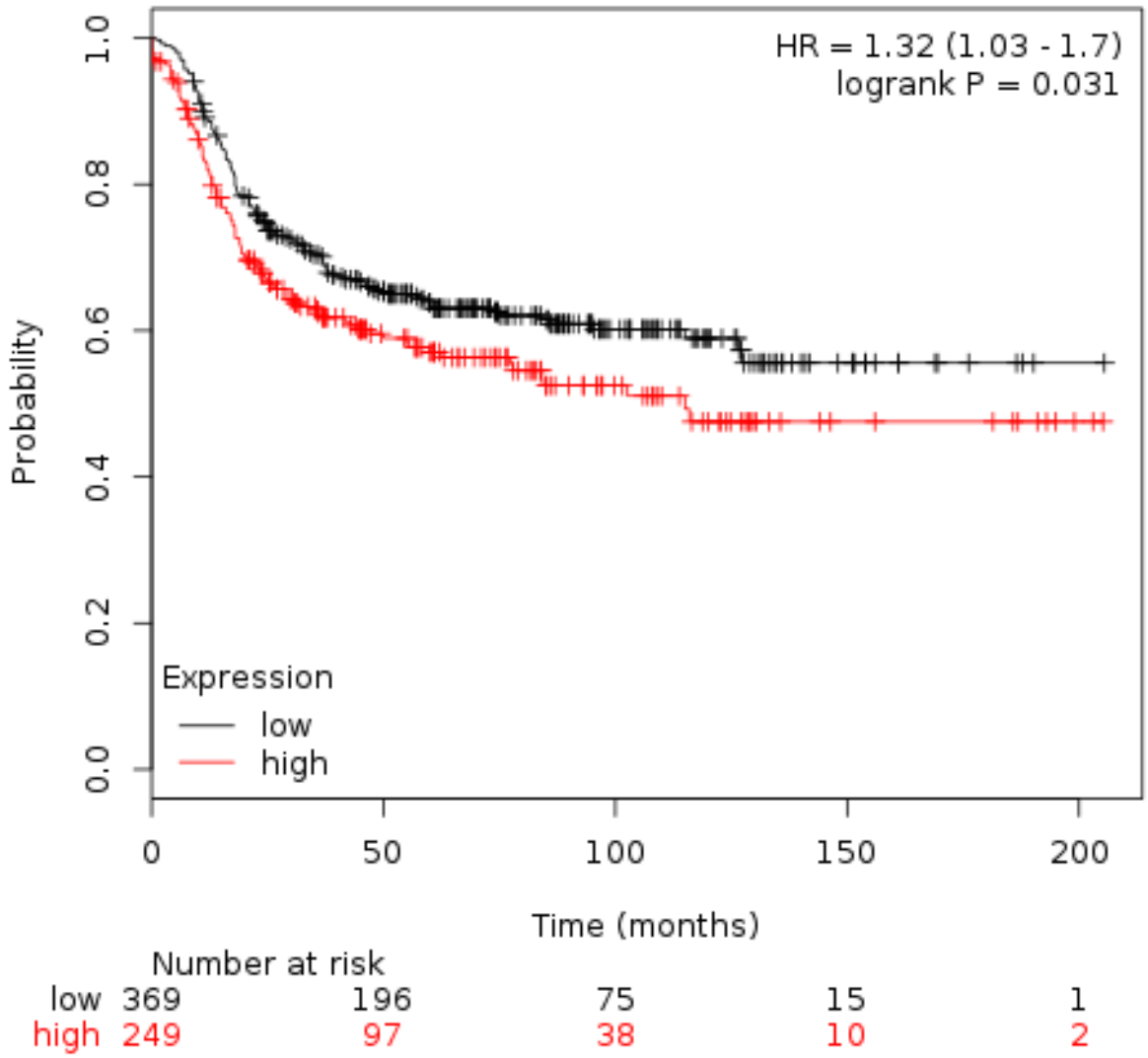

Kaplan Meier plot of GRP78 expression relative to survival in basal breast cancer patients. Analysis of GRP78 mRNA expression in terms of relapse-free survival (RFS) of patients over a period of 20 months. The basal intrinsic subtype as no triple negative subtype was available. Auto select best cut off was used (n=618, p value = 0.0308) (Szász et al. 2016).

3.4.3. Validation of target gene GRP78, expression profile

The microarray data indicated that GRP78 was expressed at a higher level in both the anoikis resistant cell lines (MDA-MB-231 and MDA-MB-468) in comparison to both the anoikis sensitive cell lines (HCC1954 and HS578T). To confirm this trend was present in the TNBC panel, Western blot analysis was performed, described in section 2.5. As seen in Figure 3-7 and Figure 3-8, the protein abundance of GRP78 was higher in both the MDA-MB-231 and MDA-MB-468 cell lines compared to both the HCC1954 and HS578T cell lines. This appears to validate the microarray data and confirms that GRP78 shows higher expression in the anoikis resistant cell lines compared to the anoikis sensitive cell lines. Following on from this, the expression of GRP78 was reduced using transient siRNA transfections and functional effects were assessed. This was used to investigate if GRP78 played a role in anoikis resistance as well as other metastatic phenotypes such as proliferation, invasion and colony formation.

Figure 3-7. Level of GRP78 and β-actin protein across a panel of TNBC cell lines

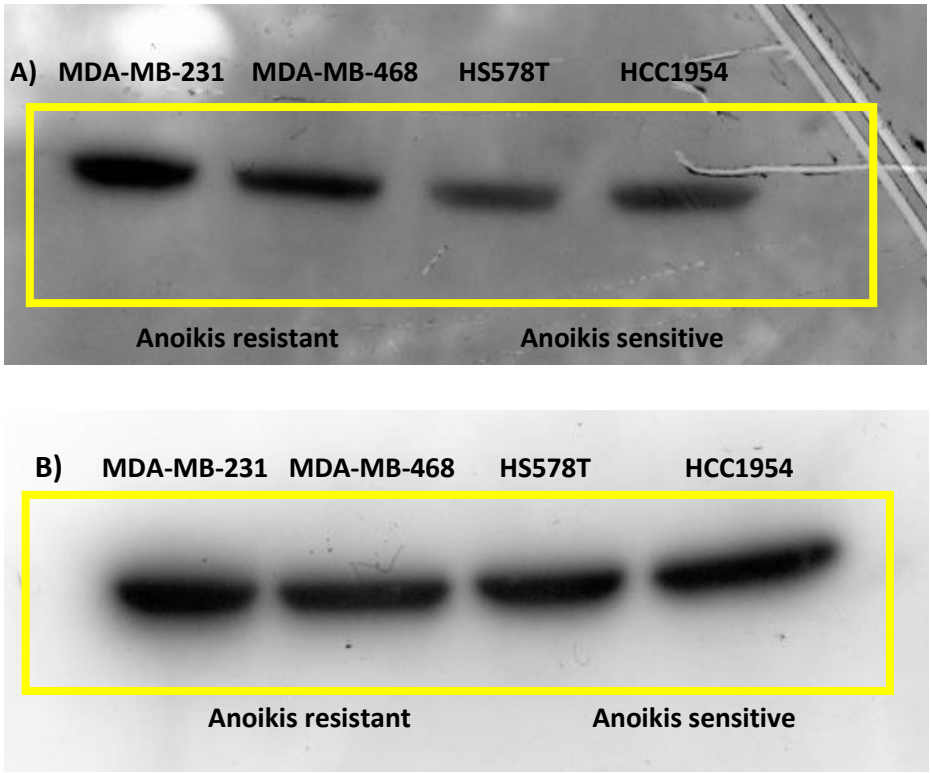

A) Trend of GRP78 protein, 78 kDa, in both anoikis resistant cell lines (MDA-MB-231 and MDA-MB-468) and both anoikis sensitive cell lines (HS578T and HCC1954) validating the microarray expression profile. B) Level of β-actin protein, 42 kDa, (loading control) in both anoikis resistant cell lines (MDA-MB-231 and MDA-MB-468) and both anoikis sensitive cell lines (HS578T and HCC1954).

Figure 3-8. Densitometry analysis of GRP78 protein across a panel of TNBC cell lines

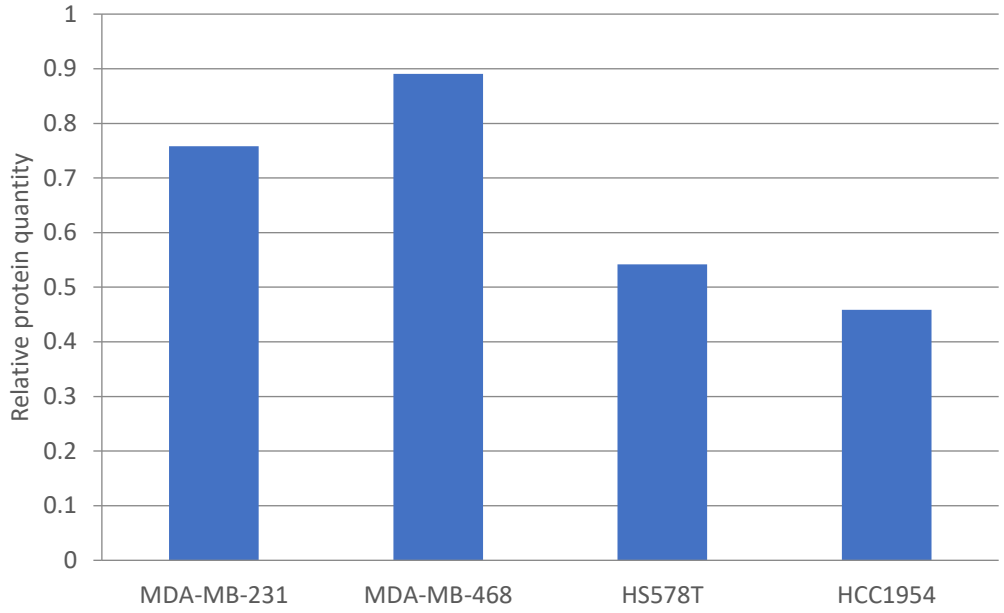

Densitometry analysis of the trend of GRP78 protein in both anoikis resistant cell lines (MDA-MB-231 and MDA-MB-468) and both anoikis sensitive cell lines (HS578T and HCC1954) using TotalLab Quant software relative to β-actin, used as the loading control (n=1).

3.5. GRP78 Knockdown Optimisation

Both breast cell lines (MDA-MB-231 and MDA-MB-468) were transfected with siRNA targeting GRP78, as described in section 2.6.2. A negative control was also included. This negative control is *Silencer*® Select Negative Control No. 2, this negative control is an siRNA sequence which does not target any known gene, as described in section 2.6.2. Originally two concentrations (3nM and 5nM) of GRP78 siRNA were assessed to examine which concentration resulted in the most efficient knockdown. GRP78 knockdown was assessed through qPCR, described in section 2.10.1. A higher level of knockdown of GRP78 was achieved in the MDA-MB-468 cells (3-fold) than in the MDA-MB-231 cells (2-fold) compared to the negative control. Following this, two higher concentrations of GRP78 siRNA (8nM and 10nM) were assessed with the aim to achieve a higher GRP78 knockdown, especially in the MDA-MB-231 cells. From these results 10nM was observed to be optimum as it achieved a 4-fold knockdown in MDA-MB-468. No greater level of

knockdown was achieved in the MDA-MB-231 cell line but a 2-fold reduction in GRP78 expression was deemed sufficient to observe functional effects. The results from both transfections can be seen in Figure 3-9.

Figure 3-9. GRP78 knockdown through optimisation of siRNA concentration

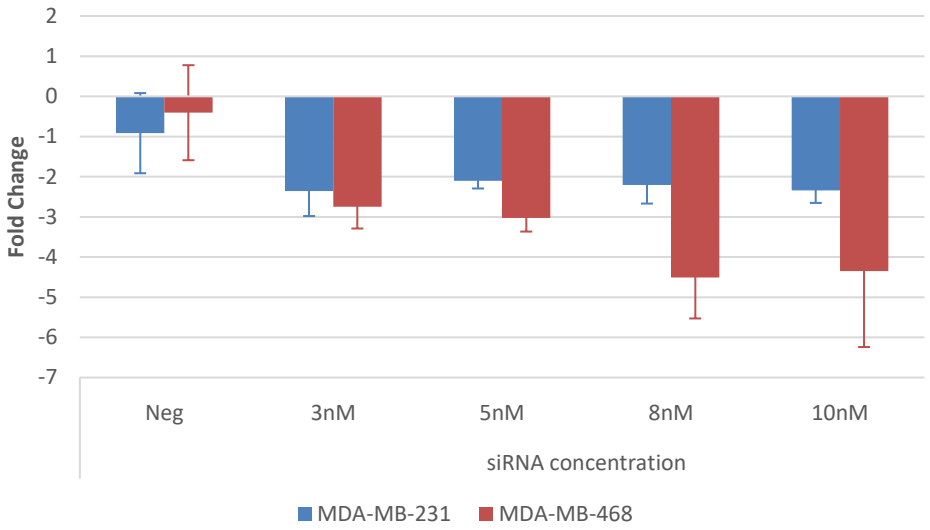

Reduction in GRP78 expression induced using varying concentrations of GRP78 siRNA (3, 5, 8, 10nM) in MDA-MB-231 and MDA-MB-468 cell lines displayed as fold change, assessed through qPCR 48hr post transfection, with a negative control (Neg) included and B2M used as an endogenous control. Error bars represent +/- standard deviation between technical replicates, (n=1).

3.6. Functional effects of GRP78 knockdown

Following knockdown of GRP78 expression using optimised siRNA conditions, functional effects of this alteration were investigated using proliferation, anoikis, invasion and colony formation assays. The percentage knockdown of GRP78 observed in each cell line as well the negative and positive control knockdown are displayed in Figure 3-10. The results from the functional assays post GRP78 knockdown can be seen in Figure 3-13 – effect on proliferation at 24hr, Figure 3-14 and Figure 3-15 – effect on anoikis, Figure 3-16 – effect on invasion, Figure 3-18 – effect on proliferation at 7days, Figure 3-19 – effect on 2D colony formation and Figure 3-21 – effect on 3D colony formation. These functions were assessed as each function plays an important role in metastasis.

Figure 3-10. Validation of transfection

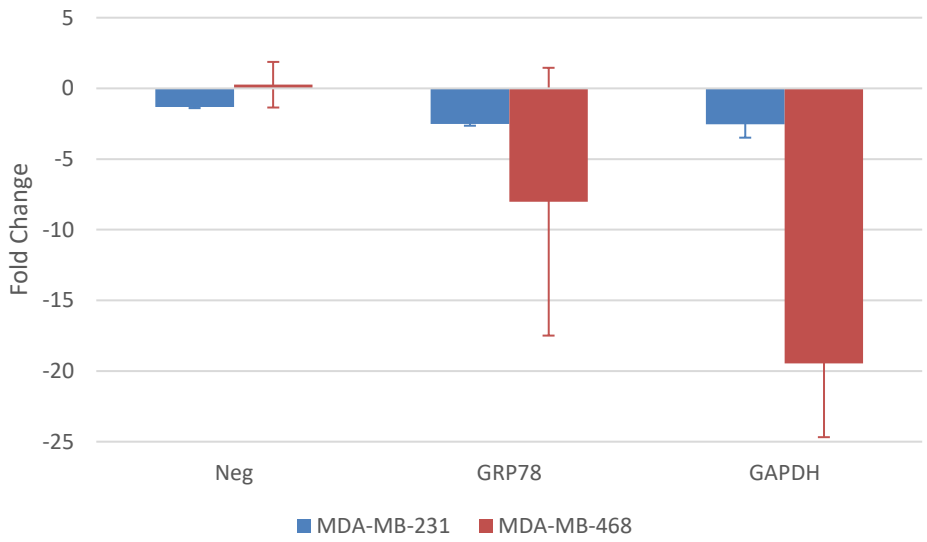

Fold change of negative control (Neg), GAPDH and GRP78 following a 48hr transfection using siRNA at a 10nM concentration in MDA-MB-231 and MDA-MB-468 cell lines. GAPDH acting as a positive control for knockdown and using B2M as an endogenous control for assessment of knockdown through qPCR. Error bars represent +/- standard deviation between technical replicates, (n=1).

Figure 3-11. GRP78 protein knockdown post transfection

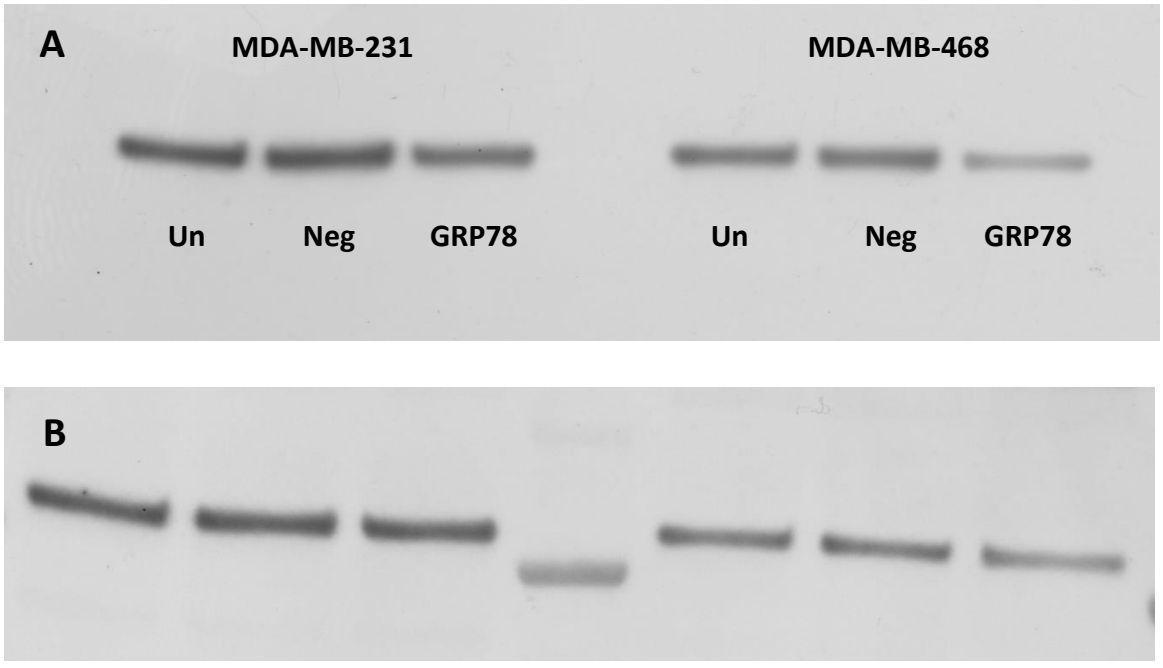

A. Western blot showing knockdown of GRP78 protein, 78 kDa, in both anoikis resistant cell lines (MDA-MB-231 and MDA-MB-468) post transfection, samples included untransfected (Un), negative control (Neg) and GRP78 KD (GRP78). **B.** α- Tubulin levels across all six samples was included as a loading control.

Figure 3-12. Densitometry analysis of GRP78 knockdown

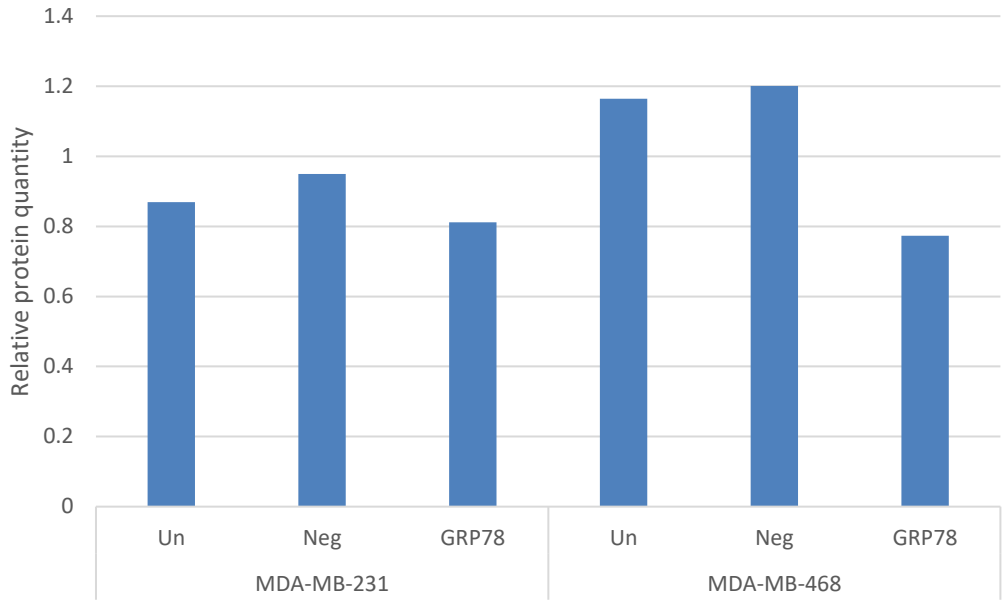

Densitometry analysis of GRP78 knockdown following a 48hr transfection using siRNA at a 10nM concentration in both anoikis resistant cell lines (MDA-MB-231 and MDA-MB-468) using TotalLab Quant software. Untransfected (Un) and negative (Neg) controls were included, relative to α-Tubulin used as the loading control (n=1).

Figure 3-10., analysis of qPCR data displays the fold change reduction of GRP78 achieved through transient transfection using siRNA of GRP78 in both the MDA-MB-231 and MDA-MB-468 cells lines as well the levels of knockdown in the negative control. A transient knockdown of GAPDH was included as a positive control. A 2-fold reduction of GAPDH was achieved in the MDA-MB-231 cell line with a 19-fold reduction present in the MDA-MB-468 cell line. The reduction in GAPDH mRNA validates that the transfection was successful. Figure 3-10 also shows that the expression of GRP78 was successfully reduced in both the anoikis resistant TNBC cell lines. MDA-MB-231 cells displayed a 2-fold decrease while the MDA-MB-468 cell lines possessed an 8-fold reduction in GRP78 expression. Figure 3-11 shows Western blot analysis of GRP78 protein knockdown post transfection. Further analysis of this protein knockdown using densitometry is displayed in Figure 3-12. Both figures are in agreement and show GRP78 protein knockdown was achieved in both the MDA-MB-231 and MDA-MB-468 cell lines. This result is in agreement with the mRNA reduction as a much greater decrease in GRP78 mRNA was induced in the MDA-MB-468 cell line compared to the MDA-MB-231 cell line. This

confirmation of successful reduction in GRP78 mRNA expression and GRP78 protein knockdown led to assessment of functional effects resulting from GRP78 knockdown.

Figure 3-13. Percentage proliferation at 24hr in both anoikis resistant cell lines post GRP78 knockdown

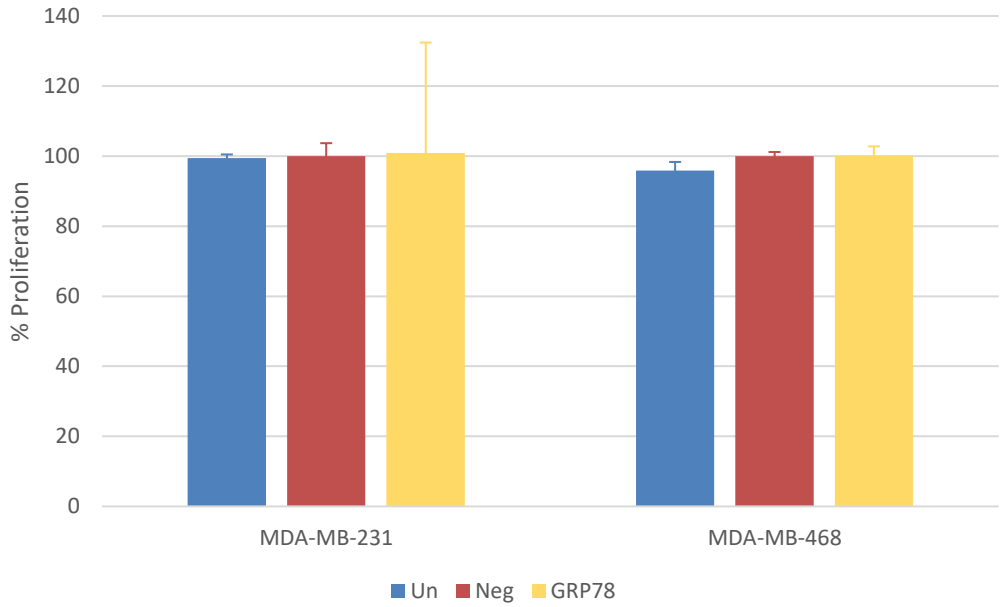

Percentage proliferation at a 24hr time-point following GRP78 knockdown post 48hr transfection in MDA-MB-231 and MDA-MB-468 cell lines relative to the negative control (Neg) with the untransfected (Un) control included. Error bars represent +/- standard deviation between biological replicates, (n=3).

Figure 3-13 displays the level of proliferation observed in both anoikis resistant TNBC cell lines after 24hr of incubation and post GRP78 knockdown. This time point was utilised to accommodate the anoikis and invasion analysis detailed below. Both functions were assessed at a 24hr timepoint therefore to ensure any changes observed in either anoikis or invasion were not due to proliferation changes, proliferation was assessed at a 24hr timepoint as well after a 7-day period. The levels of proliferation are relative to the negative control with the untransfected control included to show the effects the transfection process had on proliferation. The reduction of GRP78 expression induced no change in proliferation of either TNBC cell line after 24hr of culture.

Figure 3-14. Percentage survival of the **MDA-MB-231** cell line post GRP78 knockdown

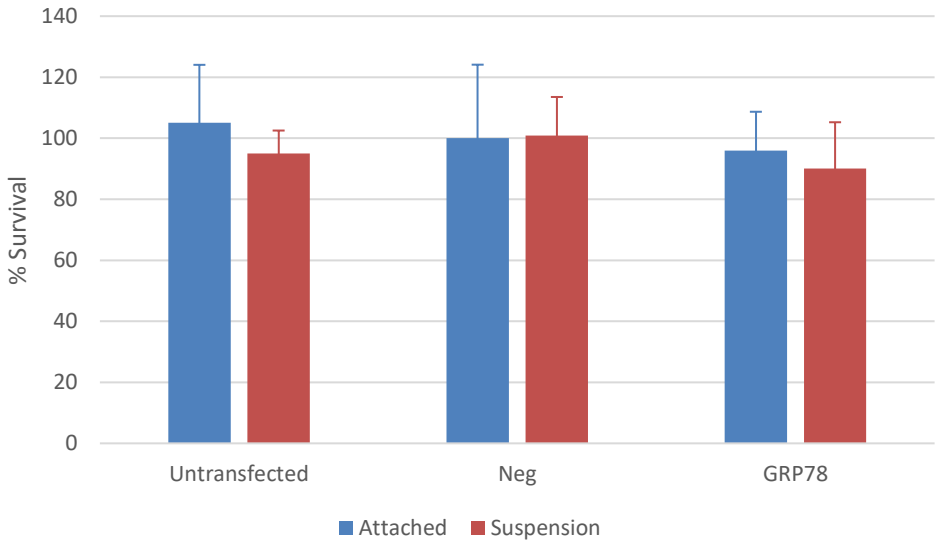

Percentage survival in both attached and anoikis i.e. suspension, conditions following GRP78 knockdown post 48hr transfection in the **MDA-MB-231** cell line relative to the negative control (Neg) in attached conditions with the untransfected (Un) control included. Error bars represent +/- standard deviation between biological replicates, (n=3).

Figure 3-15. Percentage survival of the **MDA-MB-468** cell line post GRP78 knockdown

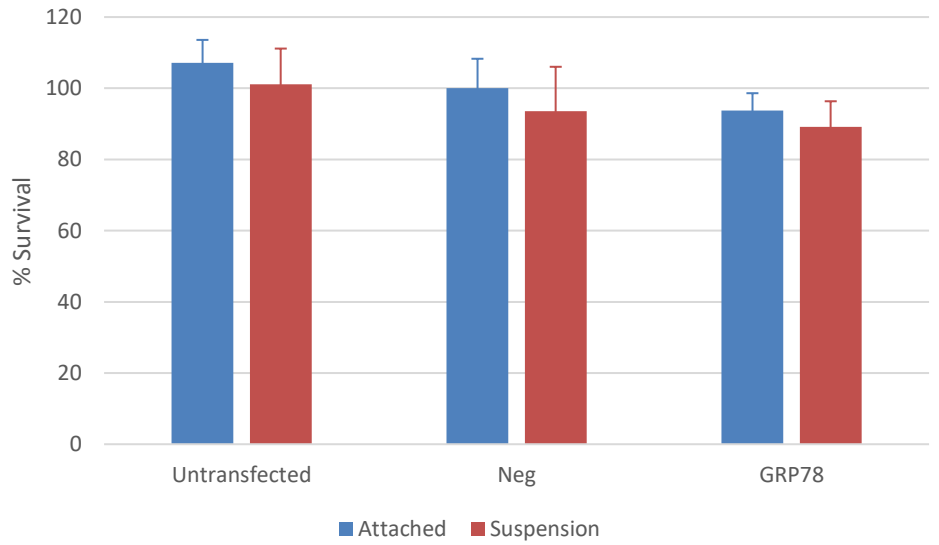

Percentage survival in both attached and anoikis i.e. suspension, conditions following GRP78 knockdown post 48hr transfection in the **MDA-MB-468** cell line relative to the negative control (Neg) in attached conditions with the untransfected (Un) control included. Error bars represent +/- standard deviation between biological replicates, (n=3).

Figure 3-14 and show the observed effects of GRP78 knockdown on anoikis i.e. survival in suspension, of both TNBC cell lines after a 48hr transfection and a further 24 hours exposed to anoikis conditions. For the evaluation of anoikis, two conditions were utilised, attached and suspension. Cells in suspension were in anoikis conditions i.e. unattached, meaning cells underwent anoikis cell death, if they were anoikis sensitive. To assess anoikis, Alamar blue was used as an indicator of cellular health through metabolic rate. Cells undergoing anoikis displayed a reduced metabolic rate and therefore induced less reduction of the Alamar blue resulting in little to no colour change. This lack of colour change was detected by the microtiter plate reader and expressed as a percentage survival i.e. the percentage of cells that are surviving while in attached and suspension conditions post GRP78 knockdown. This survival was calculated using the control sample in attached conditions as a comparison, meaning the control in attached conditions was expressed as 100% survival with other experimental conditions relative to this. Therefore, samples which reduced the Alamar blue through metabolism, to a greater or lesser extent than the control were displayed as having a greater or lesser percentage survival. Using this method of analysis, the effect of GRP78 knockdown on anoikis was determined and expressed as percentage survival for both TNBC cell lines with the negative control in attached conditions expressed as 100% survival. It was determined there was no change in the level of survival observed in either anoikis resistant cell line post GRP78 knockdown in both attached and suspension conditions relative to the negatively transfected control.

Figure 3-16. Percentage invasion post GRP78 knockdown in both anoikis resistant TNBC cell lines

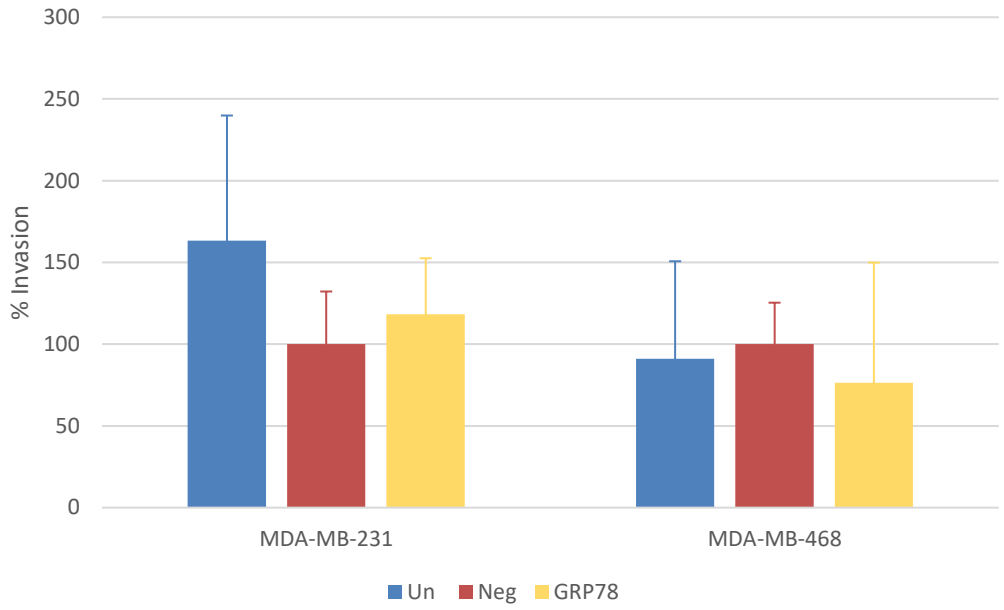

Percentage invasion of both TNBC cell lines, MDA-MB-231 (24hr) and MDA-MB-468 (48hr) following GRP78 knockdown post 48hr transfection, with percentage invasion relative to the negative control (Neg) and the untransfected (Un) control included. Error bars represent +/- standard deviation between biological replicates, (n=3).

Figure 3-17. Representative images of invasion levels of both **MDA-MB-231** and **MDA-MB-468** cells post GRP78 knockdown

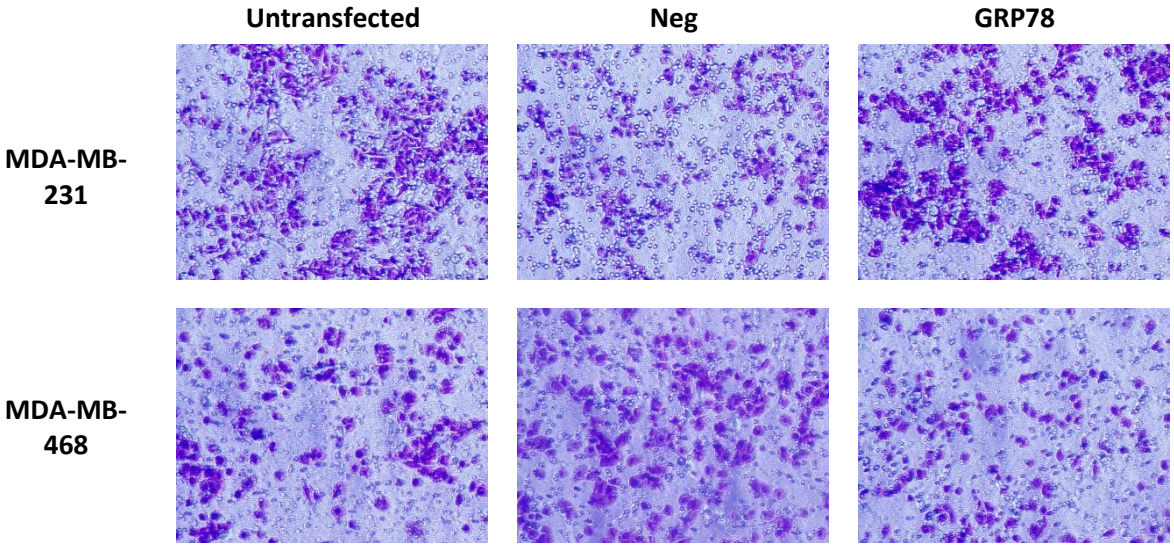

Representative images of invasion following GRP78 knockdown in both **MDA-MB-231** (24hr) and **MDA-MB-468** (48hr) cell lines with the untransfected (Un) and negative control (Neg) included.

Assessment of changes in invasion levels induced by GRP78 knockdown showed no significant effect in either TNBC cell line, as seen in . Representative images of the invasion levels in both cell lines in each transfection condition are displayed in Figure 3-17. An increase in invasion was present in the MDA-MB-231 cell line while a decrease was observed in the MDA-MB-468 cell line. Neither result showed any statistical significance due to variation between biological replicates.

Figure 3-18. Percentage proliferation over 7 days in both anoikis resistant cell lines post GRP78 knockdown

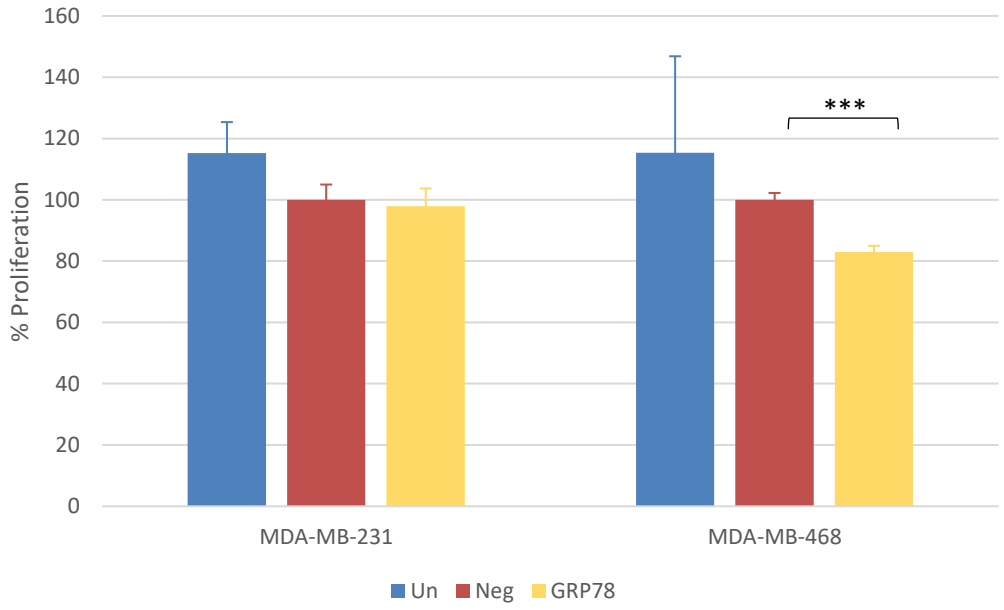

Percentage proliferation after 7 days' incubation following GRP78 knockdown post 48hr transfection in MDA-MB-231 and MDA-MB-468 cell lines relative to the negative control (Neg) with the untransfected (Un) control included. Error bars represent +/- standard deviation between biological replicates, (n=3, *** = p value ≤ 0.001).

As seen in Figure 3-13 no effect on proliferation was observed due to GRP78 knockdown at a 24hr time-point. This time point was utilised to accommodate the anoikis and invasion analysis detailed previously. To fully assess if GRP78 knockdown had any effect on proliferation acid phosphatase assays were performed after 7 days of culture. Figure 3-18 displays there was no change in proliferation in the MDA-MB-231 cell line post GRP78 knockdown. A significant 20% reduction in proliferation (p value = 0.00013) was

induced in the MDA-MB-468 cell line due to decreased GRP78, this is compared to the negative control.

Figure 3-19. Percentage 2D colony formation of the **MDA-MB-231** cell line post GRP78 knockdown

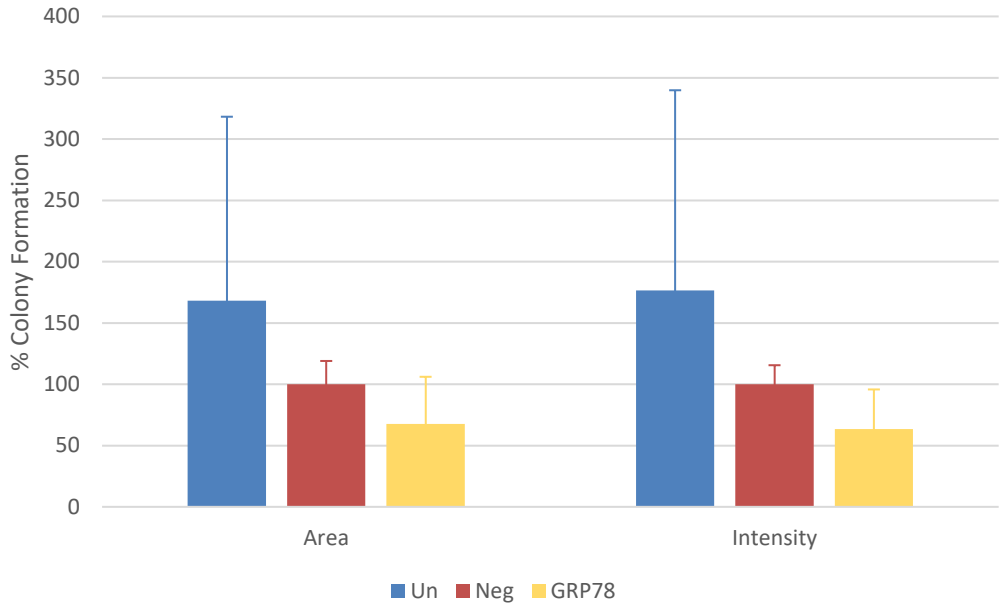

Percentage colony area and staining intensity of colonies formed over 14 days in 2D relative to the negative control (Neg) following a 48hr transfection to induce GRP78 knockdown in the **MDA-MB-231** cell line. Colonies were analysed using ImageJ software. Error bars represent +/- standard deviation between biological replicates, (n=3).

Figure 3-20. Representative image of 2D colony formation of the **MDA-MB-231** cell line post GRP78 knockdown

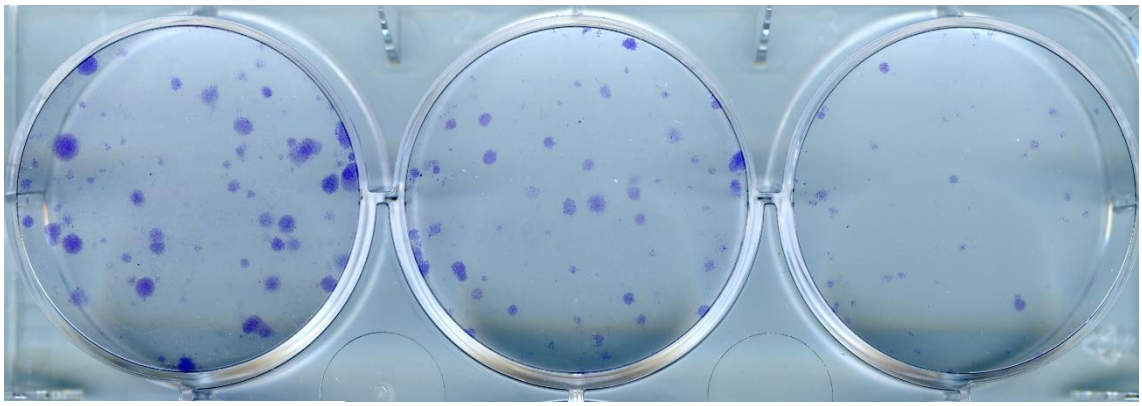

Representative image of 2D colony formation of the **MDA-MB-231** cell line at 14 days following GRP78 knockdown post 48hr transfection with the untransfected (Un) and negative control (Neg) included.

Figure 3-21. Percentage 3D colony formation of both anoikis resistant TNBC cell lines post GRP78 knockdown

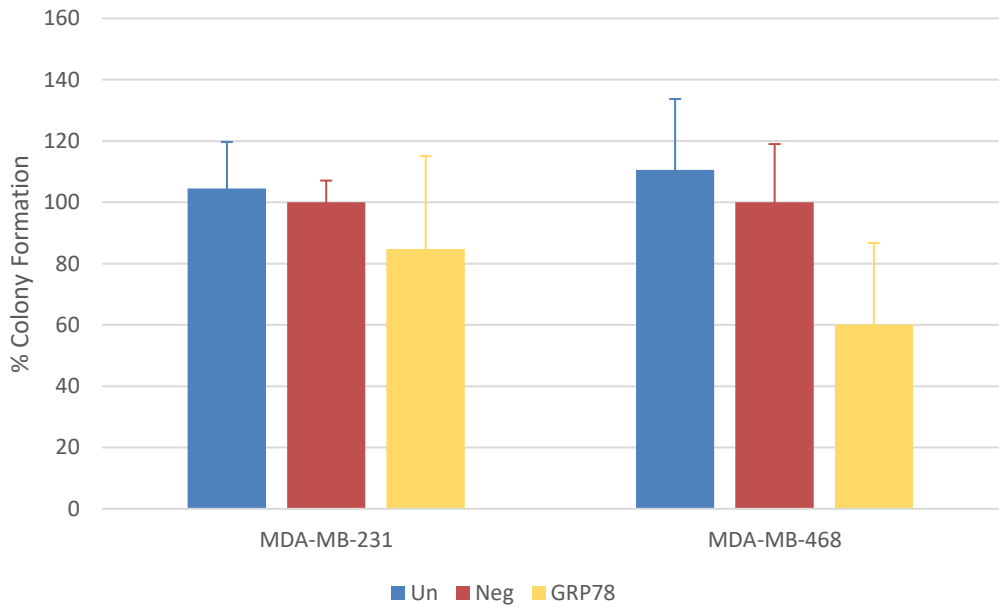

Percentage colonies formed over 14 days relative to the negative control (Neg) following GRP78 knockdown post 48hr transfection in MDA-MB-231 and MDA-MB-468 cell lines. Error bars represent +/- standard deviation between biological replicates, (n=3).

The functional effect of reduced GRP78 on the ability of the TNBC cell lines to form colonies was assessed using two different methods. The first being in 2D, with the method described in section 2.13. It was determined however that the MDA-MB-468 cells do not form colonies in 2D, meaning the effect on 2D colonies was investigated in only the MDA-MB-231 cell line. Displayed in Figure 3-19 is the percentage area and percentage intensity with area equating to colony number and intensity equating to colony size. The 2D colonies of MDA-MB-231 cells could not be analysed using the method used to analyse colonies from other cell lines i.e. Metamorph image analysis. This was due to the lack of staining of the colonies, the cells did not take up a large amount of the crystal violet stain therefore the software could not distinguish colonies from the background. Due to this a different software method was used, ImageJ. This software was similar to Metamorph but allows less control of the analysis, it was this aspect of ImageJ which led to Metamorph being the favoured software for colony formation analysis. Using ImageJ software, the percentage colony formation of MDA-MB-231 cells post GRP78 knockdown is shown in Figure 3-19 with a representative image displayed in Figure 3-20. A 40% reduction in both colony area and intensity was induced due to reduced GRP78, while no statistical significance was present, this may be due to the analysis software, a trend of reduced colony forming ability post GRP78 knockdown was present and is shown in Figure 3-20. The largest functional effect observed post GRP78 knockdown was a reduction in the TNBC cells ability to form colonies in 3D, as shown in Figure 3-21. The method used to investigate colony formation in 3D, the soft agar assay is described in section 2.14. The MDA-MB-231 cell line displayed a 15% reduction in colonies formed while a 40% reduction in colonies formed was observed in the MDA-MB-468 cell line. While no statistical significance was observed a very strong trend of reduced colony forming ability was present, with MDA-MB-468 cell line displaying a p value of 0.06.

4. Discussion – Microarray Analysis of Anoikis Resistance in Triple Negative Breast Cancer

4.1. Microarray Analysis

Microarray analysis of a panel of TNBC cell lines was performed in order to develop knowledge in the area of anoikis resistance. The ability of cancer cells to resist cell death post detachment from the ECM is an important hallmark of cancer progression. Anoikis was induced by exposing cells to suspension conditions for 4hr prior to profiling. This time point was chosen to ensure optimal cell viability. The longer the cells are detached the more viability was reduced; this was especially true for the anoikis sensitive cell lines. Gene expression profiling with microarrays was performed on the two anoikis resistant TNBC cell lines (MDA-MB-231 and MDA-MB-468) and two anoikis sensitive TNBC cell lines (HCC1954 and HS578T). The anoikis status of the four cell lines was confirmed in Figure 3-1. The anoikis sensitive cell lines (HCC1954 and HS578T) display anoikis levels of 90% and 58% respectively. The anoikis resistant cell lines (MDA-MB-231 and MDA-MB-468) display levels of only 10% and 20% anoikis respectively. There are very few publications to investigate if these anoikis levels are observed in other studies. However, one such study does exist, the MDA-MB-231 cell line is described as anoikis resistant in comparison to MCF-7 cells due to a 1.7-fold higher survival in anoikis conditions in a study of the protein profiles of anoikis resistant cell lines (Akekawatchai et al. 2016). The profiling was performed on the four cell lines in two different conditions at 4hr:

- Cells in normal monolayer cell culture conditions i.e. attached
- Cells exposed to anoikis conditions i.e. in suspension

4.2. Investigation of microarray data

The analysis compared each of the four cell lines, both anoikis resistant and anoikis sensitive, in both attached conditions and suspension conditions i.e. the genes being expressed in the MDA-MB-231 cell line in suspension were compared to the genes being expressed in the MDA-MB-231 cell line in attached conditions. This analysis focused on the genes and miRNA that were differentially expressed in both anoikis resistant cell lines in the same direction (upregulated/downregulated) when in suspension compared to attached and did not show differential expression in either anoikis sensitive cell line

in suspension compared to attached. This was with the aim of identifying a gene or miRNA which contributed to the ability of the anoikis resistant cells to survive in suspension. This profiling identified 26 significantly differentially expressed genes in the anoikis resistant cell lines when in suspension compared to attached, and not differentially expressed in the anoikis sensitive cell lines, with significance being considered as an adjusted p value <0.05. Literature mining was performed to reduce this list and using a range of literature mining tools including PubMed, Pathway Studios and Kaplan-Meier survival analysis, the target GRP78 was chosen to further investigate. GRP78 is an ER stress response protein as were several of the differentially expressed genes from the microarray analysis.

GRP78 (also known as Bip and HSPA5) is a glucose regulated protein involved in the endoplasmic reticulum (ER) stress response (Lee 2007). It is a member of the heat shock protein family, specifically the HSP70 protein family which is ubiquitously expressed in mammalian cells (Zhang and Zhang 2010). GRP78 plays an important role in cellular survival through several different functions including as a chaperone for folding, maturation and transport of proteins in the ER (Raiter, Yerushalmi and Hardy 2014). A major function of GRP78 is as part of the unfolded protein response (UPR) which is a response to stress conditions to protect the cell from apoptosis. When the protein level in the cell exceeds the folding capacity of the ER, the UPR is initiated in response to this stress (Lee 2007). This response activates several signalling pathways which result in attenuation of translation, upregulation of chaperones and folding enzymes, as well enhanced degradation of misfolded proteins (Lee 2007). The other roles of GRP78 include inhibiting aggregation of protein intermediates and Ca^{2+} binding to act as an ER stress signal regulator (Lee 2007).

Using literature mining tools, PubMed, Pathway Studios and Kaplan-Meier survival analysis, GRP78 was chosen as a target to investigate further for a functional effect on metastatic phenotypes in TNBC. The Pathway Studios analysis, shown in Figure 3-2 and Figure 3-3, indicated a function of GRP78 in TNBC as well a role in the functions of cell

survival, colony formation and anoikis. However, the literature mining did not show any evidence GRP78 played a part in anoikis in TNBC which vastly contributed to the decision to further investigate the part GRP78 played in anoikis resistance in TNBC. Additional Pathway Studios analysis was performed focusing on GRP78. This data, shown in Figure 3-4 and Figure 3-5, indicated a role of GRP78 in triple negative breast cancer, metastasis, invasion and carcinogenesis, with GRP78 playing a positive role in the majority of these conditions. Analysis of cellular processes indicated GRP78 had an effect on cell migration, invasion, survival and colony formation. The effect GRP78 had in anoikis was unknown, indicated by the grey arrow and literature mining using PubMed showed no publications directly linking GRP78 with anoikis, this contributed to the interest in investigating the part GRP78 had in anoikis resistance. The survival analysis of GRP78 utilised software and data available through kmplot.com which yielded a Kaplan-Meier (KM) survival plot, shown in Figure 3-6. The KM plot of GRP78 expression was for the basal subtype of breast cancer as no triple negative subtype option was available in the analysis software. This plot displays GRP78 mRNA expression in terms of relapse-free survival (RFS) of 618 patients over a period of 200 months (Szász et al. 2016). The KM survival analysis indicated that high expression of GRP78 was significantly (p value = 0.0308) associated with poorer RFS in basal breast cancer patients. This high expression-poorer survival relationship was in agreement with the original hypothesis that high GRP78 expression may be significant in anoikis resistance. In the data from the microarray gene expression profiling, GRP78 showed a p value of 0.001 and a log2 fold change (FC) value of 0.43 in the MDA-MB-231 cell line and a p value of 0.000004 and a log2 FC value of 0.775 in the MDA-MB-468 cell line. These values along with the knowledge gained from the Pathway Studios and Kaplan-Meier survival analysis led to GRP78 being chosen as a target to investigate in the development of anoikis resistance.

The first step in investigating the role of GRP78 in anoikis resistance was to confirm the expression levels of GRP78 across the TNBC panel. The microarray data indicated that GRP78 was expressed at a higher level in both the anoikis resistant cell lines (MDA-MB-231 and MDA-MB-468) in comparison to both the anoikis sensitive cell lines (HCC1954 and HS578T). To confirm this trend was present in the TNBC panel, Western blot analysis

was performed. As seen in Figure 3-7 the protein abundance of GRP78 was higher in both the MDA-MB-231 and MDA-MB-468 cell lines compared to both the HCC1954 and HS578T cell line. This appears to validate the microarray data and confirms that GRP78 shows higher expression in anoikis resistant cell lines compared to anoikis sensitive cell lines. With this higher expression being confirmed the next step was to determine if reduction of GRP78 mRNA could be successfully achieved using transient siRNA transfections. As seen in Figure 3-10, a 2-fold change decrease in GRP78 mRNA was induced in the MDA-MB-231 cell line and an 8-fold decrease was achieved in the MDA-MB-468 cell line. Preliminary analysis of GRP78 protein levels, shown in Figure 3-11, displays GRP78 protein knockdown in the MDA-MB-468 cell line. Figure 3-11 shows Western blot analysis of GRP78 protein knockdown post transfection with densitometry analysis of these protein levels is displayed in Figure 3-12. Both figures indicate GRP78 protein knockdown was achieved in both the MDA-MB-231 and MDA-MB-468 cell lines with a greater protein reduction displayed in the MDA-MB-468 cell line. This result is in agreement with the mRNA reduction as a much greater decrease in GRP78 mRNA was induced in the MDA-MB-468 cell line compared to the MDA-MB-231 cell line. This confirmation of successful reduction in GRP78 mRNA expression and GRP78 protein knockdown led to assessment of functional effects resulting from GRP78 knockdown.

Post knockdown, the functional effects of reduced GRP78 expression were assessed. The changes in proliferation, anoikis, invasion and colony forming ability were investigated. The microarray data showed GRP78 as upregulated in both anoikis resistant cell lines in suspension compared to attached culture, therefore, it was proposed that a reduction in GRP78 may result in the anoikis resistant cell lines having a reduced ability to survive under anoikis conditions i.e. in suspension, unattached. As seen in Figure 3-14 and Figure 3-15, this result was not observed. It appears that lowering GRP78 expression had no effect on either anoikis resistant cell lines ability to survive in suspension. As there are no publications discussing GRP78 and its direct role in anoikis, it was difficult to conclude if this data is representative of the role of GRP78 in anoikis. Basing conclusions on this data it appeared GRP78 had no influence on anoikis resistance in either the MDA-MB-231 or the MDA-MB-468 cell line. One conclusion which can be drawn from Figure 3-14

and Figure 3-15 was that the cells displayed an 80-90% survival in suspension, this re-affirms their status as anoikis resistant cell lines and reiterates the data seen in Figure 3-1.

Assessment of changes in invasion levels induced by GRP78 knockdown showed no significant effect in either TNBC cell line, as seen in and Figure 3-17. An increase in invasion was present in the MDA-MB-231 cell line while a decrease was observed in the MDA-MB-468 cell line. Neither result showed any statistical significance due to variation between biological replicates. From these results, it was difficult to determine the role GRP78 played in invasion in TNBC. A positive effect on cell invasion by GRP78 was indicated by the Pathway Studios analysis, seen in Figure 3-5. It has also been shown that overexpression of GRP78 promotes invasion levels in both triple negative breast cancer and hepatocellular carcinoma (Lee et al. 2011, Su et al. 2010). This published study of breast cancer involved the MDA-MB-231 cell line, as did this current investigation of anoikis resistance. In the published study overexpression of GRP78 was induced through silencing of MMP-26 and this led to a significant 50% increase in invasion. This result contrasted with the increase in invasion observed in the MDA-MB-231 cell line post GRP78 knockdown in this project. It was difficult to determine if this result due to GRP78 knockdown was accurate due to the lack of statistical significance however in the study of inhibition of MMP-26 several other targets as well as GRP78 were overexpressed so the increase in invasion observed may have been due to other targets or a combinational effect.

Proliferation was assessed post transfection through an acid phosphatase method as described in section 2.11. Analysis showed no significant effect on proliferation due to altered expression of GRP78 in either TNBC cell lines at a 24hr timepoint. This time point was utilised to accommodate the anoikis and invasion analysis. Both functions were assessed at a 24hr timepoint therefore to ensure any changes observed in anoikis or invasion were not due to proliferation changes, proliferation was assessed at a 24hr timepoint. It has been shown that overexpression of surface GRP78 increases

proliferation in breast cancer cells *in vitro* and that when the receptor for this surface GRP78 is blocked the level of cellular proliferation was reduced (Yao et al. 2015). This assessment of proliferation was over a 24hr period so this indicates it was possible to detect a change in proliferation due to altered GRP78 over a short time frame. As the doubling time of the TNBC cell lines is greater than 24hr (Limame et al. 2012), proliferation post GRP78 knockdown was also assessed after a 7-day period. This showed a highly significant 20% decrease in proliferation of the MDA-MB-468 cell line. The role of GRP78 in proliferation of cancer has been published, the previously mentioned paper using a 24hr assay showed overexpression of GRP78 increased the proliferation of breast cancer cells (Yao et al. 2015). Similar results have been observed in other cancer types such as gastric and colon cancer, with overexpression causing an increase in proliferation and reduced expression inducing a decrease in proliferation (Zhang et al. 2015, Fu et al. 2014, Yeung et al. 2008).

The most noteworthy functional effect due to GRP78 knockdown was a large reduction in the number of colonies formed in both cell lines. A reduction in colony formation was observed in both 2D and 3D in the MDA-MB-231 cell line. In 2D a 40% decrease was observed in both colony area and staining intensity, equating to a reduction in colony number and size in the MDA-MB-231 cell line. In 3D, a 15% reduction in colonies formed was observed in the MDA-MB-231 cell line while a 40% reduction was observed in the MDA-MB-468 cell line. This reduction in colony formation was much larger in the MDA-MB-468 cell line than in the MDA-MB-231 cell line. This may be due to the greater reduction of GRP78 expression in the MDA-MB-468 cell line, an 8-fold reduction was achieved as opposed to the 2-fold reduction observed in the MDA-MB-231 cell line. There are several reasons why greater knockdown can be achieved in one cell line over another. In terms of the two triple negative breast cancer cell lines, the apparent lesser knockdown in the MDA-MB-231 cell line may be down to doubling time. The MDA-MB-231 cell line has a shorter doubling time (31.1hr) compared to the MDA-MB-468 cell line (62.8hr) (Risinger, Dybdal-Hargreaves and Mooberry 2015). Therefore, the shorter doubling time of the MDA-MB-231 cell line may have led to GRP78 expression returning to innate levels sooner than in the MDA-MB-468 cell line. Other reasons for the greater

knockdown achieved may be innately greater levels of GRP78 in the MDA-MB-231 cell line observed through qPCR and Western blotting. There was a 1 Ct value difference between the cell lines indicating a 2-fold greater expression of GRP78 in the MDA-MB-231 cell line. This greater expression was also observed at the protein level as shown in Figure 3-7 and Figure 3-11. Therefore, while a similar transfection efficacy was achieved in both cell lines, the shorter doubling time of the MDA-MB-231 cell line and the innately greater expression levels may have led to the apparent lesser GRP78 knockdown. This may also have contributed to the greater reduction in colony formation observed in the MDA-MB-468 cell line. This reduction in colony formation was consistent with the literature; Kuo *et al.*, reduced GRP78 expression through a stable transfection and assessed the effect on colony formation in two colon cancer cell lines, HT29 and DLD-1. This group observed a reduction in colony forming units in GRP78 knockdown cells, a 50% reduction in colony formation was detected which was similar to the result shown by this current project in the MDA-MB-468 cell line. This group also observed a reduction in proliferation post GRP78 knockdown (Kuo et al. 2013). A reduction in colony formation due to decreased GRP78 expression has also been observed in renal cell carcinoma (Lin et al. 2014a). The method used in this paper was similar to the method used in this current body of work, a transient siRNA transfection was used to reduce GRP78 expression and then functional effects were assessed. A significant reduction in the ability of renal cell carcinoma cells to produce colonies was observed post GRP78 knockdown (Lin et al. 2014a). This group also observed a reduction in cell growth post GRP78 knockdown as well as colony formation at 48hr and 72hr time points (Lin et al. 2014a). Pathway Studios analysis had indicated a positive role of GRP78 in colony formation, Figure 3-5, which would agree with the data observed in this work as a reduction in GRP78 expression appeared to induce a reduction in colony forming ability. A relationship between colony formation, specifically spheroid formation, and stemness has been well established (Gauthaman et al. 2009, Cheng et al. 2013, Li et al. 2015, Li et al. 2015b). A connection between GRP78 and stemness has also been reported (Wu et al. 2010, Chiu et al. 2013, Heijmans et al. 2013, Cheng et al. 2016b). These reports may suggest that the reduction in colony forming ability of the TNBC cells due to reduced GRP78 may be linked to stemness. This is an aspect to be investigated further in future work, post GRP78 knockdown the stem-like phenotype of the cells may be investigated.

GRP78 is known to play a role in cancer progression, many publications have determined this (Yao et al. 2015, Zhang et al. 2015, Fu et al. 2014, Lin et al. 2014a, Matsumura et al. 2014, Raiter, Yerushalmi and Hardy 2014, Kuo et al. 2013, Zhang and Zhang 2010, Quinones, Ridder and Pizzo 2008, Yeung et al. 2008). This role in progression was linked to the function of GRP78 as an ER stress response protein. GRP78 was elevated in many cancers and aids the cancer cells in evading stress-induced apoptosis (Matsumura et al. 2014, Zhang and Zhang 2010, Quinones, Ridder and Pizzo 2008). The reduction in the proliferation and colony forming efficiency in TNBC observed in this work induced by reduced GRP78 expression ties in with this knowledge. The lowered expression of GRP78 reduced the breast cancer cells ability to produce colonies and proliferate. Several studies further assessed reduced proliferation and colony formation due to GRP78 knockdown using flow cytometry (Wang et al. 2015, Ji et al. 2016, Zhou et al. 2016). Due to the significant reduction in proliferation observed in the MDA-MB-468 cell line and the trend of reduced colony formation due to GRP78 knockdown, an interesting next step would be to assess which cycle of cell growth was arrested. The cell growth cycles can be easily assessed using the Guava® easyCyte Flow Cytometer available in-house in the NICB, with the Guava® Cell Cycle Assay which measures G0/G1, S and G2/M phase distributions. This analysis would identify the specific phase of cell growth that GRP78 knockdown is arresting, inducing the observed reduction in proliferation and colony formation. This may determine a role of GRP78 in specific growth cycles of TNBC cells. To further investigate the effect of GRP78 on cell growth, analysis of phosphorylation of key cell cycle regulatory proteins such as AKT, JNK and ERK1/2 could be performed (Zhou et al. 2016). Alterations to phosphorylation of key cell cycle regulators could be assessed through Western blotting post GRP78 knockdown. Determining changes of phosphorylation of cell cycle regulators may identify the key regulators which GRP78 knockdown has altered inducing the reduction in proliferation and colony formation. No change in anoikis was observed due to reduced GRP78 expression, therefore the original hypothesis did not validate. However, knowledge gained regarding the role of GRP78 in proliferation and colony formation was novel in terms of triple negative breast cancer as very few studies have investigated the role of GRP78 in TNBC. GRP78 may be a viable target to interfere and reduce triple negative breast cancer cells' ability to proliferate and colonise in the process of metastasis.

5. Results – Investigation of the Role of the Tumour Microenvironment in Pancreatic Cancer

5.1. Aim

Investigate the role of the tumour microenvironment in the progression of pancreatic cancer using an indirect co-culture model. Pancreatic cancer is one of the most lethal cancers worldwide with a 5-year survival rate of only 6%. The poor prognosis and survival rate is partially due to the early onset of metastasis, which occurs soon after the development of the cancer. Metastasis is the ability of a cell to spread to another location in the body, colonising this secondary site with tumour growth. The pancreatic tumour microenvironment plays an important role in the progression of the cancer. The defined role the stroma plays in pancreatic cancer metastasis has not yet been fully elucidated. Aiming to investigate this role of the pancreatic cancer stroma, an indirect co-culture model was developed and utilised to determine the role the tumour microenvironment plays in the progression of pancreatic cancer.

5.2. Pancreatic Cancer

Pancreatic cancer is one of the most lethal cancers worldwide. The 5-year survival rate is approximately 6%, due to late diagnosis by which time usually metastasis has occurred (Rucki and Zheng 2014). A hallmark of pancreatic cancer is a high level of stroma in the tumours as seen in Figure 1-3, which is due to fibrosis. Fibrosis is defined as an accumulation of extracellular matrix (ECM) proteins due to the loss of balance between the manufacture and degradation of ECM (Apte, Pirola and Wilson 2012). This fibrosis plays a major role in the development and progression of pancreatic cancer. This fibrosis develops due to the stromal cells present in the pancreatic microenvironment. This body of work aimed to investigate the role of stromal cells in the development and progression of pancreatic cancer. To determine this, the functional effects of indirect co-culture of pancreatic cancer cell lines with human primary fibroblasts and pancreatic stellate cells were assessed, analysing the impact of cell to cell interactions. The functional effects assessed included proliferation, anoikis, invasion and colony formation. These functions were investigated due to their important role in the cascade of metastasis.

5.3. Panel of pancreatic cancer cell lines

The first step of the project was to establish the phenotypic properties of a panel of pancreatic cancer cell lines. Table 5-1 displays the origin and a representative image of the cell line in mono culture.

Table 5-1. Characteristics of a panel of four pancreatic cancer cell lines

Cell Line	Morphology	Mutational Status	Culture
AsPc-1	Epithelial cell line which produces abundant amounts of mucin. Derived from nude mouse xenografts initiated with cells from an ascites site in a female 62-year-old patient. Produce abundant mucin.	**Mutated:** KRAS,TP53 **Wildtype:** CDKN2A/p16, SMAD4/DPC4	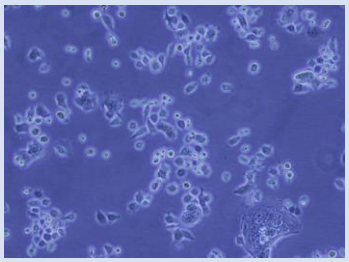
BxPc-3	Epithelial cell line which grows as tight sheets. Obtained from a female 61-year-old patient with cancer of the body of the pancreas. No metastasis had occurred	**Mutated:** TP53, SMAD4/DPC4 **Wildtype:** KRAS, CDKN2A/p16	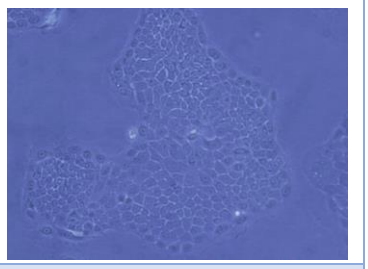
Mia PaCa-2	Epithelial cell line with a mesenchymal morphology. Developed from a tumour of a male 65-year-old patient involving the body and tail of the pancreas and had infiltrated the periaortic area	**Mutated:** KRAS,TP53, CDKN2A/p16, SMAD4/DPC4	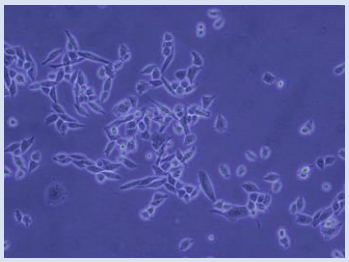
Panc-1	Epithelial cell line with a cuboidal morphology. Originated from a tumour of a female 56-year-old patient in the head of the pancreas which invaded the duodenal wall	**Mutated:** KRAS,TP53, CDKN2A/p16 **Wildtype:** SMAD4/DPC4	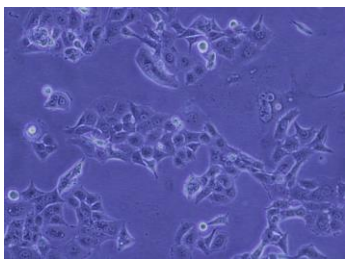

Figure 5-1. Levels of anoikis across a panel of pancreatic cancer cell lines

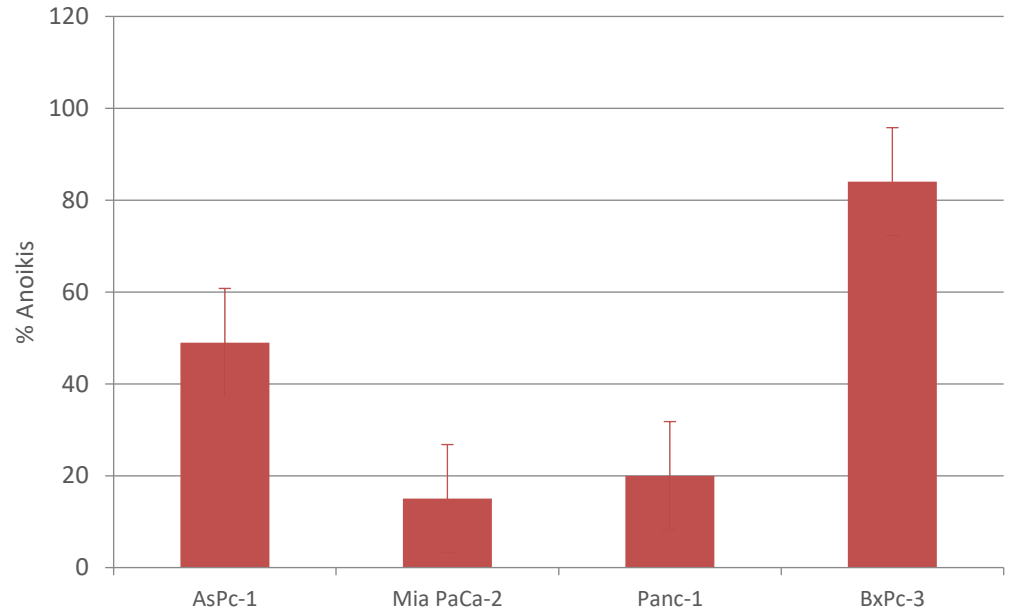

Characterisation of innate anoikis levels of four pancreatic cancer cells lines, AsPc-1, Mia PaCa-2, Panc-1 and BxPc-3. Assessment of the metabolic rate of a panel of pancreatic cancer cell lines in suspension conditions compared to attached conditions, as described in section 2.3 displayed as percentage anoikis i.e. the percentage cells surviving and metabolising in suspension conditions. Error bars represent +/- standard deviation between biological replicates, (n=3).

Figure 5-2. Levels of invasion across a panel of pancreatic cancer cell lines

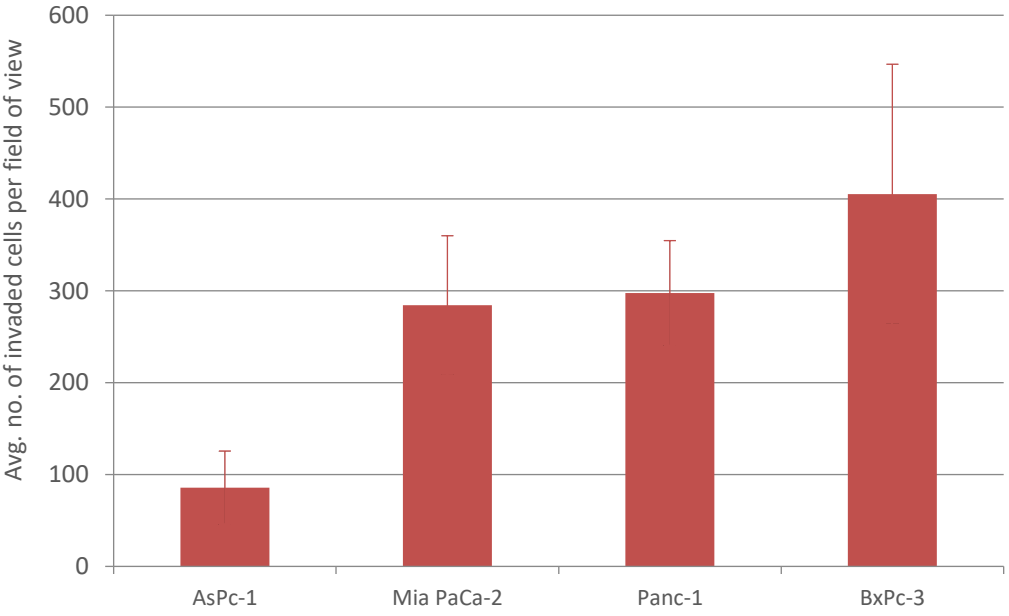

Characterisation of innate invasion levels of four pancreatic cancer cells lines, AsPc-1, Mia PaCa-2, Panc-1 and BxPc-3. Displayed as average number of invaded cells per field of view, to assess the invasive ability of a panel of pancreatic cancer cell lines. Error bars represent +/- standard deviation between biological replicates, (n=3).

Table 5-2. Relative levels of invasion and anoikis resistance across a panel of four pancreatic cancer cell lines

Characteristics	Relative Levels
Invasion	BxPc-3 > Panc-1 ≥ Mia PaCa-2 > AsPc-1
Anoikis Resistance	Mia PaCa-2 > Panc-1 > AsPc-1 > BxPc-3

Table 5-2 displays the basal levels of invasion and anoikis resistance across the panel of pancreatic cancer cell lines. The relative levels of anoikis resistance were determined from the data in Figure 5-1 and the levels of invasion are shown in Figure 5-2. These are the levels observed across the cell lines through multiple experiments. The levels of invasion observed, are in line with published data from a paper by Deer *et al.*, which reviews the phenotype and genotype of commonly used pancreatic cancer cell lines (Deer et al. 2010). Interestingly, there does not appear to be an exact correlation between invasive capabilities and ability to survive anoikis, the BxPc-3 cell possess the highest level of invasion but is the most anoikis sensitive whereas the Mia PaCa-2 cell line displays medium to low invasion levels with a high level of anoikis resistance. This panel was chosen as these four cell lines represented a wide range of levels in two of the cellular functions being assessed in this body of work.

5.4. Functional effects of 48hr indirect co-culture with stromal cell populations

This body of work aimed to investigate the role of stromal cells in the development and progression of pancreatic cancer. To determine this the functional effects of indirect co-culture of pancreatic cancer cell lines with human primary fibroblasts and pancreatic stellate cells were assessed, analysing the impact of cell to cell interactions. This work involved culturing the panel of pancreatic cancer cell lines with pancreatic stromal cells above in a co-culture insert as described in section 2.15 and shown in Figure 5-3. After 48hr of co-culture the pancreatic cancer cells were detached and assessed for changes in levels of survival in suspension i.e. anoikis, proliferation and invasion due to indirect

co-culture. These functions were investigated due to their important role in the cascade of metastasis.

5.4.1. Functional effects of 48hr indirect co-culture with tumour derived fibroblasts (Pt-102)

The patient tumour derived fibroblasts were developed in house. Tumour samples, received from St. Vincent's University Hospital, were enzymatically digested using hyaluronidase and collagenase. Following this digestion, the samples were then explanted into culture and outgrowth used to develop fibroblasts. The first fibroblast line developed, Pt-102, was derived from a poorly differentiated cholangiocarcinoma diagnosed in a 61-year-old Irish male. These patient tumour derived fibroblasts were used to investigate the role of stromal cells in the development and progression of pancreatic cancer. This work involved culturing the panel of pancreatic cancer cell lines with the tumour derived fibroblasts (Pt-102) above in a co-culture insert. After 48hr of co-culture the pancreatic cancer cells were detached and assessed for changes in levels of survival in suspension i.e. anoikis, proliferation and invasion due to indirect co-culture.

Figure 5-3. A schematic of the indirect co-culture model used to investigate the pancreatic tumour microenvironment

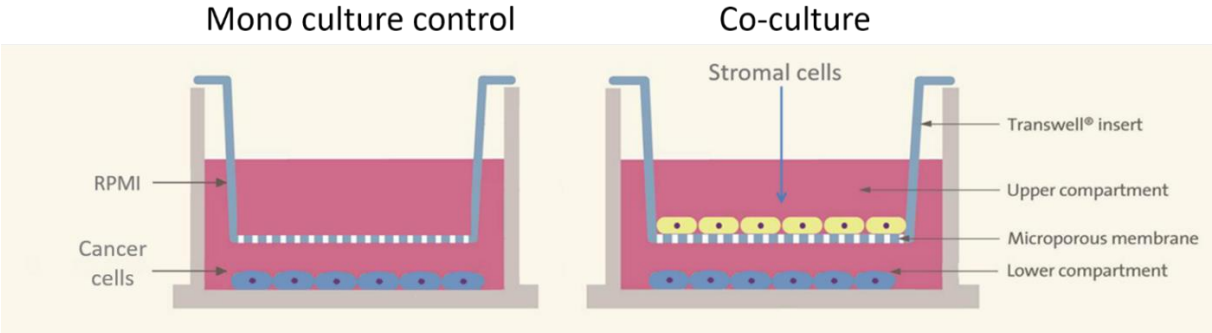

Schematic of the indirect co-culture model set up. Pancreatic cancer cells are seeded in a 6 well plate with the stromal cell population above in a co-culture insert above. The insert contains a polyester membrane with 3.0µm pores which allow secretions to pass between the two cell types (Crosson 2014).

Figure 5-4. Percentage survival in attached and suspension conditions of **Mia PaCa-2** cells post co-culture

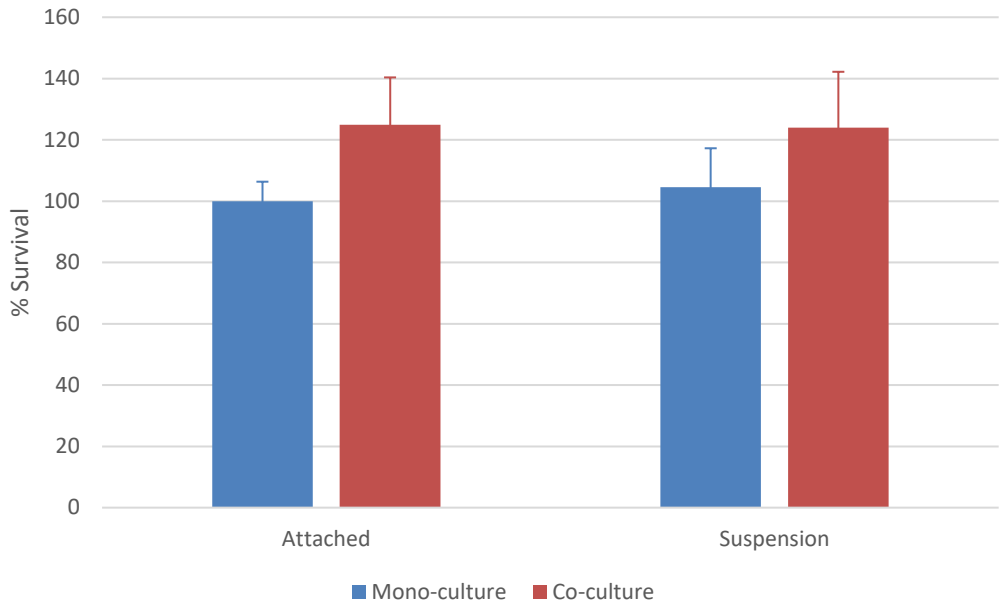

Percentage survival at 24hr in attached and suspension i.e. anoikis conditions, relative to attached mono culture of the **Mia PaCa-2** cell line following 48hr indirect co-culture with pancreatic tumour derived fibroblasts (**Pt-102**). Error bars represent +/- standard deviation between biological replicates, (n=3).

Figure 5-5. Percentage survival in attached and suspension conditions of **Panc-1** cells post co-culture

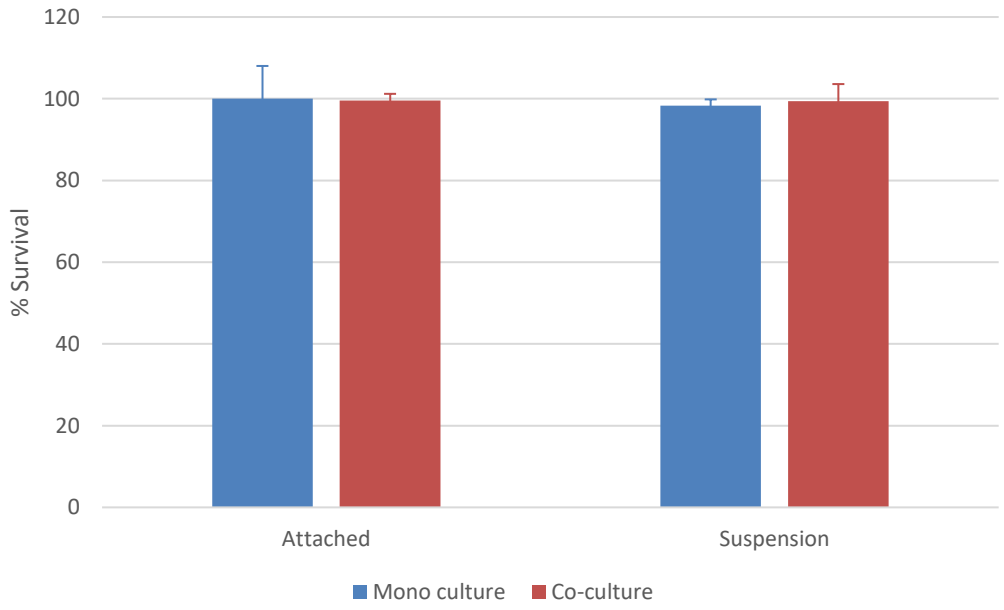

Percentage survival at 24hr, in attached and suspension i.e. anoikis conditions, relative to attached mono culture of the **Panc-1** cell line following 48hr of indirect co-culture with pancreatic tumour derived fibroblasts (**Pt-102**). Error bars represent +/- standard deviation between biological replicates, (n=3).

Following 48hrs exposure to the secondary cell type, in this instance, fibroblasts, the pancreatic cancer cells were trypsinised and in seeded into attached and suspension conditions for 24hr to assess survival post co-culture Post co-culture, in suspension conditions survival was increased by 20% compared to mono culture cells in Mia PaCa-2 cells as seen in Figure 5-4. Co-culturing the Mia PaCa-2 cells with tumour derived fibroblasts over a 48hr period appears to have increased the cancer cells ability to survive in suspension. Figure 5-4 also showed an increase in survival (25%) in attached conditions post co-culture compared to mono culture which may indicate an increase in growth. The dye used in the anoikis assay, Alamar Blue, measures metabolic activity indicating post co-culture, it appears more metabolism was present leading to the conclusion that more cells were present. No effect on survival in either attached or suspension conditions were observed post co-culture in the Panc-1 cell line, seen in Figure 5-5. AsPc-1 and BxPc-3 do not feature in the anoikis results as both these cell lines are highly anoikis sensitive it is extremely difficult to get successful data from an anoikis assay using these cell lines. The cell lines clump and metabolise the dye very little which can lead to negative readings, cells may also become senescent.

Figure 5-6. Percentage proliferation post co-culture across a panel of pancreatic cancer cell lines

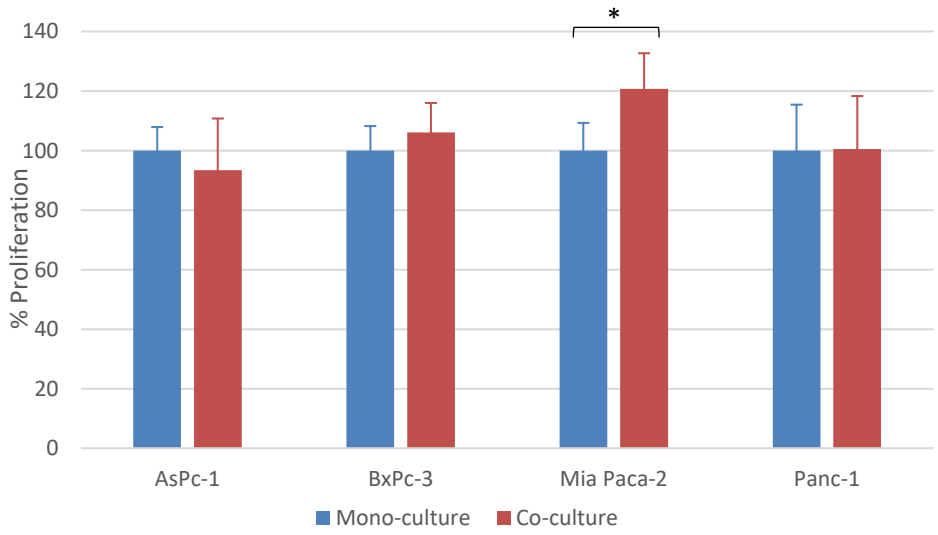

Percentage proliferation after 7 days' incubation, following 48hr of indirect co-culture relative to mono culture, of **AsPc-1**, **BxPc-3**, **Mia PaCa-2** and **Panc-1** cell lines with pancreatic tumour derived fibroblasts (**Pt-102**). Error bars represent +/- standard deviation between biological replicates, (n=3, * = p value ≤ 0.05, Mia PaCa-2 p value = 0.03).

Proliferation was assessed after 7 days of culture which was preceded by 48hr of co-culture using an acid phosphatase method described in section 2.11. The hypothesis that the increased survival of the Mia PaCa-2 cells observed post co-culture in attached conditions (Figure 5-4) was due to increased proliferation, was validated by Figure 5-6. This figure shows a significant increase in proliferation in the Mia Pa-Ca-2 cell line post co-culture compared to mono culture. The increase in proliferation across three biological replicates was calculated as 20% with this result being significant due to a p value of 0.03. There was also no effect on proliferation, in Figure 5-6, of the Panc-1 cell line relative to mono culture. There was a slight increase in proliferation in the BxPc-3 cell line post co-culture while a slight decrease in proliferation was observed in the AsPc-1 cell line, although neither result showed significance.

Figure 5-7. Percentage invasion post co-culture across a panel of pancreatic cancer cell lines

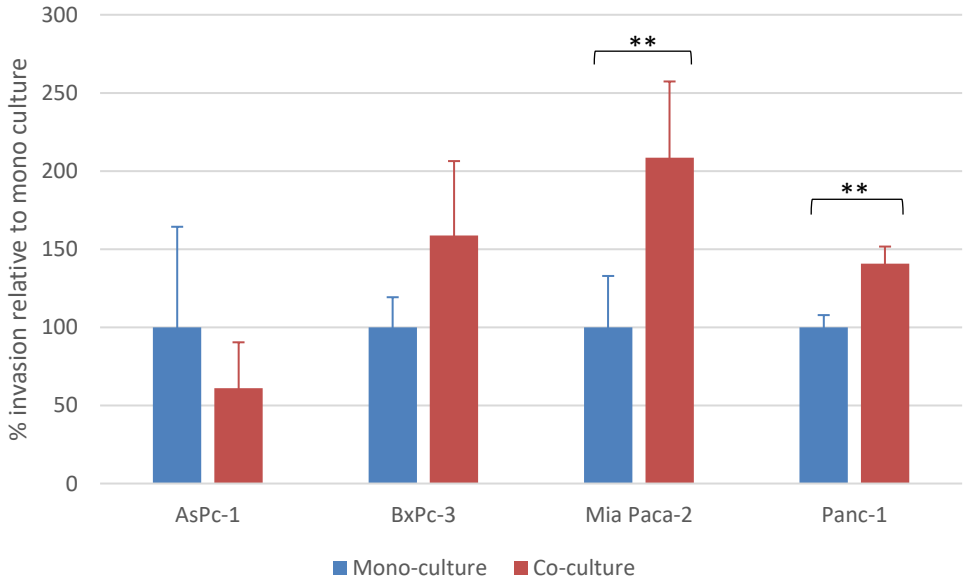

Percentage invasion at 24hr post 48hr of indirect co-culture with pancreatic tumour derived fibroblasts **(Pt-102**) relative to mono culture of **AsPc-1**, **BxPc-3**, **Mia PaCa-2** and **Panc-1** cell lines. Error bars represent +/- standard deviation between biological replicates, (n=3, ** = p value ≤ 0.01, Mia PaCa-2 p value = 0.01, Panc-1 p value = 0.003).

Figure 5-8. Representative images of invasion post a) mono culture and b) co-culture conditions across a panel of pancreatic cancer cell lines

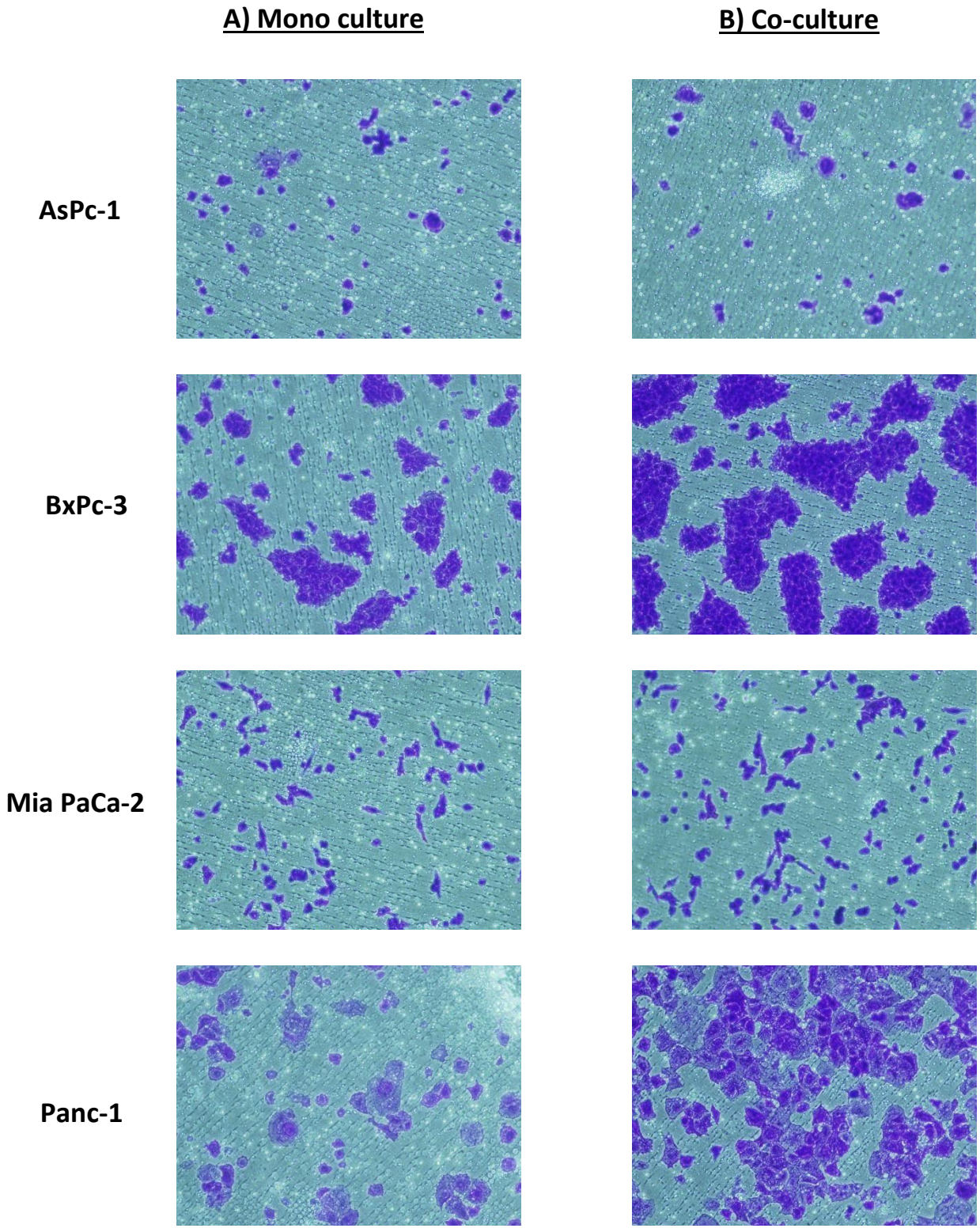

Representative images of invasion levels following both A) mono and B) co-culture of **AsPc-1**, **BxPc-3**, **Mia PaCa-2** and **Panc-1** cell lines with pancreatic tumour derived fibroblasts (**Pt-102**).

The most notable change in phenotype following co-culture with human tumour derived fibroblasts (Pt-102) was an increase in invasive capabilities in three out of the four cell lines: BxPc-3, Mia PaCa-2 and Panc-1 shown in Figure 5-7 and Figure 5-8. This increase was significant in both the Mia PaCa-2 and Panc-1 cell line with an increase of 100% and a p value of 0.01 and an increase of 40% and a p value of 0.01, respectively. BxPc-3 cells exhibited a higher level of invasion post co-culture, an increase of 60% but this result was not significant. This may be due to the high level of error observed in the invasion of the BxPc-3 cell line as these cells invaded as clumps of cells as seen in Figure 5-8. Analysing invasion using a cell counting method may be not ideal for this cell line. AsPc-1, a lowly invasive cell line appeared to become less invasive, a 40% reduction, following co-culture with the tumour derived fibroblasts. Figure 5-8 contains pictures of invasion levels for all four cell lines post mono culture and co-culture.

5.4.2. Functional effects of conditioned media of Pt-102

It was hypothesised that the significant increase in invasion post co-culture observed in both the Mia PaCa-2 and Panc-1 cell lines may be due to secretions being released by the tumour derived fibroblasts. To assess this hypothesis an experiment was designed to examine if the secretions from the fibroblasts induced the same functional effects. This involved using the exact previous co-culture set up with one main difference, instead of the fibroblasts being seeded above in a transwell insert conditioned media (CM) from the fibroblasts was used as a treatment for the pancreatic cancer cells. In an effort to maintain consistency between the two different experiment types several steps were taken. This included using media containing FBS in the conditioned media treatment, it is usual practice when performing conditioned media experiments to use serum-free media. Also, conditioned media practices generally involve concentrating the conditioned media. These steps were not used in this experiment as the aim was to maintain as much consistency as possible between the co-culture set up and the treatment i.e. serum containing media with no concentration of the conditioned media. The fibroblasts were cultured for 48hr in a 6 well format using the same cell number seeded in the co-culture insert ($1x10^5$). Conditioned media was then collected, debris

removed through centrifugation before treating the pancreatic cancer cells. The pancreatic cancer cells were treated with the CM for 48hr before being removed and assessed for functional effects.

Figure 5-9. Percentage survival in attached and suspension conditions of **Mia PaCa-2** cells post conditioned media treatment

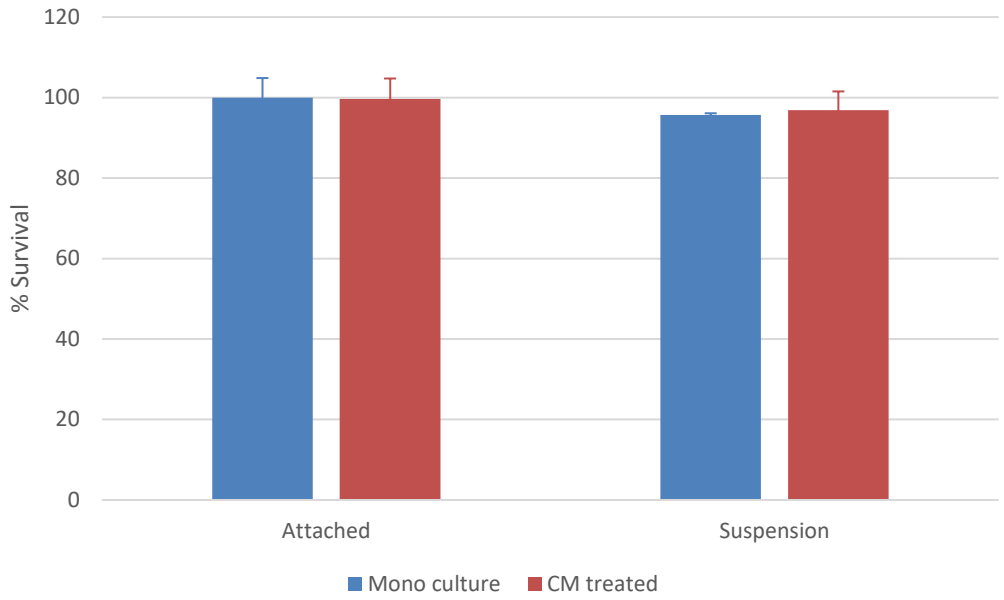

Percentage survival relative to attached mono culture, in attached and suspension i.e. anoikis, conditions of the **Mia PaCa-2** cell line following treatment with conditioned media from the pancreatic tumour derived fibroblasts (**Pt-102**). Error bars represent +/- standard deviation between biological replicates, (n=3).

Figure 5-10. Percentage survival in attached and suspension conditions of **Panc-1** cells post conditioned media treatment

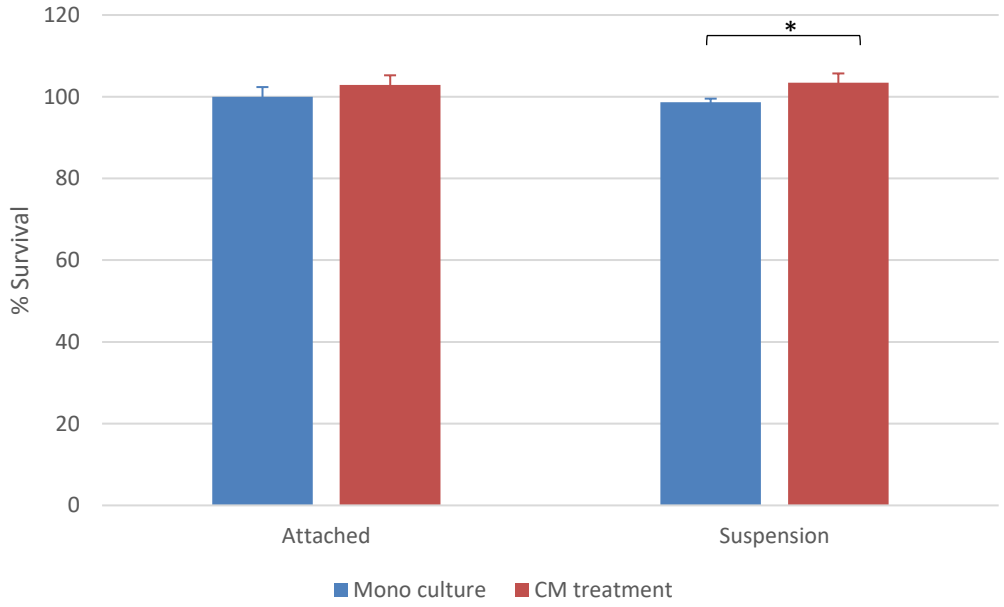

Percentage survival relative to attached mono culture, in attached and suspension i.e. anoikis, conditions of the **Panc-1** cell line following treatment with conditioned media from the pancreatic tumour derived fibroblasts (**Pt-102**). Error bars represent +/- standard deviation between biological replicates, (n=3, * = p value ≤ 0.05).

Treatment of Mia PaCa-2 cells with conditioned media from tumour derived fibroblasts (Pt-102) resulted in no change in levels of survival while in suspension or attached conditions post treatment, as seen in Figure 5-9. A slight increase in survival (5%) was observed in the Panc-1 cell line, shown in Figure 5-10, in suspension conditions post CM treatment compared to mono culture. While this result shows statistical significance, a 5% change is not sufficient to be considered biologically significant. A slight increase in the Panc-1 cells ability to survive in suspension may have been induced due to CM treatment.

Figure 5-11. Percentage proliferation in **Mia PaCa-2** and **Panc-1** cells post conditioned media treatment

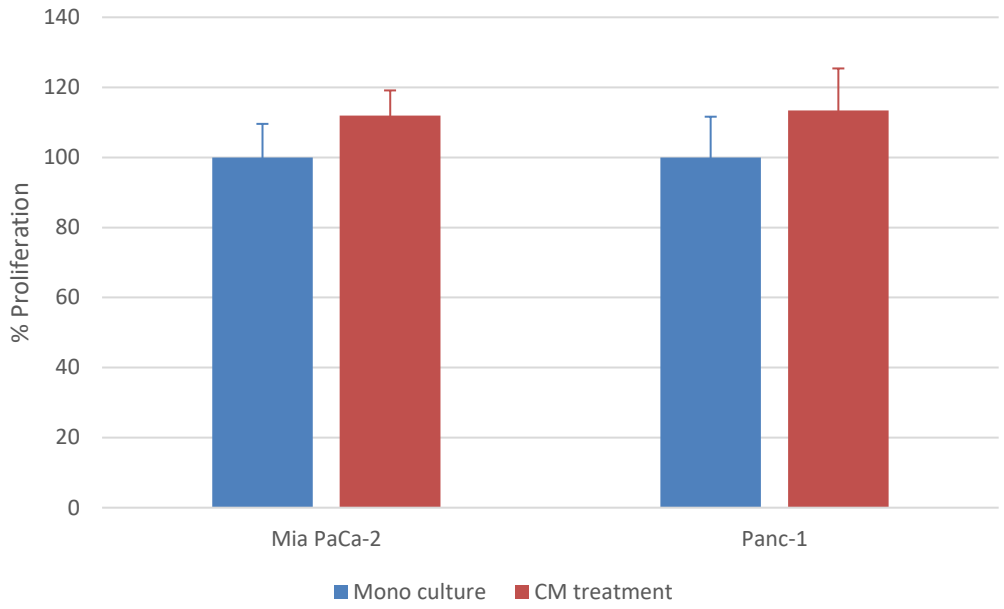

Percentage proliferation of **Mia PaCa-2** and **Panc-1** cell lines following treatment with conditioned media from the pancreatic tumour derived fibroblasts (**Pt-102**). Error bars represent +/- standard deviation between biological replicates, (n=3).

Post CM treatment a small increase in proliferation, ~10%, was observed, seen in Figure 5-11, in both the Mia PaCa-2 and Panc-1 cell lines, although analysis showed these results did not possess statistical significance. This proliferation level was measured after 7 days of culture prior to which the pancreatic cancer cells had been treated for 48hr with Pt-102 fibroblasts CM.

Figure 5-12. Percentage invasion of the **Panc-1** cell line post treatment with conditioned media

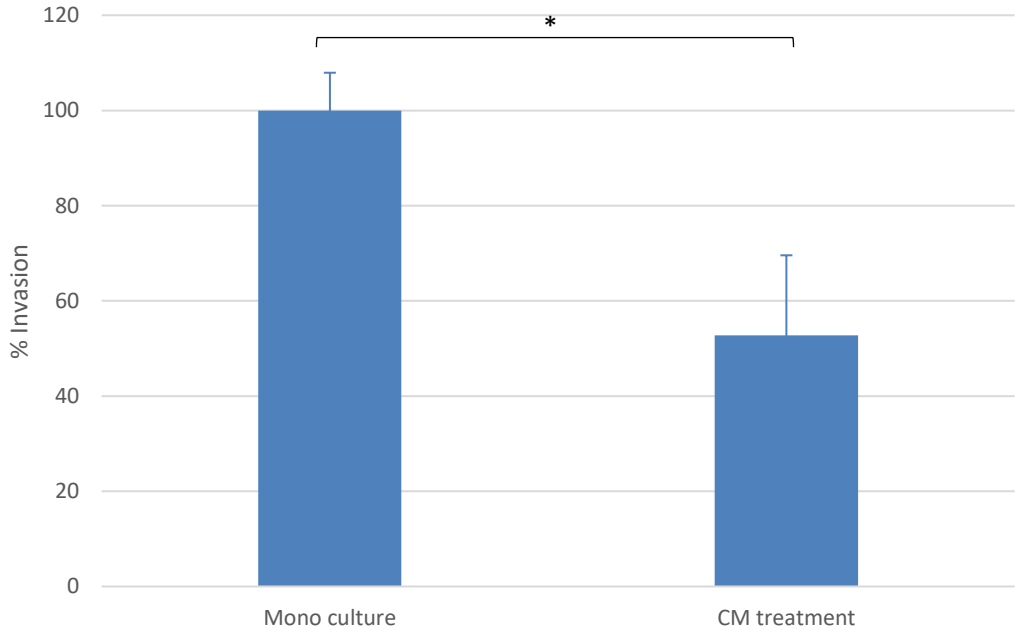

Percentage invasion of the **Panc-1** cell line post treatment with conditioned media of pancreatic tumour derived fibroblasts (**Pt-102**) relative to mono culture of the Panc-1 cell line. Error bars represent +/- standard deviation between biological replicates, (n=2, * = p value ≤ 0.05, p value = 0.05).

The most noteworthy phenotypic change post CM is displayed in Figure 5-12, showing a 50% reduction in invasion of the Panc-1 cell line relative to mono culture. Analysis showed this result to be of low significance which may be due to the presence of only two biological replicates and error between biological replicates. The pancreatic cancer cells were treated with Pt-102 fibroblasts CM for 48hr prior to assessment for changes in invasive capabilities over 24hr of culture in the invasion assay set up, described in section 2.12.

5.4.3. Functional effects of indirect co-culture with tumour derived fibroblasts (Pt-127)

To further investigate the role of stromal cells in the development and progression of pancreatic cancer, the functional effects of indirect co-culture of pancreatic cancer cell lines with a second batch of human primary fibroblasts derived from a different patient (Pt-127), were assessed. While both fibroblast primary cell lines were developed in the same way, they have differences, see section 2.1.1.. Both fibroblast populations had different pathology, levels of differentiation and invasive capabilities. Due to these differences, it was important to assess both stromal populations in the indirect co-culture model to assess if similar or different phenotypic changes were induced. It was highly important to ensure the changes observed were not batch specific and to assess differences observed due to different diagnosis or pathology. This work involved culturing the panel of pancreatic cancer cell lines with tumour derived fibroblasts above in a co-culture insert, as described in section 2.15. After 48hr the panel of pancreatic cancer cells were detached and assessed for changes in levels of survival in suspension i.e. anoikis, proliferation and invasion due to indirect co-culture. The panel of cell lines was reduced from four to two; to include just the Mia PaCa-2 and Panc-1 cell lines as these showed the most significant results in previous co-culture experiments using Pt-102 fibroblasts. These were also the most flexible and adaptable cell lines in all of the functions this work assessed. The BxPc-3 and AsPc-1 cell lines were not suitable for invasion or anoikis assays. Statistical significance was not shown in any of the phenotypic changes induced due to Pt-127 fibroblasts as before three biological replicates were performed a change in assay format occurred. This change in assay format occurred due to results observed and described in section 5.5, time-course experiment.

Figure 5-13. Percentage survival in attached and survival conditions of **Mia PaCa-2** cells post co-culture with **Pt-127**

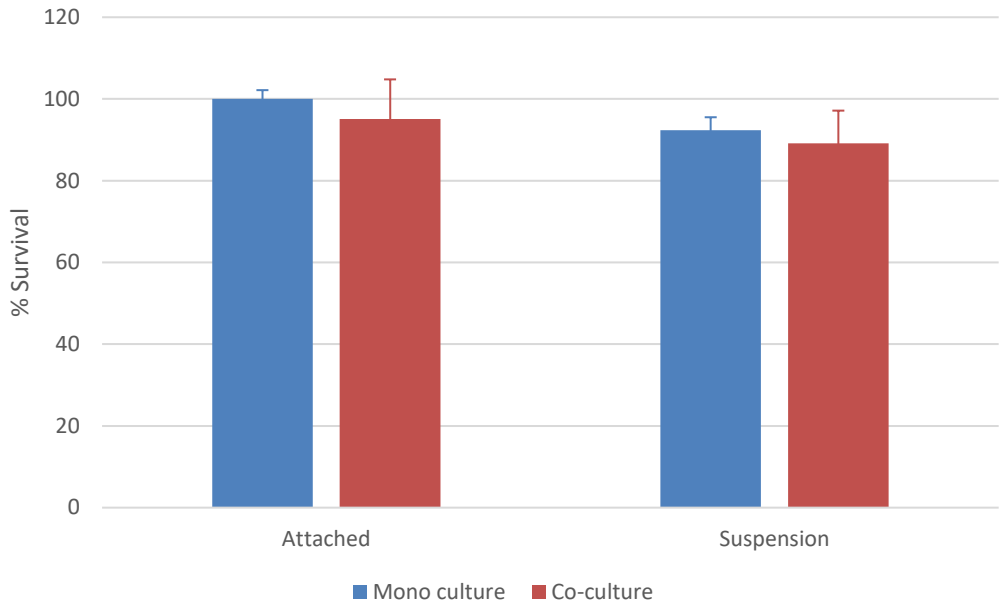

Percentage survival relative to attached mono culture, in attached and suspension i.e. anoikis, conditions of the **Mia PaCa-2** cell line following indirect co-culture with pancreatic tumour derived fibroblasts **(Pt-127**). Error bars represent +/- standard deviation between biological replicates, (n=3).

Figure 5-14. Percentage survival in attached and survival conditions of **Panc-1** cells post co-culture with **Pt-127**

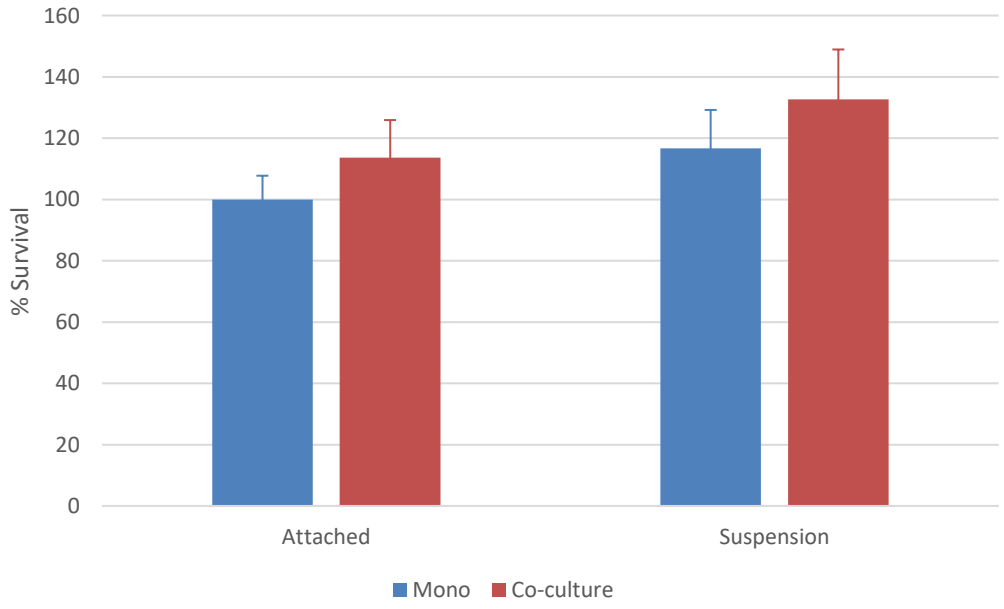

Percentage survival relative to attached mono culture, in attached and suspension i.e. anoikis, conditions of the **Panc-1** cell line following indirect co-culture with pancreatic tumour derived fibroblasts (**Pt-127**). Error bars represent +/- standard deviation between biological replicates, (n=2).

Indirect co-culture of pancreatic cancer cell lines with a different batch of fibroblasts, derived from patient 127 (Pt-127) yielded the following results. Figure 5-13 displays a small decrease in survival of the Mia PaCa-2 cell line in both attached and suspension conditions post co-culture. The opposite result was observed in the Panc-1 cell line, shown in Figure 5-14 an increase in survival in both attached (13%) and suspension (15%) conditions post co-culture. The increase in survival in attached conditions post co-culture compared to mono culture (13%) may indicate an increase in growth.

Figure 5-15. Percentage proliferation of **Mia PaCa-2** and **Panc-1** cells post co-culture with **Pt-127**

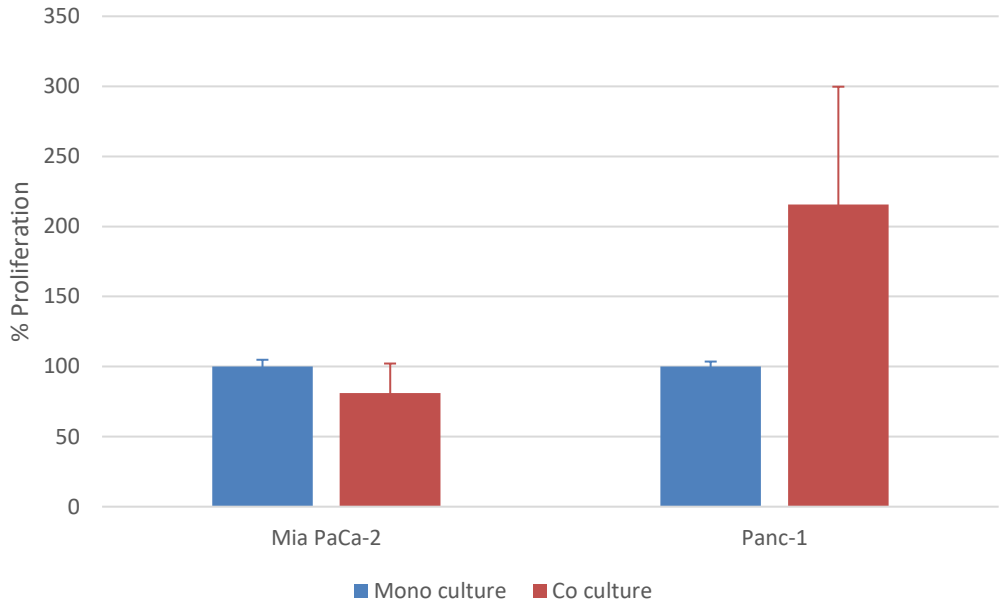

Percentage proliferation following co-culture relative to mono culture of **Mia PaCa-2** and **Panc-1** cell lines with pancreatic tumour derived fibroblasts (**Pt-127**). Error bars represent +/- standard deviation between biological replicates, (Mia PaCa-2 n=3, Panc-1 n=2).

The hypothesis that the increase in survival of the Panc-1 cells in attached conditions observed in Figure 5-14 was due to an increase in growth was confirmed, shown in Figure 5-15. This shows a large (115%) increase in proliferation in the Panc-1 cell line and it can also be seen that a reduction in proliferation (20%) was observed in Mia PaCa-2

cells post co-culture with Pt-127 fibroblasts. Neither result showed statistical significance.

Figure 5-16. Percentage invasion of **Mia PaCa-2** and **Panc-1** cells post co-culture with **Pt-127**

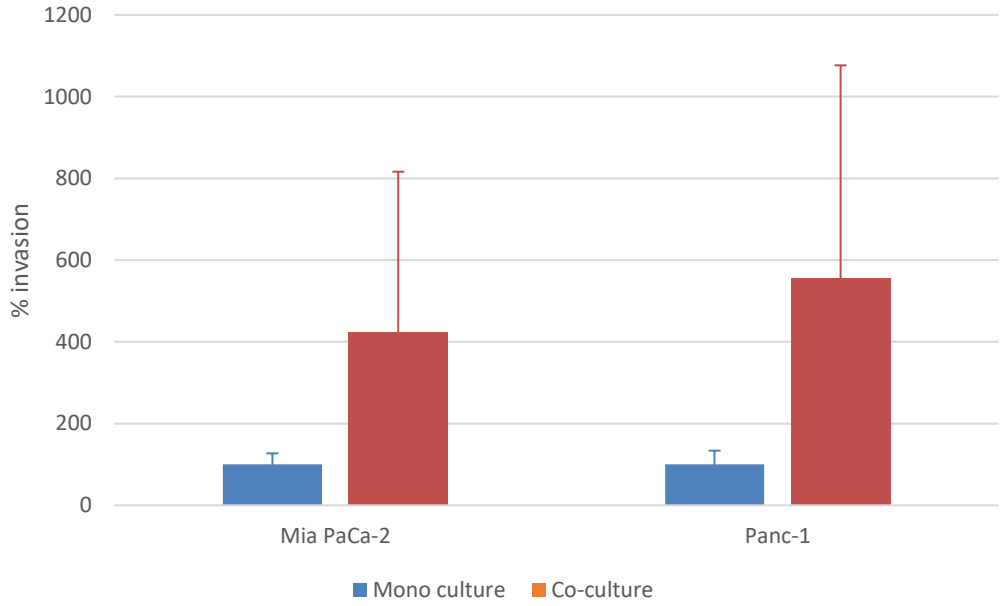

Percentage invasion following co-culture of **Mia PaCa-2** and **Panc-1** cell lines with pancreatic tumour derived fibroblasts (**Pt-127**) relative to mono culture. Error bars represent +/- standard deviation between biological replicates, (n=2).

Both cell lines displayed a large increase in invasion post co-culture as seen in Figure 5-16, 300% and 450% respectively, while large error bars are present the trend was visible with each biological replicate. More biological replicates are required to analyse if statistical significance is present, it does appear a trend of a large increase in invasion was present in both the Mia PaCa-2 and Panc-1 cell lines post co-culture with Pt-127 fibroblasts.

5.4.4. Functional effects of indirect co-culture with pancreatic stellate cells

Another aspect of the pancreatic tumour microenvironment being investigated in this work was the role of the pancreatic stellate cell. The indirect co-culture model was used with pancreatic stellate cells as the stromal component to assess phenotypic changes induced in the pancreatic cancer cells post indirect co-culture. Several different batches of human pancreatic stellate cells were donated by Dr. Masamune, based in Tohoku University in Sendai, Japan. Statistical significance was not shown in any of the phenotypic changes induced due to hPSC24 stellate cells as before three biological replicates were performed a change in assay format occurred. This change in assay format occurred due to results observed and described in section 5.5, time-course experiment.

Figure 5-17. Percentage proliferation of **Mia PaCa-2** and **Panc-1** cells post co-culture with pancreatic stellate cells (**hPSC24)**

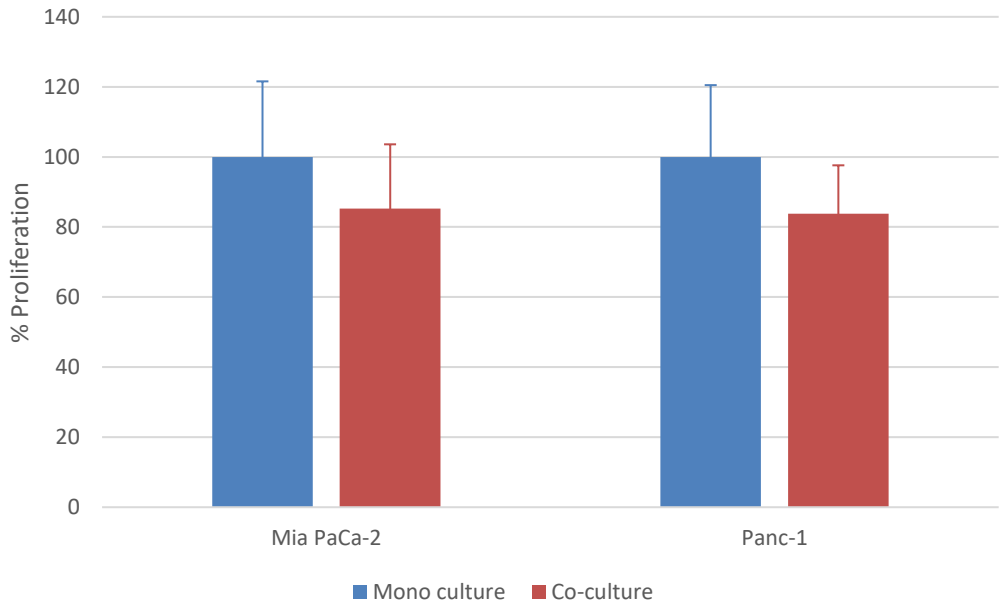

Percentage proliferation following co-culture relative to mono culture, of **Mia PaCa-2** and **Panc-1** cell lines with human pancreatic stellate cells (**hPSC24**). Error bars represent +/- standard deviation between biological replicates, (n=2).

Co-culture of the Mia PaCa-2 and Panc-1 cell lines with human pancreatic stellate cells (hPSC24) resulted in a 20% reduction in proliferation in both the Mia PaCa-2 and Panc-1 cell line, Figure 5-17. Analysis showed neither result displayed statistical significance.

Figure 5-18. Percentage invasion of **Mia PaCa-2** and **Panc-1** cells post co-culture with pancreatic stellate cells **(hPSC24**)

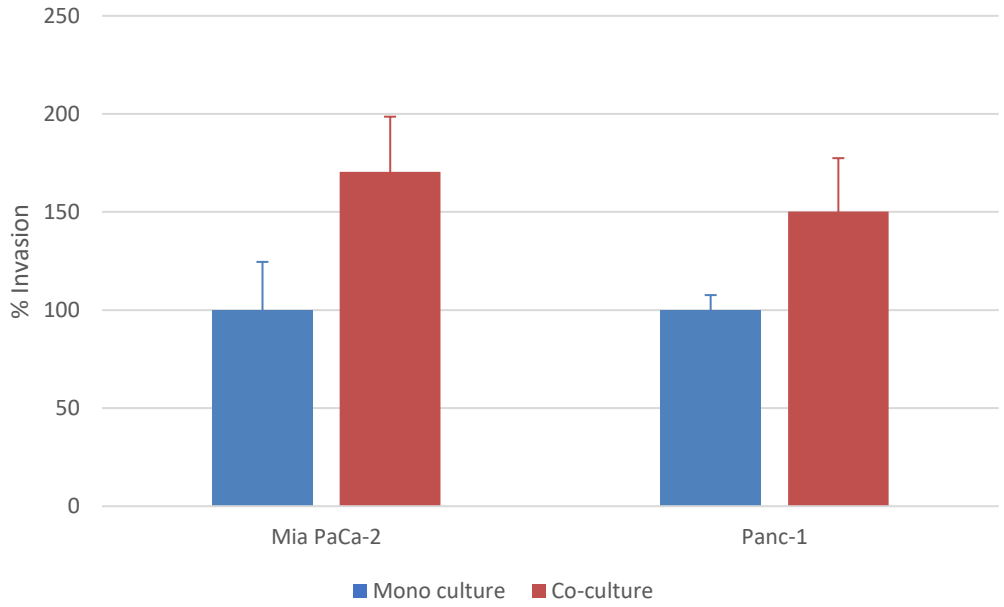

Percentage invasion following co-culture relative to mono culture, of **Mia PaCa-2** and **Panc-1** cell lines with human pancreatic stellate cells (**hPSC24**). Error bars represent +/- standard deviation between biological replicates, (Mia PaCa-2 n=1, Panc-1 n=2).

Conversely to the proliferation result in Figure 5-17 both cells lines exhibited a large increase in invasion post co-culture with hPSC24 cells, 70% and 50% respectively, shown in Figure 5-18. Due to these contrasting phenotypes, it can be deducted that this increase in invasion was not due to an increase in proliferation. These results require more biological replicates to determine if these effects were statistically significant.

5.5. Time-course experiment

In previous co-culture experiments a time-point of 48hr had been used to assess functional effects of co-culture. This time-point was chosen based on literature and publications on co-culture of stromal cells with pancreatic cancer cells (Takikawa et al. 2013, Kikuta et al. 2010, Fujita et al. 2009). Co-cultures up until this point had shown some but inconsistent effects on proliferation across the panel. Assessment of proliferation post co-culture in previous experiments has involved trypsinisation of cells post mono and co-culture. The same cell number was then seeded and incubated over five days. On the fifth day, an acid phosphatase experiment, see section 2.11, was performed to assess proliferation. To assess if this co-culture set up was optimum for assessing functional effects a time-course experiment was performed. This involved setting up indirect co-cultures of Pt-102 fibroblasts with the Mia PaCa-2 cell line and assessing for functional effects on invasion and proliferation through cell counts, after 24, 48 and 72 hours of co-culture.

Figure 5-19. Cell number of **Mia PaCa-2** cells post indirect co-culture with tumour derived fibroblasts (**Pt-102**) at a range of time-points

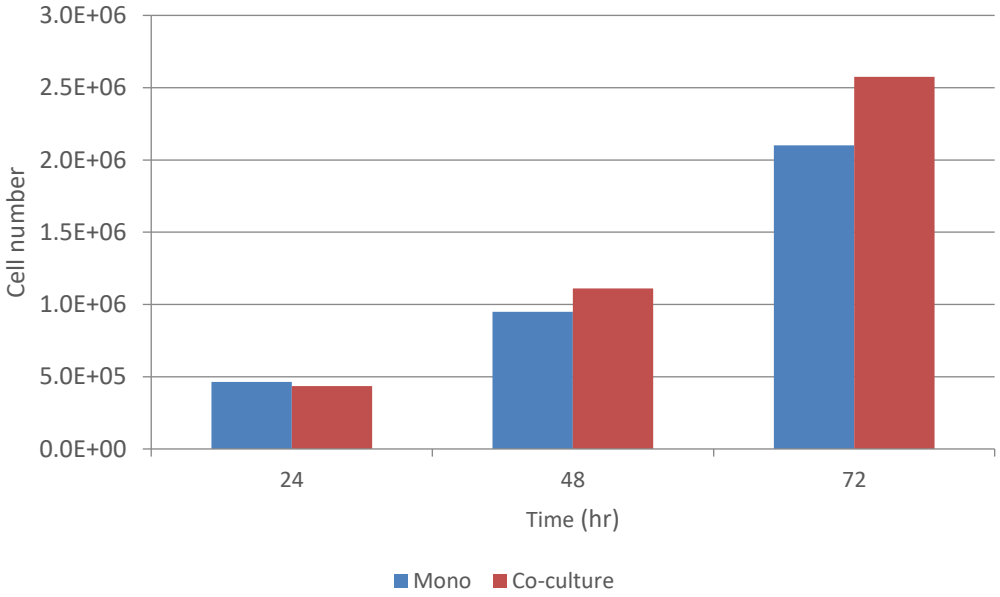

Cell number of the **Mia PaCa-2** cell line following both mono and co-culture of with pancreatic tumour derived fibroblasts (**Pt-102**) at time-points of 24hr, 48hr and 72hr assessed using a haemocytometer, (n=1).

Figure 5-20. Invasion levels of **Mia PaCa-2** cells post co-culture with tumour derived fibroblasts (**Pt-102**) at a range of time-points

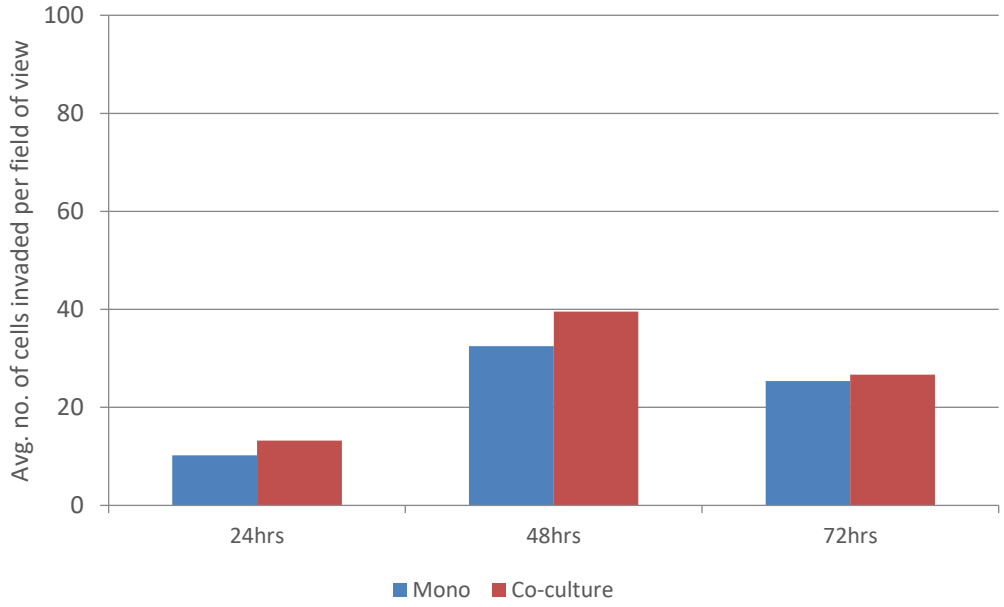

Average number of invading cells per field of view following co-culture of **Mia PaCa-2** cell line with pancreatic tumour derived fibroblasts (**Pt-102**) at time-points of 24hr, 48hr and 72hr, (n=1).

Figure 5-19 shows the cell number of the Mia PaCa-2 cell line following both mono and co-culture of with pancreatic tumour derived fibroblasts (Pt-102) at time-points of 24hr, 48hr and 72hr. While the cell number increases over time due to culture there was an increase in cell number post co-culture compared to mono culture at both the 48hr and 72hr time-points. This increase appeared to continue incrementally over the length of the time-course. Figure 5-20 shows the changes in invasion following co-culture of Mia PaCa-2 cell line with pancreatic tumour derived fibroblasts (Pt-102) at time-points of 24hr, 48hr and 72hr. An increase in invasion post co-culture was observed at both the 24 and 48hr time-point but the effect on invasion post co-culture appeared to have tapered off at the 72hr time-point. While the previous co-culture format was efficient at examining phenotypic changes in invasion post co-culture it was not sufficient to assess the changes the stromal cells induced in the proliferation levels of the pancreatic cancer cells.

5.6. In-assay indirect co-culture of Panc-1 cells with stromal cells

A hypothesis that an effect on proliferation due to co-culture was present but being missed in proliferation experiments was established due to the observation that the cell number in samples post co-culture with Pt-102 was consistently higher than mono culture samples, this effect can be seen in Figure 5-19. This hypothesis was confirmed through Figure 5-19 and Figure 5-20. This was found to be especially true for the Panc-1 cell line which consistently displayed a higher cell number post co-culture but no effect on proliferation was found, as seen in Figure 5-6. Due to this, the Panc-1 cell line was used to investigate phenotypic changes in proliferation and colony formation due to the presence of tumour derived fibroblasts with an 'in assay' co-culture format. In this format the two cell populations are indirectly co-cultured in the functional assay set up for the duration of the assay as opposed to the previous format. The previous format involved only a 48hr co-culture with the cells being trypsinised and re-seeded into functional assays. This new, 'in-assay' format involved the Panc-1 cells being seeded into functional assays (proliferation and colony formation assays) with the stromal cells above in a co-culture insert for the entire length of the assay (7 days for proliferation, 14 days for colony formation). Meaning the cancer and stromal cells were interacting throughout the time of the assay, at the end point the effect of co-culture on proliferation and colony formation was examined. Colony formation was assessed for phenotypic changes post co-culture also as it can also be an indication of changes in growth.

Figure 5-21. Percentage proliferation of **Panc-1** cells post in-assay co-culture with **Pt-102** and **hPSC24**

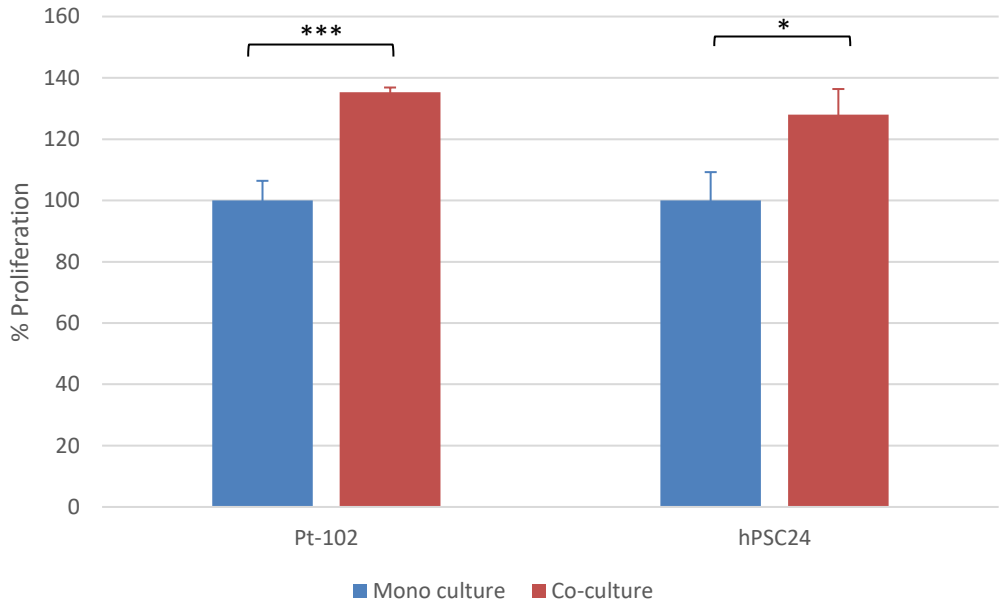

Percentage proliferation following 7 days of in-assay co-culture of **Panc-1** cell lines with pancreatic tumour derived fibroblasts (**Pt-102**) and human pancreatic stellate cells (**hPSC24**) relative to mono culture. Error bars represent +/- standard deviation between biological replicates, (n=3, * = p value ≤ 0.05, *** = p value ≤ 0.001, Pt-102 p value = 0.00066, hPSC24 p value = 0.02).

An increase in proliferation of the Panc-1 cells was observed post 7 days of in-assay co-culture with the tumour derived fibroblasts (Pt-102) and human pancreatic stellate cells (hPSC24), shown in Figure 5-21. Proliferation was assessed using the acid phosphatase method detailed in section 2.11, with the proliferation of co-cultured cells displayed relative to mono culture. The increase in proliferation post co-culture with Pt-102 fibroblasts across three biological replicates was calculated as 35% with this result being highly significant due to a p value of 0.00066. The increase in proliferation post co-culture with hPSC24 was observed to be 28% with this result being lowly significant due to a p value of 0.02.

Figure 5-22. Colony formation of **Panc-1** cells post in-assay co-culture with **Pt-102**

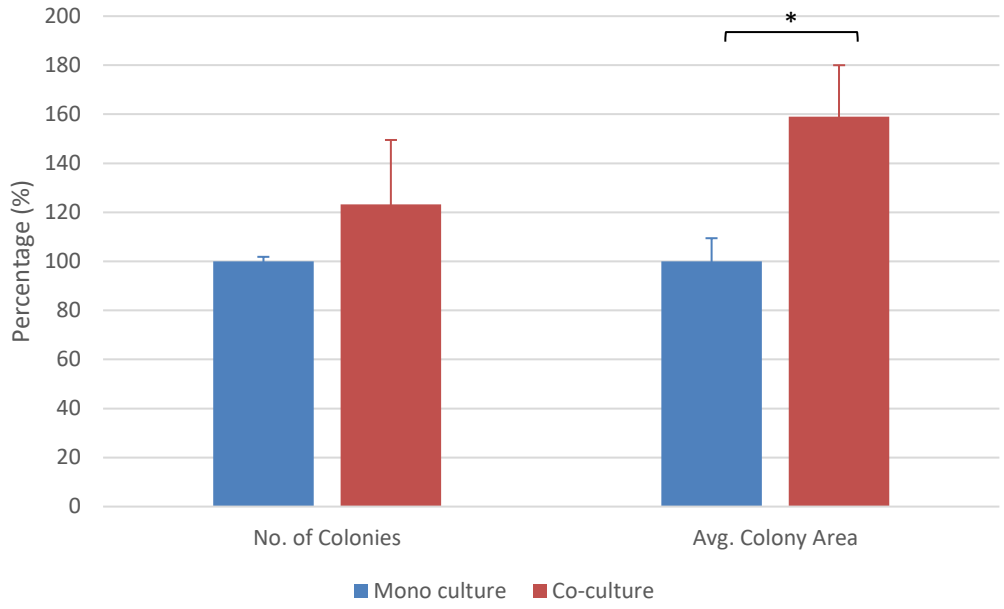

Number of colonies and average colony area percentage relative to mono culture of **Panc-1** cells observed 14 days' post mono and in-assay co-culture with tumour derived fibroblasts (**Pt-102**). Colonies were analysed using MetaMorph software. Error bars represent +/- standard deviation between biological replicates, (n=3, * = p value ≤ 0.05, p value = 0.03).

Figure 5-23. Representative image of colony formation of **Panc-1** cells post in-assay co-culture

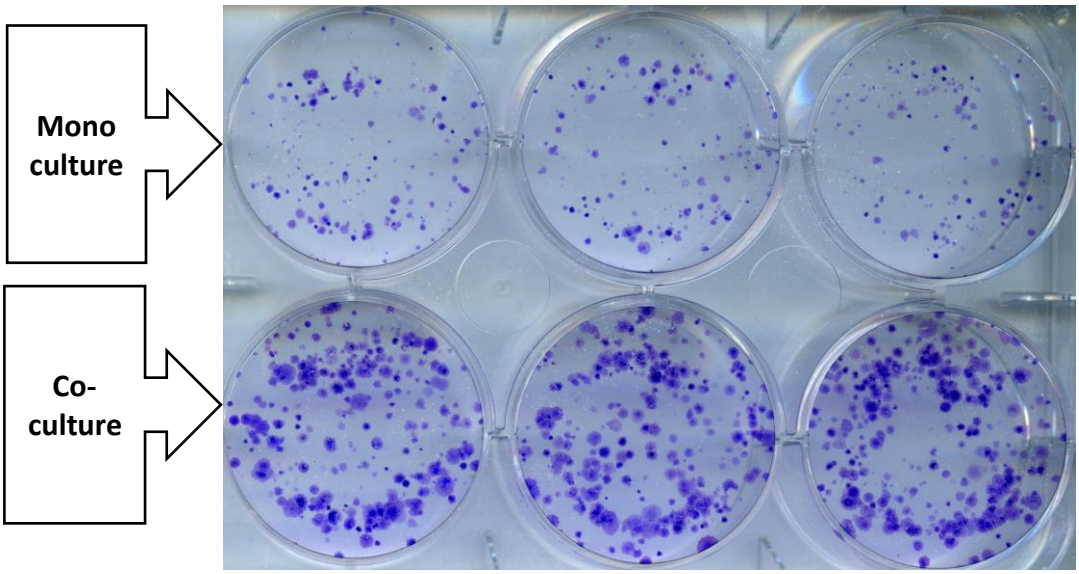

Representative image of colonies of **Panc-1** cells observed post mono and in-assay co-culture with tumour derived fibroblasts (**Pt-102**).

Post in-assay co-culture with Pt-102 fibroblasts, Panc-1 cells formed a greater number of colonies and colonies of a larger size relative to colonies of mono cultured Panc-1 cells, as seen in Figure 5-22. Analysis (MetaMorph Image Analysis software) of the number of colonies did not show a significant p value but a trend of greater number of colonies being formed post co-culture appeared to be present, as shown in Figure 5-23 The average increase in colony size across three biological replicates was 60% larger colonies formed post co-culture relative to mono culture with a p value of 0.03. The functional effect of hPSC24 on colony formation was being assessed but before three biological replicates were achieved, the results in the following sections were observed.

5.7. Determination of the optimum co-culture control

To assess if the increase in proliferation observed in Figure 5-21 was due to the presence of the stromal cell populations a range of co-culture variants were assessed. These included different media in the insert above with no cells present, the fibroblasts above in different media and a later passage number of fibroblasts above. The different media types were assessed as the pancreatic cancer cells were grown in DMEM media while each of the stromal cell populations were cultured in RPMI media. A later passage number of Pt-102 fibroblasts was used to investigated if the activity or influence of the fibroblasts diminished after long culture periods, as it was important to be aware that these cells are primary i.e. not immortal.

Figure 5-24. Proliferation of **Panc-1** cells using a range of co-culture variants

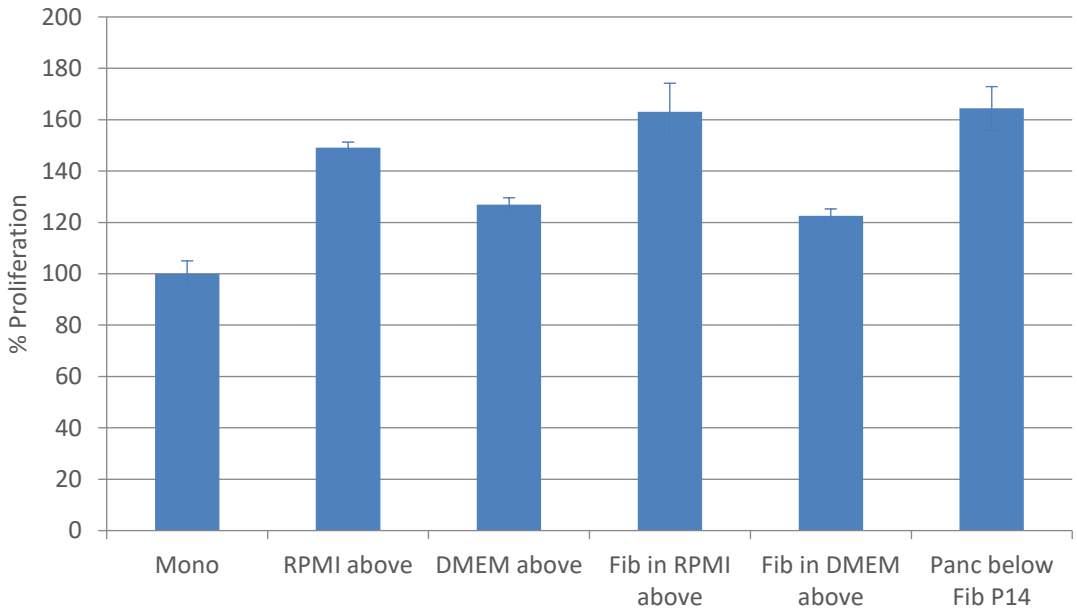

Proliferation levels of **Panc-1** cells using a range of co-culture variants including RPMI above, DMEM above, Pt-102 fibroblasts in RPMI above, Pt-102 fibroblasts in DMEM above and passage 14 Pt-102 fibroblasts in RPMI above. The mono culture control is Panc-1 cells with no insert above. Error bars represent +/- standard deviation between technical replicates, (n=1).

Figure 5-24 shows the effects of all co-culture variants investigated on proliferation in the Panc-1 cell line. This data showed that media alone, without stromal cells, above Panc-1 cells induced an increase in proliferation. The increase from RPMI alone at 50% is double the effect seen in DMEM alone, at 26%. A greater increase in proliferation, 13%, was observed when Pt-102 fibroblasts were above in RPMI than RPMI alone. There appeared to be no difference between DMEM alone and Pt-102 fibroblasts in DMEM above. Pt-102 fibroblasts at passage 14 induced a 60% increase in proliferation in Panc-1 cells relative to mono culture control i.e. no transwell insert above.

Figure 5-25. Proliferation of **Panc-1** cells using volume controls with CM treatment

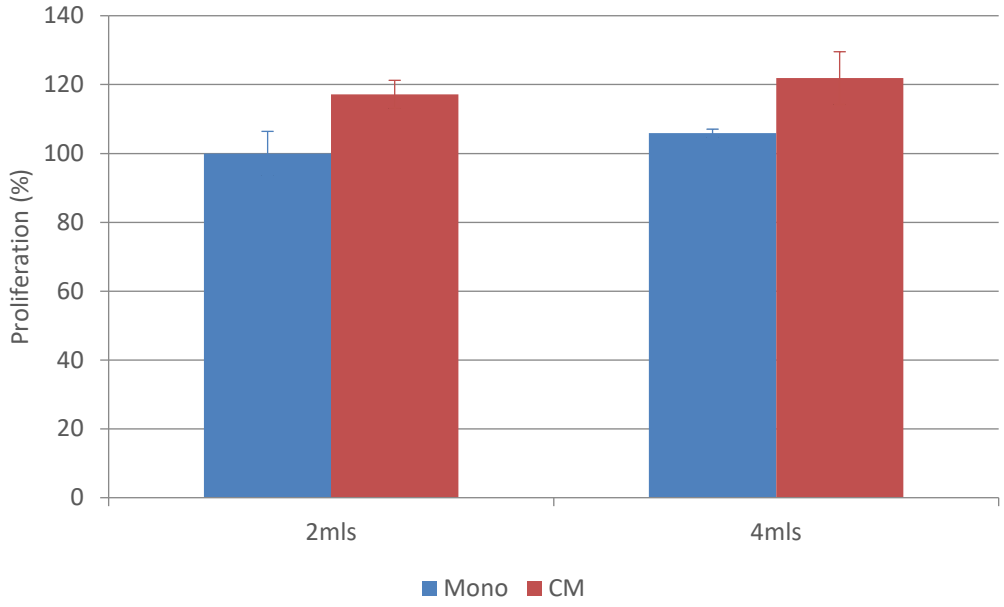

Proliferation levels of **Panc-1** cells using volume controls with conditioned media from tumour derived fibroblasts (Pt-102). Mono culture controls contain fresh DMEM media while the CM treatment contains 50% fresh DMEM with 50% conditioned RPMI media. Error bars represent +/- standard deviation between technical replicates, (n=1).

To ensure the effects on proliferation displayed in Figure 5-24 were not due to volume differences a volume control CM treatment experiment was performed. This involved two volumes, 2mL and 4mL. Previous experimental work used a mono culture control of 2mL with a co-culture of 4mL. Figure 5-25 displays an increase in proliferation in both CM treatments compared to mono culture whether 2mL or 4mL of volume was present. As there was no significant difference between the mono culture controls or CM treatments of 2mL and 4mL, the volume differences did not appear to be responsible for the phenotypic changes observed post co-culture.

Figure 5-26. Proliferation of **Panc-1** cells using a range of co-culture variants with an appropriate control

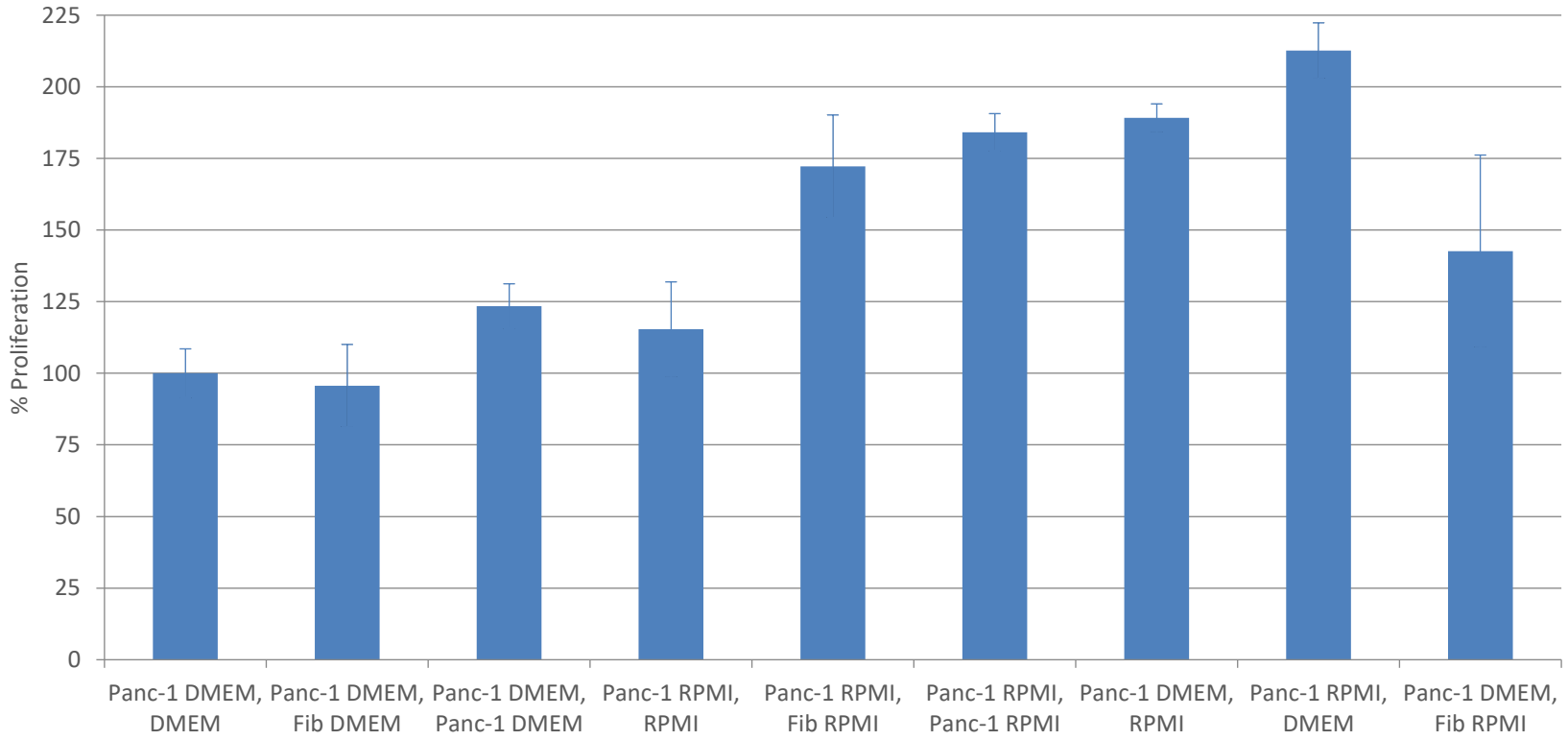

Proliferation levels of **Panc-1** cells using a range of co-culture variants with Panc-1 cells in DMEM with DMEM above as a control. The variants include Pt-102 fibroblasts in DMEM above, Panc-1 cells in DMEM above, Panc-1 cells in RPMI with RPMI above, Panc-1 cells in RPMI with Pt-102 fibroblasts in RPMI above, Panc-1 cells in RPMI with Panc-1 cells in RPMI above, Panc-1 cells in DMEM with RPMI above, Panc-1 cells in RPMI with DMEM above and Panc-1 cells in DMEM with Pt-102 fibroblasts in RPMI above. Error bars represent +/- standard deviation between technical replicates, (n=1).

The previous range of controls, Figure 5-24, displayed that complete DMEM media in a co-culture insert above induced an increase in proliferation. This result led to an investigation of volume differences. Figure 5-25 portrays that the functional changes observed post co-culture were not due to volume differences between mono and co-culture set ups. Following this, a larger screen of co-culture variants were investigated using as the mono culture control, Panc-1 cells in DMEM below a co-culture insert with complete DMEM media above, as seen in Figure 5-26. In comparison to this control, it appeared fibroblasts above in DMEM had no effect on proliferation of the cancer cells. Interestingly, Panc-1 cells in DMEM with Panc-1 cells above in DMEM induced a 20% increase in proliferation. Panc-1 cells in RPMI media with RPMI above seemed to proliferate faster than Panc-1 cells in DMEM with DMEM above, with an increase of 15% found. When Pt-102 fibroblasts were present in RPMI above Panc-1 cells in RPMI this effect on proliferation rose to an increase of 70%. When the cell population above was Panc-1 cells in RPMI instead of fibroblasts, above Panc-1 cells in RPMI the effect increased again to 85%. Surprisingly the greatest effect on proliferation was observed when no second cell population was present above but when a mix of media types was present. Panc-1 cells in DMEM with RPMI above induced a 90% increase while Panc-1 cells in RPMI with DMEM above caused a 110% increase in proliferation. Panc-1 cells in DMEM with Pt-102 fibroblasts in RPMI above, which had been the co-culture set up previously used resulted in a 40% increase in proliferation of the Panc-1 cells. This large effect present due to a mix of DMEM and RPMI may be due to the formulations of the media types providing a wider range of nutrients or nutrients in greater amounts. A brief investigation of the media formulations, identified that almost every nutrient was different between the two media types. To identify the root of the effect observed due to the mix of media, a large in-depth analysis will be necessary.

5.8. Determination of activation state of tumour derived fibroblasts

The activation state of stromal cells is an area of research gathering a lot of attention as discussed in section 1.4.3.2. Whether the stromal cells in the pancreatic tumour microenvironment are activated or quiescent has a major impact on the influence the

stromal cells have on the pancreatic cancer cells. There are a wide range of markers published to distinguish between activated and quiescent stromal cells, as discussed in section 1.4.3.2. Research focusing on the role of stromal cells is now including examinations of the activation state of the stromal cell populations. The activation state of the tumour derived fibroblasts used in this body of work was examined for the marker podoplanin. A published study of podoplanin as an activation marker in CAFs observed that CAFs positive for podoplanin expression enhanced the invasive capabilities of the pancreatic cancer cells through co-culture compared to CAFs with no podoplanin expression (Shindo et al. 2013). I aimed to assess the activation state of the tumour derived fibroblasts through podoplanin expression and also assessed if the activation state increased due to co-culture with pancreatic cancer cells as the previously mentioned study had observed this to be true.

Figure 5-27. Level of podoplanin protein in patient tumour derived fibroblasts (Pt-102)

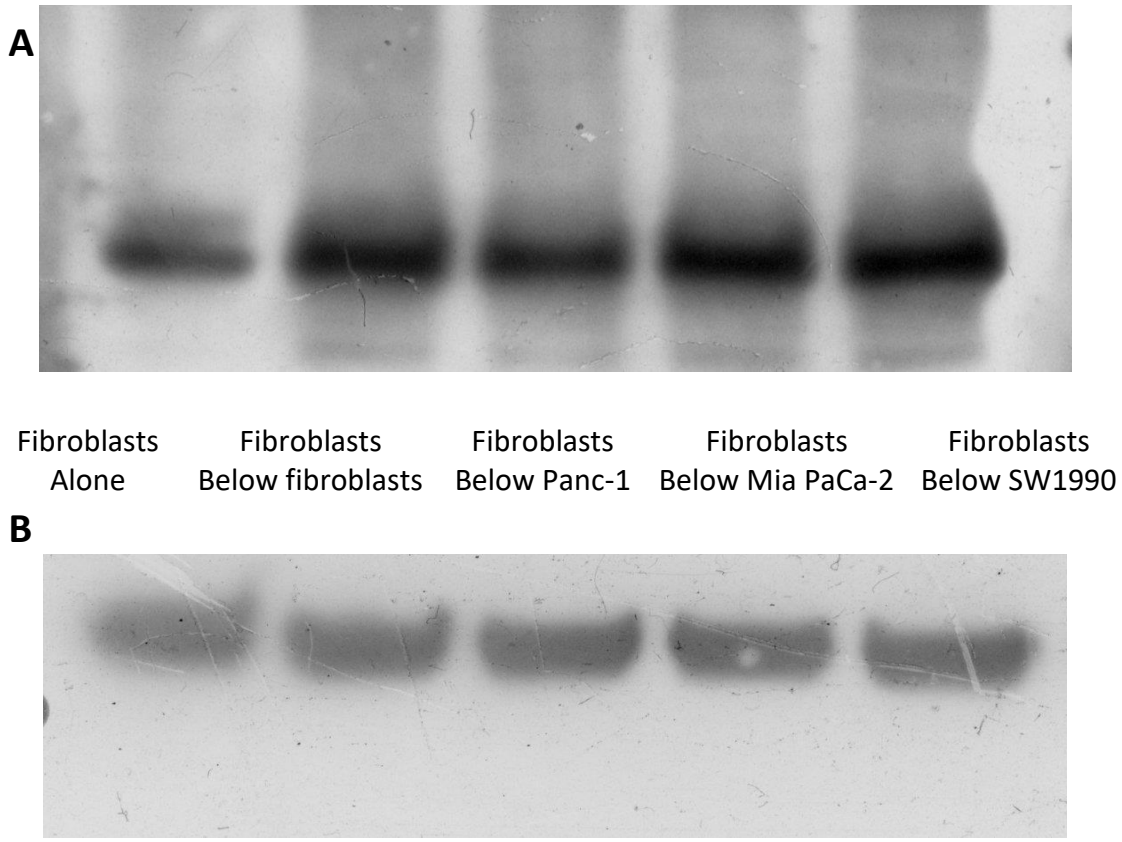

A. Western blot showing podoplanin protein, 17 kDa, levels in patient tumour derived fibroblasts (Pt-102) post 72hr co-culture with a panel of pancreatic cancer cell lines above. **B.** β-actin levels across all five samples is included as a loading control.

Figure 5-28. Densitometry analysis of podoplanin protein in patient tumour derived fibroblasts (Pt-102)

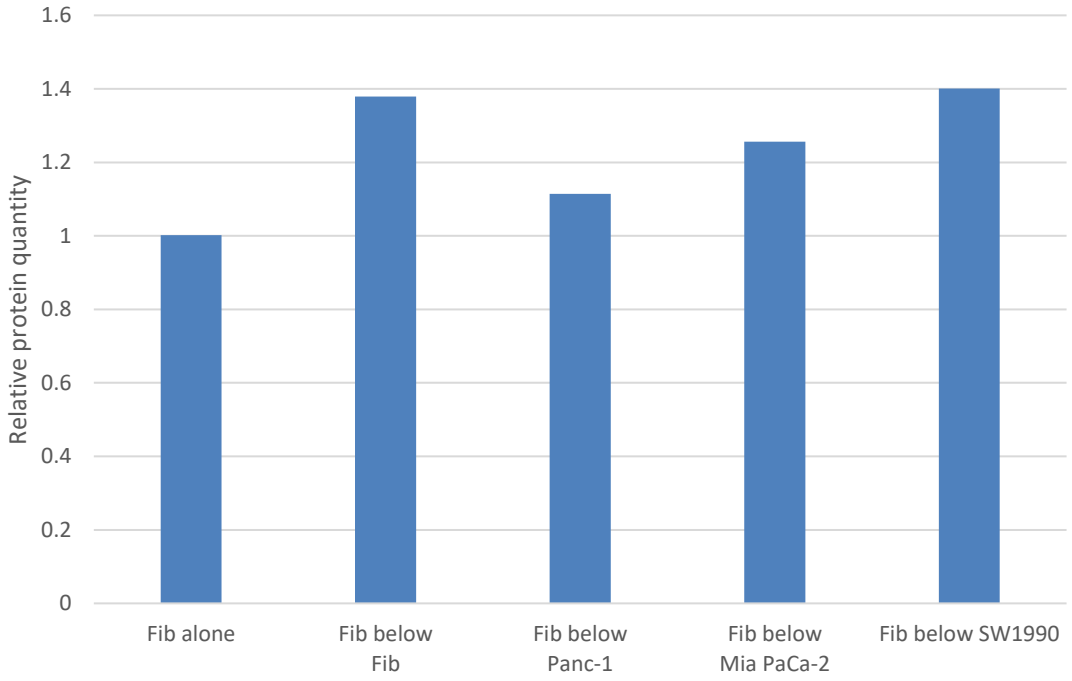

Densitometry analysis of Podoplanin protein levels in patient tumour derived fibroblasts (Pt-102) innately and following a 72hr co-culture with a panel of pancreatic cancer cells lines (Panc-1, Mia PaCa-2 and SW1990). Protein quantity was analysed using TotalLab Quant software, relative to β-actin used as the loading control (n=1).

Assessment of the activation state of Pt-102 tumour derived fibroblasts used Western blot analysis of podoplanin expression, as seen in Figure 5-27 and further analysis using densitometry, shown in Figure 5-28. It was determined that Pt-102 fibroblasts express podoplanin protein indicating that Pt-102 fibroblasts are in an activated state. Podoplanin expression was also assessed post co-culture with a panel of pancreatic cancer cell lines. This was to assess if the activation state increased due to co-culture with pancreatic cancer cells as the previously mentioned study had observed this to be true (Shindo et al. 2013). In the present study, this involved a 72hr indirect co-culture with the fibroblasts seeded in the well with the second cell population seeded above in a transwell insert. Pt-102 fibroblasts with no cells above was used as a control, with a second control of Pt-102 fibroblasts seeded above Pt-102 fibroblasts included. This control was used to determine if the presence of the pancreatic cancer cells or the

tumour derived fibroblasts induced different changes in the activation state of the stromal cells. It appears there is an increase in podoplanin protein in Pt-102 fibroblasts post co-culture in all conditions, as seen in Figure 5-27. This demonstrates that the activity of the tumour derived fibroblasts is further increased due to the presence of a second cell population. This increased expression is also induced by the Pt-102 fibroblasts co-cultured above the Pt-102 fibroblasts. This may indicate that an increase in secreted factors, whether from pancreatic cancer cells or the fibroblasts themselves, can increase the activity of tumour derived fibroblasts.

5.9. Functional effects of indirect co-culture with tumour derived fibroblasts (Pt-102) using the optimum control

Considering the effects observed in Figure 5-26 it was determined that the indirect co-culture should be performed using a more appropriate control. This control was determined to be a transwell insert above the cancer cells containing RPMI, no fibroblasts present. This control ensured no effects due to the mix media would be observed as the mix of media was present in all conditions. The previous mono culture control and the optimum mono culture control are shown in Figure 5-29. The co-culture model using the optimum control returned to the method used in section 5.4.1, i.e. co-culturing the pancreatic cancer cells (Panc-1 and BxPc-3) with the tumour derived fibroblasts (Pt-102) above in a co-culture insert for 48hr. The BxPc-3 cell line was included in this analysis as no mix of media was present in this co-culture as both the BxPc-3 cells and the fibroblasts were grown in RPMI medium, therefore any effects observed due to co-culture would not be due to a mix of media. After 48hr the pancreatic cancer cells were detached and assessed for changes in levels of survival in suspension i.e. anoikis, proliferation, colony formation and invasion due to indirect co-culture. Positive readings in anoikis assays were achieved in this section due to an increase in cell number from previous work, see section 5.4.1, although the BxPc-3 still displayed high anoikis sensitivity. Effects observed using this indirect co-culture set up should truly show the influence the tumour derived fibroblasts have on the pancreatic cancer cells.

Figure 5-29. Schematic of the previous mono culture control and the optimum mono culture control

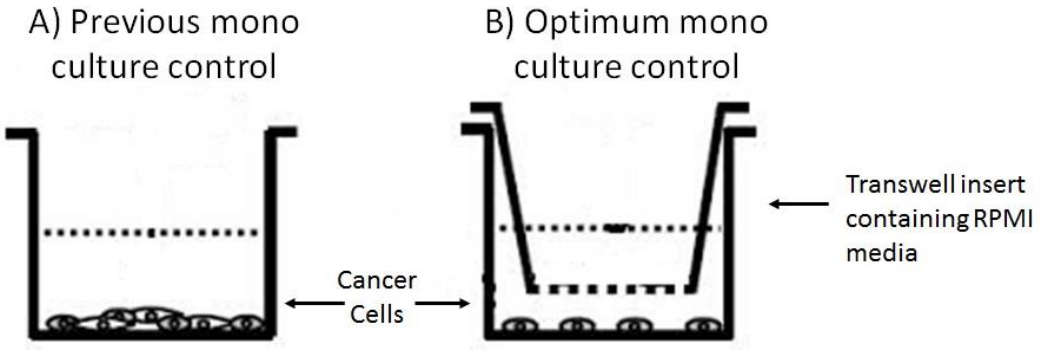

In previous co-culture experiments used mono culture set up (A). This contained the pancreatic cancer cells in 2mL of the cell specific media. The optimum mono culture control was determined to be (B). This consists of pancreatic cancer cells in 2mL of the cell specific media with a transwell insert above containing fresh RPMI media, the media specific for the stromal cell populations.

Figure 5-30. Percentage survival in attached and suspension conditions of **Panc-1** cells post co-culture with **Pt-102** fibroblasts using the optimum control.

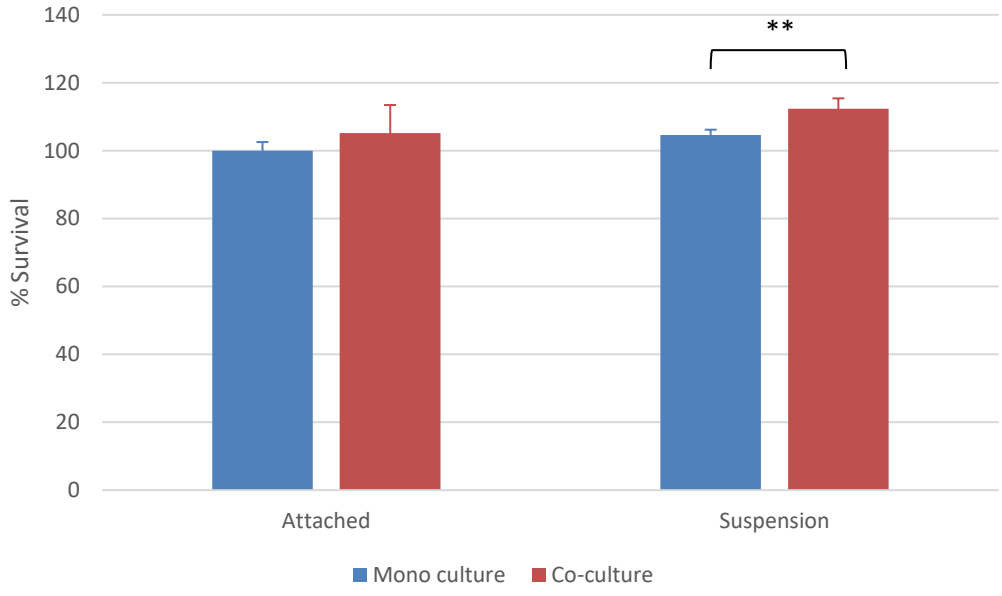

Percentage survival relative to attached mono culture, in attached and suspension i.e. anoikis, conditions of the **Panc-1** cell line following indirect co-culture with pancreatic tumour derived fibroblasts (**Pt-102**) using the optimum control. Error bars represent +/- standard deviation between biological replicates, (n=3, ** = p value ≤ 0.01, p value = 0.01).

Figure 5-31. Percentage survival in attached and suspension conditions of **BxPc-3** cells post co-culture with **Pt-102** fibroblasts using the optimum control.

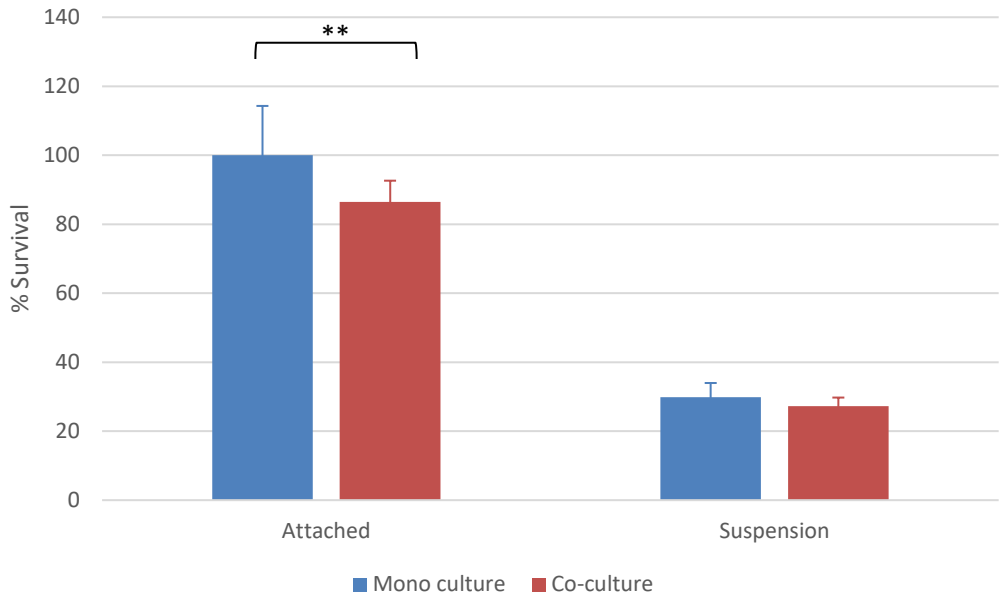

Percentage survival relative to attached mono culture, in attached and suspension i.e. anoikis, conditions of the **BxPc-3** cell line following indirect co-culture with pancreatic tumour derived fibroblasts (**Pt-102**) using the optimum control. Error bars represent +/- standard deviation between biological replicates, (n=3, ** = p value ≤ 0.01, p value = 0.01).

Co-culture of pancreatic cancer cells with tumour derived fibroblasts (Pt-102) using the optimum control induced some varied effects in comparison to the results previously seen in this work, i.e. section 5.4 and 5.6. To assess survival in suspension, the cells were trypsinised after 48hr of co-culture, the cells were then seeded into attached and suspension conditions for 24hr at which point survival was assessed. The Panc-1 cell line showed an increase in survival in both attached and suspension conditions post co-culture, as seen in Figure 5-30. Post co-culture Panc-1 cells showed a significant 8% increase in survival in suspension conditions in comparison to mono culture in suspension. There was a 5% increase in survival in attached conditions post co-culture present in Panc-1 cells, this apparent increase in survival may be due to an increase in growth. The opposite trend was observed in the BxPc-3 cell line, Figure 5-31 displays a decrease in survival post co-culture in both attached and suspension conditions. The decrease in suspension conditions was negligible while in attached conditions a

significant 14% reduction in survival was displayed. This seeming decrease in survival may be due to a reduction in growth post co-culture

Figure 5-32. Percentage proliferation of **Panc-1** and **BxPc-3** cells post co-culture with **Pt-102** fibroblasts using the optimum control

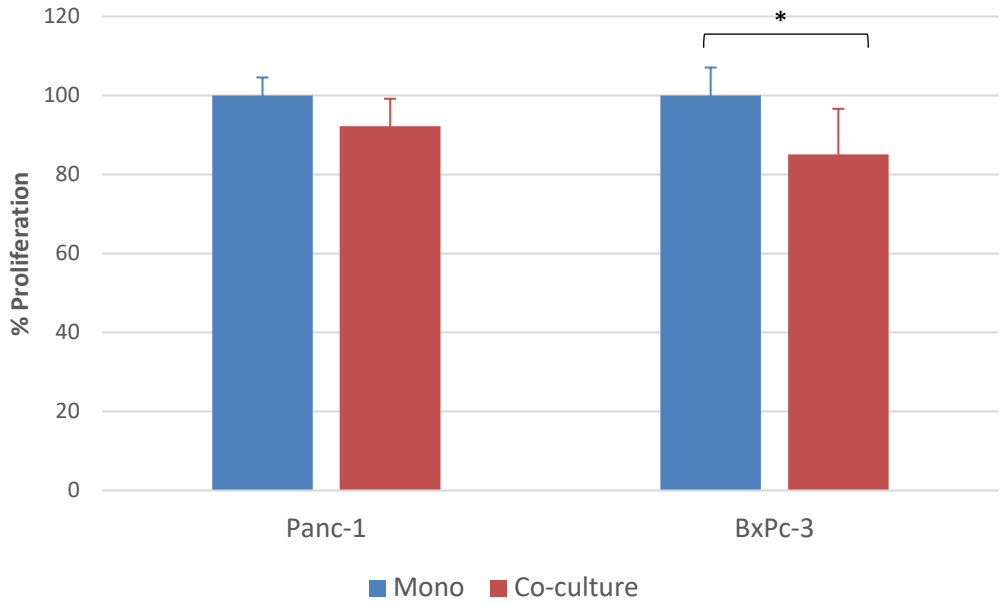

Percentage proliferation following co-culture relative to mono culture, of **Panc-1** and **BxPc-3** cell lines with pancreatic tumour derived fibroblasts (**Pt-102**) using the optimum control. Error bars represent +/- standard deviation between biological replicates, (n=3, * = p value ≤ 0.05, BxPc-3 p value = 0.04).

The hypothesis that the decreased survival of BxPc-3 cells observed post co-culture in attached conditions (Figure 5-31) was due to decreased proliferation, was confirmed by the data in Figure 5-32. Both the Panc-1 and BxPc-3 cell line had diminished proliferation levels post co-culture, displayed by Figure 5-32. An 8% reduction was present in the Panc-1 cell line while a significant 15% decrease in proliferation was seen in the BxPc-3 cell line post co-culture. Using the optimum control, the tumour derived fibroblasts were inhibiting the proliferation of the pancreatic cancer cells through indirect co-culture.

Figure 5-33. Colony formation of **Panc-1** cells post co-culture with **Pt-102** fibroblasts using the optimum control

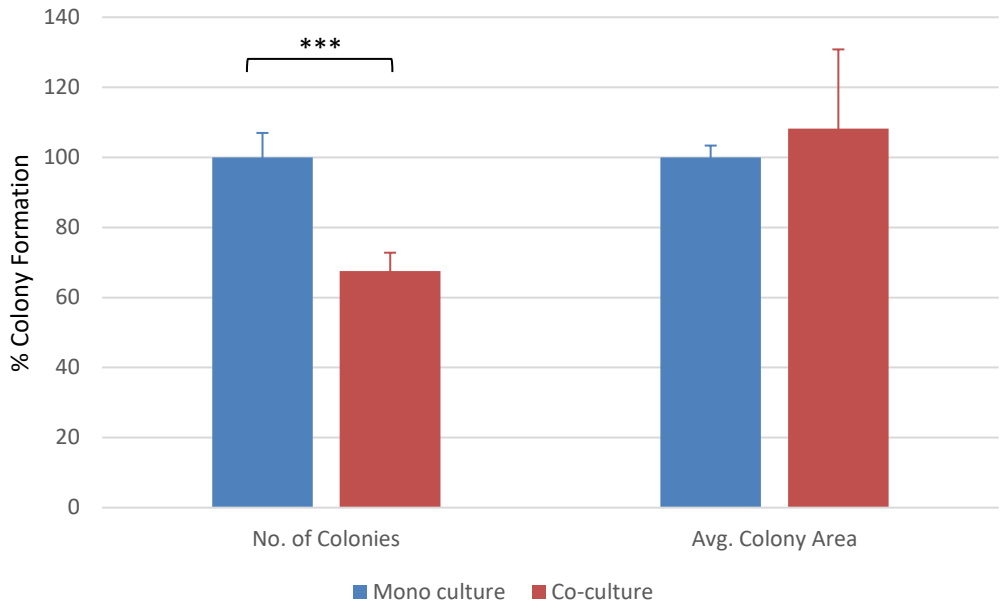

Percentage colony formation displayed as number of colonies and average colony area following co-culture relative to mono culture, of Panc-1 cells with pancreatic tumour derived fibroblasts (Pt-102) using the optimum control. Error bars represent +/- standard deviation between biological replicates, (n=3, *** = p value ≤ 0.001, p value = 0.0004).

Figure 5-34. Representative image of colony formation of **Panc-1** cells post co-culture with **Pt-102** fibroblasts using the optimum control

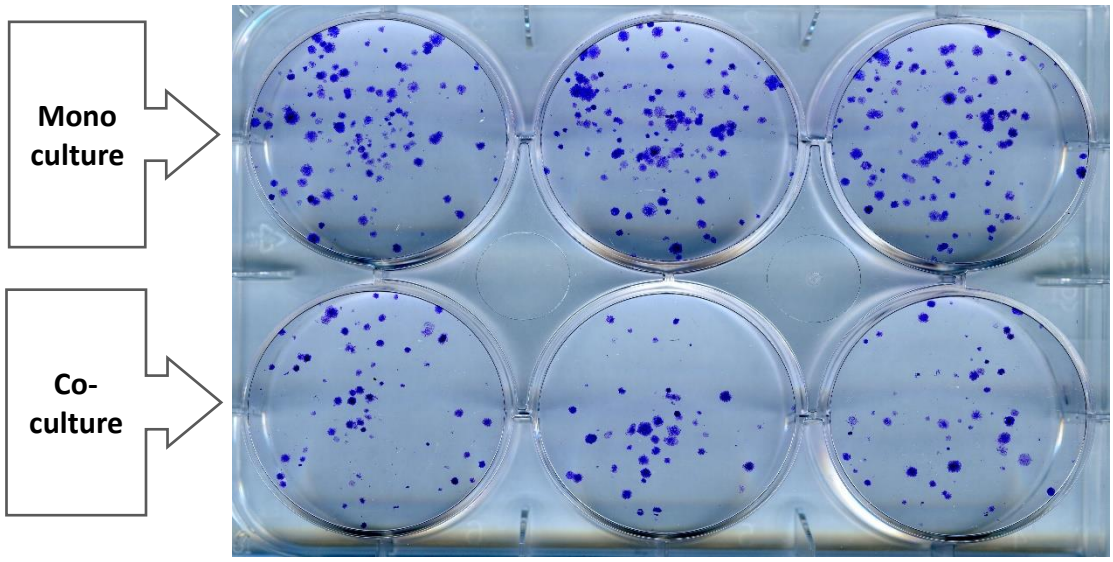

Representative image of colonies of **Panc-1** cells observed post indirect co-culture with tumour derived fibroblasts (**Pt-102**) using the optimum control.

Figure 5-35. Colony formation of **BxPc-3** cells post co-culture with **Pt-102** fibroblasts using the optimum control

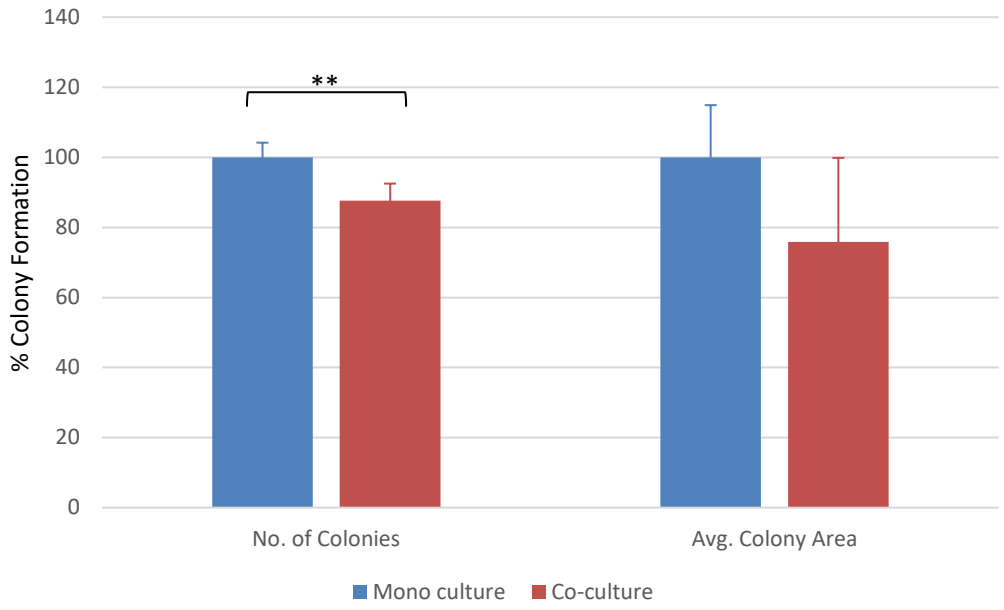

Percentage colony formation displayed as number of colonies and average colony area following co-culture relative to mono culture, of **BxPc-3** cells with pancreatic tumour derived fibroblasts (**Pt-102**) using the optimum control. Error bars represent +/- standard deviation between biological replicates, (n=3, ** = p value ≤ 0.01, p value = 0.01).

Figure 5-36. Representative image of colony formation of **BxPc-3** cells post co-culture with **Pt-102** fibroblasts using the optimum control

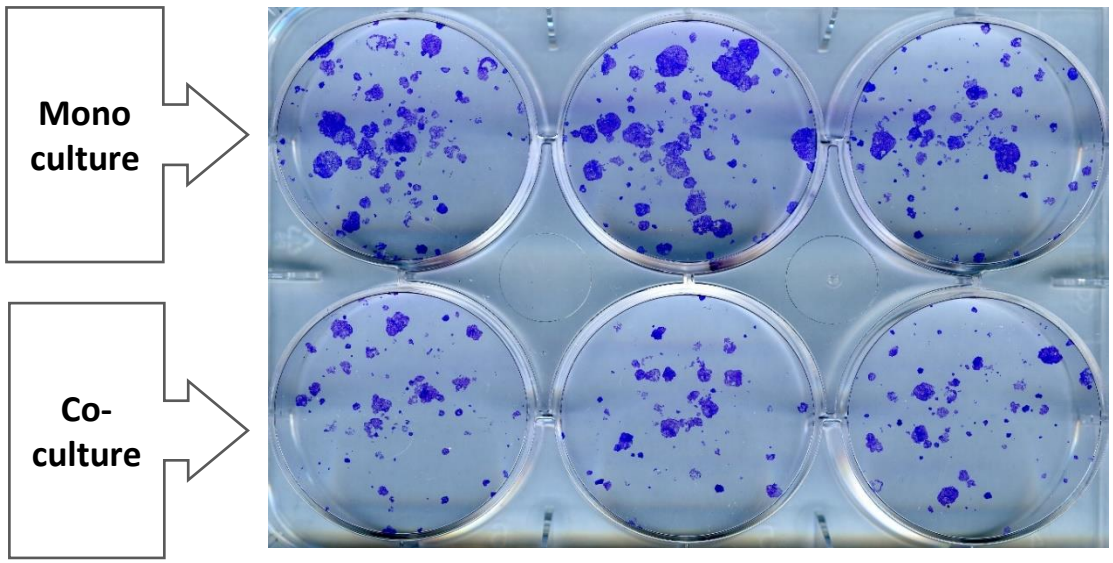

Representative image of colonies of **BxPc-3** cells observed post indirect co-culture with tumour derived fibroblasts (**Pt-102**) using the optimum control.

The analysis of colony formation was performed using MetaMorph software, the results are displayed as colony number and colony area which represents colony size. Figure 5-33 displays colony formation of the Panc-1 cell line post co-culture using the optimum control with a representative image shown in Figure 5-34. A slight increase in colony area was present at 8% but conversely a highly significant 33% reduction in colony number was induced post co-culture with a p value of 0.0004. This reduction was also seen in the BxPc-3 cell line in Figure 5-35, with a reduction in both colony area and colony number observed post co-culture. A 25% decrease in colony area was induced as well as a significant 12% reduction in colony number post co-culture in the BxPc-3 cell line with a representative image shown in Figure 5-36.

Figure 5-37. Percentage invasion of **Panc-1** and **BxPc-3** cells post co-culture with **Pt-102** fibroblasts using the optimum control

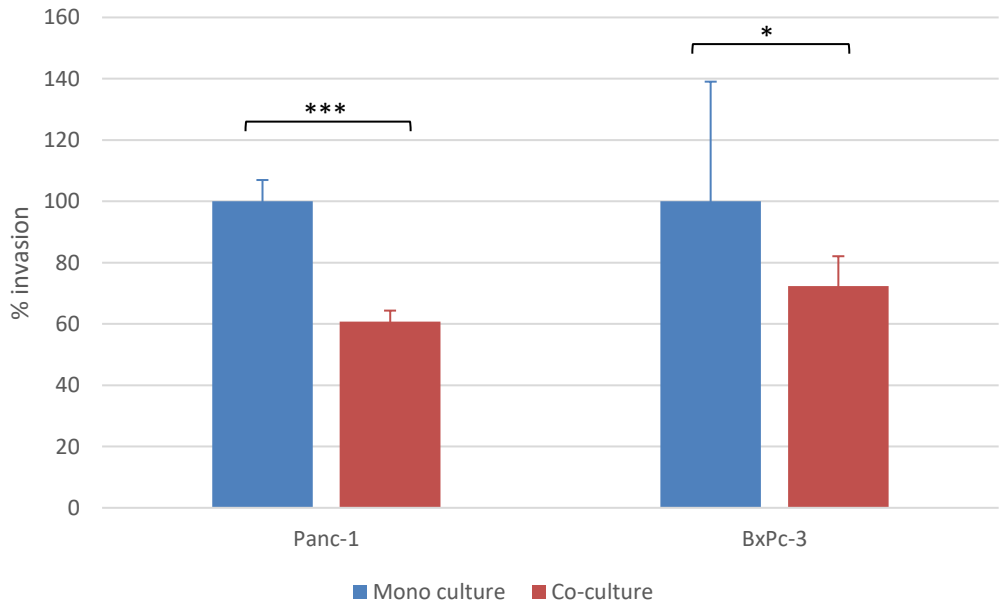

Percentage invasion following co-culture relative to mono culture, of **Panc-1** and **BxPc-3** cell lines with pancreatic tumour derived fibroblasts (**Pt-102**) using the optimum control. Error bars represent +/- standard deviation between biological replicates, (n=3, *** = p value ≤ 0.001, * = p value ≤ 0.05, Panc-1 p value = 4.47E-05, BxPc-3 p value = 0.03).

Figure 5-38. Representative images of invasion levels of both **Panc-1** and **BxPc-3** cells post mono and co-culture

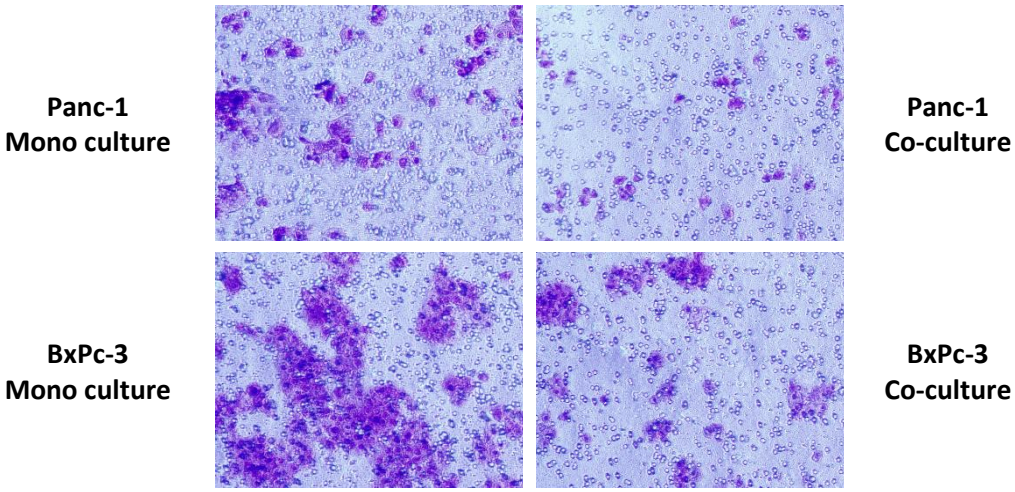

Representative images of invasion following mono culture and co-culture of **Panc-1** and **BxPc-3** cell lines with pancreatic tumour derived fibroblasts (**Pt-102**) using the optimum control.

Post co-culture with Pt-102 fibroblasts using the optimum control both pancreatic cancer cell lines displayed a large reduction in invasion relative to mono culture, shown in Figure 5-37. A significant 28% decrease was present in the BxPc-3 cell line; the low level of significance (p value of 0.03) may be due to the high level of error in the mono culture control. Also, the BxPc-3 cell line invades as clumps of cells as seen in Figure 5-38, which can lead to errors in counting. In the Panc-1 cell line the level of invasion was reduced by a highly significant 40% due to the presence of the tumour derived fibroblasts (Pt-102) with a p value of 4.47E-05. These results indicated that indirect co-culture of the pancreatic cancer cells with tumour derived fibroblasts (Pt-102) using the optimum control inhibited the invasive capabilities of the pancreatic cancer cells, this trend can be observed in Figure 5-38.

6. Discussion - Investigation of the Role of the Tumour Microenvironment in Pancreatic Cancer

Pancreatic cancer is one of the most lethal cancers worldwide due to late diagnosis by which time usually metastasis has occurred (Rucki and Zheng 2014). A hallmark of pancreatic cancer is a high level of stroma in the tumours as seen in Figure 1-3, which is due to fibrosis also known as desmoplasia. Fibrosis is defined as an accumulation of extracellular matrix (ECM) proteins due to the loss of balance between the manufacture and degradation of ECM (Apte, Pirola and Wilson 2012). In a healthy pancreas, the pancreatic microenvironment is responsible for the fine balance in production and degradation of ECM. Reasonably in a malignant situation the pancreatic tumour microenvironment is responsible for the loss of this fine balance. As the significance of the tumour microenvironment has been realised in recent years the role of fibroblasts and PSCs in the progression of pancreatic cancer has become the centre of a great deal of pancreatic cancer research. Both of these cell populations play an important role in the pancreatic microenvironment, they are responsible for several things one of which is the production of ECM, meaning they are also responsible for the fibrosis present in pancreatic cancer.

To investigate the role both fibroblasts and PSCs play in the metastasis and progression of pancreatic cancer an indirect co-culture model was developed and optimised. To begin a panel of pancreatic cancer cell lines were selected and characterised for the two metastatic functions to be investigated post co-culture, meaning anoikis and invasion. Based on this characterisation the four cell lines chosen were AsPc-1, BxPc-3, Mia PaCa-2 and Panc-1. These cell lines displayed a wide range of variety in both levels of anoikis and levels of invasion. As can be seen in

Figure 5-1, the BxPc-3 and AsPc-1 cell lines exhibited the highest levels of anoikis meaning these cell lines were highly sensitive to anoikis conditions i.e. suspension. Mia PaCa-2 and Panc-1 cells were much less sensitive to anoikis conditions, possessing a high level of anoikis resistance. A different trend was observed in invasion levels, shown in Figure 5-2. Panc-1 cells possess both a high level of invasion and anoikis resistance with AsPc-1 cells being the opposite, displaying low levels of invasion and anoikis resistance. The remaining cell lines in the panel appear to have converse characteristics; Mia PaCa-

2 cell line while being highly anoikis resistant displays a low to medium invasion level, observed in Figure 5-2. The BxPc-3 cell line is very sensitive to anoikis conditions and possess a high invasive ability.

6.1. Investigations of functional effects post 48hr indirect co-culture with multiple stromal cell populations

To investigate the functional impact of cell to cell interactions an indirect co-culture model to mimic the pancreatic tumour microenvironment was developed using pancreatic cancer cell lines with human derived stromal cells. Through the course of developing this model a range of formats were investigated to determine the efficiency of each model and the optimum conditions to investigate metastatic phenotypic changes.

The first format of the co-culture model involved culturing the pancreatic cancer cell lines below a transwell insert which contained the stromal cell population, for a 48hr time period. After 48hr the pancreatic cancer cells were detached and assessed for changes in levels of survival in suspension i.e. anoikis, proliferation and invasion due to indirect co-culture with pancreatic stromal cells. A variety of different stromal cell populations were examined for functional effects post co-culture with pancreatic cancer cells. Two different batches of human tumour derived fibroblasts were investigated, Pt-102 and Pt-127, which were fibroblasts developed in house from tumour samples of two different pancreatic cancer patients. These fibroblasts were developed in house using a combination method of enzymatic digestion and outgrowth. Full details of development and differences between the two populations can be found in section 2.1.1. Human pancreatic stellate cells were also investigated for functional effects on pancreatic cancer cells post co-culture. These stellate cells were kindly donated by Associate Professor Masamune in Tohoku University, Sendai, Japan. The metastatic phenotypes anoikis i.e. survival in suspension, proliferation and invasion were assessed for changes due to the presence of pancreatic stromal cells.

The three stromal populations investigated induced a variety of changes in both survival and proliferation across the panel of pancreatic cancer cell lines after a 48hr co-culture incubation. Phenotypic changes appear to be specific to each batch of stromal cells. The effects on survival varied post co-culture with each fibroblast batch and in each cell line examined. Post co-culture of the Mia PaCa-2 cell line with Pt-102 fibroblasts induced an increase in survival in both attached and suspension conditions shown in Figure 5-4. The opposite effect was observed post co-culture with Pt-127 fibroblasts, as seen in Figure 5-13 these fibroblasts resulted in a decrease in survival of the Mia PaCa-2 cell line in both attached and suspension conditions. Both fibroblast populations induced different changes in the Panc-1 cell line also. Figure 5-5 shows that no effect on survival in either attached or suspension conditions was displayed by the Panc-1 cell line post co-culture with Pt-102 fibroblasts. Conversely, Pt-127 fibroblasts caused an increase in survival in both attached and suspension conditions post co-culture in the Panc-1 cell line. Statistical significance was not present in any of the phenotypic assays using Pt-127 fibroblasts as while the functional effects due to indirect co-culture with Pt-127 fibroblasts was being assessed but before three biological replicates were achieved, the results in section 5.5 were observed, discussed in section 6.2. While both fibroblast primary cell lines were developed in the same way, they have differences, see section 2.1.1. Both tumours from which the fibroblast populations were derived had different pathology, levels of differentiation and invasive capabilities. Therefore, the varied phenotypic changes induced through co-culture is may be due to these differences. These investigations show that phenotypic changes in survival in suspension conditions induced by co-culture with stromal cells are both dependent on the stromal population and the pancreatic cancer cell line used. Interestingly, opposing results were observed between Pt-102 fibroblasts co-culture and Pt-102 conditioned media treatment. The co-culture induced an increase in survival in the Mia PaCa-2 cell line with no effect on survival observed in the Panc-1 cell line. Conditioned media treatment induced contrasting effects, no effect on survival was observed in the Mia PaCa-2 cell line while an increase in survival in suspension conditions was induced in the Panc-1 cell line through CM treatment. These results are displayed in Figure 5-9 and Figure 5-10

respectively. There is minimal published data on the effects of co-culture on anoikis and there is nothing investigating this in pancreatic cancer. Of the limited data, available one study determined that cancer-associated fibroblasts can inhibit anoikis in cancer cells therefore making the cancer cells behave in a more anoikis resistant manner. This anoikis inhibition was induced due to the elevated levels of insulin-like growth factor-binding proteins (IGFBPs) secreted by the CAFs, indicating this may have a role in inducing anoikis sensitivity (Weigel et al. 2014). This study however was a breast cancer investigation and used conditioned media as the co-culture model. While the assessment of the effects of stromal cells on survival in suspension post co-culture in pancreatic cancer in the present study show varied effects and there is no distinct conclusion to be drawn, it is a novel investigation due to the examination of anoikis post indirect co-culture in pancreatic cancer.

A similar variation in phenotypic changes was observed in proliferation post co-culture with the three different stromal cell populations. Human pancreatic stellate cells (hPSC24) induced a reduction in proliferation in both the Mia PaCa-2 and Panc-1 cell line post co-culture, displayed in Figure 5-17. Statistical significance was not present in any of the phenotypic assays using hPSC24 as while the changes due to indirect co-culture with hPSC24 was being assessed but before three biological replicates were achieved, the results in section 5.5 were observed, discussed in section 6.2. A reduction in proliferation was also observed in the Mia PaCa-2 cell line post co-culture with Pt-127 fibroblasts, a contrasting result was present in the Panc-1 cell line post co-culture with Pt-127 fibroblasts, where the proliferation level doubled post co-culture. Pt-102 fibroblasts induced an increase in proliferation in two out of four cell lines, an increase was observed in BxPc-3 and Mia PaCa-2 cells, with the effect on the Mia PaCa-2 cell line being significant and shown in Figure 5-6. Conditioned media from Pt-102 fibroblasts also induced an increase in proliferation in the Mia PaCa-2 cell line, interestingly, an increase in proliferation was observed in the Panc-1 cell line post CM treatment, seen in Figure 5-11. Clearly a difference between the indirect co-culture model and the CM treatment resulted in the opposing effects observed on the proliferation of Panc-1 cells. An effect may have been missed by the co-culture model or the cross-talk between the

two cell populations inhibited the increase in proliferation induced by the CM treatment. An increase in proliferation of pancreatic cancer cells post treatment with stromal cell CM has been observed in published studies. Hwang *et al*., investigated the effect of human pancreatic stellate cells (PSC) CM on pancreatic tumour progression. This work focused on the effect of conditioned media from immortalised pancreatic stellate cells on the pancreatic cell lines BxPc-3 and Panc-1. The effect of PSC conditioned media on proliferation, migration; invasion, colony formation and cell survival post treatment with gemcitabine or radiation therapy were all investigated. An increase in proliferation, migration, invasion and colony formation was induced by exposure to PSC conditioned media. This exposure also caused an inhibition of apoptosis in cells treated with gemcitabine and radiation therapy (Hwang et al. 2008). Another study performed a similar CM treatment investigation and found that the proliferation of both the Mia PaCa-2 and Panc-1 cell line was significantly increased after 24, 48 and 72hr of stellate cell CM treatment (Vonlaufen et al. 2008). These studies appear to validate the effect observed in Figure 5-11, treatment of pancreatic cancer cells with stromal cell conditioned media induced an increase in proliferation.

Conversely, other studies have found that co-culture of pancreatic cancer cells with stromal cells has had no effect on proliferation. A group in Japan who kindly donated the pancreatic stellate cells to this project, investigated phenotypic changes induced by co-culture with an immortalised pancreatic stellate cell line. This work utilised an indirect co-culture method quite similar to the model used in this present study, meaning using transwell culture inserts similar to invasion inserts but with a smaller pore size. The Japanese study determined that co-culture of PSCs with pancreatic cancer cells led to a cancer stem cell-like phenotype. Both colony formation and cell growth *in vivo* were increased due to indirect co-culture along with increased expression of several stem cell related genes including ABCG2, Nestin and LIN28 (Hamada et al. 2012). This published study also found that co-culture of pancreatic cancer cells with the immortalised pancreatic stellate cell population did not affect proliferation in any way. Interestingly, of the two pancreatic cell lines used in the Japanese study only one was investigated by the present study, AsPc-1 and this present study found a decrease in

proliferation was induced post co-culture. The effects of stromal cells post co-culture on proliferation of pancreatic cancer cells shows some variation. Many studies show a proliferation increase post treatment with stellate cell CM; however, there are few publications investigating an indirect co-culture model using transwell inserts, which is quite a different co-culture model to CM treatment. This present study has shown that converse effects can be observed between the two co-culture models. Also, there are a small number of studies which utilise patient tumour derived fibroblasts, in this study tumour derived fibroblasts from two different patients were investigated as inducers of metastatic phenotypes in pancreatic cancer cell lines.

The most consistent and significant phenotypic change observed post co-culture of pancreatic cancer cells with stromal cell populations was an increase in invasive capabilities. All three stromal cell populations investigated, Pt-102, Pt-127 and hPSC24 induced an increase in invasion levels post co-culture relative to mono culture. Pt-102 fibroblasts induced a more invasive phenotype in three out of four cell lines post co-culture, seen in Figure 5-7. The Mia PaCa-2 cell line displayed significantly double the level of invasion compared to the mono culture control with a significant 40% increase induced in the Panc-1 cell line. Considering the effects on proliferation, Figure 5-6, no effect in Panc-1 and a 20% increase in Mia PaCa-2, it can be stated that the increase in invasion is not due to an increase in proliferation. Pt-127 fibroblasts also induced an increase in invasion levels in both the Mia Paca-2 and Panc-1 cell lines post co-culture. As seen in Figure 5-16, these increases which are extremely large, 300% and 450% respectively, contain a large amount of error which inhibits any statistical significance as well as only two biological replicates being present. The increase induced in both cell lines is to a greater level than the effect observed on proliferation showing this increase in invasion is not due to an increase in proliferation. While a specific conclusion cannot be drawn from this result, it can be concluded that a trend of increased invasion is observed post culture with Pt-127 fibroblasts. A similar trend is present post co-culture with hPSC24, Figure 5-18. Mia PaCa-2 cells possessed a 70% higher level of invasion post co-culture with the Panc-1 cell line displaying a 50% increase. As a decrease in proliferation was observed post co-culture with hPSC24 this increase in invasion is not

due to an effect on proliferation, the increase in invasion may be greater than shown considering the reduction on proliferation. Due to the level in variability and need for more biological replicates this result on invasion did not show significance but a trend of increased invasion induced by hPSCs can be drawn. This conclusion has been observed in several published studies. Virtually every publication that has investigated the role of stromal cell populations in cancer cell invasion has observed that the invasion capabilities of the cancer cells are increased through stromal cell interactions (Goicoechea et al. 2014, Shindo et al. 2013, Farrow, Berger and Rowley 2009, Hwang et al. 2008). While the increase in invasion post co-culture, is present throughout the publications, the method used to assess this change is quite varied across the wide range of publications. Several groups use stromal cell CM treatment (Hwang et al. 2008), which contrasts with the results seen in Figure 5-12 showing a significant 50% reduction in invasion of Panc-1 cells post CM treatment. These opposite effects may be due to differences between the methods of the two studies. The Texas group (Hwang et al. 2008) used concentrated hPSC media while the CM used in this study was not concentrated in an attempt to replicate the 48hr co-culture system used in section 5.4.1. Hwang *et al.,* also treated the pancreatic cancer cells with CM in the invasion assay set up. In the present study, the pancreatic cancer cells were treated for 48hr before trypsinisation and seeding into the invasion assay inserts. In some experimental investigations, direct co-culture is used to assess phenotypic changes in invasion, as opposed to the indirect co-culture method used in this study (Zheng et al. 2015, Goicoechea et al. 2014, Farrow, Berger and Rowley 2009). Some investigations utilised an indirect co-culture method which involved the cancer cells seeded in the invasion insert above with the stromal cells seeded below in the insert in the well, similar to a chemoattractant used in invasion (Zheng et al. 2015, Shindo et al. 2013). There is a wide range of published methods investigating the influence of stromal cells on pancreatic cancer which has led to variation in the effects seen on proliferation, colony formation, drug treatment etc. but virtual all investigations report an increase in invasion due to stromal cell interactions. The fact that this result is present despite the variation in the methods used gives more power to the result overall.

6.2. Time-course experiment

The co-culture set up discussed in the previous section, 6.1, involved the pancreatic cancer cells incubated in the indirect co-culture model for 48hr before removing from the set up and seeding into functional assays to assess phenotypic changes post co-culture. This previous co-culture set up showed some inconsistent effects on proliferation across the panel and stromal cell populations. The time-course experiment, seen in Figure 5-19 and Figure 5-20, investigated if this co-culture set up and time-point was optimum for assessing functional effects. These results showed that the time-point was indeed optimum but led to a hypothesis that an effect on proliferation due to co-culture was present but being missed using acid phosphatase experiments to assess proliferation. This hypothesis was formed due to the observation that the cell number in co-culture samples was consistently higher than mono culture samples, this was then validated by the result seen in Figure 5-19. In order to optimally assess phenotypic changes in both proliferation and colony formation an in-assay co-culture format was developed. This differed from the original model in that the two cell populations were co-cultured for the duration of the functional assay, as described in section 5.6. It was determined that this was a more appropriate model to evaluate phenotypic changes in proliferation and colony formation due to the presence of the stromal cells.

6.3. Assessment of in-assay indirect co-culture set up

Due to an observation of increased cell number of pancreatic cancer cells post co-culture but no proliferation changes detected using the acid phosphatase assay, an in-assay co-culture format was developed. This differed from the original model in that the two cell populations were co-cultured for the duration of the functional assay as opposed to 48hr. In detail this in-assay co-culture format involved the pancreatic cancer cells being seeded into functional assays (proliferation and colony formation assays) with the stromal cells above in a co-culture insert for the entire length of the assay (7 days for proliferation, 14 days for colony formation). Meaning the cancer and stromal cells were

interacting throughout the time of the assay. It was determined that this was a more appropriate model to evaluate phenotypic changes in proliferation due to the continually presence of the stromal cells. Colony formation was also assessed for phenotypic changes post co-culture also as it can be an indication of changes in growth. This alternative format involved the cells being seeded at the required cell densities into proliferation and colony formation assays with the stromal cells above in a co-culture insert for the entire length of the assay.

Two stromal cell populations were assessed in this in-assay indirect co-culture format, Pt-102 and hPSC24, as both these populations previously showed the most consistent effects across the panel of pancreatic cancer cell lines. Also, the original hypothesis, that an increase in proliferation was present post co-culture but not being assessed sufficiently, was developed due to the observation that the cell number in samples post co-culture with Pt-102 was consistently higher than mono culture samples. This effect was most apparent in the Panc-1 cell line, no effect on proliferation is seen in Figure 5-6 but the cell number post co-culture was consistently higher. Due to this, the Panc-1 cell line was used to develop the in-assay indirect co-culture method. Both stromal cell populations, Pt-102 and hPSC24, induced a significant increase in proliferation and colony formation in the Panc-1 cell line, shown in Figure 5-21 and Figure 5-22. As previously stated a large proportion of co-culture investigations use CM treatment as the indirect method. A small number of publications use a similar in-assay indirect co-culture format (Hamada et al. 2012, Fujita et al. 2009). Interestingly, these groups saw contrasting results to the effects observed in this body of work, both observed that in-assay indirect co-culture had no significant effect on the proliferation of the pancreatic cancer cells. While Hamada *et al.*, reported no effect on proliferation this published work did state a significant increase in spheroid formation was induced through in-assay co-culture. A parallel between this result and the increase in colony formation observed in Figure 5-22 can be made and may validate the role of pancreatic stromal cells have in increasing the colony forming ability of pancreatic cancer cells. The results in section 5.6 appear to validate the hypothesis that an effect on proliferation due to stromal cell co-culture is more efficiently assessed using this in-assay co-culture model. The Panc-1 cell

line showed no effect on proliferation post Pt-102 co-culture and a decrease in proliferation was induced post hPSC24 co-culture. This validation ties in with the theoretical idea that the co-culture effects are more efficiently assessed when the stromal cell population is present at the end point assessment of the phenotypic change. To examine a phenotypic change due to 48hr of co-culture after 5 days (proliferation) or 14 days (colony formation) post co-culture may be an excessive expectation of the power of the co-culture model.

6.4. Determination of the optimum indirect co-culture control

In order to confirm that the increase in proliferation post in-assay co-culture was induced by the stromal cell populations, a range of co-culture variants were investigated for effects on proliferation of the Panc-1 cell line. These variants included different media in the insert above with no cells present, the fibroblasts above in different media and a later passage number of fibroblasts above. As this result, Figure 5-24, showed an increase in Panc-1 proliferation induced by complete medium above in a co-culture insert, it became clear that the mono-culture control previously used needed to be optimised. In order to determine the optimum control for the indirect co-culture model a larger screen of co-culture variants were investigated, using Panc-1 cells in DMEM below a co-culture insert with complete DMEM media above as the mono culture control. Figure 5-26 displays some highly surprising and interesting results. The most startling result observed was a doubling in the proliferation rate of the Panc-1 cell line when a mix of media types, DMEM and RPMI, was present in the co-culture model. A brief insight into the formulations of both media types, DMEM and RPMI, revealed that virtually every component is different between the two media types. Due to the hundreds of variables that could be the cause of the increase in proliferation observed, a large investigation would be required to fully elucidate the exact cause.

The increase in proliferation due to a mix of media types was greater than the increase induced when the Pt-102 fibroblasts were present in any of the other variants. While

this result was only one biological replicate, it led to the determination that the optimum control for the indirect co-culture model was a co-culture insert containing RPMI above the pancreatic cancer cells. This control ensured no effects due to the mix media were observed as the mix of media was present in all conditions. A brief insight into the formulations of both media types, DMEM and RPMI, revealed that virtually every single component is different between the two media types. Due to the hundreds of variables that could be the cause of the increase in proliferation observed, a large investigation would be required to fully elucidate the exact cause. A thorough investigation of the published data on indirect co-culture models produced inconclusive results on the mono culture control used in each publication. Each study states the use of a mono culture control but very few are explicit in exactly what this control was. It is hoped that each study is using an appropriate control but there is a possibility that some results observed may be due to an inappropriate control. Whether that proves to be true or not, it is necessary for publications to be hugely more overt and exact in the description of the mono culture control. This body of work has shown the momentous importance of determining the optimum control while developing an indirect co-culture model.

6.5. Functional effects of indirect co-culture with tumour derived fibroblasts (Pt-102) using the optimum control

Based on the results observed in Figure 5-26 the optimum control for this indirect co-culture method was determined to be a transwell insert above the cancer cells containing RPMI, no fibroblasts present. This control ensured no effects due to the mix media would be observed as the mix of media was present in all conditions. This format returned to the method used in section 5.4.1, i.e. co-culturing the pancreatic cancer cells (Panc-1 and BxPc-3) with tumour derived fibroblasts (Pt-102) above in a co-culture insert for 48hr. After 48hr the pancreatic cancer cells were detached and assessed for phenotypic changes. Using the more appropriate control ensured any changes observed were wholly due to the interactions with the patient tumour derived fibroblasts.

This interaction with the tumour derived fibroblasts produced interesting results which were in contrast to all previous observed results, results observed without the optimum control present. Previously results varied but appear to show an increase in proliferation, colony formation and invasion post co-culture. Once the optimum control was introduced to the model, the opposite trend appears to be induced. The majority of the effects observed have negative phenotypes with the exception of a slight increase in survival induced in the Panc-1 cell line. A decrease in survival post co-culture in both attached and suspension conditions was produced post co-culture in the BxPc-3 cell line. The significant decrease in survival in attached conditions is most likely due to a decrease in proliferation. This decrease in proliferation was validated in Figure 5-32 which shows a reduction in proliferation in both the Panc-1 and BxPc-3 cell lines. In agreement with this observation, co-culture also produced a significant reduction in colony number in both the Panc-1 and the BxPc-3 cell line. As proliferation and colony formation share similar characteristics, it was encouraging to observe a reduction was produced in both functions through stromal cell interactions. The final negative phenotype observed post co-culture was a significant reduction in invasion levels in both the Panc-1 and BxPc-3 cell line as seen in Figure 5-37. This was in complete contrast to the trend of an increase in invasion post co-culture with multiple stromal cell populations observed in section 5.4.1. To further investigate the inhibition of metastatic phenotypes observed in this project, there are several approaches available. A more in-depth analysis could be performed on the reduced proliferation and colony formation post co-culture using flow cytometry to assess which cycle of cell growth was arrested (Gundewar et al. 2014, Haqq et al. 2015). The cell growth cycles can be easily assessed using the Guava® easyCyte Flow Cytometer available in-house in the NICB, with the Guava® Cell Cycle Assay which measures G0/G1, S and G2/M phase distributions. This analysis would identify the specific phase of cell growth of the pancreatic cancer cells that is being arrested due to the presence of the stromal cells, inducing the observed reduction in proliferation and colony formation. To further investigate the reduction in invasion levels due to co-culture the levels of MMPs and TIMPs is an interesting aspect to analyse. MMPs and TIMPs play a major role in the invasive capabilities of a cell, meaning there is most likely a change in either or both present post co-culture indicated by the inhibited invasion levels. Alteration to MMP and TIMP levels could be assessed

using zymography or at a molecular level using qPCR post co-culture (Tjomsland et al. 2016). Determining changes of MMPs and TIMPS may identify the key regulators of invasion which co-culture has altered inducing the reduction in invasive capabilities of the pancreatic cancer cells.

While the inhibition of metastatic phenotypes observed in this study were unexpected, there are published studies to confirm these observations (Leake 2014, Rhim et al. 2014, Özdemir et al. 2014). Rhim *et al.*, found that suppressing the stroma in pancreatic cancer led to more aggressive, vascularised, undifferentiated tumours with increased proliferation. This group concluded that the pancreatic tumour stroma can act to restrain tumour progression (Rhim et al. 2014). This conclusion was also drawn by Özdemir *et al.*, this investigation determined that depletion of the stroma produced invasive, undifferentiated tumours with enhanced EMT and hypoxia. This group also observed reduced animal survival and a correlation between reduced patient survival and reduced myofibroblast presence (Özdemir et al. 2014). Another group produced similar results, Lee *et al.*, presented data that suppression of the stroma in pancreatic cancer induced accelerated disease progression (Lee et al. 2014). These studies showed reducing the stroma induced a more aggressive phenotype which corresponds to the phenotypes observed in this present study where the presence of the tumour stroma reduced metastatic phenotypes. These phenotypes indicated that the presence of the stromal cells appears to restrain and inhibit the development of a more aggressive phenotype. A highly important pancreatic cancer clinical trial corroborates these findings. The clinical trial published by Olive *et al.*, used hedgehog inhibitors to target the stroma with the aim to increase drug perfusion of the tumours and therefore stabilise the progression of the disease. This hypothesis was based on studies showing the positive effects of targeting the stroma through hedgehog signalling inhibition in mouse pancreatic cancer models which showed increased drug delivery and survival post hedgehog inhibition (Olive et al. 2009). Unfortunately, and un-expectantly, the clinical trial observed no increase in survival through a combination treatment of gemcitabine and a hedgehog inhibitor. In fact, the gemcitabine and placebo group displayed higher survival in comparison appearing to indicate that disease progression

may be induced by stromal ablation (Madden 2012). This startling result brought about an immediate halt and termination of the trial. While many *in vitro* studies have portrayed the stroma as a promising target to inhibit pancreatic cancer progression this present study found the opposite to be true. Considering this data, recent publications and the significant termination of the clinical trial it appears targeting the pancreatic cancer stroma may not be the ideal therapeutic approach it once seemed.

7. Results – Investigation of the Role of miRNA in Metastatic Phenotypes in Pancreatic Cancer

7.1. Aim

Investigate the role of miRNA expression in the progression of pancreatic cancer using sponge knockdown and overexpression vectors. Pancreatic cancer is one of the most lethal cancers worldwide with a 5-year survival rate of only 6%. The poor prognosis and survival rate is partially due to the early onset of metastasis, which occurs soon after the development of the cancer. Metastasis is the ability of a cell to spread to another location in the body, colonising this secondary site with tumour growth. miRNA are key regulators of gene expression and therefore have an important role in virtually all cellular functions including metastasis. There are several methods to alter miRNA expression, inducing either up- or downregulation. A novel approach used in this investigation, is a sponge knockdown vector to reduce the target miRNAs activity. In addition to this approach, overexpression vectors inducing upregulated expression of the target miRNA were utilised as well as Pre-miRs and Anti-miRs to induce transient alterations in miRNA expression. This body of work aimed to investigate the role miRNA expression plays in the progression of pancreatic cancer, specifically in metastatic phenotypes.

7.2. Alteration of miRNA expression

Despite an influx of research in pancreatic cancer in recent years very little progress has been made and the development of new, more effective therapies is needed. One such area which shows promise for these new developments is the area of miRNA in pancreatic cancer (Chitkara, Mittal and Mahato 2015). Investigations of miRNA in pancreatic cancer have covered several topics from large studies aiming to profile pancreatic cancer through both cells and tumour samples, to studies of miRNA as biomarkers and the therapeutic potential of miRNA. Many studies have investigated the impact miRNA have on pancreatic cancer with some miRNA being involved in progression of the disease, some inhibiting its development etc. (Li et al. 2013, Takikawa et al. 2013). A range of tools to stably alter miRNA expression had previously been developed in house by Alan Costello of the molecular biology group. These tools included sponge knockdown and overexpression vectors. Also, available through the

molecular biology group was a range of Pre-miRs and Anti-miRs which are commercial tools used to transiently alter miRNA expression. Transient alteration of miRNA expression is a temporary change where as stable alteration is a permanent alteration. The cell line becomes permanently altered, not only due to the change in altered miRNA expression but also due to the selection of a subpopulation which have been transfected with a plasmid vector. An in-depth description of these tools has been detailed in section 1.5.5.3. These tools were used to alter miRNA expression in the Panc-1 cell line. Functional changes due to altered miRNA expression were assessed in anoikis i.e. survival in suspension, proliferation, colony formation and invasion.

7.2.1. Investigation of transiently altered miRNA expression

Assessment of functional changes due to transiently altered miRNA expression were examined using a transient transfection. These investigations of increased and decreased miRNA expression were performed in the Panc-1 cell line. 48hr after transfection, method described in section 2.6.3, functional changes were assessed in both proliferation and colony formation. The miRNA investigated using a transient approach are displayed . An untransfected control was included in each experiment as well as a negative control, either a Pre-miR negative control or Anti-miR negative control. These negative controls are random sequences which have been shown to have no effect on known miRNA function as described in section 2.6.3. In this body of work some phenotypic changes were observed due to transfection using a negative control. As a result of this, all functional comparisons were to the untransfected control. The miRNA listed in were chosen for several reasons, the first being an unbiased approach. A large, diverse cohort of miRNA Pre-miRs and Anti-miRs were available in-house through the molecular biology group. From this cohort three Pre-miR and three Anti-miR targets were chosen to investigate further, these choices are detailed in the following sections.

Table 7-1. miRNA investigated in a transient manner

Pre-miR	Anti-miR
miR-204	**miR-224**
miR-224	**miR-320a**
miR-320a	**miR-378**

A literature review was performed to determine the level of novelty of these miRNA targets and the role, if any, they play in pancreatic cancer.

miR-204 had been shown to be downregulated in pancreatic cancer cell lines and linked to the upregulation of Mcl-1 (Chen et al. 2013). Mcl-1 protects cancer cells from cell death and contributes to chemoresistance. It had also been shown to be upregulated in pancreatic tumour tissues compared to adjacent normal tissue. This same study also determined that overexpression of miR-204 using a Pre-miR, reduced expression of Mcl-1 and subsequently cell viability of the pancreatic cancer cells (Chen et al. 2013). This publication indicated that miR-204 acts as a tumour suppressor in pancreatic cancer, studies of several different cancer types had also identified a role of miR-204 as a tumour suppressor (Imam et al. 2012, Ying et al. 2013, Sacconi et al. 2012). The Mcl-1 study was performed in the Mia PaCa-2 and S2-VP10 pancreatic cancer cell lines, the study in this body of work used the Panc-1 cell line. The Panc-1 cell line was transiently transfected with Pre-miR-204, firstly, to assess if the tumour suppressor role of miR-204 was observed in another pancreatic cancer cell line and also as proof of concept to assess if the tumour suppressor properties of miR-204 were observed.

There were very few investigations of the role of miR-224 in pancreatic cancer, one that does exist identified that miR-224 was significantly upregulated in highly metastatic pancreatic cancer cell lines (Mees et al. 2009). This paper appeared to suggest that miR-224 is an oncogenic miRNA in pancreatic cancer. In relation to other cancer types there are conflicting roles of miR-224 reported. In cervical cancer miR-224 showed higher expression in tumour vs normal tissues with *in vitro* transient overexpression inducing

increased proliferation, migration and invasion (Huang et al. 2016a). Converse results to this were observed in breast cancer. miR-224 was found to have an inverse relationship with aggressiveness in a range of breast cancer subtype cell lines (Liu et al. 2016). This study also found transient overexpression reduced proliferation and migration as well as growth *in vivo* while transient knockdown induced the opposite effects i.e. increased proliferation and migration (Liu et al. 2016). Due to these reports of conflicting aspects of miR-224, its role in pancreatic cancer was investigated in two ways, over and reduced expression with both being a transient alteration.

There is very little research available to show the function of miR-320a in pancreatic cancer. Although the role in pancreatic cancer had been unknown until this point, in many other cancers miR-320a had been shown to be a tumour suppressor miRNA such as colorectal cancer, glioma, NSCLC (Lei et al. 2016, Tadano et al. 2016, Sun et al. 2015). In NSCLC miR-320 expression was found to be significantly downregulated in tumour vs normal tissue samples. This study also observed that transient overexpression of miR-320 induced a decrease in growth, migration and invasion (Lei et al. 2016). An investigation of miR-320 in cervical cancer found an inverse relationship between miR-320 and the anti-apoptotic protein, Mcl-1 in cervical cancer tissues (Zhang et al. 2016). Transient overexpression of miR-320 reduced proliferation, migration and invasion while increasing apoptosis in cervical cancer cell lines. This is similar to the relationship previously mentioned, discussing the role of miR-204 with Mcl-1 in pancreatic cancer (Chen et al. 2013). While miR-320 had been shown to function as a tumour suppressor in several other cancer types, there was very little investigation in pancreatic cancer. Due to this, this study investigated the role of miR-320a in pancreatic cancer using both a Pre-miR and Anti-miR separately.

Lastly, miR-378 was chosen to be investigated. It had been found to have minimal association to pancreatic cancer, a small number of publications currently exist and these had a tenuous link. One such study assessed miRNA in patient sera using miRNA microarrays. miR-378 was identified as a circulating miRNA which was significantly

elevated in pancreatic cancer sera compared with control groups (Li et al. 2013). Studies into other cancer types had observed a role of miR-378 as a tumour suppressor. An investigation into nasopharyngeal carcinoma observed upregulation of miR-378 induced an increase in proliferation, migration, invasion and colony formation (Yu et al. 2014). A study of stable overexpression of miR-378 in cancer found that overexpression enhanced colony formation as well as cell survival (Deng et al. 2013). These findings as well as increased drug resistance were observed due to overexpression of miR-378 in glioblastoma (Wu et al. 2012). These two studies identified miR-378 as a tumour suppressor while one of the few pancreatic cancer studies appeared to suggest miR-378 as an oncomiR. To investigate this oncomiR role of miR-378 in pancreatic cancer an Anti-miR was chosen as downregulated expression may exhibit reduced metastatic phenotypes.

Figure 7-1. Percentage proliferation of **Panc-1** cells post transient transfection with a range of **Pre-miRs**

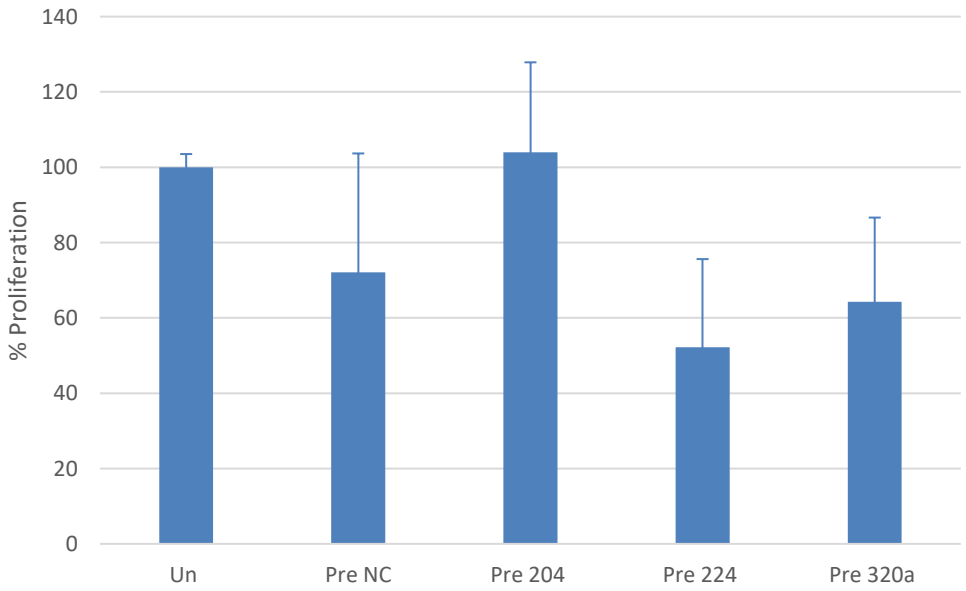

Percentage proliferation of the **Panc-1** cell line following transient overexpression of **miRNA 204**, **224** and **320a** with a negative control (Pre NC) included. All values are relative to untransfected control (Un). Error bars represent +/- standard deviation between biological replicates, (n=3).

Figure 7-2. Percentage proliferation of **Panc-1** cells post transient transfection with a range of **Anti-miRs**

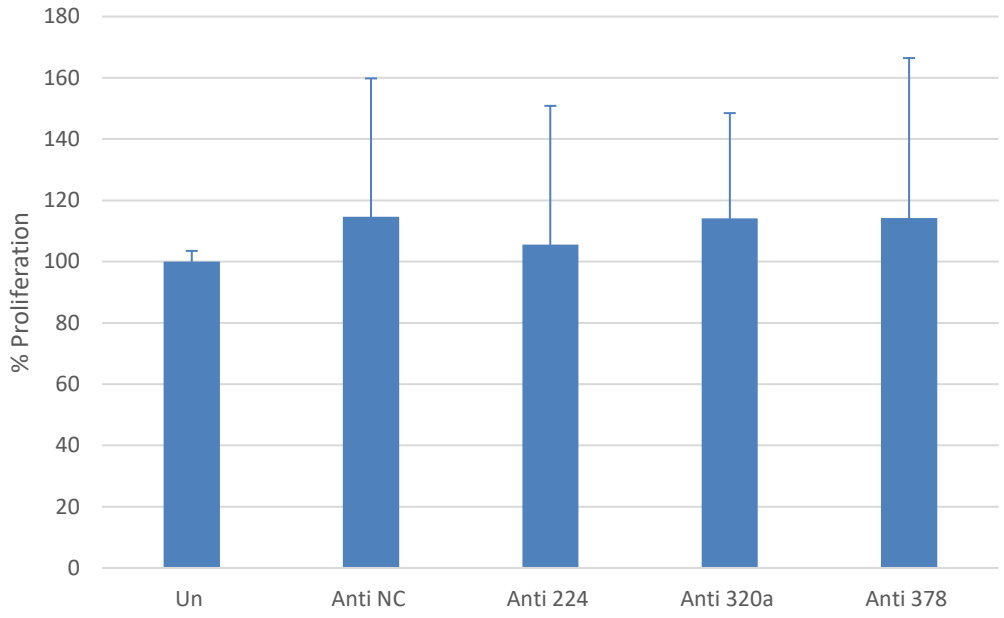

Percentage proliferation of the **Panc-1** cell line following transient knockdown of **miRNA 224**, **320a** and **378** with a negative control (Anti NC) included. All values are relative to untransfected control (Un). Error bars represent +/- standard deviation between biological replicates, (n=3).

The level of proliferation of Panc-1 cells was altered by increased expression of selected miRNA. Figure 7-1 displays the changes observed post 48hr transfection with Pre-miRs for miR-204, 224 and 320a. Transient overexpression of miR-224 induced a 50% reduction in proliferation, a 40% reduction was observed due to overexpression of miR-320a. While both of these results displayed no significance a trend of reduced proliferation was observed and the lack of significance may be due to variability between biological replicates. All values are relative to Panc-1 untransfected cells. No trend of changes in proliferation were observed due to transient reduction of miRNA expression as seen in Figure 7-2.

Figure 7-3. Percentage colony formation of **Panc-1** cells post transient transfection with a range of **Pre-miRs**

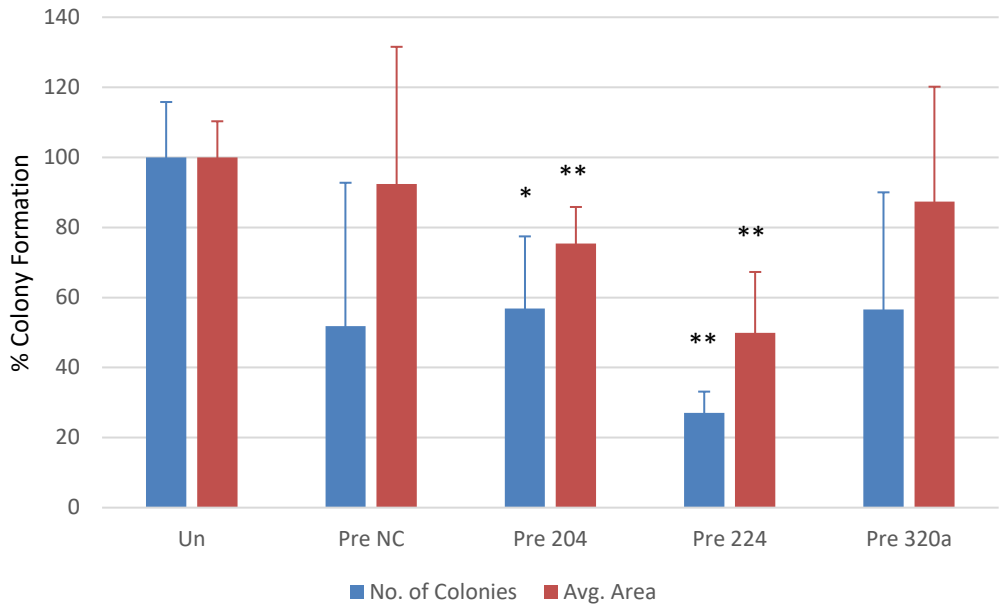

Percentage colony number and colony area of the **Panc-1** cell line following transient overexpression of miRNA **204**, **224** and **320a** with a negative control (Pre NC) included. All values are relative to untransfected control (Un). Error bars represent +/- standard deviation between biological replicates, (n=3, * = p value ≤ 0.05, ** = p value ≤ 0.01, p values = 0.02, 0.01, 0.002, 0.007).

Figure 7-4. Representative image of colony formation of **Panc-1** cells following transient miRNA overexpression

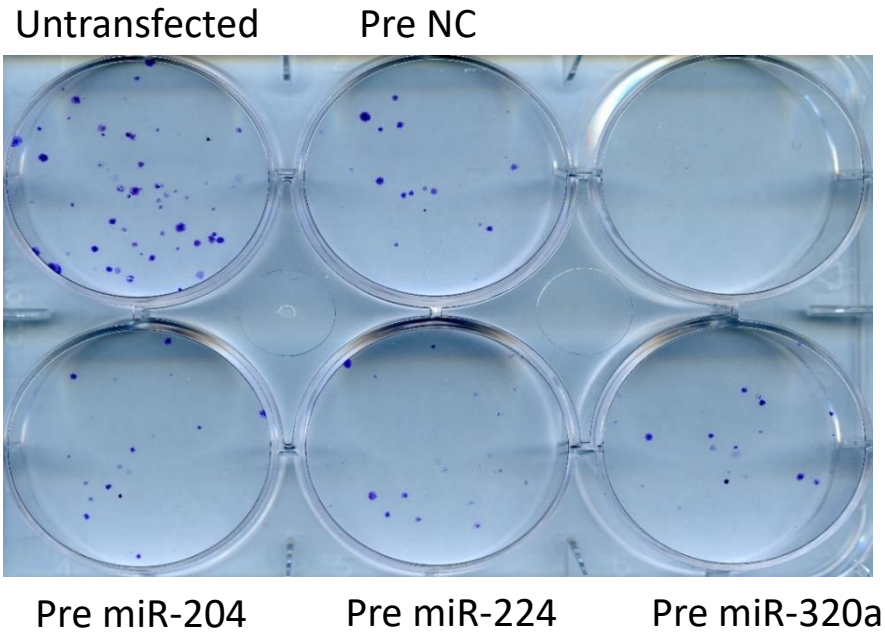

Representative image of colony formation of the **Panc-1** cell line following transient overexpression of **miRNA 204**, **224** and **320a** with a negative control (Pre NC) and untransfected control (Un) included.

The level of colony formation was effected by both over and reduced expression of selected miRNA. The changes observed post 48hr transfection with Pre-miRs for miR-204, 224 and 320a are shown in Figure 7-3. It displays a significant 40% reduction in colony number and a significant 25% reduction in colony area due to transient overexpression of Pre-204, p values of 0.02 and 0.01 respectively. Overexpression of miR-224 induced a significant 70% reduction in colony number, p value of 0.002. The colony size was also reduced by miR-224 overexpression, by a significant 50% with a p value of 0.007 as seen in Figure 7-4. A reduction in both colony number and size due to increased miR-320a was present but not statistically significant due to error between biological replicates. There appears to be a trend of reduced colony number due to a 40% reduction being present.

Figure 7-5. Percentage colony formation of **Panc-1** cells post transient transfection with a range of **Anti-miRs**

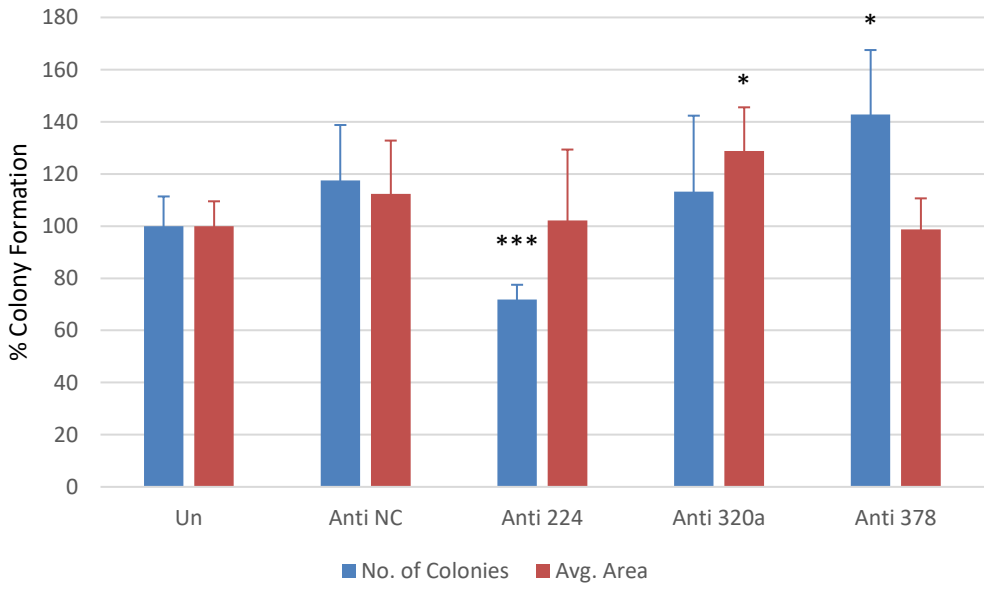

Percentage colony number of the **Panc-1** cell line following transient knockdown of **miRNA 224**, **320a** and **378** with a negative control (Anti NC) included. All values are relative to untransfected control (Un). Error bars represent +/- standard deviation between biological replicates, (n=3, * = p value ≤ 0.05, *** = p value ≤ 0.001, p values = 0.0009, 0.04, 0.04).

Figure 7-6. Representative image of colony formation of Panc-1 cells following transient miRNA reduction

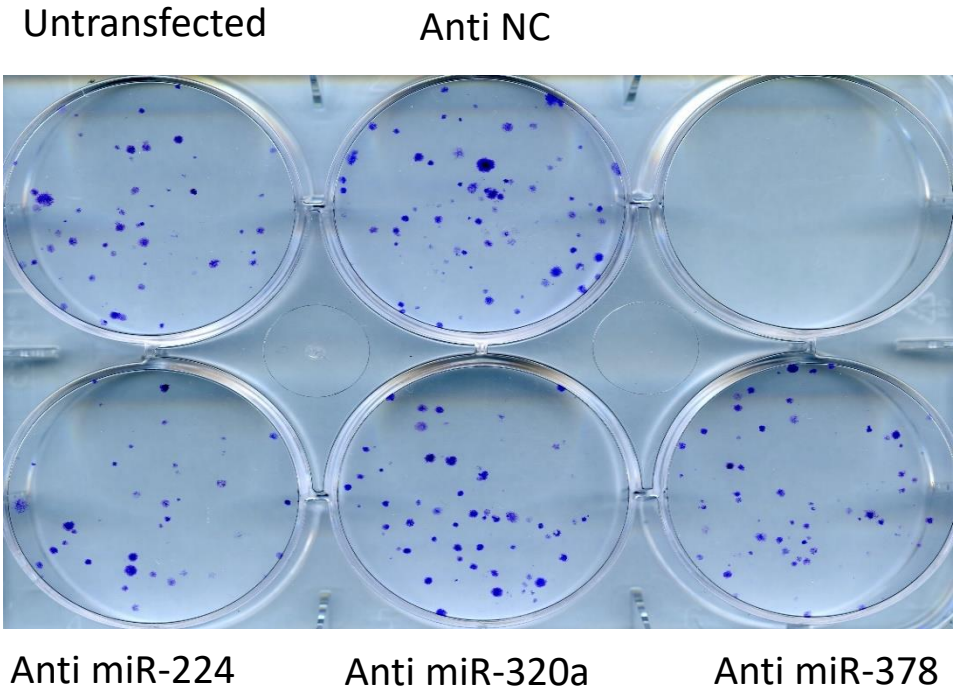

Representative image of colony formation of the **Panc-1** cell line following transient overexpression of **miRNA 204**, **224** and **320a** with a negative control (Anti NC) and untransfected control (Un) included.

Converse to proliferation, a functional effect on colony formation was induced due to transfection of Panc-1 cells with Anti-miRs, seen in Figure 7-5. A highly significant 30% reduction in colony number resulted from miR-224 reduced expression, p value of 0.0009. No change in colony size was observed due to miR-224 alteration. Reduced expression of miR-320a caused a significant 30% increase in colony size with a p value of 0.04. An increase in colony number, 40%, was induced post reduction of miR-378 expression, p value of 0.04 as seen in .

7.2.2. Development of stable cell lines to alter miRNA expression

A wide range of plasmid vectors to induce miRNA expression changes were available in-house. These tools included both overexpression and sponge knockdown vectors, a list of these are displayed in Table 7-2. All these vectors can be used to generate stable cell

lines. Vectors are transfected into the cells which then undergo a selection process as described in 2.6.4 and 2.6.5. This process selects for cells successfully transfected, a selection marker is included in the vector. The selection marker used in these vectors was Hygromycin B. Hygromycin B is an antibiotic which can be used to select for cells which have acquired a plasmid containing Hygromycin resistance. This aims to remove untransfected cells from the cell population, thus allowing for a greater examination of functional changes due to the expression alteration. The vectors in Table 7-2 are inducible vectors, meaning that the action of the vector can be controlled to a certain extent. The transcription of the vector is controlled through treatment with an inducement agent. Whether a sponge or overexpression vector, the alteration of the miRNA expression level should not occur until the inducer is added. Doxycycline Hyclate was the inducer for the vectors in Table 7-2. This is an antibiotic which activates transcription of the sponge/overexpression miRNA target. Vector maps for both sponge knockdown and overexpression are shown in Figure 7-7 and Figure 7-8.

Table 7-2. Overexpression and sponge knockdown vectors available for a wide range of miRNA

Overexpression	Knockdown	
miR-7	miR-7	miR-409*
miR-34a	miR-23b	miR-451
miR-10a	miR-34a	miR-455
miR-206	miR-144	miR-455*
	miR-204	miR-497
	miR-338	miR-497*
	miR-378	miR-505
	miR-378*	miR-505*
	miR-409	

Figure 7-7. Vector map of miRNA sponge knockdown of target miRNA

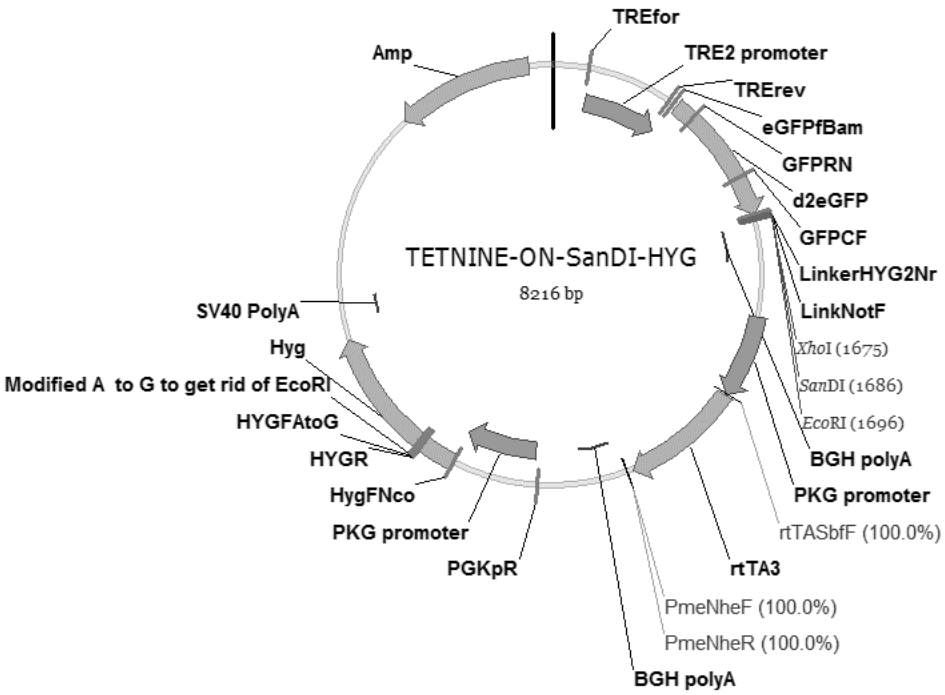

Inducible miRNA sponge vector, TET-NINE-SanDI-HYG. This construct contains a reporter gene, GFP, driven by an inducible TRE2 promoter and multiple cloning sites for sponge cloning. A trans-activator, rtTA3, which is driven by a PKG promoter, regulates the transcriptional activation of the reporter gene, GFP, in the presence of the induction agent Doxycycline. This sponge vector also encodes for the selective marker Hygromycin to allow for generation of stable cell lines.

Figure 7-8. Vector map of miRNA overexpression of target miRNA

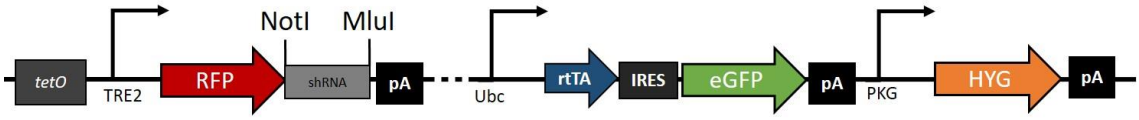

miRNA overexpression vector, TET-ON-HYG. This vector encodes for the reporter gene, RFP which is driven by a TRE2 promoter with transcription activated by the trans-activator rtTA3. The rtTA3 is co-expressed with an eGFP reporter. This sponge vector also encodes for the selective marker Hygromycin to allow for generation of stable cell lines.

7.2.3. Generation of stably altered cell lines

7.2.3.1. Optimisation of selection agent concentration, Hygromycin B

To generate stable cell lines, the minimum concentration of selection agent required to kill untransfected, parental cells needed to be determined. To do this a kill curve was used, this involved testing a range of Hygromycin B concentrations, 400µg/mL - 1200µg/mL, on Panc-1 parental cells.

Figure 7-9. Optimisation of selection agent concentration, Hygromycin B

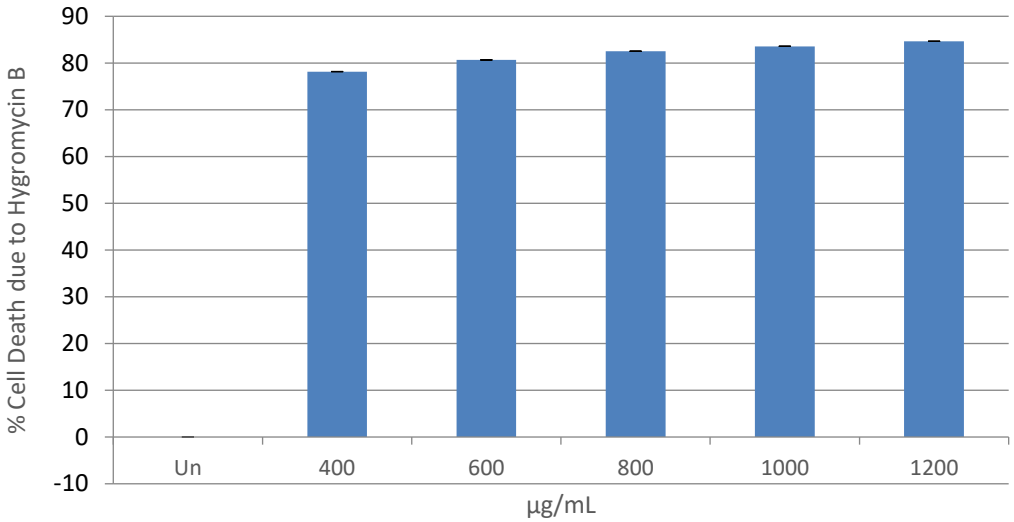

Percentage cell death of **Panc-1** cells using a varying range of selection agent, Hygromycin B concentrations. Untransfected (Un) Panc-1 cells act as the control and all values are relative to this. The concentrations examined are 400, 600, 800, 1000 and 1200µg/mL, (n=1).

7.2.3.2. Optimisation of transfection reagent concentration, Mirus TransIT X2 and vector concentration

To generate stable cell lines, the optimum concentration of transfection reagent and plasmid vector required for sufficient transfection efficiency was investigated. To do this a range of concentrations for both parameters were examined. Then fluorescence of reporter gene GFP was assessed under the microscope to confirm transfection and determine transfection efficiency.

Table 7-3. Optimisation of transfection reagent concentration, Mirus TransIT X2 and vector concentration using miR-505 Sponge KD vector

Sample	Fluorescence only	Overlay
Untransfected		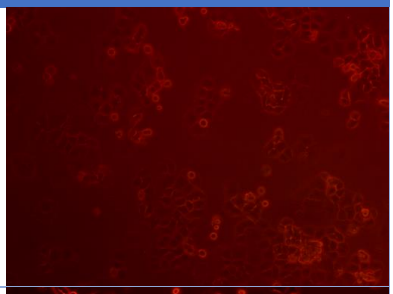
Mirus only		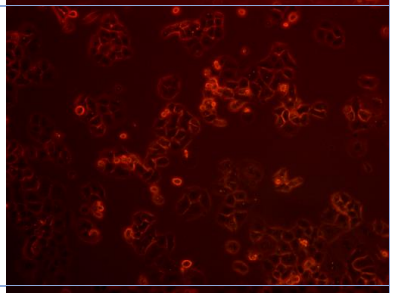
1.5µg in 1µL of Mirus	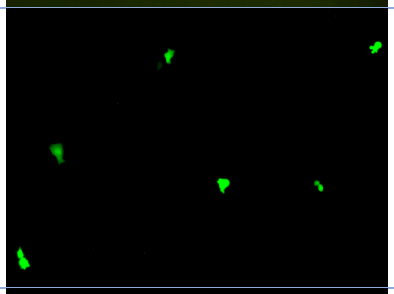	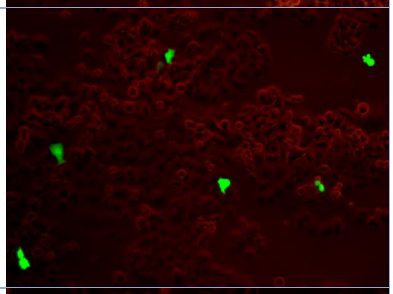
3µg in 3µL of Mirus	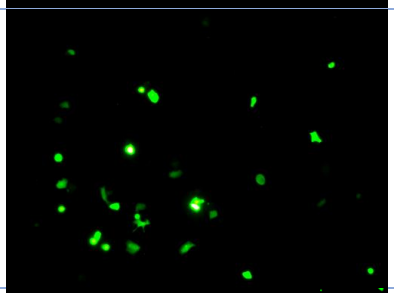	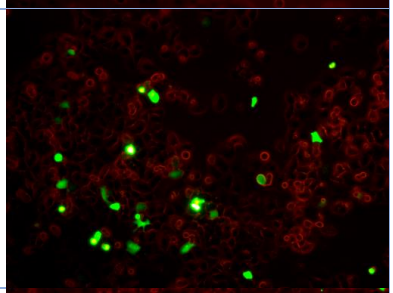
5µg in 5µL of Mirus	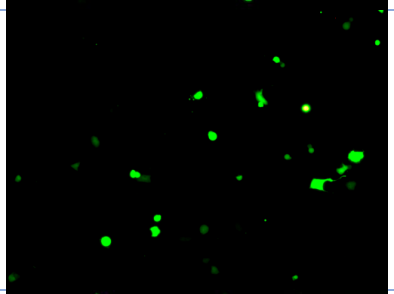	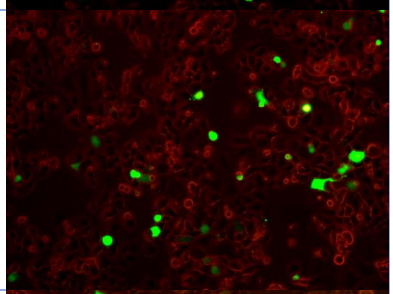
5µg in 7.5µL of Mirus	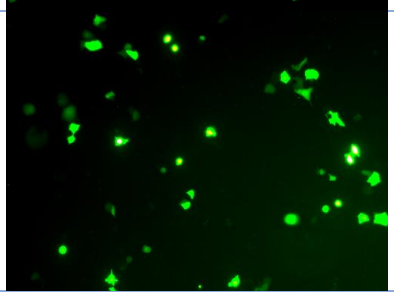	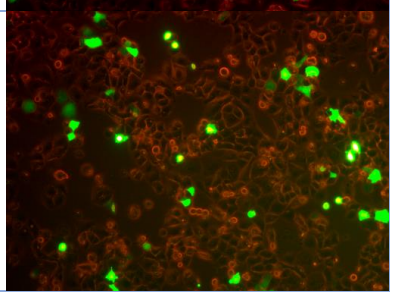

7.2.3.3. Confirmation of inducement of Panc-1 cells with miR-505 sponge

To confirm these vectors were behaving as inducible vectors i.e. altering expression after treatment with Doxycycline, fluorescence was visualised 4 days' post induction. Without inducement, the reporter gene, GFP, should be not expressed meaning no florescence should be detected.

Table 7-4. Confirmation of inducement of Panc-1 cells with miR-505 sponge

Un-induced	Induced	Induced Overlay
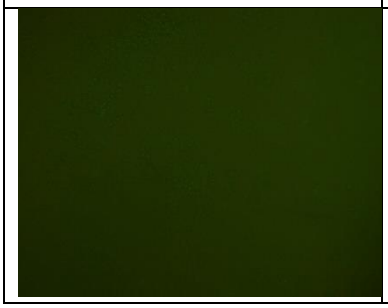	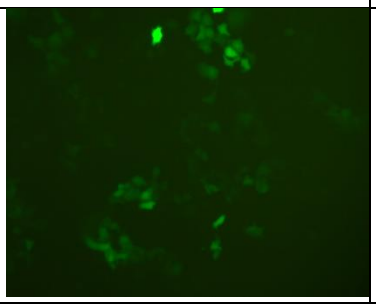	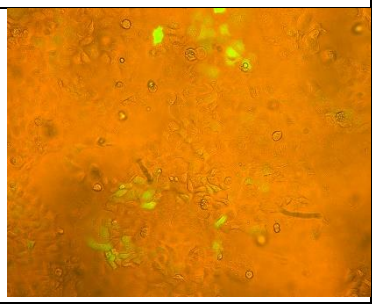

The optimum conditions for generation of stable cell lines was determined through optimisation. The kill curve shown in Figure 7-9 determined that at a concentration of 400µg/mL ~80% cell death occurred. This was the minimum concentration in the range tested, required to kill untransfected, parental Panc-1 cells. Table 7-3 displays the highest level of fluorescence and therefore the highest transfection efficiency was produced using 5µg of vector and 7.5ul of Mirus TransIT X2 transfection reagent. To confirm these vectors were inducible i.e. altering expression after treatment with Doxycycline, fluorescence was visualised 4 days' post induction. Table 7-4 displays minimal fluorescence without Doxycycline treatment ensuring the vector was not functioning when induction was not present. Post induction fluorescence was observed confirming the vector was functional post induction.

7.2.4. miRNA target selection and validation of altered miRNA expression

A large cohort of plasmid vectors to induce miRNA expression changes were available in-house. These tools included both overexpression and sponge knockdown vectors, a list of these are displayed in Table 7-2. The miRNA listed were the beginning of the choice of target miRNA using an unbiased approach. From this large cohort miRNA targets for overexpression and sponge knockdown were chosen to investigate. The first step in target selection was to elucidate the innate, basal expression levels of each miRNA member of the cohort across a panel of pancreatic cancer cell lines. Figure 7-10 shows the basal expression level of the possible target miRNA across the panel with a normal cell line, human mammary epithelial cell (HMEC) included. Expression levels are displayed as Ct value evaluated through qPCR as described in 2.10.2. Data from qPCR analysis indicates the level of expression through Ct values. These values are on a scale of 1-40, this is due to the number of cycles ran through the qPCR. In simple terms a high Ct value indicates low expression of the target; a low Ct value meaning high expression of the target. This is due to the number of cycles it requires for the target to cross the threshold, hence the name Cycle Threshold (Ct). This means the more cycles required to reach the threshold the less target expression present in the sample. Ct values between 20-30 Ct are considered reliable data, outside of this range the data can contain variability and false readings. These basal levels along with a review of the current knowledge of each miRNA, were used to determine which miRNA targets were most appropriate for expression alteration using the tools listed in Table 7-2. These choices are detailed in the following sections.

Figure 7-10. Screen of basal miRNA expression across a panel of pancreatic cancer cell lines

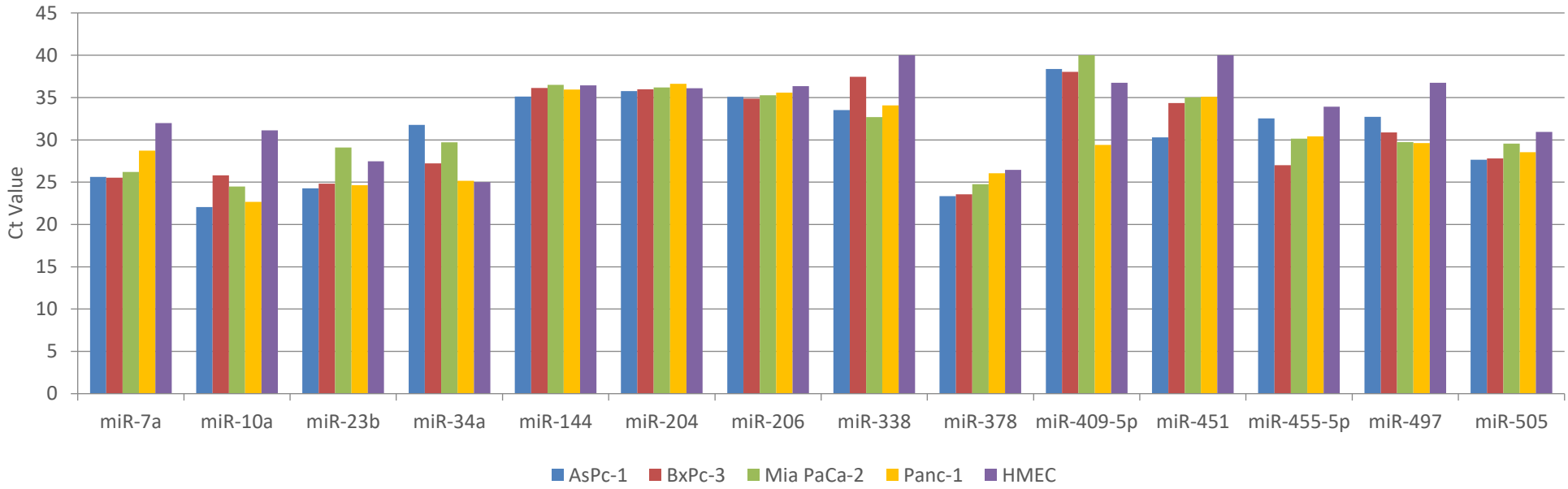

Basal expression of a panel of 14 miRNA displayed as Ct value across a panel of pancreatic cancer cell lines (AsPc-1, BxPc-3, Mia PaCa-2 and Panc-1) with HMEC included as a normal cell line. The miRNA listed were the beginning of the choice of target miRNA using an unbiased approach. From this large cohort miRNA targets for overexpression and sponge knockdown were chosen to investigate further based on the innate basal expression levels.

There were limited published investigations of the role of miR-7a in pancreatic cancer. One study examined the effect of Curcumin which had an anti-tumour activity on pancreatic cancer. This treatment caused an increase in miR-7 expression as well as suppression of growth, migration and invasion along with an increase in apoptosis indicating a tumour suppressor role of miR-7a in pancreatic cancer (Ma et al. 2014a). A small number of publications investigated the role of miR-7 in invasion in a range of cancer types, such as cervical cancer, gastric cancer, colorectal cancer and melanoma. Across this range of diseases miR-7 was very lowly expressed and overexpression inhibited migration, invasion and cell growth, identifying miR-7 as a tumour suppressor miRNA (Giles et al. 2016, Zeng et al. 2016, Hao et al. 2015, Xie et al. 2014). Similar results were also observed in NSCLC (Cao et al. 2016). All of these studies showed miR-7a functioning as a tumour suppressor miRNA in a range of diverse cancer types. miR-7a showed medium expression, Ct value of ~25, across the panel of cancer cell lines with low expression observed in the normal HMEC cell line, seen in Figure 7-10. As a Ct value of 28 was observed in the Panc-1 cell line and considering the published cancer studies showed miR-7a to play a tumour suppressor role, an overexpression vector for miR-7a was deemed most appropriate to investigate if miR-7a acts as a tumour suppressor in pancreatic cancer.

Publications had shown miR-34a as a tumour suppressor miRNA that is commonly deleted in several cancers including lung, breast, liver and colon. This miRNA was involved in the p53 and Wnt/β-catenin pathways and restoration of its expression through a transient Pre-miR transfection inhibited tumour growth and progression (Liu et al. 2011). It has also been stated that miR-34a is frequently absent in pancreatic cancers (Chang et al. 2007). This study showed overexpression of miR-34a induced apoptosis through an apoptotic program triggered by the tumour suppressor protein p53, evidence indicated miR-34a to be a direct transcriptional target of p53. Overexpression of miR-34a was also shown to dramatically inhibit proliferation in Panc-1 and Mia PaCa-2 cell lines (Ikeda et al. 2012). A Pre-miR for miR-34a known as MRX34 entered clinical testing in 2013. Unfortunately, as of September 2016, this clinical trial was halted due to immune related adverse effects. Downregulation of the target

resulted in an increase in cell cycle progression and angiogenesis as well as a decrease in apoptosis and DNA repair in pancreatic cancer (Rachagani, Kumar and Batra 2010). More evidence of the tumour suppressor function of miR-34a was observed *in vivo*, overexpression of miR-34a inhibited growth and proliferation while increasing apoptosis in mice xenografts tissues (Pramanik et al. 2011). Conversely, miR-34a was a part of the 10 miRNA index discussed below in relation to miR-505, which exhibited higher expression in pancreatic cancer patients compared to healthy controls (Schultz et al. 2014). This paper suggested an oncogenic role for miR-34a but this study was in the minority with its suggestion (Ikeda et al. 2012). miR-34a was expressed at varied levels across the pancreatic cancer panel shown in Figure 7-10, with the Panc-1 cell line displaying medium expression with a Ct value of 25. Considering this either a sponge or overexpression vector was appropriate, an overexpression vector was chosen due to the fact that miR-34a is frequently absent in pancreatic cancer (Chang et al. 2007).

A small number of publications have shown miR-206 to act as a tumour suppressor miRNA in pancreatic cancer. Two publications stated that miR-206 is significantly decreased in pancreatic cancer patient tissues in comparison to normal controls (Ju et al. 2016, Keklikoglou et al. 2014). These studies observed that overexpression of miR-206 inhibited progression of pancreatic cancer through decreased growth, migration and invasion. Growth *in vivo* in mice xenografts was reduced as well as proliferation, with apoptosis being increased, shown through tissue staining of Ki67 and TUNEL (Ju et al. 2016, Keklikoglou et al. 2014). *In vitro* overexpression in both the Panc-1 and BxPc-3 cell lines induced significant decreases in cell proliferation, migration and invasion (Keklikoglou et al. 2014). These studies showed a tumour suppressor role of miR-206 in pancreatic cancer. Due to no/low expression of miR-206 observed across the panel of pancreatic cancer cell lines, as seen in Figure 7-10 and the previous publications mentioned, an overexpression vector was determined most suitable and may confirm a tumour suppressor role of miR-206 on pancreatic cancer.

miR-378 has very little link to pancreatic cancer with a patient sera array analysis being the only substantial published study. This showed miR-378 as a circulating miRNA which was significantly elevated in pancreatic cancer sera compared with control groups (Li et al. 2013). There are a small number of publications addressing the role of miR-378 in invasion in a range of cancer types. In different cancer types this miRNA appeared to play a different role in invasion. For instance, in both glioma and colorectal cancers, miR-378 overexpression reduced migration, invasion and in colorectal cancer a reduction in proliferation was also observed, miR-378 appears to act as an oncomiR in these cancer types (Li et al. 2015a, Zhang et al. 2014). However, in liver and non-small cell lung cancer, miR-378 overexpression was associated with increased migration and invasion as well as increased proliferation in liver cancer and increased angiogenesis in NSCLC, meaning it played a role as a tumour suppressor (Ma et al. 2014b, Chen et al. 2012). miR-378 was expressed at medium to high levels across the pancreatic cancer panel with a Ct value of 26 being present in the Panc-1 cell line, shown in Figure 7-10, therefore, a miRNA sponge was deemed the most appropriate for alteration of miR-378 expression.

There is little published data on the role of miR-505 in cancer. The majority of the papers which do mention this target are miRNA screens and profiles which reference miR-505 in a list of differential expression. One of the few functional studies observed that miR-505 transient overexpression in endometrial cancer reduced proliferation, migration and invasion (Chen et al. 2016b). One pancreatic cancer paper exists which addresses miR-505, this paper assessed miRNA as biomarkers for pancreatic cancer in blood. miR-505 was a part of two diagnostic panels used to distinguish patients with pancreatic cancer from healthy controls. miR-505 was among a 10 miRNA index which exhibited higher expression in pancreatic cancer patients compared to healthy controls (Schultz et al. 2014). Low expression of miR-505 was present across the panel of cell lines, with Panc-1 displaying a Ct value of 28, seen in Figure 7-10. It was determined to alter miR-505 expression with a sponge knockdown vector. This was due to no overexpression vector being available and due to the level of novelty of miR-505 in pancreatic cancer, any assessment of its role in pancreatic cancer was deemed valuable.

7.2.5. Confirmation of altered miRNA expression

Figure 7-11 through to Figure 7-15 display the relative quantification of each miRNA target. Once stable cell lines had been developed, confirmation of altered miRNA expression was required. qPCR was used to investigate the level of, if any, altered miRNA expression, qPCR method described in section 2.10.2. Figure 7-11 and Figure 7-12 display no significant change in fold change in either miR-378 or miR-505 in the stable cell lines. In fact, it appears an overexpression is present in miR-505. However, taking into account the Ct values displayed in Table 7-5, a 1 Ct value difference is displayed between the induced negative control and the induced target miRNA. An increase in Ct value indicates a decrease in expression, as described in section 7.2.4, also 1 Ct value equates to a 2-fold change (Morey, Ryan and Van Dolah 2006). This reduction in expression caused by the sponge knockdown was not found in the qPCR Relative Quantification analysis, this was due to changes in the Ct value of the endogenous control, Let-7e (data not shown) and also due to expression changes in the negative control when induced, seen in Table 7-5. Treatment with the induction agent Doxycycline appeared to cause alteration in miRNA expression levels in the negative control. There appeared to be no overexpression of miR-7a as seen in Figure 7-13 and Table 7-5. The same is true for miR-34a, shown in Figure 7-14, however, the Ct values displayed in Table 7-5, show an increase of 1.2 Ct (indicating an increase in expression) in miR-34a between the induced negative control and the induced target miRNA. This indicates a 2-fold increase in miR-34a expression. This was not found in the qPCR Relative Quantification analysis due to changes in the Ct values of the endogenous control, Let-7e (data not shown) and also due to expression changes in the negative control when induced, seen in Table 7-5. Successful overexpression of miR-206 was achieved, displayed in Figure 7-15 as well as Table 7-5. A vast increase of miR-206 expression was achieved, ~230-fold change. It appeared a reduction in miRNA expression of miR-378 and miR-505 was achieved using sponge knockdown and overexpression was achieved for miR-34a and miR-206 but more qPCR analysis is required to show this conclusively. The change of miRNA expression in the negative control post inducement must also be addressed.

Figure 7-11. Relative quantification of **miR-378** expression post sponge knockdown

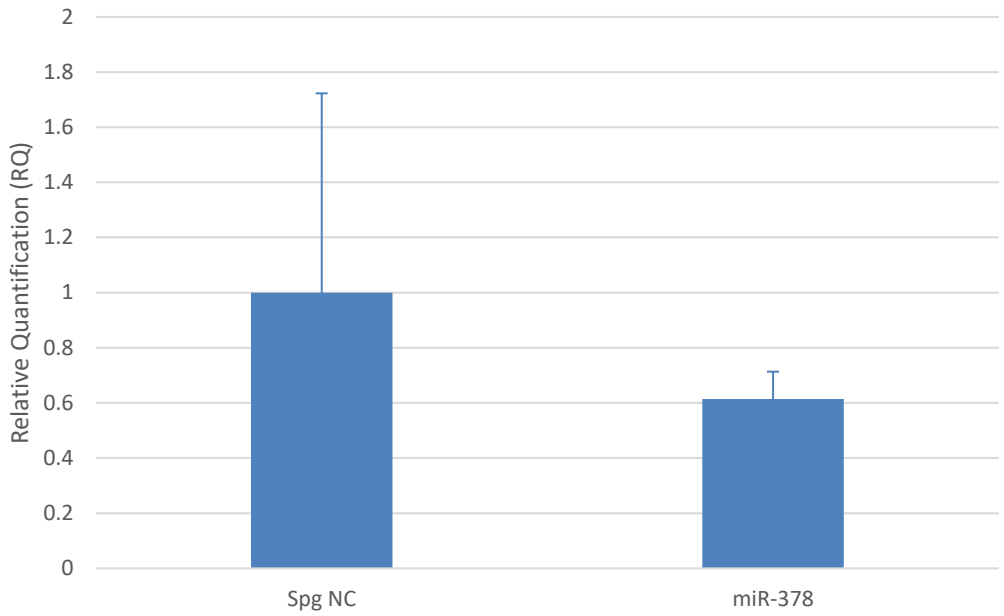

Relative quantification of **miR-378** expression in the **Panc-1** cell line 24hr post induction of sponge knockdown relative to the sponge negative control using Let-7e as an endogenous control.

Figure 7-12. Relative quantification of **miR-505** expression post sponge knockdown

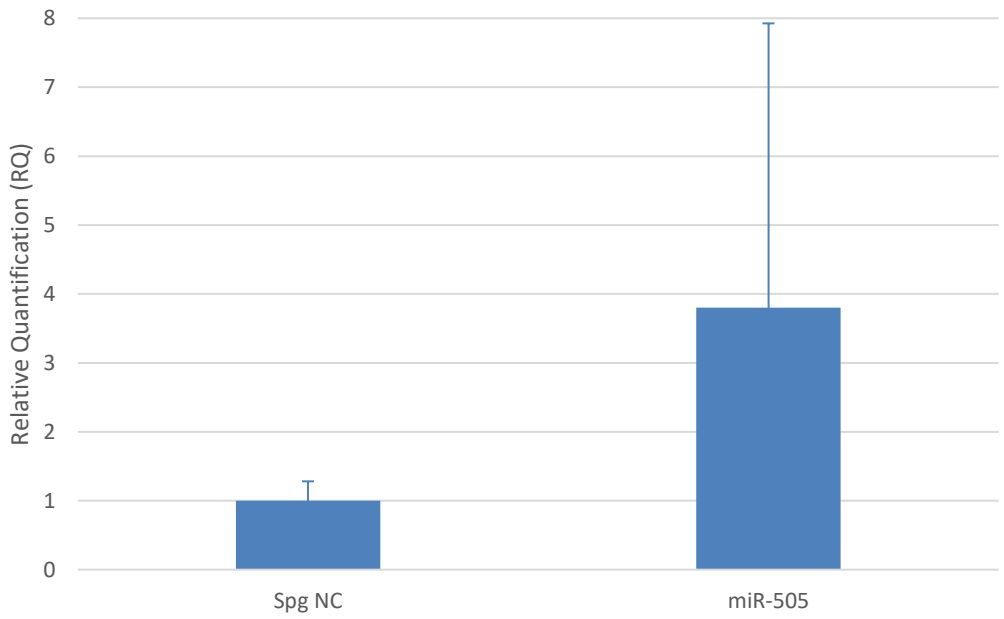

Relative quantification of **miR-505** expression in the **Panc-1** cell line post 24hr induction of sponge knockdown relative to the sponge negative control using Let-7e as an endogenous control.

Figure 7-13. Relative quantification of **miR-7a** overexpression post transfection

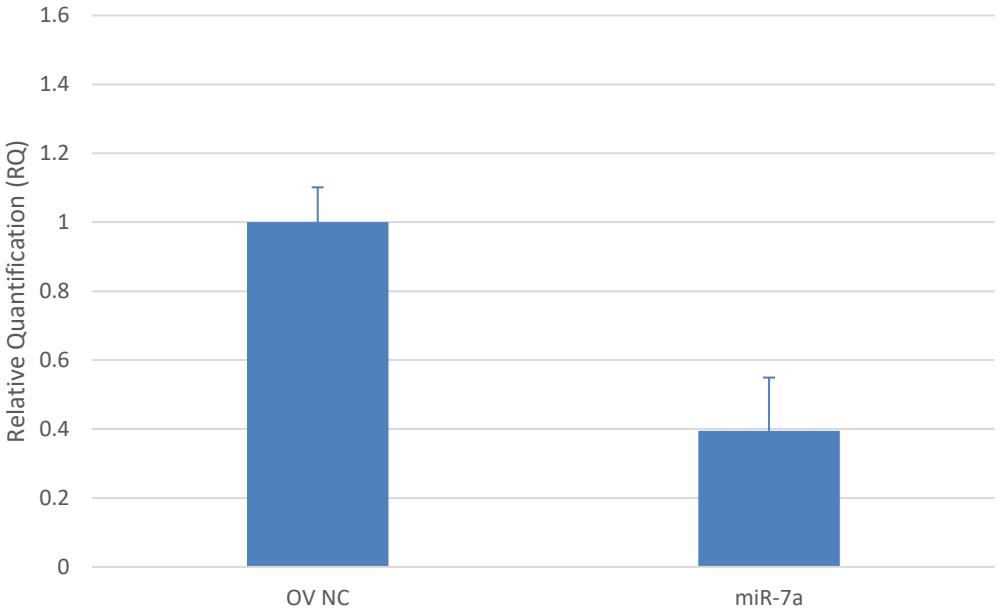

Relative quantification of **miR-7a** expression in the **Panc-1** cell line post 24hr induction of overexpression relative to the overexpression negative control using Let-7e as an endogenous control.

Figure 7-14. Relative quantification of **miR-34a** overexpression post transfection

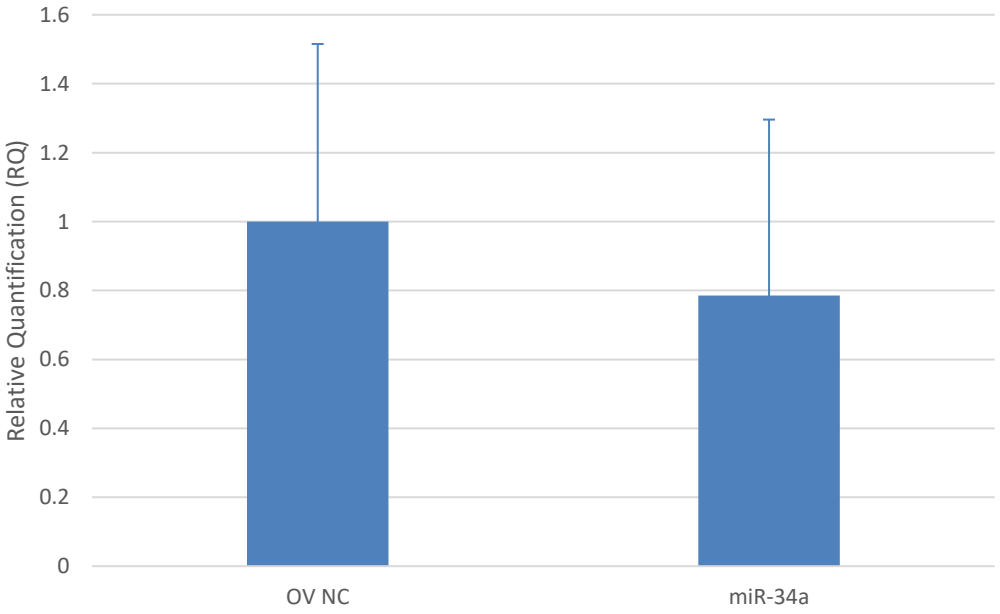

Relative quantification of **miR-34a** expression in the **Panc-1** cell line post 24hr induction of overexpression relative to the overexpression negative control using Let-7e as an endogenous control.

Figure 7-15. Relative quantification of **miR-206** overexpression post transfection

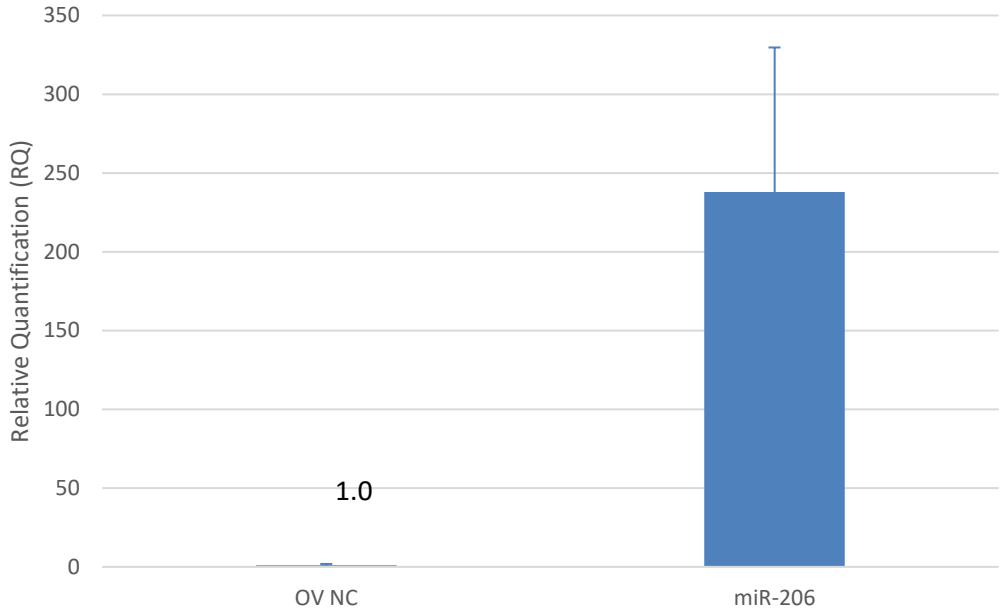

Relative quantification of **miR-206** expression in the **Panc-1** cell line post 24hr induction of overexpression relative to the overexpression negative control using Let-7e as an endogenous control.

Table 7-5. Ct values of each miRNA target, un-induced and induced.

miR-378	Ct Value
Spg NC Un	22.5
miR-378 Un	23.9
Spg NC In	25.7
miR-378 In	27.0

miR-505	Ct Value
Spg NC Un	25.5
miR-505 Un	27.9
Spg NC In	26.8
miR-505 In	27.8

miR-7a	Ct Value
OV NC Un	27.6
miR-7a Un	28.4
OV NC In	28.2
miR-7a In	28.0

miR-34a	Ct Value
OV NC Un	25.0
miR-34a Un	25.9
OV NC In	22.8
miR-34a In	24.0

miR-206	Ct Value
OV NC Un	32.4
miR-206 Un	25.1
OV NC In	31.7
miR-206 In	22.9

The Ct values of each miRNA target with the negative control included, Ct values in both un-induced (Un) and induced (In) conditions are displayed.

7.2.6. Functional effects of stable enduring alteration of miRNA expression

Once cell lines with stably altered miRNA expression were generated and confirmed, functional changes due to altered miRNA expression were investigated. Functional changes due to reduced expression of miR-378 and miR-505 and increased expression of miR-7a, miR-34a and miR-206 were assessed in anoikis, proliferation, colony formation and invasion. An untransfected control was included in each experiment as well as a negative control, either a sponge negative control or an overexpression negative control. All functional effects were assessed with inducement i.e. Doxycycline present in assay.

Figure 7-16. Percentage survival of induced and un-induced **Panc-1** cells

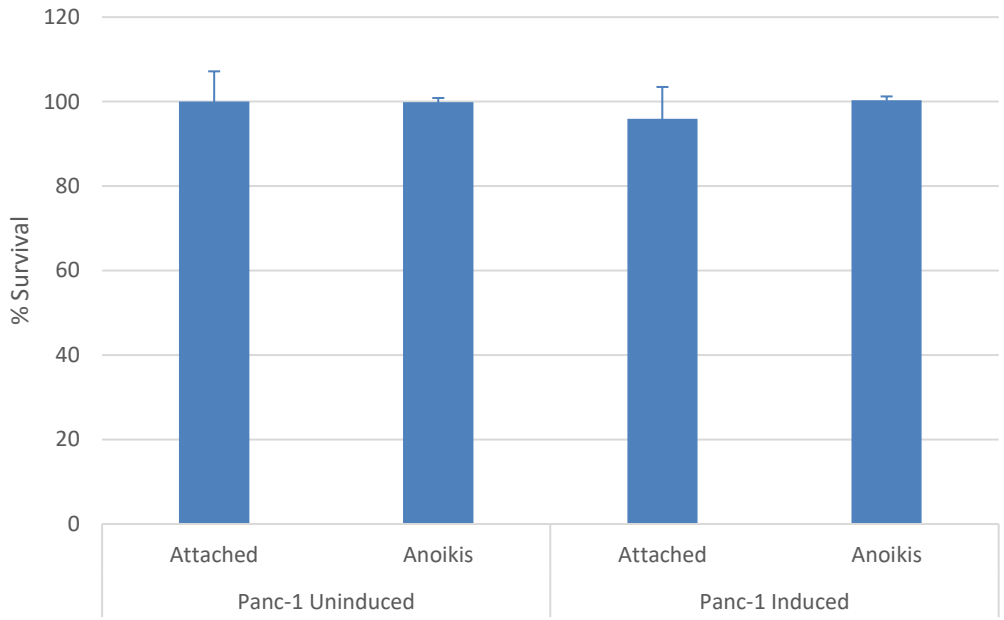

Percentage survival of **Panc-1** cells un-induced and induced, in both attached and anoikis i.e. suspension conditions relative to attached un-induced as the control. Induction with 1µg/mL of Doxycycline is present throughout the assay in the induced samples. Error bars represent +/- standard deviation between biological replicates, (n=3).

Figure 7-17. Percentage survival of **Panc-1** cells post sponge knockdown of miRNA expression

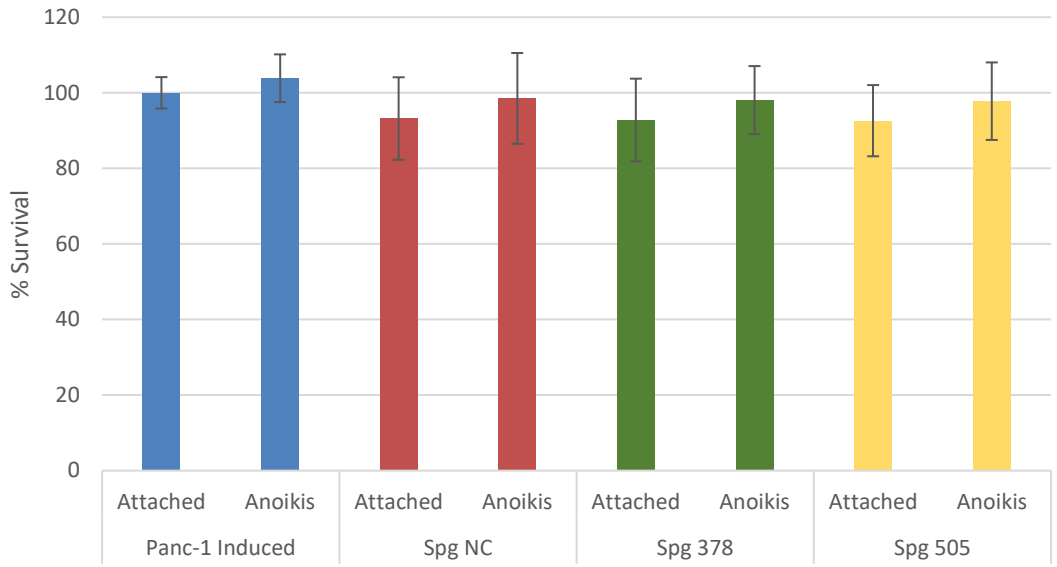

Percentage survival of **Panc-1** cells in both anoikis i.e. suspension and attached conditions with Panc-1 induced cells acting as the control. Survival post miRNA expression reduction is displayed by Sponge negative control, **Spg 378** and **Spg 505**. Induction with 1µg/mL of Doxycycline is present throughout the assay. Error bars represent +/- standard deviation between biological replicates, (n=5).

Figure 7-18. Percentage survival of **Panc-1** cells post miRNA overexpression

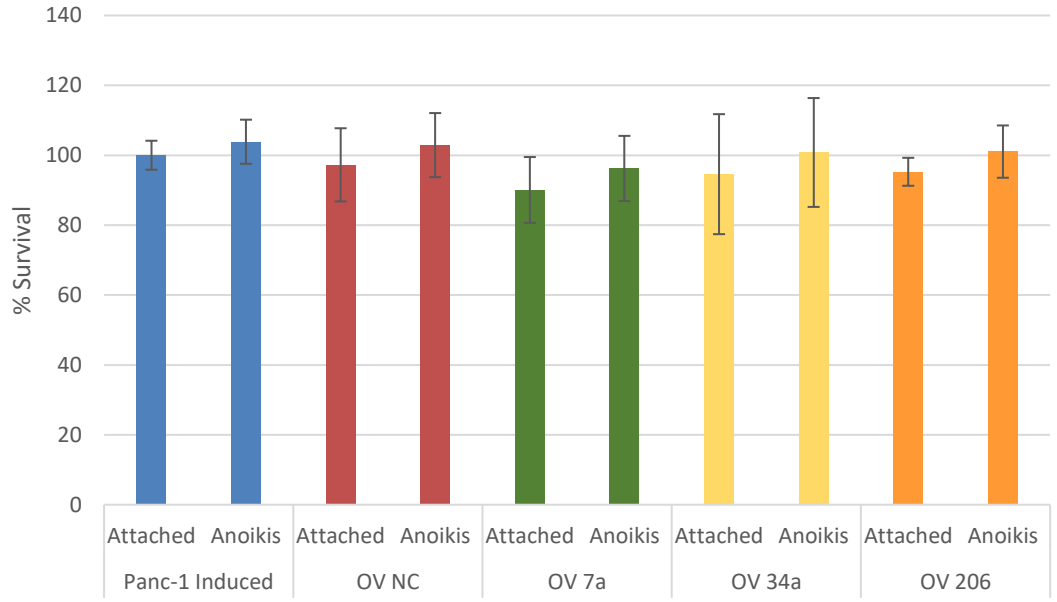

Percentage survival of **Panc-1** cells in both suspension and attached conditions with Panc-1 induced cells acting as the control. Survival post miRNA overexpression is displayed by overexpression negative control, **OV 7a**, **OV 34a** and **OV 206**. Induction with 1µg/mL of Doxycycline is present throughout the assay. Error bars represent +/- standard deviation between biological replicates, (n=5).

Treatment of parental Panc-1 cells with doxycycline, the inducer, had no effect on survival in either attached or suspension conditions, as seen in Figure 7-16. Neither sponge knockdown or overexpression of any target miRNA had any effect on survival in either suspension or attached conditions, displayed in Figure 7-17 and Figure 7-18. The alteration of miR-7a, 34a, 206, 378 and 505 expression did not show any effect on the ability of Panc-1 cells to survive in suspension.

Figure 7-19. Percentage proliferation of induced and un-induced **Panc-1** cells

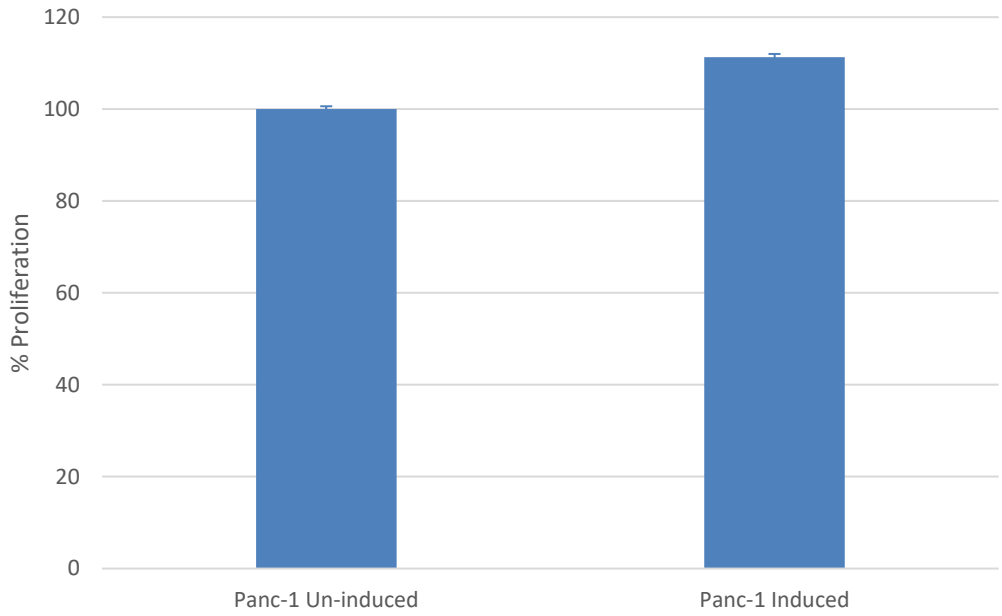

Percentage proliferation of **Panc-1** cells un-induced and induced after 7 days' incubation, relative to un-induced as the control. Induction with 1µg/mL of Doxycycline is present throughout the assay in the induced samples. Error bars represent +/- standard deviation between technical replicates, (n=1).

Figure 7-20. Percentage proliferation of **Panc-1** cells post sponge knockdown of miRNA expression

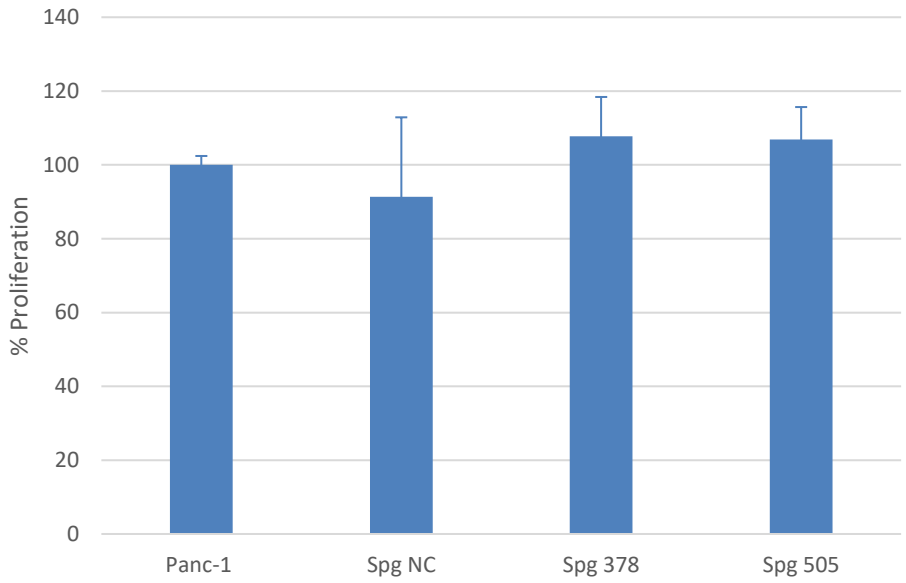

Percentage proliferation of **Panc-1** cells with Panc-1 induced cells acting as the control. Proliferation post miRNA expression reduction is displayed by Sponge negative control, **Spg 378** and **Spg 505**. Induction with 1µg/mL of Doxycycline is present throughout the assay. Error bars represent +/- standard deviation between biological replicates, (n=4).

Figure 7-21. Percentage proliferation of **Panc-1** cells post miRNA overexpression

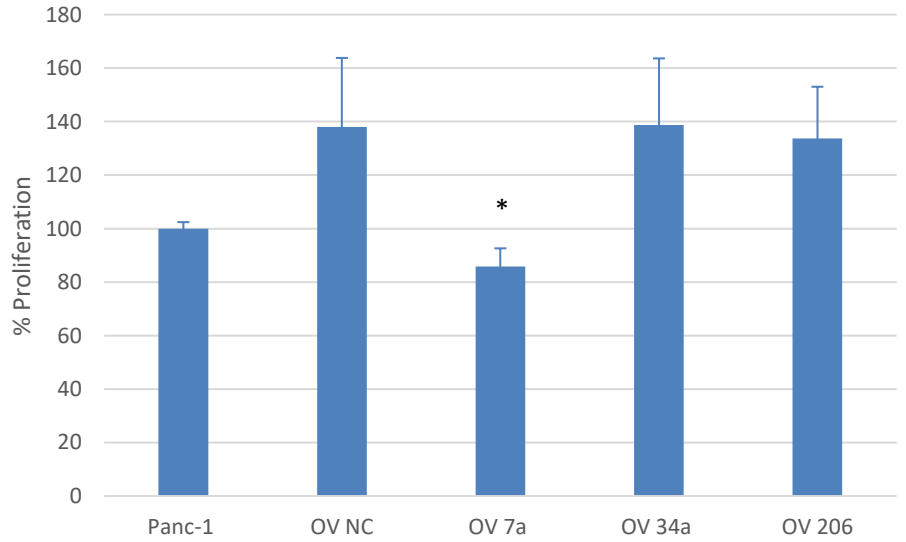

Percentage proliferation of **Panc-1** cells with Panc-1 induced cells acting as the control. Proliferation post miRNA overexpression is displayed by overexpression negative control, **OV 7a**, **OV 34a** and **OV 206**. Induction with 1µg/mL of Doxycycline is present throughout the assay. Error bars represent +/- standard deviation between biological replicates, (n=4, p value = 0.02).

The inducer, Doxycycline, increased proliferation of Panc-1 cells by 10%, seen in Figure 7-19. Due to this, induced Panc-1 cells were used as the control and all proliferation values were calculated relative to this. No effect on proliferation was observed due to sponge knockdown alteration of miRNA expression, shown in Figure 7-20. Figure 7-21 displays proliferation changes due to overexpression of miR-7a, miR-34a and miR-206 with an untransfected control and overexpression negative control included. Interestingly, a 40% increase in proliferation resulted from the OV NC, this change validated that induced parental Panc-1 cells were the most appropriate control as the negative control vector caused changes in the cell line. A significant 15% reduction in proliferation was due to miR-7a overexpression with a p value of 0.02. Overexpression of both miR-34 and miR-206 caused an increase in proliferation, 40% and 30%, but these changes were not statistically significant.

Figure 7-22. Percentage colony formation of **Panc-1** cells post sponge knockdown of miRNA expression

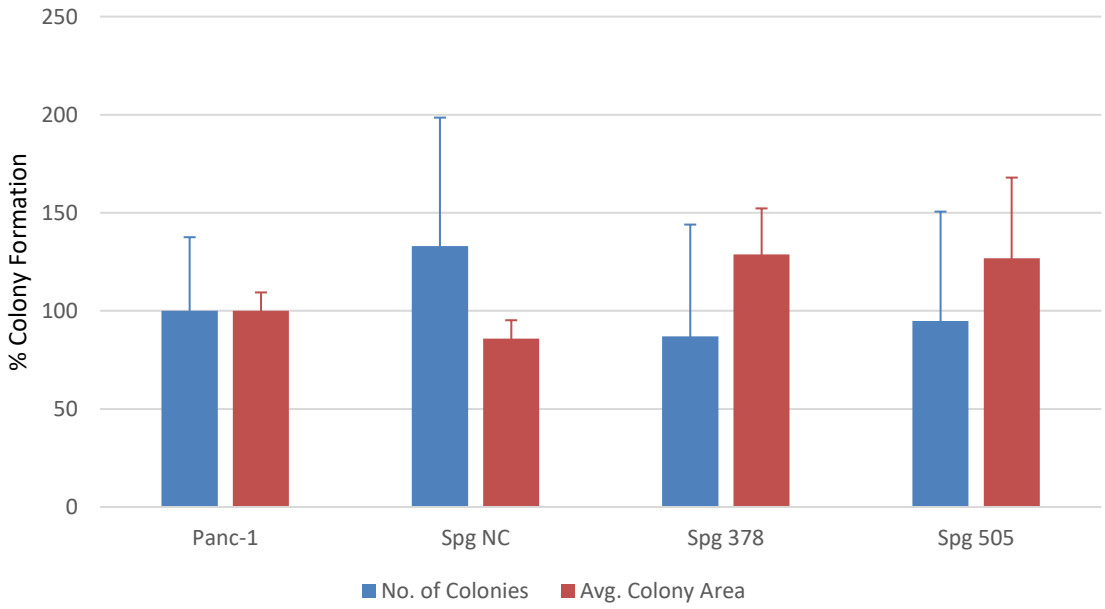

Percentage number of colonies and colony area of **Panc-1** cells with Panc-1 induced cells acting as the control. Colony formation post miRNA expression reduction is displayed by Sponge negative control, **Spg 378** and **Spg 505**. Induction with 1µg/mL of Doxycycline is present throughout the assay. Error bars represent +/- standard deviation between biological replicates, (n=3).

Figure 7-23. Representative image of colony formation of **Panc-1** post sponge knockdown

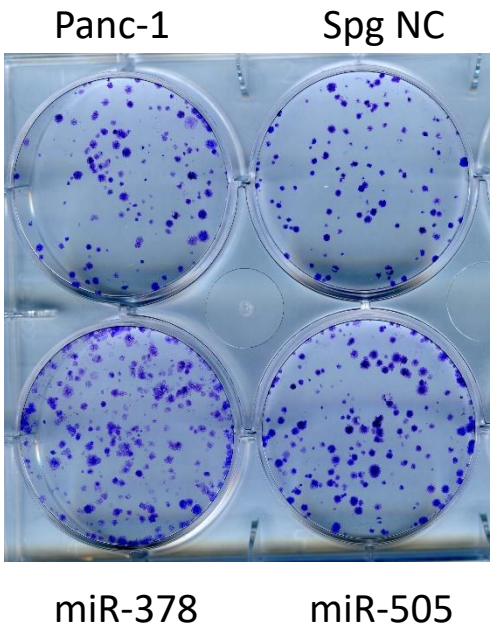

Representative image of colony formation of the **Panc-1** cell line following sponge knockdown of **miR-378** and **miR-505**. With parental Panc-1 and Sponge negative control included.

Figure 7-24. Percentage colony formation of **Panc-1** cells post miRNA overexpression

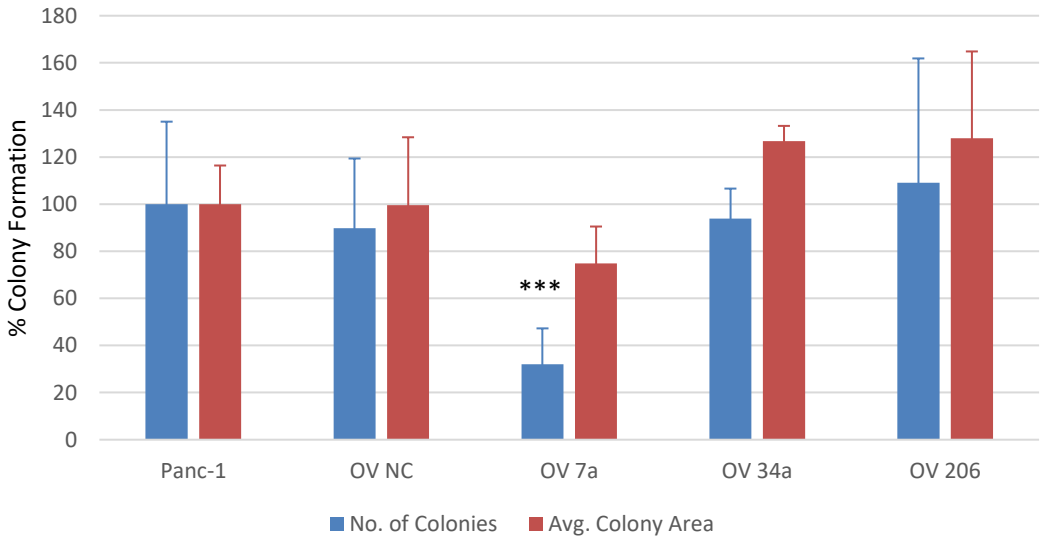

Percentage number of colonies and colony area of **Panc-1** cells with Panc-1 induced cells acting as the control. Colony formation post miRNA overexpression is displayed by overexpression negative control, **OV 7a**, **OV 34a** and **OV 206**. Induction with 1µg/mL of Doxycycline is present throughout the assay. Error bars represent +/- standard deviation between biological replicates, (n=3, *** = p value ≤ 0.001, p value = 0.001).

Figure 7-25. Representative image of colony formation of **Panc-1** cells post miRNA overexpression

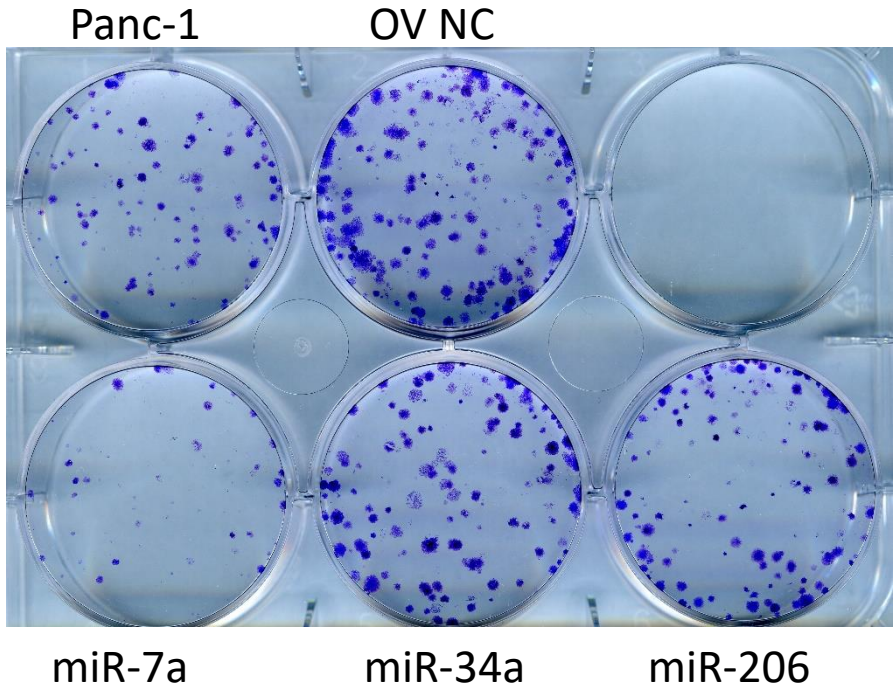

Representative image of colony formation of the **Panc-1** cell line following overexpression of **miR-7a**, **miR-34a** and **miR-206**. With parental Panc-1 and Overexpression negative control included.

Figure 7-22 displays no significant change in colony formation resulted from miRNA sponge knockdown of miR-378 or miR-505. A representative image of colony formation post sponge knockdown as well as parental Panc-1 cells treated with the inducer, Doxycycline is shown in Figure 7-23. A highly significant decrease in colony number and a decrease in colony size resulted from miR-7a overexpression, observed in Figure 7-24. The number of colonies was reduced by 70% compared to induced Panc-1 parental cells with a p value of 0.001. The reduction in colony size of 25% did not show statistical significance. A representative image is seen in Figure 7-25. Overexpression of miR-34a and miR-206 had no effect on colony number but caused an increase in colony size, although no statistical significance was present.

Figure 7-26. Percentage invasion of induced and un-induced **Panc-1** cells

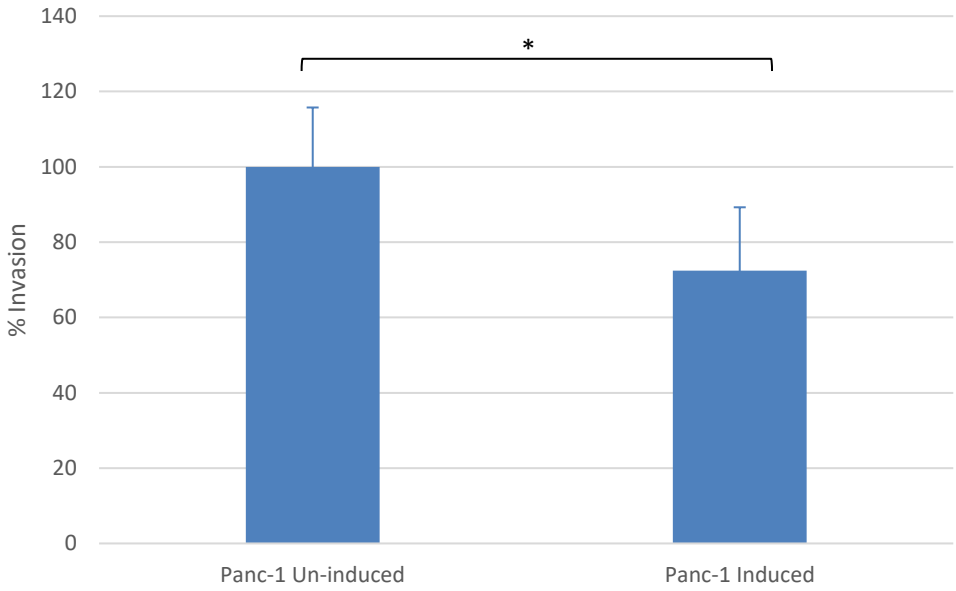

Percentage invasion of **Panc-1** cells un-induced and induced after 24 hours, relative to un-induced as the control. Induction with 1µg/mL of Doxycycline is present throughout the assay in the induced samples. Error bars represent +/- standard deviation between biological replicates, (n=3, p value = 0.04).

Figure 7-27. Percentage invasion of **Panc-1** cells post sponge knockdown of miRNA expression

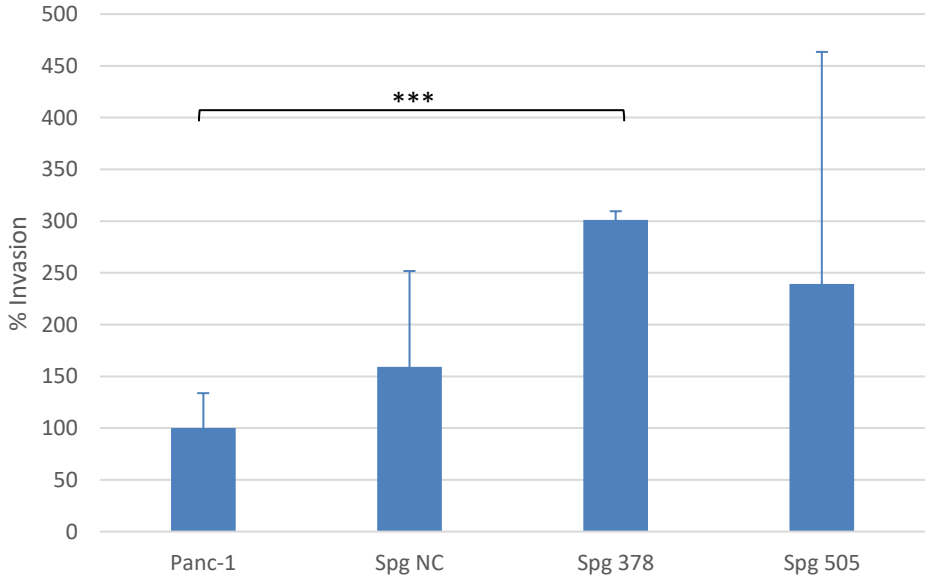

Percentage invasion of **Panc-1** cells with Panc-1 induced cells acting as the control. Invasion post miRNA expression reduction is displayed by Sponge negative control, **Spg 378** and **Spg 505**. Induction with 1µg/mL of Doxycycline is present throughout the assay. Error bars represent +/- standard deviation between biological replicates, (n=2, *** = p value ≤ 0.001, Spg 378 p value = 0.0008).

Figure 7-28. Percentage invasion of **Panc-1** cells post miRNA overexpression

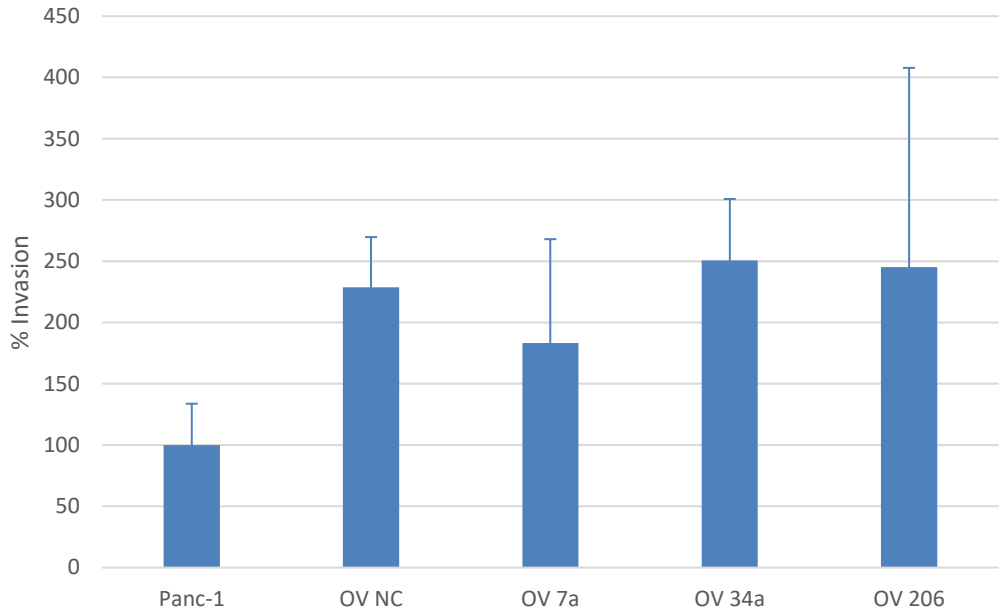

Percentage invasion of **Panc-1** cells with Panc-1 induced cells acting as the control. Invasion post miRNA overexpression is displayed by overexpression negative control, **OV 7a**, **OV 34a** and **OV 206**. Induction with 1µg/mL of Doxycycline is present throughout the assay. Error bars represent +/- standard deviation between biological replicates, (n=2).

Figure 7-29. Representative images of invasion of Panc-1 cells post miRNA expression alteration

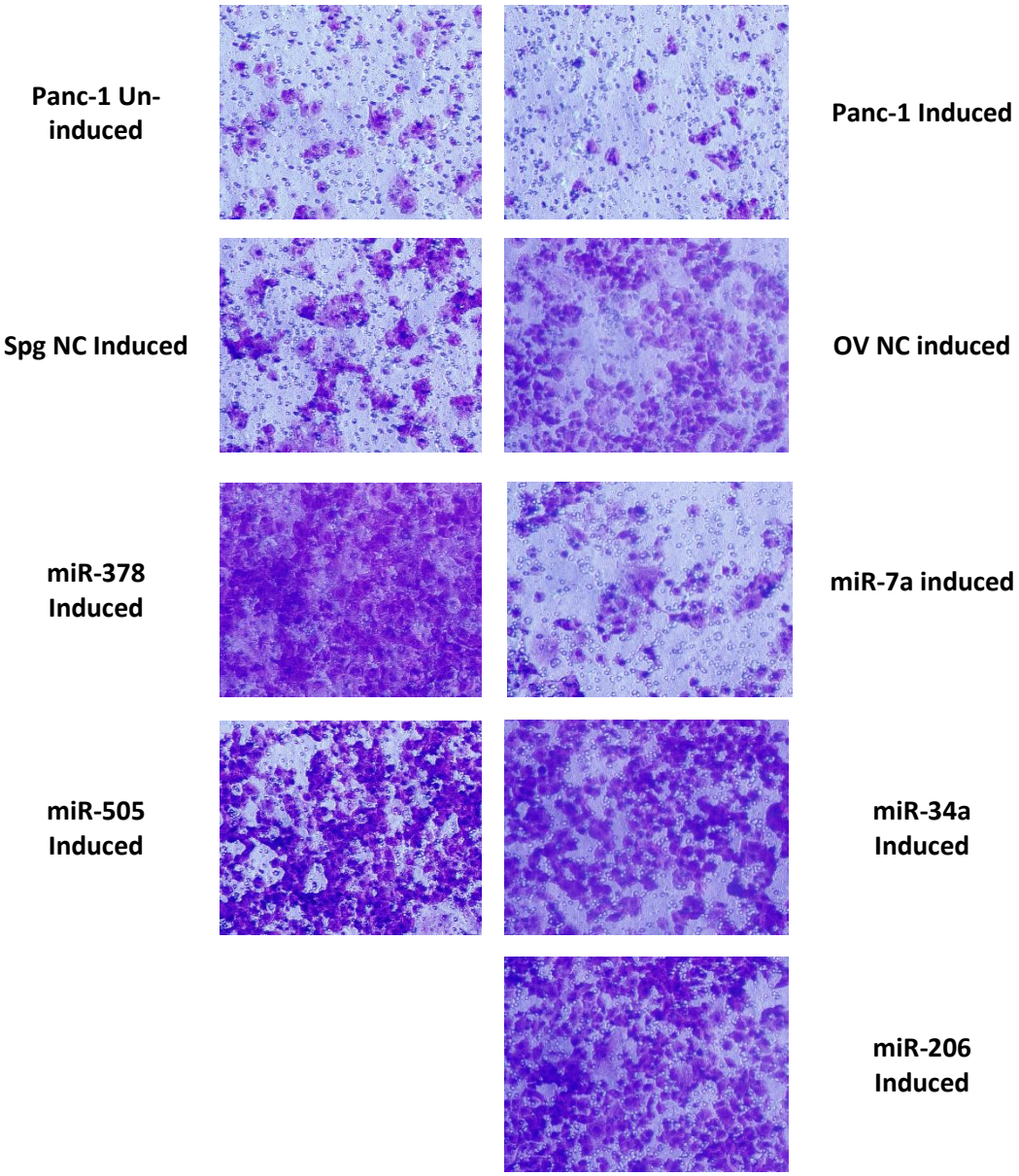

Representative images of invasion of **Panc-1** cells un-induced and induced. The effects due to sponge knockdown are displayed as **Spg NC**, **miR-378** and **miR-505** all induced. The effects due to miRNA overexpression are displayed as **OV NC**, **miR-7a**, **miR-34a** and **miR-206** all induced.

A slightly significant reduction in invasion was caused due to inducement of Panc-1 cells. Figure 7-29 displays a 30% reduction in invasion levels post treatment with Doxycycline with a p value of 0.04. This may be due to Doxycycline functioning as an inhibitor of MMPs. Several studies have shown an inhibitory effect of Doxycycline on MMP function (Uitto et al. 1994, Hanemaaijer et al. 1998, Prall et al. 2002). As MMPs play a highly important role in invasion, they function to allow the cell to break down the ECM, therefore the reduction observed in invasion of the parental Panc-1 cell line post induction may be due to the Doxycycline acting as an MMP inhibitor. Due to this, induced Panc-1 cells were used as the control and all invasion values were calculated relative to this. Sponge NC appeared to induce a 60% increase in invasion, observed in Figure 7-27. This change validated that induced parental Panc-1 cells are the most appropriate control as the negative control caused changes in the cell line. Sponge knockdown of miR-378 resulted in a highly significant increase in the invasive capability of Panc-1 cells. Invasion levels increased by 200% with a p value of 0.0008 due to reduced expression of miR-378. Figure 7-27 also shows that sponge knockdown of miR-505 induced a 140% increase in invasion, unfortunately this result did not show statistical significance due to large error between biological replicates. While significance was not detected a trend of increased invasion post miR-505 knockdown was observed. Similar to the Sponge NC, OV NC appears to induce a 130% increase in invasion, observed in Figure 7-28. This change validated that induced parental Panc-1 cells are the most appropriate control as the negative control had a large effect. Overexpression of each miRNA, miR-7a, miR-34a and miR-206 all induced an increase in invasion, 80%, 150% and 145% respectively, displayed in Figure 7-28. Due to the level of error and considering the increase induced by OV NC, these results were not found to be significant. Representative images of invasion of Panc-1 cells un-induced and induced as well as all sponge knockdown and overexpression miRNA targets can be seen in Figure 7-29 .

Following the observation of the phenotypic changes due to stably altered miRNA expression, survival analysis was also performed. This analysis utilised software and data available through the PROGmiR program which yielded a Kaplan-Meier (KM) survival

plot. This software analysed approximately 1050 human miRNAs in 33 major cancer types and used data from Gene Expression Omnibus (GEO) and The Cancer Genome Atlas (TCGA) to analyse the prognostic value of miRNA. These databases provide both sequencing/expression data as well as survival data for the clinical samples producing a Kaplan-Meier survival analysis yielding a plot, hazard ratio and P value. A significant role of miR-7a in pancreatic cancer survival was observed and is shown in Figure 7-30. This KM plot displays miR-7 expression in terms of overall survival (OS) of 191 patients over a period of 5 years (Goswami and Nakshatri 2012). The KM survival analysis indicated that high expression of miR-7 was significantly (p value = 0.0016) associated with greater OS in pancreatic cancer patients. The low expression cohort of patients possessed a median survival time of 607 days while the high expression cohort displayed a median survival time of 702 days. This high expression-greater survival relationship is in agreement with the phenotypic changes observed in this body of work which indicated miR-7a overexpression inhibited metastatic phenotypes.

Figure 7-30. Kaplan Meier plot showing the relationship of miR-7 expression with survival

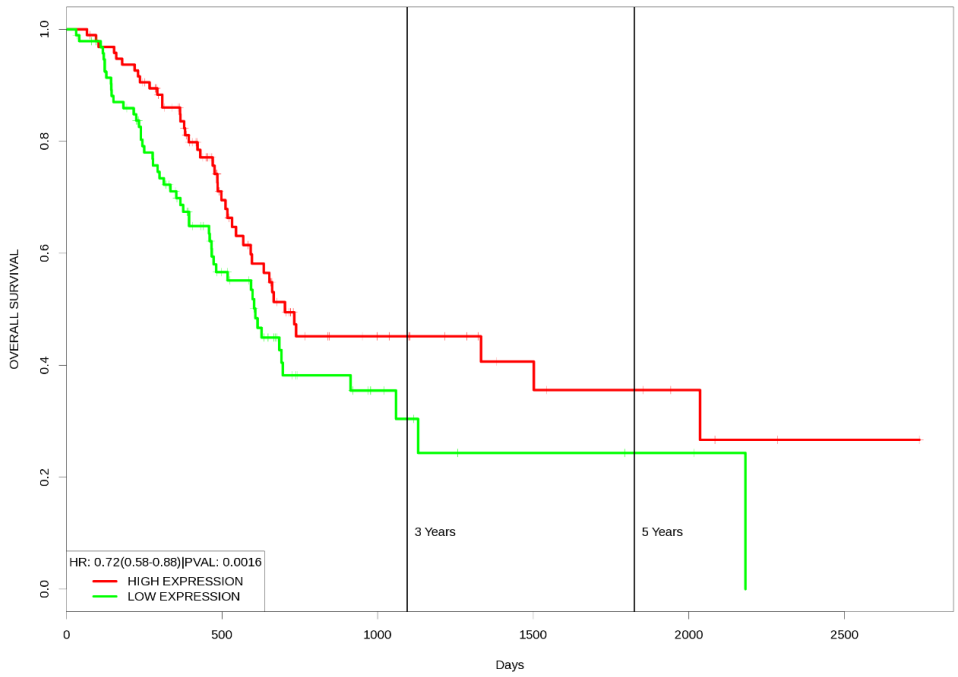

Kaplan Meier plot of miR-7 expression relative to survival in pancreatic cancer patients. Analysis of miR-7 expression in terms of overall survival (OS) of patients over a period of 5 years. The KM survival analysis indicates that high expression of miR-7 is significantly (p value = 0.0016) associated with greater OS in pancreatic cancer patients (n=191, p value = 0.0016) (Goswami and Nakshatri 2012).

8. Discussion – Investigation of the Role of miRNA in Metastatic Phenotypes in Pancreatic Cancer

8.1. Functional effects of transient alteration of miRNA in Panc-1 cells

Assessment of functional changes due to altered miRNA expression were examined in a transient fashion. Investigations of increased and decreased miRNA expression were performed in the Panc-1 cell line. 48hr after transfection, method described in section 2.6.3, functional changes were assessed in both proliferation and colony formation. The miRNA investigated using a transient approach are displayed . An untransfected control was included in each experiment as well as a negative control, either a Pre-miR negative control or Anti-miR negative control which are random sequences which have been shown to have no effect on known miRNA function as described in section 2.6.3. In this body of work some phenotypic changes were observed due to transfection using a negative control, due to this all functional comparisons were to the untransfected control. The miRNA listed in were chosen for several reasons, the first being beginning with an unbiased approach. A large cohort of miRNA Pre-miRs and Anti-miRs were available in-house, this cohort was the beginning of the choice of target miRNA. From this large cohort three Pre-miR and three Anti-miR targets were chosen to investigate further, these choices are detailed in section 7.2.1.

Overexpression of miR-204 using a Pre-miR significantly reduced colony number and colony size, meaning Panc-1 cells had a reduced ability to form colonies due to increased miR-204 expression. A similar result was observed in thyroid cancer, a transient overexpression of miR-204 induced reduced proliferation and a significant reduced ability to form colonies (Wu et al. 2015). There are several studies investigating miR-204 in pancreatic cancer. One study observed that miR-204 expression was repressed in pancreatic cancer tissues compared to normal tissue. This work also found that transient overexpression of miR-204 reduced cell viability i.e. induced cancer cell death (Chen et al. 2013). It was also discovered that Pre-204 negatively regulates Mcl-1 which is anti-apoptotic protein and the reduced cell viability induced by transient overexpression of miR-204 was concluded to be due to loss of Mcl-1 expression (Chen et al. 2013). High miR-204 expression in patients post gemcitabine treatment possessed a longer survival time, 33 months' vs 16.3 months in patients with low miR-204 expression post

treatment (Ohuchida et al. 2011). This work suggested miR-204 as a promising predictive marker for chemotherapeutic response in resected patients. As well as possessing a role as a predictive marker, miR-204 appears to function as a tumour suppressor in pancreatic cancer. The reduction in colony formation observed in this work appears to validate the role of miR-204 as a tumour suppressor in pancreatic cancer.

The role of miR-224 in pancreatic cancer was investigated in two ways, over and reduced expression with both being a transient alteration. Transient overexpression of miR-224 caused major reduction in metastatic phenotypes. Proliferation was reduced by 50% with colony formation showing a significant 70% reduction in colony number and a highly significant 50% reduction in colony size. Conversely reduction of miR-224 expression resulted in a highly significant 30% reduction in colony number. These results in terms of colony formation are in conflict with each other. There are very few investigations of the role of miR-224 in pancreatic cancer, one that does exist identified that miR-224 is significantly upregulated in highly metastatic pancreatic cancer cell lines (Mees et al. 2009). This paper appears to suggest that miR-224 is an oncogenic miRNA in pancreatic cancer. In terms of other cancer types there are conflicting roles of miR-224 reported. In cervical cancer miR-224 shows higher expression in tumour vs normal tissues with *in vitro* transient overexpression inducing an increase in proliferation, migration and invasion (Huang et al. 2016a). This is in contrast to this study of pancreatic cancer as transient overexpression of miR-224 reduced proliferation and colony formation. Phenotypic changes similar to this have been observed in breast cancer. miR-224 was found to have an inverse relationship with aggressiveness in a range of breast cancer subtype cell lines (Liu et al. 2016). This study also found transient overexpression reduced proliferation and migration as well as growth *in vivo* with transient knockdown inducing the opposite effects i.e. an increase in proliferation and migration (Liu et al. 2016). Considering these contrasting publications and the conflicting results observed due to transient alteration of miR-224 in this pancreatic cancer study, it was difficult to concisely conclude the role miR-224 plays in the progression of pancreatic cancer.

A clearer picture was able to be drawn from the results due to altered expression of miR-320a. Transient overexpression of miR-320a induced a 40% reduction in both proliferation and number of colonies formed. These results did not show statistical significant but promisingly contrastingly results were observed due to reduced miR-320a expression. A significant 30% increase in colony size was observed due to decreased miR-320a expression. These results appear to show miR-320a plays a role in the ability of pancreatic cancer cells to form colonies meaning miR-320a acts as a tumour suppressor in pancreatic cancer. There is very little research available to show the role of miR-320a in pancreatic cancer so this may be a novel insight. Although the role in pancreatic cancer has been unknown until this point, in many other cancers miR-320a has been shown to be a tumour suppressor miRNA such as colorectal cancer, glioma, NSCLC (Lei et al. 2016, Tadano et al. 2016, Sun et al. 2015). In NSCLC miR-320 expression was found to be significantly downregulated in tumour vs normal tissue samples. This study also observed that transient overexpression of miR-320 induced a decrease in growth, migration and invasion (Lei et al. 2016). An investigation of miR-320 in cervical cancer found an inverse relationship between miR-320 and the anti-apoptotic protein, Mcl-1 in cervical cancer tissues (Zhang et al. 2016). Transient overexpression of miR-320 reduced proliferation, migration and invasion while increasing apoptosis in cervical cancer cell lines. This is similar to the relationship previously mentioned, discussing the role of miR-204 with Mcl-1 in pancreatic cancer (Chen et al. 2013). As this present investigation of miR-320a in pancreatic cancer identified its role as a tumour suppressor this function may be carried out through targeting and inhibition of Mcl-1.

The final target investigated in a transient manner was miR-378. Reduced expression of miR-378 in Panc-1 cells induced a significant 40% increase in colony number. Decreased miR-378 expression appears to increase the ability of Panc-1 cells to form colonies. This would imply that miR-378 behaves as a tumour suppressor in pancreatic cancer as reduced expression induces a more metastatic phenotype. miR-378 has very little link to pancreatic cancer, only one publication currently exists. This study assessed miRNA in patient sera using miRNA microarrays. miR-378 was identified as a circulating miRNA which was significantly elevated in pancreatic cancer sera compared with control groups

(Li et al. 2013). Studies into other cancer types have also observed a role of miR-378 as a tumour suppressor. An investigation into triple negative breast cancer observed transient upregulation of miR-378 inhibited migration and invasion (Browne et al. 2016). Another study of transient overexpression of miR-378 in cancer found that overexpression suppressed migration and invasion and promoted apoptosis in prostate cancer (Chen et al. 2016a). While both of these studies used transient overexpression, the present pancreatic cancer study used transient downregulation, promisingly both approaches identified miR-378 as a tumour suppressor. It appears that miR-378 functions as a tumour suppressor in pancreatic cancer as well as other cancer types as have been published.

8.2. Phenotypic changes of Panc-1 cells with stably altered miRNA expression

A large cohort of plasmid vectors to induce miRNA expression changes were available in-house. These tools included both overexpression and sponge knockdown vectors, a list of these are displayed in Table 7-2. The miRNA listed were the beginning of the choice of target miRNA using an unbiased approach. From this large cohort miRNA targets for overexpression and sponge knockdown were chosen to investigate. The first step in target selection was to elucidate the innate, basal expression levels of each miRNA member of the cohort across a panel of pancreatic cancer cell lines. Figure 7-10 shows the basal expression level of the possible target miRNA across the panel with a normal cell line, HMEC, included. These basal levels along with a review of the current knowledge of each miRNA, were used to determine which miRNA targets were most appropriate for expression alteration using the tools listed in Table 7-2. These choices are detailed in section 7.2.4.

8.2.1. Functional effects of sponge knockdown of miRNA in Panc-1 cells

Sponge knockdown technology has only begun to be used as an investigative tool in the last decade with the number of publications being small over a 10-year period. In terms of pancreatic cancer there are very little investigations of sponge knockdown

technology, with only 2 publications being listed (Neault, Mallette and Richard 2016, Jung et al. 2015). In this work, sponge knockdown was used to reduce expression of miR-378 and miR-505. No significant effect was observed post knockdown in anoikis, proliferation or colony formation. There is little published data on the role of miR-505 in cancer. The majority of the papers which do mention this target are miRNA screens and profiles which mention miR-505 in the list of differential expression. One of the few functional studies observed that miR-505 transient overexpression in endometrial cancer reduced proliferation, migration and invasion (Chen et al. 2016b). One pancreatic cancer paper exists which mentions miR-505, this paper assessed miRNA as biomarkers for pancreatic cancer in blood. miR-505 was a part of two diagnostic panels used to distinguish patients with pancreatic cancer from healthy controls. miR-505 was among a 10 miRNA index which exhibited higher expression in pancreatic cancer patients compared to healthy controls (Schultz et al. 2014). Using a sponge knockdown vector for miR-505 in this work no significant change in phenotype was observed, an increase in invasion may be present but no statistical significance was detected. This trend of increased invasion post sponge knockdown is in line with the results observed in endometrial cancer, miR-505 overexpression decreased invasion in that study (Chen et al. 2016b). Conversely, in this study miR-505 knockdown may have induced an increase in invasion. A significant increase in invasion was observed due to the other sponge knockdown target in this body of work, miR-378. A 200% increase in invasion with a p value of 0.0008 was induced by knockdown of miR-378 relative to induced parental Panc-1 cells. As previously mentioned miR-378 has very little link to pancreatic cancer with the patient sera array analysis being the only substantial published study. This showed miR-378 as a circulating miRNA which was significantly elevated in pancreatic cancer sera compared with control groups (Li et al. 2013). There are a small number of publications addressing the role of miR-378 in invasion in a range of cancer types. In different cancer types this miRNA appears to play a different role in invasion. For instance, in both glioma and colorectal cancers, miR-378 overexpression reduces migration, invasion and in colorectal cancer a reduction in proliferation also, miR-378 appears to act as an oncomiR in these cancer types (Li et al. 2015a, Zhang et al. 2014). However, in liver and non-small cell lung cancer, miR-378 overexpression is associated with an increase in migration and invasion as well as increased proliferation in liver

cancer and increased angiogenesis in NSCLC, meaning it plays a role as a tumour suppressor (Ma et al. 2014b, Chen et al. 2012). While no effect on proliferation was detected using sponge knockdown in this investigation, a significant increase in invasion was observed showing miR-378 may play a similar role as a tumour suppressor in pancreatic cancer as previously seen in liver and non-small cell lung cancer. miR-378 was unique in this investigation as both transient and stable expression reduction were investigated. Both interventions induced different phenotypic changes. Transient expression reduction induced a significant increase in colony formation while stable expression reduction induced a significant increase in invasion with no effect on colony formation. While different phenotypic changes were observed both indicate a role of miR-378 as a tumour suppressor in pancreatic cancer, the fact that different forms of intervention led to the same conclusion may validate miR-378 as a tumour suppressor in pancreatic cancer. The effect of miR-378 on invasion of Panc-1 cells was the most significant result observed from the sponge knockdown investigations but the validation of sponge knockdown technology in pancreatic cancer is valuable, as is the knowledge gained of miR-378 and miR-505, two novel miRNA in pancreatic cancer.

8.2.2. Functional effects of stable miRNA overexpression in Panc-1 cells

The use of stable overexpression of miRNA offers a powerful insight into the role miRNA play in disease progression especially as miRNA can act as tumour suppressors in cancer. Overexpression of a miRNA target which has a low basal level may restore the tumour suppressor function of the target miRNA i.e. metastatic phenotypes may be inhibited or reverse due to overexpression of tumour suppressor miRNA. The miRNA targets investigated for tumour suppressor role in pancreatic cancer were miR-7a, miR-34a and miR-206.

miR-206 overexpression induced no effect in anoikis or colony formation of Panc-1 cells. An increase in both proliferation and invasion was observed due to miR-206 overexpression although these did not show statistical significance due to variability

between biological replicates. It was also a concern that the OV NC induced similar increases in both these metastatic functions. Considering this, it was difficult to draw a specific conclusion from the overexpression of miR-206. Publications have shown miR-206 to act as a tumour suppressor miRNA. Two publications have stated that miR-206 is significantly decreased in pancreatic cancer patient tissues in comparison to normal controls (Ju et al. 2016, Keklikoglou et al. 2014). These studies observed that overexpression of miR-206 inhibited progression of pancreatic cancer through decreased growth, migration and invasion. Growth *in vivo* in mice xenografts was reduced as well as proliferation with apoptosis being increased, shown through tissue staining of Ki67 and TUNEL (Ju et al. 2016, Keklikoglou et al. 2014). *In vitro* overexpression in both the Panc-1 and BxPc-3 cell lines induced significant decrease in cell proliferation, migration and invasion (Keklikoglou et al. 2014). These studies show a tumour suppressor role of miR-206 in pancreatic cancer, unfortunately no conclusion could be drawn from miR-206 overexpression in this project but no tumour suppressor functions were observed.

Phenotypic changes observed due to miR-34a overexpression were similar to the results observed due to miR-206 overexpression. No effect was observed on anoikis or colony formation. An increase in both proliferation and invasion was induced due to miR-34a overexpression but did not show statistical significance due to error between biological replicates. Again, the fact that the OV NC induced similar increases in both these metastatic functions is still a concern, making it difficult to draw a specific conclusion from the overexpression of miR-34a. Publications have shown miR-34a as a tumour suppressor miRNA that is commonly deleted in several cancers including lung, breast, liver and colon. This miRNA is involved in the p53 and Wnt/β-catenin pathways and restoration of its expression through a transient Pre-miR transfection has been shown to inhibit tumour growth and progression (Liu et al. 2011). It has also been shown that miR-34a is frequently absent in pancreatic cancers (Chang et al. 2007). This study showed overexpression of miR-34a to induce apoptosis through an apoptotic program triggered by the tumour suppressor protein p53, with evidence indicating that miR-34a is a direct transcriptional target of p53. Overexpression of miR-34a has also been shown

to dramatically inhibit proliferation in Panc-1 and Mia PaCa-2 cell lines (Ikeda et al. 2012). A Pre-miR for miR-34a known as MRX34 entered clinical testing in 2013. Unfortunately, as of September 2016, this clinical trial was halted due to immune related adverse effects. Downregulation of the target resulted in an increase in cell cycle progression and angiogenesis as well as a decrease in apoptosis and DNA repair in pancreatic cancer (Rachagani, Kumar and Batra 2010). More evidence of the tumour suppressor function of miR-34a was observed *in vivo*, overexpression of miR-34a inhibited growth and proliferation while increasing apoptosis in mice xenografts tissues (Pramanik et al. 2011). Conversely, miR-34a was a part of the 10 miRNA index previously mentioned in relation to miR-505, which exhibited higher expression in pancreatic cancer patients compared to healthy controls (Schultz et al. 2014). This paper suggested an oncogenic role for miR-34a but this study is in the minority with its suggestion (Ikeda et al. 2012). Unfortunately, no conclusion could be drawn from miR-34a overexpression in this project but no tumour suppressor functions were observed.

Overexpression of miR-7a exhibited the most significant change in metastatic phenotypes due to miRNA overexpression. Surprisingly, no overexpression of miR-7a was detected through qPCR. Due to cells expressing fluorescence, the success of the transfection was validated and due to the functional effects induced it was accepted that miR-7a overexpression was present but undetected. To further analyse this, qPCR will be carried out to detect RFP expression, this will be an indicator of the overexpression achieved. The RFP sequence is transcribed from the same promotor as the miRNA target indicating that the target miRNA is transcribed along with the reporter gene, RFP. As with each of the other target miRNA, no effect on anoikis was observed due to altered miRNA expression, but there was one conclusion to be made from the investigation into miRNA in anoikis. For all targets, it appears that survival in suspension is slightly increased after induction. Meaning that treatment with Doxycycline is allowing the pancreatic cancer cells to resist anoikis i.e. death due to suspension. This observation has been observed by other groups, inducible fibroblasts displayed positive phenotypes such as greater proliferation and survival in suspension with Doxycycline present (Fluri et al. 2012). Overexpression of miR-7a induced an increase in invasion but

this result was not statistically significant and a trend of increased invasion was not observed in each biological replicate. The most significant change in phenotype due to overexpression of miR-7a was a significant reduction in proliferation and a highly significant reduction in colony formation. Due to the link between proliferation and colony formation a reduction in both was promising. A decrease of 80% was induced in the number of colonies formed and this result was highly significant, p value of 0.001. A significant reduction in colony formation was observed in each biological replicate leading to the conclusion that miR-7a plays a highly important role in the ability of pancreatic cancer cells to form colonies. It has been widely reported that miR-7a targets EGFR, Panc-1 cells have been shown to highly express EGFR and also inhibition of EGFR in cancer has been associated with a reduction in colony forming ability (Li et al. 2016, Ali et al. 2005). Therefore, inhibition of EGFR through miR-7a overexpression may be responsible for the reduction in colony formation observed (Giles et al. 2016, Kefas et al. 2008). It is possible that overexpression of miR-7a is inhibiting colony formation of Panc-1 cells through downregulation of EGFR.

Following the observation of the phenotypic changes due to stably altered miRNA expression, survival analysis was also performed. This analysis utilised software and data available through PROGmiR program which yielded a Kaplan-Meier (KM) survival plot. A significant role of miR-7a in pancreatic cancer survival was observed and is shown in Figure 7-30. This KM plot displays miR-7 expression in terms of OS of 191 patients over a period of 5 years (Goswami and Nakshatri 2012). The KM survival analysis indicates that high expression of miR-7 is significantly (p value = 0.0016) associated with greater OS in pancreatic cancer patients. This high expression-greater survival is in agreement with the phenotypic changes observed which indicated miR-7a acts as a tumour suppressor in pancreatic cancer and may indicate a possible role of miR-7 as a prognostic indicator (Goswami and Nakshatri 2012).

There are limited published investigations of the role of miR-7a in pancreatic cancer. One study examined the effect of Curcumin which has an anti-tumour activity on

pancreatic cancer. This treatment caused an increase in miR-7 expression as well as suppression of growth, migration and invasion along with an increase in apoptosis indicating a tumour suppressor role of miR-7a in pancreatic cancer (Ma et al. 2014a). A small number of publications investigated the role of miR-7 in invasion in a range of cancer types, such as cervical cancer, gastric cancer, colorectal cancer and melanoma. Across this range of diseases miR-7 was very lowly expressed and overexpression inhibited migration, invasion and cell growth, identifying miR-7 as a tumour suppressor miRNA (Giles et al. 2016, Zeng et al. 2016, Hao et al. 2015, Xie et al. 2014). Similar results were also observed in NSCLC (Cao et al. 2016).Promisingly, the study investigating miR-7 in melanoma observed that overexpression of miR-7 significantly reduced the cancer cells ability to form colonies in both 2D and 3D with the effect being as drastic as the effect found by this project. This appears to confirm that miR-7a plays an important role in the ability of cancer cells to form colonies. All of these studies show miR-7a functioning as a tumour suppressor miRNA in a range of diverse cancers. Considering this, it appears the role of miRNA as a tumour suppressor in pancreatic cancer observed through this work is confirmed by these studies. The significant role of miR-7a in colony formation and overall as a tumour suppressor in pancreatic cancer is a novel and significant finding.

9. Concluding Discussion

9.1. Concluding Discussion

The aim of this project was to investigate mechanisms of metastasis in triple negative breast cancer and pancreatic cancer. Metastasis is the ability of a cell to spread to another location in the body which contributes to approximately 90% of cancers fatalities (Hu et al. 2016). Both TNBC and pancreatic cancer possess poor prognosis, limited therapeutic options and the risk of each becoming metastatic remains a major risk and concern. This body of work aimed to investigate metastasis through several metastatic phenotypes, specifically anoikis (anchorage independence), colony formation, proliferation and invasion. Each of these aspects of metastasis are critical in the metastatic cascade. These mechanisms of metastasis were investigated through three approaches, the first being microarray profiling to investigate anoikis resistance. The second approach analysed the role of the tumour microenvironment using an indirect co-culture model. The final approach determined the changes in metastatic phenotypes due to altered miRNA expression. Each approach identified unique influences on the metastatic capabilities of both TNBC and pancreatic cancer cells.

Through microarray profiling 26 genes were identified as differentially expressed in anoikis resistant cell lines. Specifically, GRP78 was identified as a regulator of growth in TNBC through proliferation and colony formation, with GRP78 acting as an oncogene. GRP78 has long been known as a potential target in cancer treatment but its role as an oncogene in TNBC is a novel insight and further research can investigate its potential as a therapeutic target in TNBC. The development of an indirect co-culture model allowed insight into the complicated role of the tumour microenvironment in pancreatic cancer. This investigation led to the observation that the stroma can act to inhibit and restrain the progression of pancreatic cancer. The overall conclusion from this model of the tumour microenvironment was that the stroma is diverse and complex with a more advanced and all-inclusive model needed before distinct conclusions on the role of the stroma in pancreatic cancer can be determined. Altering miRNA expression led to the identification of a range of tumour suppressor miRNA including miR-7a, miR-204 and miR-378. Each induced different changes in metastatic phenotypes including a reduction

in proliferation and colony formation and an extreme increase in invasion. A highly novel finding was the validity of using sponge knockdown vectors as a valuable research tool in pancreatic cancer. miRNA are key regulators of gene expression and therefore can give a powerful insight into the mechanisms of metastasis in cancer cells.

Through the three different approaches used, possible effective therapies were identified. GRP78 acting as an oncogene in TNBC may be a possible drug target with a wide range of inhibitors available such as arctigenin, verrucosidin and metformin (Sun et al. 2011, Thomas et al. 2013, Jagannathan et al. 2015). Investigations of GRP78 as a druggable target have not advanced to the clinical trial stage as of yet, but there is a possibility that GRP78 may provide a more compelling treatment option in TNBC. A valuable insight gained is that of the tumour microenvironment, in that targeting the pancreatic cancer stroma may not be the ideal therapeutic approach it once seemed. Targeting the stroma with the current level of understanding of the role of the tumour microenvironment is not a viable therapeutic plan, a much greater knowledge of the stroma is required before determining whether targeting the stroma is a beneficial strategy. The identification of miR-7a, miR-224 and miR-378 as tumour suppressors in pancreatic cancer could lead to the identification of drug targets with the targets of miR-7a being involved in cell growth and the targets of miR-378 being involved in invasion. The emergence of CRISPR technology is also an exciting future aspect, the potential targets of miR-7a, miR-224 and miR-378 could be evaluated and eventually targeted in pancreatic cancer patients as a potential highly effective therapy. Concluding from this body of work, the individual processes of metastasis investigated in this thesis, anoikis, proliferation, colony formation and invasion can be greatly influenced by gene expression, the tumour microenvironment and miRNA expression. Using these three approaches a greater understanding of metastasis has been gained and led to a further understanding of the progression of both TNBC and pancreatic cancer, with this greater understanding comes a greater possibility of developing effective therapies.

10. Conclusions and Future Work

10.1. Conclusions

1. Microarray analysis of anoikis resistance in triple negative breast cancer
    - Microarray analysis identified 26 genes as differentially expressed in two anoikis resistant TNBC cell lines in suspension compared to attached. The microarray data was validated as GRP78 protein was more abundant in both anoikis resistant cells lines compared to both anoikis sensitive cell lines
    - Transient transfection to reduce GRP78 expression did not affect the TNBC cells' ability to resist anoikis. Therefore, GRP78 did not validate as a gene involved in anoikis resistance, the original hypothesis was not validated
    - Reduced GRP78 expression significantly inhibited proliferation and colony formation in both 2D and 3D. GRP78 has a role in the ability of TNBC cells to proliferate and colonise meaning it may be a viable target to inhibit triple negative breast cancer cells' ability to proliferate and colonise in the process of metastasis.

2. Investigation of the role of the tumour microenvironment in pancreatic cancer
    - Development of an accurate co-culture model requires optimisation of a wide array of parameters. It is extremely important to determine the optimum control in the development process. Inappropriate controls can lead to misleading information and determining a control as optimum or inappropriate can require a lot of vigilant research
    - The type of media used in in-direct co-culture models can be highly significant. If a mix of media types is present, this must be tightly controlled for and an effect due to this mix of media types should be investigated.
    - Publications need to be hugely more overt and exact in the description of controls. It is hoped that each study is using an appropriate control but there is a possibility that some results published may be due to use of

inappropriate controls. This is needed to be sure published data can be replicated and confirmed. If different controls are being used in an area of research it is extremely difficult to draw conclusions as a scientific community.

- Patient tumour derived fibroblasts act to inhibit the metastatic phenotypes of pancreatic cancer cells. Indirect co-culture with Pt-102 fibroblasts significantly reduced the ability of two pancreatic cancer cells to proliferate, form colonies and invade. The tumour microenvironment appears to function in a protective manner by inhibiting the metastasis of PDAC. Targeting the pancreatic cancer stroma may not be the ideal therapeutic approach it once seemed.
- The role of the tumour microenvironment is complex, there is published evidence of the tumour microenvironment both inhibiting and progressing pancreatic cancer. It appears the tumour microenvironment can play both roles, the next step is to investigate what determines which role is being played. Activation of the stromal cell populations may be a factor.

3. Investigation of the role of miRNA in metastatic phenotypes in pancreatic cancer
    - Alteration of miRNA expression, both transiently and stably inhibited metastatic phenotypes of pancreatic cancer
    - Transient alteration of miRNA expression identified three miRNA, miR-204, miR-320a and miR-378, to be tumour suppressors in pancreatic cancer. Overexpression inhibited metastatic phenotypes of proliferation and colony formation while reduced expression increased these metastatic phenotypes. The role of miR-320a and miR-378 as a tumour suppressor in pancreatic cancer is a novel finding.
    - The role of miR-378 as a tumour suppressor was validated further through a stable sponge knockdown of miR-378 expression. Generation of a cell line which was induced to reduce miR-378 expression had

increased invasive capabilities. The use of both transient and stable miRNA alteration technologies led to the same conclusion, a role as a tumour suppressor although both showed an effect on different phenotypes.

- A highly novel finding of this work is that miRNA expression can be altered successfully using sponge knockdown technology in pancreatic cancer *in* vitro. This technology can induce changes in metastatic phenotypes.
- miR-7a was identified as a tumour suppressor miRNA in pancreatic cancer as stable overexpression induced a significant reduction in proliferation and a highly significant reduction in colony formation in PDAC. The role of miR-7 as a tumour suppressor has been published in other cancers but this is a novel finding in pancreatic cancer, as is its highly significant role in the ability of pancreatic cancer cells to form colonies.
- miRNA transient and stable expression alteration can be successfully used to induce significant changes in the metastatic phenotype of pancreatic cancer cells. This work led to the identification of miR-204, miR-320a, miR-378 and miR-7a as tumour suppressor miRNA in pancreatic cancer. The fact that all the miRNA identified were tumour suppressors ties into the knowledge that universally miRNA expression is downregulated in cancer

10.2. Future Work

1. Microarray analysis of anoikis resistance in triple negative breast cancer
    - Investigate the specific phase of cell growth that GRP78 knockdown is arresting using flow cytometry, specifically the Guava Cell Cycle assays using the Guava easyCyte Flow Cytometer. This may determine a role of GRP78 in specific phases of the cell cycle of TNBC cells.
    - Analyse phosphorylation of a range of key cell cycle regulatory proteins such as AKT, JNK and ERK1/2 using Western blotting post GRP78 knockdown. Determining changes of phosphorylation of cell cycle regulators may identify the key regulators which GRP78 knockdown has altered inducing the reduction in proliferation and colony formation.
    - Use stable overexpression of GRP78 to investigate phenotypic changes in two anoikis sensitive cell lines. May show a role of GRP78 in anoikis resistance.

2. Investigation of the role of the tumour microenvironment in pancreatic cancer
    - Investigate the phenotypic effects of indirect co-culture of PDAC cell using the optimum control with multiple batches of pancreatic stellate cells and tumour derived fibroblasts from different patients. This could show that the phenotypic changes induced were not patient specific thus giving greater validity to the results observed.
    - Investigate the specific phase of cell growth that co-culture with the stromal cells is arresting using flow cytometry, specifically the Guava Cell Cycle assays using the Guava easyCyte Flow Cytometer. This may determine the specific phases of the cell cycle which the stromal cells inhibit in the pancreatic cancer cells.
    - Further analyse the reduction in invasion levels through determining changes in MMP and TIMPs levels post co-culture using zymography and qPCR. Determining changes of MMPs and TIMPS may identify the key

regulators of invasion which co-culture has altered inducing the reduction in invasive capabilities of the pancreatic cancer cells.

- Assess miRNA changes in the pancreatic cancer cells post co-culture. A profiling study may identify miRNA expression changes induced due to co-culture which then may lead to identification of the miRNA responsible for the phenotypic changes observed post co-culture.
- Develop a direct co-culture model to investigate the tumour microenvironment. This would give a different insight to the tumour microenvironment as the cells would be in physical contact, cell to cell junctions would be formed. This would require labelling the cell lines, for example with GFP. This is required as it is necessary to be able to distinguish between the two cell populations in the co-culture model. This would allow for a comparison between direct and in-direct co-culture.
- Develop a triple co-culture model to investigate the tumour microenvironment using PDAC cells, patient derived fibroblasts and pancreatic stellate cells. A triple co-culture model could take many form, indirect, direct or a mix of both. While the development may be complex it would yield a high level of insight into the tumour microenvironment, as it is closer to the clinical tumour microenvironment which is a mix of different cells interacting to induce phenotypes.
- Explore the potential of investigating the effects of co-culture on metastasis *in vivo*. The two cell populations could be co-cultured before implantation *in vivo* or both cell types mixed together could be implanted, this would be a direct co-culture *in vivo*. This would allow investigation of the role of the tumour microenvironment in an *in vivo* setting.

3. Investigation of the role of miRNA in metastatic phenotypes in pancreatic cancer
    - Confirm miR-7a overexpression through analysis of RFP expression using qPCR. Assess the mRNA levels of validated targets of miR-7a, if the expression of these targets is reduced compared to the parental Panc-1 cell line this would validate that overexpression of miR-7a was achieved.
    - Develop stably transfected cell lines for miR-7a and miR-378 across the panel of pancreatic cancer cell lines. Assess if similar phenotypic changes are observed across the panel due to altered miRNA expression. This may confirm the roles of these miRNA as tumour suppressors in pancreatic cancer, confirming it was not a cell line specific effect.
    - Investigate the panel of miRNA investigated transiently across a panel of pancreatic cancer cell lines. This may confirm the roles of miR-204, miR-320a and miR-378 as tumour suppressors in pancreatic cancer, confirming it was not a cell line specific effect. Investigating miR-224 in a panel of pancreatic cancer cell lines may identify if this miRNA plays a tumour suppressor or oncogenic role in pancreatic cancer as no conclusion could be drawn from the effects observed in the Panc-1 cell line.
    - Investigate which protein-coding genes are being targeted by the miRNA vectors. This could be at a transcriptional and proteomic level and could lead to identification of gene targets involved in metastasis. miR-7a has been shown to target EGFR, overexpression of miR-7a may have induced downregulated expression of EGFR leading to the inhibition of metastatic phenotypes. This would also validate overexpression of miR-7a was achieved. Similarly, miR-320a has been shown to target Mcl-2. Expression of both these targets as well as others could be investigated.
    - Explore the potential of investigating the effects of miR-7a and miR-378 stably transfected cells on metastasis *in vivo*. Several studies have implanted transfected cells in mice, this would allow for investigation of the role of miR-7a and miR-378 in metastatic phenotypes in an *in vivo* setting.

11. Bibliography

Akekawatchai, C., Roytrakul, S., Kittisenachai, S., Isarankura-Na-Ayudhya, P. and Jitrapakdee, S. 2016. Protein profiles associated with anoikis resistance of metastatic MDA-MB-231 breast cancer cells. *Asian Pacific Journal of Cancer Prevention,* 17(2), pp.581-590.

Albini, A. 1998. Tumor and endothelial cell invasion of basement membranes. *Pathology & Oncology Research,* 4(3), pp.230-241.

Ali, S., Ahmad, A., Aboukameel, A., Ahmed, A., Bao, B., Banerjee, S., Philip, P.A. and Sarkar, F.H. 2014. Deregulation of miR-146a expression in a mouse model of pancreatic cancer affecting EGFR signaling. *Cancer Letters,* 351(1), pp.134-142.

Ali, S., El-Rayes, B.F., Sarkar, F.H. and Philip, P.A. 2005. Simultaneous targeting of the epidermal growth factor receptor and cyclooxygenase-2 pathways for pancreatic cancer therapy. *Molecular Cancer Therapeutics,* 4(12), pp.1943-1951.

Alizadeh, A.M., Shiri, S. and Farsinejad, S. 2014. Metastasis review: From bench to bedside. *Tumour Biology : The Journal of the International Society for Oncodevelopmental Biology and Medicine,* 35(9), pp.8483-8523.

Allegra, D., Bilan, V., Garding, A., Döhner, H., Stilgenbauer, S., Kuchenbauer, F. and Mertens, D. 2014. Defective DROSHA processing contributes to downregulation of MiR-15/-16 in chronic lymphocytic leukemia. *Leukemia,* 28(1), pp.98-107.

Al-Nasiry, S., Geusens, N., Hanssens, M., Luyten, C. and Pijnenborg, R. 2007. The use of alamar blue assay for quantitative analysis of viability, migration and invasion of choriocarcinoma cells. *Human Reproduction (Oxford, England),* 22(5), pp.1304-1309.

Ambros, V., Bartel, B., Bartel, D.P., Burge, C.B., Carrington, J.C., Chen, X., Dreyfuss, G., Eddy, S.R., Griffiths-Jones, S., Marshall, M., Matzke, M., Ruvkun, G. and Tuschl, T. 2003. A uniform system for microRNA annotation. *RNA (New York, N.Y.),* 9(3), pp.277-279.

Amirikia, K.C., Mills, P., Bush, J. and Newman, L.A. 2011. Higher population-based incidence rates of triple-negative breast cancer among young African-American women. *Cancer,* 117(12), pp.2747-2753.

Anders, C.K. and Carey, L.A. 2009. Biology, metastatic patterns, and treatment of patients with triple-negative breast cancer. *Clinical Breast Cancer,* 9pp.S73-S81.

Apte, M.V., Pirola, R.C. and Wilson, J.S. 2012. Pancreatic stellate cells: A starring role in normal and diseased pancreas. *Frontiers in Physiology,* 3pp.344.

Attwell, S., Roskelley, C. and Dedhar, S. 2000. The integrin-linked kinase (ILK) suppresses anoikis. *Oncogene,* 19(33),

Audeh, M.W. 2014. Novel treatment strategies in triple-negative breast cancer: Specific role of poly(adenosine diphosphate-ribose) polymerase inhibition. *Pharmacogenomics and Personalized Medicine,* 7pp.307-316.

Bachem, M.G., Schünemann, M., Ramadani, M., Siech, M., Beger, H., Buck, A., Zhou, S., Schmid-Kotsas, A. and Adler, G. 2005. Pancreatic carcinoma cells induce fibrosis by stimulating proliferation and matrix synthesis of stellate cells. *Gastroenterology,* 128(4), pp.907-921.

Bachem, M.G., Schneider, E., Groß, H., Weidenbach, H., Schmid, R.M., Menke, A., Siech, M., Beger, H., Grünert, A. and Adler, G. 1998. Identification, culture, and characterization of pancreatic stellate cells in rats and humans. *Gastroenterology,* 115(2), pp.421-432.

Bader, A., Brown, D., Stoudemire, J. and Lammers, P. 2011. Developing therapeutic microRNAs for cancer. *Gene Therapy,* 18(12), pp.1121-1126.

Baines, C.P., Kaiser, R.A., Sheiko, T., Craigen, W.J. and Molkentin, J.D. 2007. Voltage-dependent anion channels are dispensable for mitochondrial-dependent cell death. *Nature Cell Biology,* 9(5), pp.550-555.

Bartel, D.P. 2009. MicroRNAs: Target recognition and regulatory functions. *Cell,* 136(2), pp.215-233.

Baumann, V. and Winkler, J. 2014. miRNA-based therapies: Strategies and delivery platforms for oligonucleotide and non-oligonucleotide agents. *Future Medicinal Chemistry,* 6(17), pp.1967-1984.

Bliss, L.A., Sams, M.R., Deep-Soboslay, A., Ren-Patterson, R., Jaffe, A.E., Chenoweth, J.G., Jaishankar, A., Kleinman, J.E. and Hyde, T.M. 2012. Use of postmortem human dura mater and scalp for deriving human fibroblast cultures. *PloS One,* 7(9), pp.e45282.

Brentnall, T.A., Lai, L.A., Coleman, J., Bronner, M.P., Pan, S. and Chen, R. 2012. Arousal of cancer-associated stroma: Overexpression of palladin activates fibroblasts to promote tumor invasion. *PloS One,* 7(1), pp.e30219.

Browne, G., Dragon, J.A., Hong, D., Messier, T.L., Gordon, J.A., Farina, N.H., Boyd, J.R., VanOudenhove, J.J., Perez, A.W. and Zaidi, S.K. 2016. MicroRNA-378-mediated suppression of Runx1 alleviates the aggressive phenotype of triple-negative MDA-MB-231 human breast cancer cells. *Tumor Biology,* 37(7), pp.8825-8839.

Burk, U., Schubert, J., Wellner, U., Schmalhofer, O., Vincan, E., Spaderna, S. and Brabletz, T. 2008. A reciprocal repression between ZEB1 and members of the miR-200 family promotes EMT and invasion in cancer cells. *EMBO Reports,* 9(6), pp.582-589.

Calin, G.A., Dumitru, C.D., Shimizu, M., Bichi, R., Zupo, S., Noch, E., Aldler, H., Rattan, S., Keating, M., Rai, K., Rassenti, L., Kipps, T., Negrini, M., Bullrich, F. and Croce, C.M. 2002. Frequent deletions and down-regulation of micro- RNA genes miR15 and miR16 at

13q14 in chronic lymphocytic leukemia. *Proceedings of the National Academy of Sciences of the United States of America,* 99(24), pp.15524-15529.

Calin, G.A., Sevignani, C., Dumitru, C.D., Hyslop, T., Noch, E., Yendamuri, S., Shimizu, M., Rattan, S., Bullrich, F., Negrini, M. and Croce, C.M. 2004. Human microRNA genes are frequently located at fragile sites and genomic regions involved in cancers. *Proceedings of the National Academy of Sciences of the United States of America,* 101(9), pp.2999-3004.

Cao, Q., Mao, Z.D., Shi, Y.J., Chen, Y., Sun, Y., Zhang, Q., Song, L. and Peng, L.P. 2016. MicroRNA-7 inhibits cell proliferation, migration and invasion in human non-small cell lung cancer cells by targeting FAK through ERK/MAPK signaling pathway. *Oncotarget,*

Cardinale, V., Carpino, G., Reid, L., Gaudio, E. and Alvaro, D. 2012. Multiple cells of origin in cholangiocarcinoma underlie biological, epidemiological and clinical heterogeneity. *World J Gastrointest Oncol,* 4(5), pp.94-102.

Carey, L.A., Perou, C.M., Livasy, C.A., Dressler, L.G., Cowan, D., Conway, K., Karaca, G., Troester, M.A., Tse, C.K. and Edmiston, S. 2006. Race, breast cancer subtypes, and survival in the carolina breast cancer study. *Jama,* 295(21), pp.2492-2502.

Carey, L., Winer, E., Viale, G., Cameron, D. and Gianni, L. 2010. Triple-negative breast cancer: Disease entity or title of convenience? *Nature Reviews Clinical Oncology,* 7(12), pp.683-692.

Carey, L.A., Perou, C.M., Livasy, C.A., Dressler, L.G., Cowan, D., Conway, K., Karaca, G., Troester, M.A., Tse, C.K., Edmiston, S., Deming, S.L., Geradts, J., Cheang, M.C., Nielsen, T.O., Moorman, P.G., Earp, H.S. and Millikan, R.C. 2006. Race, breast cancer subtypes, and survival in the carolina breast cancer study. *JAMA : The Journal of the American Medical Association,* 295(21), pp.2492-2502.

Chang, T., Wentzel, E.A., Kent, O.A., Ramachandran, K., Mullendore, M., Lee, K.H., Feldmann, G., Yamakuchi, M., Ferlito, M. and Lowenstein, C.J. 2007. Transactivation of miR-34a by p53 broadly influences gene expression and promotes apoptosis. *Molecular Cell,* 26(5), pp.745-752.

Cheang, M.C., Chia, S.K., Voduc, D., Gao, D., Leung, S., Snider, J., Watson, M., Davies, S., Bernard, P.S., Parker, J.S., Perou, C.M., Ellis, M.J. and Nielsen, T.O. 2009. Ki67 index, HER2 status, and prognosis of patients with luminal B breast cancer. *Journal of the National Cancer Institute,* 101(10), pp.736-750.

Chen, H., Ding, A. and Wang, F. 2015. Prognostic effect analysis of molecular subtype on young breast cancer patients. *Chinese Journal of Cancer Research,* 27(4), pp.428-436.

Chen, L., Xu, S., Xu, H., Zhang, J., Ning, J. and Wang, S. 2012. MicroRNA-378 is associated with non-small cell lung cancer brain metastasis by promoting cell migration, invasion and tumor angiogenesis. *Medical Oncology,* 29(3), pp.1673-1680.

Chen, Q., Zhou, W., Han, T., Du, S., Li, Z., Zhang, Z., Shan, G. and Kong, C. 2016a. MiR-378 suppresses prostate cancer cell growth through downregulation of MAPK1 in vitro and in vivo. *Tumor Biology,* 37(2), pp.2095-2103.

Chen, S., Sun, K., Liu, B., Zong, Z. and Zhao, Y. 2016b. MicroRNA-505 functions as a tumor suppressor in endometrial cancer by targeting TGF-α. *Molecular Cancer,* 15(1), pp.1.

Chen, Z., Sangwan, V., Banerjee, S., Mackenzie, T., Dudeja, V., Li, X., Wang, H., Vickers, S.M. and Saluja, A.K. 2013. miR-204 mediated loss of myeloid cell leukemia-1 results in pancreatic cancer cell death. *Molecular Cancer,* 12(1), pp.1.

Cheng, F., Shen, Y., Mohanasundaram, P., Lindström, M., Ivaska, J., Ny, T. and Eriksson, J.E. 2016a. Vimentin coordinates fibroblast proliferation and keratinocyte differentiation in wound healing via TGF-β–Slug signaling. *Proceedings of the National Academy of Sciences,* 113(30), pp.E4320-E4327.

Cheng, L., Hung, K., Huang, T., Hsieh, H., Wang, S., Huang, C. and Lo, J. 2016b. Attenuation of cancer-initiating cells stemness properties by abrogating S100A4 calcium binding ability in head and neck cancers. *Oncotarget,* 7(48), pp.78946-78957.

Cheng, N., Chen, S., Li, J. and Young, T. 2013. Short-Term spheroid formation enhances the regenerative capacity of Adipose-Derived stem cells by promoting stemness, angiogenesis, and chemotaxis. *Stem Cells Translational Medicine,* 2(8), pp.584-594.

Chiarugi, P. and Giannoni, E. 2008. Anoikis: A necessary death program for anchorage-dependent cells. *Biochemical Pharmacology,* 76(11), pp.1352-1364.

Chiche, A., Moumen, M., Romagnoli, M., Petit, V., Lasla, H., Jézéquel, P., de la Grange, P., Jonkers, J., Deugnier, M. and Glukhova, M. 2016. p53 deficiency induces cancer stem cell pool expansion in a mouse model of triple-negative breast tumors. *Oncogene,*

Chitkara, D., Mittal, A. and Mahato, R.I. 2015. miRNAs in pancreatic cancer: Therapeutic potential, delivery challenges and strategies. *Advanced Drug Delivery Reviews,* 81pp.34-52.

Chiu, C., Lee, L., Li, Y., Chen, Y., Lu, Y., Li, Y., Wang, H., Chang, J. and Cheng, A. 2013. Grp78 as a therapeutic target for refractory head–neck cancer with CD24− CD44 stemness phenotype. *Cancer Gene Therapy,* 20(11), pp.606-615.

Chunhacha, P., Sriuranpong, V. and Chanvorachote, P. 2013. Epithelial-mesenchymal transition mediates anoikis resistance and enhances invasion in pleural effusion-derived human lung cancer cells. *Oncology Letters,* 5(3), pp.1043-1047.

Crosson, S. 2012. *The scientific approach* [Online]. Available from: http://www.unc.edu/depts/our/hhmi/hhmi-ft_learning_modules/2012/biologymodule/science.html [Accessed June 10th 2014].

Danial, N.N. 2007. BCL-2 family proteins: Critical checkpoints of apoptotic cell death. *Clinical Cancer Research : An Official Journal of the American Association for Cancer Research,* 13(24), pp.7254-7263.

Dedes, K.J., Natrajan, R., Lambros, M.B., Geyer, F.C., Lopez-Garcia, M.A., Savage, K., Jones, R.L. and Reis-Filho, J.S. 2011. Down-regulation of the miRNA master regulators drosha and dicer is associated with specific subgroups of breast cancer. *European Journal of Cancer,* 47(1), pp.138-150.

Deer, E.L., Gonzalez-Hernandez, J., Coursen, J.D., Shea, J.E., Ngatia, J., Scaife, C.L., Firpo, M.A. and Mulvihill, S.J. 2010. Phenotype and genotype of pancreatic cancer cell lines. *Pancreas,* 39(4), pp.425-435.

Deng, Z., Du, W.W., Fang, L., Shan, S.W., Qian, J., Lin, J., Qian, W., Ma, J., Rutnam, Z.J. and Yang, B.B. 2013. The intermediate filament vimentin mediates microRNA miR-378 function in cellular self-renewal by regulating the expression of the Sox2 transcription factor. *The Journal of Biological Chemistry,* 288(1), pp.319-331.

Dent, R., Trudeau, M., Pritchard, K.I., Hanna, W.M., Kahn, H.K., Sawka, C.A., Lickley, L.A., Rawlinson, E., Sun, P. and Narod, S.A. 2007. Triple-negative breast cancer: Clinical features and patterns of recurrence. *Clinical Cancer Research : An Official Journal of the American Association for Cancer Research,* 13(15 Pt 1), pp.4429-4434.

Di Leva, G., Garofalo, M. and Croce, C.M. 2014. MicroRNAs in cancer. *Annual Review of Pathology,* 9pp.287-314.

Ebert, M.S., Neilson, J.R. and Sharp, P.A. 2007. MicroRNA sponges: Competitive inhibitors of small RNAs in mammalian cells. *Nature Methods,* 4(9), pp.721-726.

Ebert, M.S. and Sharp, P.A. 2010. MicroRNA sponges: Progress and possibilities. *RNA (New York, N.Y.),* 16(11), pp.2043-2050.

Elsamany, S. and Abdullah, S. 2014. Triple-negative breast cancer: Future prospects in diagnosis and management. *Medical Oncology (Northwood, London, England),* 31(2), pp.834-013-0834-y. Epub 2014 Jan 5.

Farazi, T.A., Spitzer, J.I., Morozov, P. and Tuschl, T. 2011. miRNAs in human cancer. *The Journal of Pathology,* 223(2), pp.102-115.

Farmer, P., Bonnefoi, H., Becette, V., Tubiana-Hulin, M., Fumoleau, P., Larsimont, D., Macgrogan, G., Bergh, J., Cameron, D., Goldstein, D., Duss, S., Nicoulaz, A.L., Brisken, C., Fiche, M., Delorenzi, M. and Iggo, R. 2005. Identification of molecular apocrine breast tumours by microarray analysis. *Oncogene,* 24(29), pp.4660-4671.

Farrow, B., Berger, D.H. and Rowley, D. 2009. Tumor-derived pancreatic stellate cells promote pancreatic cancer cell invasion through release of thrombospondin-2. *The Journal of Surgical Research,* 156(1), pp.155-160.

Ferlay, J., Soerjomataram, I., Ervik, M., Dikshit, R., Eser, S., Mathers, C., Rebelo, M., Parkin, D., Forman, D. and Bray, F. 2013. Cancer incidence and mortality worldwide: IARC CancerBase no. 11 [internet] *GLOBOCAN 2012* 1pp. 11/08/14. Available from:

Fluri, D.A., Tonge, P.D., Song, H., Baptista, R.P., Shakiba, N., Shukla, S., Clarke, G., Nagy, A. and Zandstra, P.W. 2012. Derivation, expansion and differentiation of induced pluripotent stem cells in continuous suspension cultures. *Nature Methods,* 9(5), pp.509-516.

Foulkes, W.D., Smith, I.E. and Reis-Filho, J. 2010. Triple-negative breast cancer. *N Engl J Med,* 363(20), pp.1938-1948.

Friedl, P. and Alexander, S. 2011. Cancer invasion and the microenvironment: Plasticity and reciprocity. *Cell,* 147(5), pp.992-1009.

Friedl, P. and Gilmour, D. 2009. Collective cell migration in morphogenesis, regeneration and cancer. *Nature Reviews.Molecular Cell Biology,* 10(7), pp.445-457.

Friedl, P., Locker, J., Sahai, E. and Segall, J.E. 2012. Classifying collective cancer cell invasion. *Nature Cell Biology,* 14(8), pp.777-783.

Friedl, P. and Wolf, K. 2003. Tumour-cell invasion and migration: Diversity and escape mechanisms. *Nature Reviews.Cancer,* 3(5), pp.362-374.

Frisch, S.M. and Francis, H. 1994. Disruption of epithelial cell-matrix interactions induces apoptosis. *The Journal of Cell Biology,* 124(4), pp.619-626.

Fu, R., Yang, P., Wu, H.L., Li, Z.W. and Li, Z.Y. 2014. GRP78 secreted by colon cancer cells facilitates cell proliferation via PI3K/Akt signaling. *Asian Pacific Journal of Cancer Prevention : APJCP,* 15(17), pp.7245-7249.

Fujita, H., Ohuchida, K., Mizumoto, K., Egami, T., Miyoshi, K., Moriyama, T., Cui, L., Yu, J., Zhao, M., Manabe, T. and Tanaka, M. 2009. Tumor-stromal interactions with direct cell contacts enhance proliferation of human pancreatic carcinoma cells. *Cancer Science,* 100(12), pp.2309-2317.

Gaggioli, C., Hooper, S., Hidalgo-Carcedo, C., Grosse, R., Marshall, J.F., Harrington, K. and Sahai, E. 2007. Fibroblast-led collective invasion of carcinoma cells with differing roles for RhoGTPases in leading and following cells. *Nature Cell Biology,* 9(12), pp.1392-1400.

Gauthaman, K., Venugopal, J.R., Yee, F.C., Peh, G.S.L., Ramakrishna, S. and Bongso, A. 2009. Nanofibrous substrates support colony formation and maintain stemness of human embryonic stem cells. *Journal of Cellular and Molecular Medicine,* 13(9b), pp.3475-3484.

Geiger, T.R. and Peeper, D.S. 2009. Metastasis mechanisms. *Biochimica Et Biophysica Acta,* 1796(2), pp.293-308.

Geiger, T.R. and Peeper, D.S. 2005. The neurotrophic receptor TrkB in anoikis resistance and metastasis: A perspective. *Cancer Research,* 65(16), pp.7033-7036.

Gibson, G.R., Qian, D., Ku, J.K. and Lai, L.L. 2005. Metaplastic breast cancer: Clinical features and outcomes. *The American Surgeon,* 71(9), pp.725-730.

Giles, K.M., Brown, R., Ganda, C., Podgorny, M.J., Candy, P.A., Wintle, L.C., Richardson, K.L., Kalinowski, F.C., Stuart, L.M. and Epis, M.R. 2016. microRNA-7-5p inhibits melanoma cell proliferation and metastasis by suppressing RelA/NF-κB. *Oncotarget,* 7(22), pp.31663-31680.

Gilmore, A.P. 2005. Anoikis. *Cell Death and Differentiation,* 12 Suppl 2pp.1473-1477.

Goicoechea, S.M., Bednarski, B., Stack, C., Cowan, D.W., Volmar, K., Thorne, L., Cukierman, E., Rustgi, A.K., Brentnall, T. and Hwang, R.F. 2010. Isoform-specific upregulation of palladin in human and murine pancreas tumors. *PloS One,* 5(4), pp.e10347.

Goicoechea, S.M., Garcia-Mata, R., Staub, J., Valdivia, A., Sharek, L., McCulloch, C.G., Hwang, R.F., Urrutia, R., Yeh, J.J., Kim, H.J. and Otey, C.A. 2014. Palladin promotes invasion of pancreatic cancer cells by enhancing invadopodia formation in cancer-associated fibroblasts. *Oncogene,* 33(10), pp.1265-1273.

Goswami, C.P. and Nakshatri, H. 2012. PROGmiR: A tool for identifying prognostic miRNA biomarkers in multiple cancers using publicly available data. *Journal of Clinical Bioinformatics,* 2(1), pp.23.

Gundewar, C., Ansari, D., Tang, L., Wang, Y., Liang, G., Rosendahl, A.H., Saleem, M.A. and Andersson, R. 2014. Antiproliferative effects of curcumin analog L49H37 in pancreatic stellate cells: A comparative study. *Annals of Gastroenterology: Quarterly Publication of the Hellenic Society of Gastroenterology,* 28(3), pp.389-396.

Guo, X., Liao, Q., Chen, P., Li, X., Xiong, W., Ma, J., Li, X., Luo, Z., Tang, H. and Deng, M. 2012. The microRNA-processing enzymes: Drosha and dicer can predict prognosis of nasopharyngeal carcinoma. *Journal of Cancer Research and Clinical Oncology,* 138(1), pp.49-56.

Ha, M. and Kim, V.N. 2014. Regulation of microRNA biogenesis. *Nature Reviews Molecular Cell Biology,* 15(8), pp.509-524.

Haag, M., Van Linthout, S., Schröder, S.E., Freymann, U., Ringe, J., Tschöpe, C. and Sittinger, M. 2010. Endomyocardial biopsy derived adherent proliferating cells—a potential cell source for cardiac tissue engineering. *Journal of Cellular Biochemistry,* 109(3), pp.564-575.

Hainfellner, J.A., Voigtlander, T., Strobel, T., Mazal, P.R., Maddalena, A.S., Aguzzi, A. and Budka, H. 2001. Fibroblasts can express glial fibrillary acidic protein (GFAP) in vivo. *Journal of Neuropathology and Experimental Neurology,* 60(5), pp.449-461.

Hamada, S., Masamune, A., Takikawa, T., Suzuki, N., Kikuta, K., Hirota, M., Hamada, H., Kobune, M., Satoh, K. and Shimosegawa, T. 2012. Pancreatic stellate cells enhance stem cell-like phenotypes in pancreatic cancer cells. *Biochemical and Biophysical Research Communications,* 421(2), pp.349-354.

Hanahan, D. and Coussens, L.M. 2012. Accessories to the crime: Functions of cells recruited to the tumor microenvironment. *Cancer Cell,* 21(3), pp.309-322.

Hanemaaijer, R., Visser, H., Koolwijk, P., Sorsa, T., Salo, T., Golub, L.M. and Van Hinsbergh, V. 1998. Inhibition of MMP synthesis by doxycycline and chemically modified tetracyclines (CMTs) in human endothelial cells. *Advances in Dental Research,* 12(1), pp.114-118.

Hao, Z., Yang, J., Wang, C., Li, Y., Zhang, Y., Dong, X., Zhou, L., Liu, J., Zhang, Y. and Qian, J. 2015. MicroRNA-7 inhibits metastasis and invasion through targeting focal adhesion kinase in cervical cancer. *International Journal of Clinical and Experimental Medicine,* 8(1), pp.480-487.

Haqq, J., Howells, L.M., Garcea, G. and Dennison, A.R. 2015. Targeting pancreatic cancer using a combination of gemcitabine with the omega-3 polyunsaturated fatty acid emulsion, lipidem™. *Molecular Nutrition & Food Research,*

Hastak, K., Alli, E. and Ford, J.M. 2010. Synergistic chemosensitivity of triple-negative breast cancer cell lines to poly(ADP-ribose) polymerase inhibition, gemcitabine, and cisplatin. *Cancer Research,* 70(20), pp.7970-7980.

Hawa, Z., Haque, I., Ghosh, A., Banerjee, S., Harris, L. and Banerjee, S.K. 2016. The miRacle in pancreatic cancer by miRNAs: Tiny angels or devils in disease progression. *International Journal of Molecular Sciences,* 17(6), pp.809.

Hayes, M.J., Thomas, D., Emmons, A., Giordano, T.J. and Kleer, C.G. 2008. Genetic changes of wnt pathway genes are common events in metaplastic carcinomas of the breast. *Clinical Cancer Research : An Official Journal of the American Association for Cancer Research,* 14(13), pp.4038-4044.

Heijmans, J., de Jeude, Jooske F van Lidth, Koo, B., Rosekrans, S.L., Wielenga, M.C., van de Wetering, M., Ferrante, M., Lee, A.S., Onderwater, J.J. and Paton, J.C. 2013. ER stress causes rapid loss of intestinal epithelial stemness through activation of the unfolded protein response. *Cell Reports,* 3(4), pp.1128-1139.

Hibio, N., Hino, K., Shimizu, E., Nagata, Y. and Ui-Tei, K. 2012. Stability of miRNA 5' terminal and seed regions is correlated with experimentally observed miRNA-mediated silencing efficacy. *Scientific Reports,* 2pp.996.

Hu, Y., Yu, X., Xu, G. and Liu, S. 2016. Metastasis: An early event in cancer progression. *Journal of Cancer Research and Clinical Oncology,* pp.1-13.

Hu, Y., Ou, Y., Wu, K., Chen, Y. and Sun, W. 2012. miR-143 inhibits the metastasis of pancreatic cancer and an associated signaling pathway. *Tumor Biology,* 33(6), pp.1863-1870.

Hu, Q., Chen, W.X., Zhong, S.L., Li, J., Luo, Z., Tang, J.H. and Zhao, J.H. 2013. Current progress in the treatment of metaplastic breast carcinoma. *Asian Pacific Journal of Cancer Prevention : APJCP,* 14(11), pp.6221-6225.

Huang, Y., Li, Y., Wang, F.F., Lv, W., Xie, X. and Cheng, X. 2016a. Over-expressed miR-224 promotes the progression of cervical cancer via targeting RASSF8. *PloS One,* 11(9), pp.e0162378.

Huang, Y., Lan, Q., Lorusso, G., Duffey, N. and Rüegg, C. 2016b. The matricellular protein CYR61 promotes breast cancer lung metastasis by facilitating tumor cell extravasation and suppressing anoikis. *Oncotarget,* 5

Hugh, J., Hanson, J., Cheang, M.C., Nielsen, T.O., Perou, C.M., Dumontet, C., Reed, J., Krajewska, M., Treilleux, I., Rupin, M., Magherini, E., Mackey, J., Martin, M. and Vogel, C. 2009. Breast cancer subtypes and response to docetaxel in node-positive breast cancer: Use of an immunohistochemical definition in the BCIRG 001 trial. *Journal of Clinical Oncology : Official Journal of the American Society of Clinical Oncology,* 27(8), pp.1168-1176.

Huse, J.T., Brennan, C., Hambardzumyan, D., Wee, B., Pena, J., Rouhanifard, S.H., Sohn-Lee, C., le Sage, C., Agami, R., Tuschl, T. and Holland, E.C. 2009. The PTEN-regulating microRNA miR-26a is amplified in high-grade glioma and facilitates gliomagenesis in vivo. *Genes & Development,* 23(11), pp.1327-1337.

Hwang, R.F., Moore, T., Arumugam, T., Ramachandran, V., Amos, K.D., Rivera, A., Ji, B., Evans, D.B. and Logsdon, C.D. 2008. Cancer-associated stromal fibroblasts promote pancreatic tumor progression. *Cancer Research,* 68(3), pp.918-926.

Idogawa, M., Adachi, M., Minami, T., Yasui, H. and Imai, K. 2003. Overexpression of BAD preferentially augments anoikis. *International Journal of Cancer,* 107(2), pp.215-223.

Ikeda, Y., Tanji, E., Makino, N., Kawata, S. and Furukawa, T. 2012. MicroRNAs associated with mitogen-activated protein kinase in human pancreatic cancer. *Molecular Cancer Research : MCR,* 10(2), pp.259-269.

Imam, J.S., Plyler, J.R., Bansal, H., Prajapati, S., Bansal, S., Rebeles, J., Chen, H.H., Chang, Y., Panneerdoss, S. and Zoghi, B. 2012. Genomic loss of tumor suppressor miRNA-204 promotes cancer cell migration and invasion by activating AKT/mTOR/Rac1 signaling and actin reorganization. *PloS One,* 7(12), pp.e52397.

Jagannathan, S., Abdel-Malek, M., Malek, E., Vad, N., Latif, T., Anderson, K. and Driscoll, J. 2015. Pharmacologic screens reveal metformin that suppresses GRP78-dependent autophagy to enhance the anti-myeloma effect of bortezomib. *Leukemia,*

Janmaat, C., de Rooij, K., Locher, H., de Groot, S., de Groot, J., Frijns, J. and Huisman, M. 2015. Human dermal fibroblasts demonstrate positive immunostaining for neuron-and glia-specific proteins. *PloS One,* 10(12), pp.e0145235.

Jaster, R. 2004. Molecular regulation of pancreatic stellate cell function. *Molecular Cancer,* 3pp.26.

Ji, Q.X., Liu, L.L., Li, L. and Xing, X.M. 2016. Roles of glucose-regulated protein 78 in proliferation and migration of human colorectal carcinoma cell line RKO. *Zhonghua Bing Li Xue Za Zhi = Chinese Journal of Pathology,* 45(6), pp.401-406.

Jiang, W., Sanders, A., Katoh, M., Ungefroren, H., Gieseler, F., Prince, M., Thompson, S., Zollo, M., Spano, D. and Dhawan, P. 2015. Tissue invasion and metastasis: Molecular, biological and clinical perspectives. *IN:* Tissue invasion and metastasis: Molecular, biological and clinical perspectives. *Seminars in Cancer Biology.* Elsevier, pp.S244-S275.

Jiao, L.R., Frampton, A.E., Jacob, J., Pellegrino, L., Krell, J., Giamas, G., Tsim, N., Vlavianos, P., Cohen, P. and Ahmad, R. 2012. MicroRNAs targeting oncogenes are down-regulated in pancreatic malignant transformation from benign tumors. *PloS One,* 7(2), pp.e32068.

Jiao, Q., Wu, A., Shao, G., Peng, H., Wang, M., Ji, S., Liu, P. and Zhang, J. 2014. The latest progress in research on triple negative breast cancer (TNBC): Risk factors, possible therapeutic targets and prognostic markers. *Journal of Thoracic Disease,* 6(9), pp.1329-1335.

Ju, H., Zhuang, Z., Li, H., Tian, T., Lu, Y., Fan, X., Zhou, H., Mo, H., Sheng, H. and Chiao, P.J. 2016. Regulation of the nampt-mediated NAD salvage pathway and its therapeutic implications in pancreatic cancer. *Cancer Letters,* 379(1), pp.1-11.

Jung, J., Yeom, C., Choi, Y.S., Kim, S., Lee, E., Park, M.J., Kang, S.W., Kim, S.B. and Chang, S. 2015. Simultaneous inhibition of multiple oncogenic miRNAs by a multi-potent microRNA sponge. *Oncotarget,* 6(24), pp.20370-20387.

Kalluri, R. 2016. The biology and function of fibroblasts in cancer. *Nature Reviews Cancer,* 16(9), pp.582-598.

Kalluri, R. and Zeisberg, M. 2006. Fibroblasts in cancer. *Nature Reviews Cancer,* 6(5), pp.392-401.

Karginova, O., Siegel, M.B., Van Swearingen, A.E., Deal, A.M., Adamo, B., Sambade, M.J., Bazyar, S., Nikolaishvili-Feinberg, N., Bash, R., O'Neal, S., Sandison, K., Parker, J.S., Santos, C., Darr, D., Zamboni, W., Lee, Y.Z., Miller, C.R. and Anders, C.K. 2015. Efficacy of carboplatin alone and in combination with ABT888 in intracranial murine models of BRCA-mutated and BRCA-wild-type triple-negative breast cancer. *Molecular Cancer Therapeutics,* 14(4), pp.920-930.

Kasinski, A.L. and Slack, F.J. 2012. Arresting the culprit: Targeted antagomir delivery to sequester oncogenic miR-221 in HCC. *Molecular Therapy.Nucleic Acids,* 1pp.e12.

Katz, M.H., Wang, H., Fleming, J.B., Sun, C.C., Hwang, R.F., Wolff, R.A., Varadhachary, G., Abbruzzese, J.L., Crane, C.H. and Krishnan, S. 2009. Long-term survival after multidisciplinary management of resected pancreatic adenocarcinoma. *Annals of Surgical Oncology,* 16(4), pp.836.

Keenan, J., Joyce, H., Aherne, S., O'Dea, S., Doolan, P., Lynch, V. and Clynes, M. 2012. Olfactomedin III expression contributes to anoikis-resistance in clonal variants of a human lung squamous carcinoma cell line. *Experimental Cell Research,* 318(5), pp.593-602.

Kefas, B., Godlewski, J., Comeau, L., Li, Y., Abounader, R., Hawkinson, M., Lee, J., Fine, H., Chiocca, E.A., Lawler, S. and Purow, B. 2008. microRNA-7 inhibits the epidermal growth factor receptor and the akt pathway and is down-regulated in glioblastoma. *Cancer Research,* 68(10), pp.3566-3572.

Keklikoglou, I., Hosaka, K., Bender, C., Bott, A., Koerner, C., Mitra, D., Will, R., Woerner, A., Muenstermann, E. and Wilhelm, H. 2014. MicroRNA-206 functions as a pleiotropic modulator of cell proliferation, invasion and lymphangiogenesis in pancreatic adenocarcinoma by targeting ANXA2 and KRAS genes. *Oncogene,*

Kennecke, H., Yerushalmi, R., Woods, R., Cheang, M.C.U., Voduc, D., Speers, C.H., Nielsen, T.O. and Gelmon, K. 2010. Metastatic behavior of breast cancer subtypes. *Journal of Clinical Oncology,* 28(20), pp.3271-3277.

Khalil, A.A. and Friedl, P. 2010. Determinants of leader cells in collective cell migration. *Integrative Biology : Quantitative Biosciences from Nano to Macro,* 2(11-12), pp.568-574.

Kikuta, K., Masamune, A., Watanabe, T., Ariga, H., Itoh, H., Hamada, S., Satoh, K., Egawa, S., Unno, M. and Shimosegawa, T. 2010. Pancreatic stellate cells promote epithelial-mesenchymal transition in pancreatic cancer cells. *Biochemical and Biophysical Research Communications,* 403(3-4), pp.380-384.

Kim, Y.N., Koo, K.H., Sung, J.Y., Yun, U.J. and Kim, H. 2012. Anoikis resistance: An essential prerequisite for tumor metastasis. *International Journal of Cell Biology,* 2012pp.306879.

Kleivi Sahlberg, K., Bottai, G., Naume, B., Burwinkel, B., Calin, G.A., Borresen-Dale, A.L. and Santarpia, L. 2015. A serum microRNA signature predicts tumor relapse and survival in triple-negative breast cancer patients. *Clinical Cancer Research : An Official Journal of the American Association for Cancer Research,* 21(5), pp.1207-1214.

Kota, J., Chivukula, R.R., O'Donnell, K.A., Wentzel, E.A., Montgomery, C.L., Hwang, H., Chang, T., Vivekanandan, P., Torbenson, M. and Clark, K.R. 2009. Therapeutic microRNA delivery suppresses tumorigenesis in a murine liver cancer model. *Cell,* 137(6), pp.1005-1017.

Kozlowski, J., Kozlowska, A. and Kocki, J. 2015. Breast cancer metastasis - insight into selected molecular mechanisms of the phenomenon. *Postepy Higieny i Medycyny Doswiadczalnej (Online),* 69pp.447-451.

Kreike, B., van Kouwenhove, M., Horlings, H., Weigelt, B., Peterse, H., Bartelink, H. and van de Vijver, M.J. 2007. Gene expression profiling and histopathological characterization of triple-negative/basal-like breast carcinomas. *Breast Cancer Research : BCR,* 9(5), pp.R65.

Krützfeldt, J., Rajewsky, N., Braich, R., Rajeev, K.G., Tuschl, T., Manoharan, M. and Stoffel, M. 2005. Silencing of microRNAs in vivo with 'antagomirs'. *Nature,* 438(7068), pp.685-689.

Kumar, M.S., Pester, R.E., Chen, C.Y., Lane, K., Chin, C., Lu, J., Kirsch, D.G., Golub, T.R. and Jacks, T. 2009. Dicer1 functions as a haploinsufficient tumor suppressor. *Genes & Development,* 23(23), pp.2700-2704.

Kümmel, A., Kümmel, S., Barinoff, J., Heitz, F., Holtschmidt, J., Weikel, W., Lorenz-Salehi, F., du Bois, A., Harter, P. and Traut, A. 2015. Prognostic factors for local, loco-regional and systemic recurrence in early-stage breast cancer. *Geburtshilfe Und Frauenheilkunde,* 75(07), pp.710-718.

Kuo, L.J., Hung, C.S., Chen, W.Y., Chang, Y.J. and Wei, P.L. 2013. Glucose-regulated protein 78 silencing down-regulates vascular endothelial growth factor/vascular endothelial growth factor receptor 2 pathway to suppress human colon cancer tumor growth. *The Journal of Surgical Research,* 185(1), pp.264-272.

Lagos-Quintana, M., Rauhut, R., Lendeckel, W. and Tuschl, T. 2001. Identification of novel genes coding for small expressed RNAs. *Science (New York, N.Y.),* 294(5543), pp.853-858.

Lai, S., Chen, Y., Kuo, W., Lien, H., Wang, M., Lu, Y., Lo, C., Kuo, S., Cheng, A. and Huang, C. 2016. Locoregional recurrence risk for postmastectomy breast cancer patients with T1–2 and one to three positive lymph nodes receiving modern systemic treatment without radiotherapy. *Annals of Surgical Oncology,* 23(12), pp.3860-3869.

Lambertz, I., Nittner, D., Mestdagh, P., Denecker, G., Vandesompele, J., Dyer, M.A. and Marine, J. 2010. Monoallelic but not biallelic loss of Dicer1 promotes tumorigenesis in vivo. *Cell Death & Differentiation,* 17(4), pp.633-641.

Lancaster, M.V. and Fields, R.D. 1996. *Antibiotic and Cytotoxic Drug Susceptibility Assays using Resazurin and Poising Agents,*

Lardon, J., Rooman, I. and Bouwens, L. 2002. Nestin expression in pancreatic stellate cells and angiogenic endothelial cells. *Histochemistry and Cell Biology,* 117(6), pp.535-540.

Leake, I. 2014. Pancreatic cancer: Surprising role for fibrosis. *Nature Reviews Gastroenterology & Hepatology,* 11(7), pp.396-396.

Lee, A.S. 2007. GRP78 induction in cancer: Therapeutic and prognostic implications. *Cancer Research,* 67(8), pp.3496-3499.

Lee, J.J., Perera, R.M., Wang, H., Wu, D.C., Liu, X.S., Han, S., Fitamant, J., Jones, P.D., Ghanta, K.S., Kawano, S., Nagle, J.M., Deshpande, V., Boucher, Y., Kato, T., Chen, J.K., Willmann, J.K., Bardeesy, N. and Beachy, P.A. 2014. Stromal response to hedgehog signaling restrains pancreatic cancer progression. *Proceedings of the National Academy of Sciences of the United States of America,* 111(30), pp.E3091-100.

Lee, S., Terry, D., Hurst, D.R., Welch, D.R. and Sang, Q.X. 2011. Protein signatures in human MDA-MB-231 breast cancer cells indicating a more invasive phenotype following knockdown of human Endometase/Matrilysin-2 by siRNA. *Journal of Cancer,* 2pp.165-176.

Lehmann, B.D., Jovanović, B., Chen, X., Estrada, M.V., Johnson, K.N., Shyr, Y., Moses, H.L., Sanders, M.E. and Pietenpol, J.A. 2016. Refinement of triple-negative breast cancer molecular subtypes: Implications for neoadjuvant chemotherapy selection. *PLoS One,* 11(6), pp.e0157368.

Lehmann, B.D. and Pietenpol, J.A. 2014. Identification and use of biomarkers in treatment strategies for triple-negative breast cancer subtypes. *The Journal of Pathology,* 232(2), pp.142-150.

Lehmann, B.D., Bauer, J.A., Chen, X., Sanders, M.E., Chakravarthy, A.B., Shyr, Y. and Pietenpol, J.A. 2011. Identification of human triple-negative breast cancer subtypes and preclinical models for selection of targeted therapies. *The Journal of Clinical Investigation,* 121(7), pp.2750-2767.

Lei, T., Zhu, Y., Jiang, C., Wang, Y., Fu, J., Fan, Z. and Qin, H. 2016. MicroRNA-320 was downregulated in non-small cell lung cancer and inhibited cell proliferation, migration and invasion by targeting fatty acid synthase. *Molecular Medicine Reports,* 14(2), pp.1255-1262.

Lewis, B.P., Burge, C.B. and Bartel, D.P. 2005. Conserved seed pairing, often flanked by adenosines, indicates that thousands of human genes are microRNA targets. *Cell,* 120(1), pp.15-20.

Li, B., Wang, Y., Li, S., He, H., Sun, F., Wang, C., Lu, Y., Wang, X. and Tao, B. 2015a. Decreased expression of miR-378 correlates with tumor invasiveness and poor prognosis of patients with glioma. *International Journal of Clinical and Experimental Pathology,* 8(6), pp.7016.

Li, H., Dai, Y., Shu, J., Yu, R., Guo, Y. and Chen, J. 2015b. Spheroid cultures promote the stemness of corneal stromal cells. *Tissue and Cell,* 47(1), pp.39-48.

Li, W., Yue, W., Wang, H., Lai, B., Yang, X., Zhang, C., Wang, Y. and Gu, M. 2016. Cyclooxygenase-2 is associated with malignant phenotypes in human lung cancer. *Oncology Letters,* 12(5), pp.3836-3844.

Li, Y., Guo, G., Li, L., Chen, F., Bao, J., Shi, Y. and Bu, H. 2015. Three-dimensional spheroid culture of human umbilical cord mesenchymal stem cells promotes cell yield and stemness maintenance. *Cell and Tissue Research,* 360(2), pp.297-307.

Li, A., Yu, J., Kim, H., Wolfgang, C.L., Canto, M.I., Hruban, R.H. and Goggins, M. 2013. MicroRNA array analysis finds elevated serum miR-1290 accurately distinguishes patients with low-stage pancreatic cancer from healthy and disease controls. *Clinical Cancer Research : An Official Journal of the American Association for Cancer Research,* 19(13), pp.3600-3610.

Limame, R., Wouters, A., Pauwels, B., Fransen, E., Peeters, M., Lardon, F., De Wever, O. and Pauwels, P. 2012. Comparative analysis of dynamic cell viability, migration and invasion assessments by novel real-time technology and classic endpoint assays. *PloS One,* 7(10), pp.e46536.

Lin, J., Fang, S., Su, C., Hsiao, C., Chang, C., Lin, Y. and Cheng, C. 2014a. Silencing glucose-regulated protein 78 induced renal cell carcinoma cell line G1 cell-cycle arrest and resistance to conventional chemotherapy. *IN:* Silencing glucose-regulated protein 78 induced renal cell carcinoma cell line G1 cell-cycle arrest and resistance to conventional chemotherapy. *Urologic Oncology: Seminars and Original Investigations.* Elsevier, pp.29. e1-29. e11.

Lin, K., Farahani, M., Yang, Y., Johnson, G.G., Oates, M., Atherton, M., Douglas, A., Kalakonda, N. and Pettitt, A.R. 2014b. Loss of MIR15A and MIR16-1 at 13q14 is associated with increased TP53 mRNA, de-repression of BCL2 and adverse outcome in chronic lymphocytic leukaemia. *British Journal of Haematology,* 167(3), pp.346-355.

Liu, A., Shao, C., Jin, G., Liu, R., Hao, J., Song, B., Ouyang, L. and Hu, X. 2014. miR-208-induced epithelial to mesenchymal transition of pancreatic cancer cells promotes cell metastasis and invasion. *Cell Biochemistry and Biophysics,* 69(2), pp.341-346.

Liu, B., Wu, X., Liu, B., Wang, C., Liu, Y., Zhou, Q. and Xu, K. 2012. MiR-26a enhances metastasis potential of lung cancer cells via AKT pathway by targeting PTEN. *Biochimica Et Biophysica Acta (BBA)-Molecular Basis of Disease,* 1822(11), pp.1692-1704.

Liu, C., Kelnar, K., Liu, B., Chen, X., Calhoun-Davis, T., Li, H., Patrawala, L., Yan, H., Jeter, C. and Honorio, S. 2011. The microRNA miR-34a inhibits prostate cancer stem cells and metastasis by directly repressing CD44. *Nature Medicine,* 17(2), pp.211-215.

Liu, F., Liu, Y., Shen, J., Zhang, G. and Han, J. 2016. MicroRNA-224 inhibits proliferation and migration of breast cancer cells by down-regulating fizzled 5 expression. *Oncotarget,*

Lu, J., Getz, G., Miska, E.A., Alvarez-Saavedra, E., Lamb, J., Peck, D., Sweet-Cordero, A., Ebert, B.L., Mak, R.H. and Ferrando, A.A. 2005. MicroRNA expression profiles classify human cancers. *Nature,* 435(7043), pp.834-838.

Lu, Y., Lu, J., Li, X., Zhu, H., Fan, X., Zhu, S., Wang, Y., Guo, Q., Wang, L. and Huang, Y. 2014. MiR-200a inhibits epithelial-mesenchymal transition of pancreatic cancer stem cell. *BMC Cancer,* 14(1), pp.85.

Ma, J., Fang, B., Zeng, F., Pang, H., Zhang, J., Shi, Y., Wu, X., Cheng, L., Ma, C. and Xia, J. 2014a. Curcumin inhibits cell growth and invasion through up-regulation of miR-7 in pancreatic cancer cells. *Toxicology Letters,* 231(1), pp.82-91.

Ma, J., Lin, J., Qian, J., Qian, W., Yin, J., Yang, B., Tang, Q., Chen, X., Wen, X., Guo, H. and Deng, Z. 2014b. MiR-378 promotes the migration of liver cancer cells by down-regulating fus expression. *Cellular Physiology and Biochemistry : International Journal of Experimental Cellular Physiology, Biochemistry, and Pharmacology,* 34(6), pp.2266-2274.

Madden, J. 2012. Infinity reports update from phase 2 study of saridegib plus gemcitabine in patients with metastatic pancreatic cancer. *USA: Infinity Pharmaceuticals,*

Marsh, T., Pietras, K. and McAllister, S.S. 2013. Fibroblasts as architects of cancer pathogenesis. *Biochimica Et Biophysica Acta (BBA)-Molecular Basis of Disease,* 1832(7), pp.1070-1078.

Martin, A. and Clynes, M. 1991. Acid phosphatase: Endpoint for in vitro toxicity tests. *In Vitro Cellular & Developmental Biology-Animal,* 27(3), pp.183-184.

Martinez, J., Patkaniowska, A., Urlaub, H., Lührmann, R. and Tuschl, T. 2002. Single-stranded antisense siRNAs guide target RNA cleavage in RNAi. *Cell,* 110(5), pp.563-574.

Matsumura, K., Sakai, C., Kawakami, S., Yamashita, F. and Hashida, M. 2014. Inhibition of cancer cell growth by GRP78 siRNA lipoplex via activation of unfolded protein response. *Biological & Pharmaceutical Bulletin,* 37(4), pp.648-653.

Mawji, I.A., Simpson, C.D., Gronda, M., Williams, M.A., Hurren, R., Henderson, C.J., Datti, A., Wrana, J.L. and Schimmer, A.D. 2007. A chemical screen identifies anisomycin as an anoikis sensitizer that functions by decreasing FLIP protein synthesis. *Cancer Research,* 67(17), pp.8307-8315.

Mees, S.T., Mardin, W.A., Sielker, S., Willscher, E., Senninger, N., Schleicher, C., Colombo-Benkmann, M. and Haier, J. 2009. Involvement of CD40 targeting miR-224 and miR-486 on the progression of pancreatic ductal adenocarcinomas. *Annals of Surgical Oncology,* 16(8), pp.2339-2350.

Miao, L., Xiong, X., Lin, Y., Cheng, Y., Lu, J., Zhang, J. and Cheng, N. 2014. miR-203 inhibits tumor cell migration and invasion via caveolin-1 in pancreatic cancer cells. *Oncology Letters,* 7(3), pp.658-662.

Mizejewski, G.J. 1999. Role of integrins in cancer: Survey of expression patterns. *Proceedings of the Society for Experimental Biology and Medicine.Society for Experimental Biology and Medicine (New York, N.Y.),* 222(2), pp.124-138.

Morey, J.S., Ryan, J.C. and Van Dolah, F.M. 2006. Microarray validation: Factors influencing correlation between oligonucleotide microarrays and real-time PCR. *Biol Proced Online,* 8(1), pp.175-193.

National Cancer Registry Ireland 2016. *Cancer trends no 29. breast cancer.* www.ncri.ie: National Cancer Registry Ireland.

Neault, M., Mallette, F.A. and Richard, S. 2016. miR-137 modulates a tumor suppressor network-inducing senescence in pancreatic cancer cells. *Cell Reports,* 14(8), pp.1966-1978.

O'Brien, J., Wilson, I., Orton, T. and Pognan, F. 2000. Investigation of the alamar blue (resazurin) fluorescent dye for the assessment of mammalian cell cytotoxicity. *European Journal of Biochemistry,* 267(17), pp.5421-5426.

Ohuchida, K., Mizumoto, K., Kayashima, T., Fujita, H., Moriyama, T., Ohtsuka, T., Ueda, J., Nagai, E., Hashizume, M. and Tanaka, M. 2011. MicroRNA expression as a predictive marker for gemcitabine response after surgical resection of pancreatic cancer. *Annals of Surgical Oncology,* 18(8), pp.2381-2387.

Olive, K.P., Jacobetz, M.A., Davidson, C.J., Gopinathan, A., McIntyre, D., Honess, D., Madhu, B., Goldgraben, M.A., Caldwell, M.E., Allard, D., Frese, K.K., Denicola, G., Feig, C., Combs, C., Winter, S.P., Ireland-Zecchini, H., Reichelt, S., Howat, W.J., Chang, A., Dhara, M., Wang, L., Ruckert, F., Grutzmann, R., Pilarsky, C., Izeradjene, K., Hingorani, S.R., Huang, P., Davies, S.E., Plunkett, W., Egorin, M., Hruban, R.H., Whitebread, N., McGovern, K., Adams, J., Iacobuzio-Donahue, C., Griffiths, J. and Tuveson, D.A. 2009. Inhibition of hedgehog signaling enhances delivery of chemotherapy in a mouse model of pancreatic cancer. *Science (New York, N.Y.),* 324(5933), pp.1457-1461.

Omary, M.B., Lugea, A., Lowe, A.W. and Pandol, S.J. 2007. The pancreatic stellate cell: A star on the rise in pancreatic diseases. *The Journal of Clinical Investigation,* 117(1), pp.50-59.

O'Shaughnessy, J., Osborne, C., Pippen, J.E., Yoffe, M., Patt, D., Rocha, C., Koo, I.C., Sherman, B.M. and Bradley, C. 2011. Iniparib plus chemotherapy in metastatic triple-negative breast cancer. *New England Journal of Medicine,* 364(3), pp.205-214.

Özdemir, B.C., Pentcheva-Hoang, T., Carstens, J.L., Zheng, X., Wu, C., Simpson, T.R., Laklai, H., Sugimoto, H., Kahlert, C. and Novitskiy, S.V. 2014. Depletion of carcinoma-

associated fibroblasts and fibrosis induces immunosuppression and accelerates pancreas cancer with reduced survival. *Cancer Cell,* 25(6), pp.719-734.

Pai, P., Rachagani, S., Are, C. and K Batra, S. 2013. Prospects of miRNA-based therapy for pancreatic cancer. *Current Drug Targets,* 14(10), pp.1101-1109.

Pancreatic Cancer Action *Trends in cancer survival by tumour site 1971_2011* [Online]. Available from: https://pancreaticcanceraction.org/about-pancreatic-cancer/stats-facts/prognosis-survival/trends-in-cancer-survival-by-tumour-site-1971_2011/ [Accessed March 2017].

Paoli, P., Giannoni, E. and Chiarugi, P. 2013. Anoikis molecular pathways and its role in cancer progression. *Biochimica Et Biophysica Acta,* 1833(12), pp.3481-3498.

Pasquinelli, A.E. 2012. MicroRNAs and their targets: Recognition, regulation and an emerging reciprocal relationship. *Nature Reviews Genetics,* 13(4), pp.271-282.

Pellegrino, B., Bella, M., Michiara, M., Zanelli, P., Naldi, N., Porzio, R., Bortesi, B., Boggiani, D., Zanoni, D. and Camisa, R. 2016. Triple negative status and BRCA mutations in contralateral breast cancer: A population-based study. *Acta Bio Medica Atenei Parmensis,* 87(1), pp.54-63.

Perou, C.M. 2010. Molecular stratification of triple-negative breast cancers. *The Oncologist,* 15 Suppl 5pp.39-48.

Perou, C.M., Sorlie, T., Eisen, M.B., van de Rijn, M., Jeffrey, S.S., Rees, C.A., Pollack, J.R., Ross, D.T., Johnsen, H., Akslen, L.A., Fluge, O., Pergamenschikov, A., Williams, C., Zhu, S.X., Lonning, P.E., Borresen-Dale, A.L., Brown, P.O. and Botstein, D. 2000. Molecular portraits of human breast tumours. *Nature,* 406(6797), pp.747-752.

Phillips, P. 2012. Pancreatic stellate cells and fibrosis *IN:* Grippo PJ, M.H. (ed.) *Pancreatic Cancer and Tumor Microenvironment.* Trivandrum, India.: Transworld Research Network, pp.Chapter 3.

Prall, A.K., Longo, G.M., Mayhan, W.G., Waltke, E.A., Fleckten, B., Thompson, R.W. and Baxter, B.T. 2002. Doxycycline in patients with abdominal aortic aneurysms and in mice: Comparison of serum levels and effect on aneurysm growth in mice. *Journal of Vascular Surgery,* 35(5), pp.923-929.

Pramanik, D., Campbell, N.R., Karikari, C., Chivukula, R., Kent, O.A., Mendell, J.T. and Maitra, A. 2011. Restitution of tumor suppressor microRNAs using a systemic nanovector inhibits pancreatic cancer growth in mice. *Molecular Cancer Therapeutics,* 10(8), pp.1470-1480.

Puchsaka, P., Chaotham, C. and Chanvorachote, P. 2016. α-Lipoic acid sensitizes lung cancer cells to chemotherapeutic agents and anoikis via integrin β1/β3 downregulation. *International Journal of Oncology,* 49(4), pp.1445-1456.

Quinones, Q.J., Ridder, G.G.d. and Pizzo, S.V. 2008. GRP78, a chaperone with diverse roles beyond the endoplasmic reticulum.

Rachagani, S., Kumar, S. and Batra, S.K. 2010. MicroRNA in pancreatic cancer: Pathological, diagnostic and therapeutic implications. *Cancer Letters,* 292(1), pp.8-16.

Rachagani, S., Macha, M.A., Heimann, N., Seshacharyulu, P., Haridas, D., Chugh, S. and Batra, S.K. 2015. Clinical implications of miRNAs in the pathogenesis, diagnosis and therapy of pancreatic cancer. *Advanced Drug Delivery Reviews,* 81pp.16-33.

Radosa, J.C., Eaton, A., Stempel, M., Khander, A., Liedtke, C., Solomayer, E., Karsten, M., Pilewskie, M., Morrow, M. and King, T.A. 2016. Evaluation of local and distant recurrence patterns in patients with triple-negative breast cancer according to age. *Annals of Surgical Oncology,* pp.1-7.

Raiter, A., Yerushalmi, R. and Hardy, B. 2014. Pharmacological induction of cell surface GRP78 contributes to apoptosis in triple negative breast cancer cells. *Oncotarget,* 5(22), pp.11452-11463.

Rampersad, S.N. 2012. Multiple applications of alamar blue as an indicator of metabolic function and cellular health in cell viability bioassays. *Sensors,* 12(9), pp.12347-12360.

Reis-Filho, J.S. and Pusztai, L. 2011. Gene expression profiling in breast cancer: Classification, prognostication, and prediction. *Lancet,* 378(9805), pp.1812-1823.

Ressler, S., Mlineritsch, B. and Greil, R. 2010. Triple negative breast cancer. *Magazine of European Medical Oncology,* 3pp.185-189.

Rhim, A.D., Oberstein, P.E., Thomas, D.H., Mirek, E.T., Palermo, C.F., Sastra, S.A., Dekleva, E.N., Saunders, T., Becerra, C.P. and Tattersall, I.W. 2014. Stromal elements act to restrain, rather than support, pancreatic ductal adenocarcinoma. *Cancer Cell,* 25(6), pp.735-747.

Risinger, A.L., Dybdal-Hargreaves, N.F. and Mooberry, S.L. 2015. Breast cancer cell lines exhibit differential sensitivities to microtubule-targeting drugs independent of doubling time. *Anticancer Research,* 35(11), pp.5845-5850.

Robertson, B., Amand, A.S. and Vermeulen, A. Modulating endogenous microRNA targets with thermo scientific miRIDIAN microRNA mimics and inhibitors: MiR-122 in hepatocarcinoma cells (huh-7).

Romero-Cordoba, S.L., Salido-Guadarrama, I., Rodriguez-Dorantes, M. and Hidalgo-Miranda, A. 2014. miRNA biogenesis: Biological impact in the development of cancer. *Cancer Biology & Therapy,* 15(11), pp.1444-1455.

Rossi, J.J. 2008. Expression strategies for short hairpin RNA interference triggers. *Human Gene Therapy,* 19(4), pp.313-317.

Ruberti, F., Barbato, C. and Cogoni, C. 2012. Targeting microRNAs in neurons: Tools and perspectives. *Experimental Neurology,* 235(2), pp.419-426.

Rucki, A.A. and Zheng, L. 2014. Pancreatic cancer stroma: Understanding biology leads to new therapeutic strategies. *World Journal of Gastroenterology : WJG,* 20(9), pp.2237-2246.

Sacconi, A., Biagioni, F., Canu, V., Mori, F., Di Benedetto, A., Lorenzon, L., Ercolani, C., Di Agostino, S., Cambria, A. and Germoni, S. 2012. miR-204 targets bcl-2 expression and enhances responsiveness of gastric cancer. *Cell Death & Disease,* 3(11), pp.e423.

Sarkar, S., Dubaybo, H., Ali, S., Goncalves, P., Kollepara, S.L., Sethi, S., Philip, P.A. and Li, Y. 2013. Down-regulation of miR-221 inhibits proliferation of pancreatic cancer cells through up-regulation of PTEN, p27 (kip1), p57 (kip2), and PUMA. *Am J Cancer Res,* 3(5), pp.465-477.

Savagner, P. 2010. The epithelial-mesenchymal transition (EMT) phenomenon. *Annals of Oncology : Official Journal of the European Society for Medical Oncology / ESMO,* 21 Suppl 7pp.vii89-92.

Schmuck, R.B., Carvalho-Fischer, C.V., Neumann, C., Pratschke, J. and Bahra, M. 2016. Distal bile duct carcinomas and pancreatic ductal adenocarcinomas: Postulating a common tumor entity. *Cancer Medicine,* 5(1), pp.88-99.

Schultz, N.A., Dehlendorff, C., Jensen, B.V., Bjerregaard, J.K., Nielsen, K.R., Bojesen, S.E., Calatayud, D., Nielsen, S.E., Yilmaz, M. and Holländer, N.H. 2014. MicroRNA biomarkers in whole blood for detection of pancreatic cancer. *Jama,* 311(4), pp.392-404.

Seux, M., Peuget, S., Montero, M., Siret, C., Rigot, V., Clerc, P., Gigoux, V., Pellegrino, E., Pouyet, L. and N'guessan, P. 2011. TP53INP1 decreases pancreatic cancer cell migration by regulating SPARC expression. *Oncogene,* 30(27), pp.3049-3061.

Shindo, K., Aishima, S., Ohuchida, K., Fujiwara, K., Fujino, M., Mizuuchi, Y., Hattori, M., Mizumoto, K., Tanaka, M. and Oda, Y. 2013. Podoplanin expression in cancer-associated fibroblasts enhances tumor progression of invasive ductal carcinoma of the pancreas. *Molecular Cancer,* 12(1), pp.168-4598-12-168.

Siegel, R.L., Miller, K.D. and Jemal, A. 2015. Cancer statistics, 2015. *CA: A Cancer Journal for Clinicians,* 65(1), pp.5-29.

Song, W., Wang, L., Huang, W., Cai, X., Cui, J. and Wang, L. 2013. MiR-21 upregulation induced by promoter zone histone acetylation is associated with chemoresistance to gemcitabine and enhanced malignancy of pancreatic cancer cells. *Asian Pacific Journal of Cancer Prevention,* 14(12), pp.7529-7536.

Sotiriou, C., Neo, S.Y., McShane, L.M., Korn, E.L., Long, P.M., Jazaeri, A., Martiat, P., Fox, S.B., Harris, A.L. and Liu, E.T. 2003. Breast cancer classification and prognosis based on

gene expression profiles from a population-based study. *Proceedings of the National Academy of Sciences of the United States of America,* 100(18), pp.10393-10398.

Sotiriou, C., Phil, D. and Pusztai, L. 2003. Gene-expression signatures in breast cancer. *N Engl J Med,* 348(17), pp.1715-1717.

Staudacher, L., Cottu, P.H., Dieras, V., Vincent-Salomon, A., Guilhaume, M.N., Escalup, L., Dorval, T., Beuzeboc, P., Mignot, L. and Pierga, J.Y. 2011. Platinum-based chemotherapy in metastatic triple-negative breast cancer: The institut curie experience. *Annals of Oncology : Official Journal of the European Society for Medical Oncology,* 22(4), pp.848-856.

Su, A., He, S., Tian, B., Hu, W. and Zhang, Z. 2013. MicroRNA-221 mediates the effects of PDGF-BB on migration, proliferation, and the epithelial-mesenchymal transition in pancreatic cancer cells. *PLoS One,* 8(8), pp.e71309.

Su, R., Li, Z., Li, H., Song, H., Bao, C., Wei, J. and Cheng, L. 2010. Grp78 promotes the invasion of hepatocellular carcinoma. *BMC Cancer,* 10(1), pp.1.

Sugimoto, H., Mundel, T.M., Kieran, M.W. and Kalluri, R. 2006. Identification of fibroblast heterogeneity in the tumor microenvironment. *Cancer Biology & Therapy,* 5(12), pp.1640-1646.

Sun, J., Xiao, W., Wang, F., Wang, Y., Zhu, Y., Wu, Y., Miao, Z. and Lin, Y. 2015. MicroRNA-320 inhibits cell proliferation in glioma by targeting E2F1. *Molecular Medicine Reports,* 12(2), pp.2355-2359.

Sun, S., Wang, X., Wang, C., Nawaz, A., Wei, W., Li, J., Wang, L. and Yu, D. 2011. Arctigenin suppresses unfolded protein response and sensitizes glucose deprivation-mediated cytotoxicity of cancer cells. *Planta Medica,* 77(02), pp.141-145.

Sun, Y., Ding, H., Li, X.Q. and Li, L. 2014. Effects of poly(ADP-ribose)polymerase inhibitor AG014699 combined with chemotherapy on the proliferation of triple-negative breast cancer cell line MDA-MB-231. *Zhongguo Yi Xue Ke Xue Yuan Xue Bao.Acta Academiae Medicinae Sinicae,* 36(2), pp.135-139.

Szász, A.M., Lánczky, A., Nagy, Á., Förster, S., Hark, K., Szabó, A. and Győrffy, B. 2016. Cross-validation of survival associated biomarkers in gastric cancer using transcriptomic data of 1,065 patients. *Oncotarget,* pp.49322-49333.

Tadano, T., Kakuta, Y., Hamada, S., Shimodaira, Y., Kuroha, M., Kawakami, Y., Kimura, T., Shiga, H., Endo, K. and Masamune, A. 2016. MicroRNA-320 family is downregulated in colorectal adenoma and affects tumor proliferation by targeting CDK6. *World Journal of Gastrointestinal Oncology,* 8(7), pp.532.

Taddei, M.L., Giannoni, E., Fiaschi, T. and Chiarugi, P. 2012. Anoikis: An emerging hallmark in health and diseases. *The Journal of Pathology,* 226(2), pp.380-393.

Takikawa, T., Masamune, A., Hamada, S., Nakano, E., Yoshida, N. and Shimosegawa, T. 2013. miR-210 regulates the interaction between pancreatic cancer cells and stellate cells. *Biochemical and Biophysical Research Communications,* 437(3), pp.433-439.

Tan, K., Goldstein, D., Crowe, P. and Yang, J. 2013. Uncovering a key to the process of metastasis in human cancers: A review of critical regulators of anoikis. *Journal of Cancer Research and Clinical Oncology,* 139(11), pp.1795-1805.

Tay, F.C., Lim, J.K., Zhu, H., Hin, L.C. and Wang, S. 2015. Using artificial microRNA sponges to achieve microRNA loss-of-function in cancer cells. *Advanced Drug Delivery Reviews,* 81pp.117-127.

Terada, T., Nakanuma, Y. and Kakita, A. 1990. Pathologic observations of intrahepatic peribiliary glands in 1000 consecutive autopsy livers: Heterotopic pancreas in the liver. *Gastroenterology,* 98(5), pp.1333-1337.

Thakral, S. and Ghoshal, K. 2015. miR-122 is a unique molecule with great potential in diagnosis, prognosis of liver disease, and therapy both as miRNA mimic and antimir. *Current Gene Therapy,* 15(2), pp.142-150.

Thomas, S., Sharma, N., Gonzalez, R., Pao, P., Hofman, F.M., Chen, T.C., Louie, S.G., Pirrung, M.C. and Schönthal, A.H. 2013. Repositioning of verrucosidin, a purported inhibitor of chaperone protein GRP78, as an inhibitor of mitochondrial electron transport chain complex I. *PloS One,* 8(6), pp.e65695.

Tiwari, N., Gheldof, A., Tatari, M. and Christofori, G. 2012. EMT as the ultimate survival mechanism of cancer cells. *Seminars in Cancer Biology,* 22(3), pp.194-207.

Tjomsland, V., Pomianowska, E., Aasrum, M., Sandnes, D., Verbeke, C.S. and Gladhaug, I.P. 2016. Profile of MMP and TIMP expression in human pancreatic stellate cells: Regulation by IL-1α and TGFβ and implications for migration of pancreatic cancer cells. *Neoplasia,* 18(7), pp.447-456.

Torres, A., Torres, K., Paszkowski, T., Jodłowska-Jędrych, B., Radomański, T., Książek, A. and Maciejewski, R. 2011. Major regulators of microRNAs biogenesis dicer and drosha are down-regulated in endometrial cancer. *Tumor Biology,* 32(4), pp.769-776.

Tutt, A., Ellis, P., Kilburn, L., Gilett, C., Pinder, S., Abraham, J., Barrett, S., Barrett-Lee, P., Chan, S. and Cheang, M. 2015. *Abstract S3-01: The TNT Trial: A Randomized Phase III Trial of Carboplatin (C) Compared with Docetaxel (D) for Patients with Metastatic Or Recurrent Locally Advanced Triple Negative Or BRCA1/2 Breast Cancer (CRUK/07/012),*

Uitto, V., Firth, J.D., Nip, L. and Golub, L.M. 1994. Doxycycline and chemically modified tetracyclines inhibit gelatinase A (MMP-2) gene expression in human skin keratinocytes. *Annals of the New York Academy of Sciences,* 732(1), pp.140-151.

Valastyan, S. and Weinberg, R.A. 2011. Tumor metastasis: Molecular insights and evolving paradigms. *Cell,* 147(2), pp.275-292.

Van De Rijn, M., Perou, C.M., Tibshirani, R., Haas, P., Kallioniemi, O., Kononen, J., Torhorst, J., Sauter, G., Zuber, M. and Köchli, O.R. 2002. Expression of cytokeratins 17 and 5 identifies a group of breast carcinomas with poor clinical outcome. *The American Journal of Pathology,* 161(6), pp.1991-1996.

Voduc, K.D., Cheang, M.C., Tyldesley, S., Gelmon, K., Nielsen, T.O. and Kennecke, H. 2010. Breast cancer subtypes and the risk of local and regional relapse. *Journal of Clinical Oncology : Official Journal of the American Society of Clinical Oncology,* 28(10), pp.1684-1691.

Volinia, S., Calin, G.A., Liu, C.G., Ambs, S., Cimmino, A., Petrocca, F., Visone, R., Iorio, M., Roldo, C., Ferracin, M., Prueitt, R.L., Yanaihara, N., Lanza, G., Scarpa, A., Vecchione, A., Negrini, M., Harris, C.C. and Croce, C.M. 2006. A microRNA expression signature of human solid tumors defines cancer gene targets. *Proceedings of the National Academy of Sciences of the United States of America,* 103(7), pp.2257-2261.

Vonlaufen, A., Joshi, S., Qu, C., Phillips, P.A., Xu, Z., Parker, N.R., Toi, C.S., Pirola, R.C., Wilson, J.S., Goldstein, D. and Apte, M.V. 2008. Pancreatic stellate cells: Partners in crime with pancreatic cancer cells. *Cancer Research,* 68(7), pp.2085-2093.

Wang, P., Chen, L., Zhang, J., Chen, H., Fan, J., Wang, K., Luo, J., Chen, Z., Meng, Z. and Liu, L. 2014. Methylation-mediated silencing of the miR-124 genes facilitates pancreatic cancer progression and metastasis by targeting Rac1. *Oncogene,* 33(4), pp.514-524.

Wang, Y., Yu, H., Zhang, J., Gao, J., Ge, X. and Lou, G. 2015. Hesperidin inhibits HeLa cell proliferation through apoptosis mediated by endoplasmic reticulum stress pathways and cell cycle arrest. *BMC Cancer,* 15(1), pp.682.

Wazir, U., Orakzai, M.M., Khanzada, Z.S., Jiang, W.G., Sharma, A.K., Kasem, A. and Mokbel, K. 2015. The role of death-associated protein 3 in apoptosis, anoikis and human cancer. *Cancer Cell International,* 15(1), pp.1.

Wei, X., Wang, W., Wang, L., Zhang, Y., Zhang, X., Chen, M., Wang, F., Yu, J., Ma, Y. and Sun, G. 2016. MicroRNA-21 induces 5-fluorouracil resistance in human pancreatic cancer cells by regulating PTEN and PDCD4. *Cancer Medicine,*

Weigel, K.J., Jakimenko, A., Conti, B.A., Chapman, S.E., Kaliney, W.J., Leevy, W.M., Champion, M.M. and Schafer, Z.T. 2014. CAF-secreted IGFBPs regulate breast cancer cell anoikis. *Molecular Cancer Research : MCR,* 12(6), pp.855-866.

Weiss, F.U., Marques, I.J., Woltering, J.M., Vlecken, D.H., Aghdassi, A., Partecke, L.I., Heidecke, C., Lerch, M.M. and Bagowski, C.P. 2009. Retinoic acid receptor antagonists inhibit miR-10a expression and block metastatic behavior of pancreatic cancer. *Gastroenterology,* 137(6), pp.2136-2145. e7.

Wilson, J.S., Pirola, R.C. and Apte, M.V. 2014. Stars and stripes in pancreatic cancer: Role of stellate cells and stroma in cancer progression. *Frontiers in Physiology,* 5pp.52.

Winter, J., Jung, S., Keller, S., Gregory, R.I. and Diederichs, S. 2009. Many roads to maturity: MicroRNA biogenesis pathways and their regulation. *Nature Cell Biology,* 11(3), pp.228-234.

Wolf, K., Wu, Y.I., Liu, Y., Geiger, J., Tam, E., Overall, C., Stack, M.S. and Friedl, P. 2007. Multi-step pericellular proteolysis controls the transition from individual to collective cancer cell invasion. *Nature Cell Biology,* 9(8), pp.893-904.

Wu, K., Hu, G., He, X., Zhou, P., Li, J., He, B. and Sun, W. 2013. MicroRNA-424-5p suppresses the expression of SOCS6 in pancreatic cancer. *Pathology & Oncology Research,* 19(4), pp.739-748.

Wu, M., Jan, C., Tsay, Y., Yu, Y., Huang, C., Lin, S., Liu, C., Chen, Y., Lo, J. and Yu, C. 2010. Elimination of head and neck cancer initiating cells through targeting glucose regulated protein78 signaling. *Molecular Cancer,* 9(1), pp.283.

Wu, Q., Xie, Y., Deng, Z., Li, X., Yang, W., Jiao, C., Fang, L., Li, S., Pan, H. and Yee, A.J. 2012. Ergosterol peroxide isolated from ganoderma lucidum abolishes microRNA miR-378-mediated tumor cells on chemoresistance. *PLoS One,* 7(8), pp.e44579.

Wu, Z., Wang, S., Chen, Z., Huv, S., Huang, K., Huang, B., Du, J., Huang, C., Peng, L. and Jian, Z. 2015. MiR-204 regulates HMGA2 expression and inhibits cell proliferation in human thyroid cancer. *Cancer Biomarkers,* 15(5), pp.535-542.

Xie, J., Chen, M., Zhou, J., Mo, M., Zhu, L., Liu, Y., Gui, Q., Zhang, L. and Li, G. 2014. miR-7 inhibits the invasion and metastasis of gastric cancer cells by suppressing epidermal growth factor receptor expression. *Oncology Reports,* 31(4), pp.1715-1722.

Xu, D., Wang, Q., An, Y. and Xu, L. 2013. miR-203 regulates the proliferation, apoptosis and cell cycle progression of pancreatic cancer cells by targeting survivin. *Molecular Medicine Reports,* 8(2), pp.379-384.

Xu, J., Zeng, J.Q., Wan, G., Hu, G.B., Yan, H. and Ma, L.X. 2009. Construction of siRNA/miRNA expression vectors based on a one-step PCR process. *BMC Biotechnology,* 9pp.53-6750-9-53.

Yao, X., Liu, H., Zhang, X., Zhang, L., Li, X., Wang, C. and Sun, S. 2015. Cell surface GRP78 accelerated breast cancer cell proliferation and migration by activating STAT3. *PloS One,* 10(5), pp.e0125634.

Yazbeck, A. and Bjornberg, A. 2014. *Euro pancreatic cancer index 2014.* Taby, Sweden: Health Consumer Powerhouse.

Yeung, B., Kwan, B., He, Q., Lee, A., Liu, J. and Wong, A. 2008. Glucose-regulated protein 78 as a novel effector of BRCA1 for inhibiting stress-induced apoptosis. *Oncogene,* 27(53), pp.6782-6789.

Yi, R., Doehle, B.P., Qin, Y., Macara, I.G. and Cullen, B.R. 2005. Overexpression of exportin 5 enhances RNA interference mediated by short hairpin RNAs and microRNAs. *RNA (New York, N.Y.),* 11(2), pp.220-226.

Ying, Z., Li, Y., Wu, J., Zhu, X., Yang, Y., Tian, H., Li, W., Hu, B., Cheng, S.Y. and Li, M. 2013. Loss of miR-204 expression enhances glioma migration and stem cell-like phenotype. *Cancer Research,* 73(2), pp.990-999.

Yu, B., Peng, X., Zhao, F., Liu, X., Lu, J., Wang, L., Li, G., Chen, H. and Li, X. 2014. MicroRNA-378 functions as an onco-miR in nasopharyngeal carcinoma by repressing TOB2 expression. *International Journal of Oncology,* 44(4), pp.1215-1222.

Yu, S.J., Hu, J.Y., Kuang, X.Y., Luo, J.M., Hou, Y.F., Di, G.H., Wu, J., Shen, Z.Z., Song, H.Y. and Shao, Z.M. 2013. MicroRNA-200a promotes anoikis resistance and metastasis by targeting YAP1 in human breast cancer. *Clinical Cancer Research : An Official Journal of the American Association for Cancer Research,* 19(6), pp.1389-1399.

Zeng, C., Zhan, Y., Huang, J. and Chen, Y. 2016. MicroRNA-7 suppresses human colon cancer invasion and proliferation by targeting the expression of focal adhesion kinase. *Molecular Medicine Reports,* 13(2), pp.1297-1303.

Zeng, Y., Wagner, E.J. and Cullen, B.R. 2002. Both natural and designed micro RNAs can inhibit the expression of cognate mRNAs when expressed in human cells. *Molecular Cell,* 9(6), pp.1327-1333.

Zhang, G., Zhou, H., Xiao, H., Li, Y. and Zhou, T. 2014. MiR-378 is an independent prognostic factor and inhibits cell growth and invasion in colorectal cancer. *BMC Cancer,* 14(1), pp.1.

Zhang, L. and Zhang, X. 2010. Roles of GRP78 in physiology and cancer. *Journal of Cellular Biochemistry,* 110(6), pp.1299-1305.

Zhang, S., Liu, C., Li, L., Sun, T., Luo, Y., Yun, W. and Zhang, J. 2013. Examination of artificial MiRNA mimics with Centered–Site complementarity for gene targeting. *PloS One,* 8(8), pp.e72062.

Zhang, T., Zou, P., Wang, T., Xiang, J., Cheng, J., Chen, D. and Zhou, J. 2016. Down-regulation of miR-320 associated with cancer progression and cell apoptosis via targeting mcl-1 in cervical cancer. *Tumor Biology,* pp.1-10.

Zhang, X., Zhang, L., Wang, S., Wu, D. and Yang, W. 2015. Decreased functional expression of Grp78 and Grp94 inhibits proliferation and attenuates apoptosis in a human gastric cancer cell line in vitro. *Oncology Letters,* 9(3), pp.1181-1186.

Zhao, C., Zhang, J., Zhang, S., Yu, D., Chen, Y., Liu, Q., Shi, M., Ni, C. and Zhu, M. 2013. Diagnostic and biological significance of microRNA-192 in pancreatic ductal adenocarcinoma. *Oncology Reports,* 30(1), pp.276-284.

Zhao, L. and Burt, A.D. 2007. The diffuse stellate cell system. *Journal of Molecular Histology,* 38(1), pp.53-64.

Zheng, B., Ohuchida, K., Chijiiwa, Y., Zhao, M., Mizuuchi, Y., Cui, L., Horioka, K., Ohtsuka, T., Mizumoto, K., Oda, Y., Hashizume, M., Nakamura, M. and Tanaka, M. 2015. CD146 attenuation in cancer-associated fibroblasts promotes pancreatic cancer progression. *Molecular Carcinogenesis,*

Zhou, X., Xing, X., Zhang, S., Liu, L., Wang, C., Li, L., Ji, Q. and Liu, H. 2016. Glucose-regulated protein 78 contributes to the proliferation and tumorigenesis of human colorectal carcinoma via AKT and ERK pathways. *Oncology Reports,* 36(5), pp.2723-2730.